ACTING ON BEHAVIORALLY RELEVANT EVENTS AND THE IMPACT THIS HAS ON ATTENTION AND MEMORY

A Dissertation
Presented to the Faculty of the Graduate School
of Cornell University
In Partial Fulfillment of the Requirements for the Degree of
Doctor of Philosophy

by
Hamid Turker
May 2022

ACTING ON BEHAVIORALLY RELEVANT EVENTS
AND THE IMPACT THIS HAS ON ATTENTION AND MEMORY

Hamid Turker, Ph.D.
Cornell University 2022

We attend to and, subsequently, remember some moments in time better than other ones. Understanding such interactions between attention and memory has been a longstanding topic in behavioral and brain sciences. One factor is the occurrence of behaviorally relevant events, which make attention fluctuate over time. These are events which require us to act on them in some fashion, to bring our ongoing behavior back in alignment with our task goals. Despite being more cognitively demanding than not acting, this somehow results in better memory for stimuli being encoded during that moment in time compared to stimuli encoded at other moments. Why is that? This dissertation investigates some of the cognitive, computational, and neural characteristics related to this phenomenon. In the first of four empirical articles covered herein, I replicate and extend previous findings on this phenomenon, demonstrating that the enhancement occurs not only for stimuli being intentionally encoded, but also for the incidentally encoded relational features between concurrent items. The second article utilizes diffusion decision modeling to reveal that the impact on memory is primarily on evidence accumulation. In the latter two empirical articles, I investigate what the neural origins of this phenomenon may be. Its underpinnings must involve a mechanism that is triggered by decision processes related to the appearance of behaviorally relevant events and thereby transiently facilitates processing in perceptual and memory regions. A promising candidate mechanism is the locus coeruleus neuromodulatory system. The third article investigates how, using functional magnetic resonance imaging, methodological decisions will affect characterization of this system's functional

connectivity in the brain. In the fourth article, the locus coeruleus is contrasted to a different neuromodulatory system and shown to uniquely account for variance in activity in perceptual and memory areas, strengthening the idea that this system in particular may play an important role in this phenomenon. Combined, the studies presented in this dissertation reveal novel insights into the cognitive and computational characteristics of this phenomenon and argue that the locus coeruleus neuromodulatory system is a likely contributor to its manifestation.

BIOGRAPHICAL SKETCH

Hamid Turker was born and raised in The Hague, the Netherlands, where he attended elementary school Waalse Louise de Coligny and grammar school Gymnasium Sorghvliet. He graduated from Leiden University with a B.Sc. in Psychology (‘11) and M.Sc. in Cognitive Neuroscience (‘13). In 2011, through the Royal Netherlands Academy of Arts & Sciences, he first gained experience with human neuroimaging, collecting fMRI data on children and adolescents. In 2012, he was a Visiting Student Research Collaborator at Princeton University, working on model-based and model-free reinforcement learning. Following this, in 2013, he was a research trainee at Harvard University, studying visual attention and memory with eyetracking and pupillometry. Combining this experience, he joined Cornell University in 2015 to pursue his Ph.D. and was awarded the Sage Fellowship. His research focuses on the cognitive, computational, and neural foundations of attention and memory.

To my parents, Levend and Hafize. Sizsiz buralara kadar gelemezdim.

ACKNOWLEDGMENTS

First and foremost, I would like to thank my parents. Your guidance, support, and love has brought me to where I am today. At every step along the way, you have made decisions that propelled me forward in life. It takes a lot of courage to pack your bags and move to a different country, with a different culture, and a different language in one's twenties, the way both of you did. It was a lot easier for me, no doubt, but your story inspired me to undertake a similar adventure in my twenties, as well. It wasn't until halfway through my Ph.D. that I realized a fun coincidence. The origins of your names – Levend, referring to an 'incidental troop of soldiers', and Hafize, from 'guardian' and 'memory' – and their relationship to the topic under investigation here: the boosting of incidental information into memory which may otherwise be lost.

My wonderful girlfriend Julia. We met in the first moments of the first class on the first day of my Ph.D. and you have been my biggest support throughout this process ever since. I will forever be thankful to Cornell for bringing you into my life. I am endlessly proud of you.

My brilliant friends and lab mates. Gandalf, whom I stayed with during interviews and who is one of the friendliest and funniest people I met here. I still cannot believe you talked that waitress into giving us free fries in Florida. I will keep your staff safe until we meet again. Roy, we instantly clicked during interviews and picked up right where we left off, over burgers at the Ale House, when we returned to Ithaca in 2015 to start this journey. It's been a whirlwind of laughter and deep conversations about the brain ever since. Office B105/95 will forever be the Türmoyal lab to me. Adam, we have collected hours of fMRI, EEG, and pupillometry data together and I have enjoyed all of it. I'm thankful to call you a friend and colleague. Let's continue to collaborate, scientifically and musically. Kava bar open mic! Also, let's never try that Caroline Reaper chip challenge again – it is the biggest regret of my Ph.D. Norma, thank you for your unconditional support, friendship, and great birthday gifts. I have lost count of the times we would sit in my office trying to figure out research and figure out life. Karen, I am thankful for all your sharp insights and inspiring research. Iris, thank you for enthusiasm and your lovely piano playing.

The fantastic staff in the Department of Psychology and Human Development: Pam, Cindy, Linda, Julie, Lisa, Caroline, and Kathy. I would have been lost without all of you. The staff at the Cornell Magnetic Resonance Imaging Facility: Emily Qualls and Roy Proper. My collaborators on our neuroimaging research, Lissa Riley, Stan Colcombe, and Wen-Ming Luh. All my research assistants in the lab and all the participants. My kind and insightful committee: Morten for his vast knowledge of statistical learning and cognitive science, Shimon for his deep understanding of computation, Tom for knowing how to relate my work to the real world.

Finally, an immeasurable thank you to Khena for giving me a chance, for trailblazing the work that my dissertation is based on, for some of the most inspiring conversations I have had on brains and behaviors, and for being the kind of supervisor every Ph.D. student dreams of. I hope I can always be a part of the AMP family, no matter where I go.

TABLE OF CONTENTS

LIST OF FIGURES

LIST OF TABLES

LIST OF ABBREVIATIONS

1.5T, 3T, 7T:	1.5, 3, 7 Tesla, field strength of the MRI scanner
1E-fMRI:	single-echo fMRI
2AFC, 4AFC:	two-alternative forced choice, four-alternative forced choice
4V:	4th ventricle
ABE:	attentional boost effect
AC:	auditory cortex
AFNI:	"analysis of functional neuroimages", a popular software suite to analyze (f)MRI images
ANATICOR:	anatomical image correction to denoise fMRI scans
ANOVA:	analysis of variance
b5:	blurring in the fMRI data brought up to approximately 5 mm FWHM
BA:	Brodmann area
BET:	brain extraction tool, a software module in FSL that identifies and deletes non-brain tissue (e.g., skull tissue) from structural MRI images ("skull-stripping")
BOLD:	blood oxygen level dependent
cm:	centimeters
CA1:	"cornu Ammonis" area 1, a subfield of the HPC
CA2/3:	"cornu Ammonis" areas 2-3, two subfields of the HPC
CRT:	cathode-ray tube, a type of analog display device/monitor
DDM:	diffusion decision model (a.k.a. drift diffusion model)
DG:	dentate gyrus, a subfield of the HPC
DIC:	deviance information criterion
DMC:	Dynamic Models of Choice toolbox (Heathcote et al., 2019)
DVARS:	delta variation signal, defined as root mean square average of the first derivatives of fMRI signals, reflecting how much the average signal intensity has changed between successive time points (lower is better)
E2:	second echo (out of three) of multi-echo data
E2a:	E2+R,4 with the addition of ICA-AROMA in lieu of basic motion regression
E2+R,4:	basic denoising, with the addition of both 4V and RETROICOR denoising
EC:	Euler characteristic
EPI:	echo-planar imaging, a popular scan sequence to collect functional MRI images
FDR:	false discovery rate
FLIRT:	FMRIB software library's linear image registration tool
fMRI:	functional magnetic resonance imaging
FNIRT:	FMRIB software library's non-linear image registration tool
FSL:	FMRIB software library, a popular software suite to analyze fMRI images in clinical and research settings

FWHM:	full width at half maximum, the length across the x-axis of a Gaussian distribution at half its amplitude, representing a measure for amount of blurring in fMRI data
GM:	gray matter
GS:	global signal
HPC:	hippocampus
Hz:	Hertz
ICA:	independent components analysis
ICA-AROMA:	automatic removal of motion artifacts through ICA to denoise fMRI scans
iFC:	intrinsic functional connectivity
K1, K2:	binary atlas from Keren, Lozar, Harris, Morgan, & Eckert (2009), 1SD and 2SD
LC:	locus coeruleus
LPI:	Left-Posterior-Inferior, a coordinate system for MRI data
MATLAB:	matrix laboratory, a popular software suite used for numeric computing
MC:	motor cortex
MCFLIRT:	FMRIB software library's motion correction tool based on FLIRT
ME:	ME-ICA pipeline, with RETROICOR, WM, 4V, and 6 motion parameters (no derivatives) on the multi-echo data (l-ME, s-ME)
MELODIC:	FMRIB software library's tool for multivariate exploratory linear optimized decomposition into independent components
MEMB:	multi-echo multi-band fMRI scanning
ME-fMRI:	multi-echo fMRI
mm:	millimeters
MNI152:	T1 MNI-152 0.5 mm iso-voxel standard atlas
MNIa:	MNIa_caez_N27 standard atlas
MPRAGE:	magnetization-prepared rapid gradient-echo, a popular scan sequence for structural brain imaging in clinical and research settings
NE:	norepinephrine
nb:	native blurring of the fMRI data, without any further blurring applied, it is at least the maximum resolution of the fMRI voxels (e.g., 3 mm voxels means at least 3 mm native blurring)
nmT1:	neuromelanin-weighted T1
OCV:	optimal combination volume
PT:	pontine tegmentum
RETROICOR:	retrospective image correction to denoise fMRI scans
ROI(s):	region(s) of interest
s:	seconds
SPM12:	statistical parametric mapping v.12, a popular software suite to analyze (f)MRI images
T2*:	transverse relaxation signal decay rate, one of the critical factors determining the contrast in MRI, allowing us to identify different tissue types

TE:	echo time
TR:	repetition time, reflecting the rate at which a functional scan is taken, e.g., a TR=2 s means that the fMRI scan consists of a functional image taken every 2 seconds
tSNR:	temporal signal-to-noise ratio, defined as the mean of a time course divided by its standard deviation, used as a measure for fMRI data quality (higher is better)
T&S:	Turker & Swallow (2019), Chapter 2 in the current dissertation
V1, V2:	primary visual cortex (area 1), secondary visual cortex (area 2)
vmPFC:	ventral medial prefrontal cortex
WM:	white matter

LIST OF SYMBOLS

a: boundary separation
v: drift rate
t0: non-decision time
z: bias

PREFACE

Imagine yourself on May 7th, 1989, as Michael Jordan, in the playoff game between the Cleveland Cavaliers and the Chicago Bulls. It's Game 5, with the best-of-five series tied 2-2. It's the fourth quarter and the Bulls are down 97-98. There's only 10 seconds left in the game. It's not looking good. You'll need to do something if you still want to win. Fortunately, the Bulls are in possession of the ball, Pippen passes to you, and you hit a jumper. It's now 99-98 and the Bulls are ahead, with 6 seconds on the clock. Good – you're back on track. The Cavs call a time-out to adjust their play and the game resumes two minutes later with Cleveland in possession of the ball. Ehlo inbounds the ball to Nance, gets it back, and drives to the hoop: 99-100, 3 seconds to go. Cleveland is back in the lead again. So, it's another moment that calls for an adjustment on your end and the Bulls call a time-out. When you head back out onto the court, Cleveland sees your new positioning for the last play of the game and they call another time-out. Both teams keep adjusting their plays based on what has happened and what signals they're getting from the other team. The game restarts and the Bulls' Sellars will inbound the ball. Three seconds left. He looks around. Ehlo and Nance are covering you. So, you move right, push Nance away, and cut left. You're open. Two seconds. Sellars gets the ball to you. One second. You put it up. It's good! The Bulls win 101-100 and the buzzer-beater eliminates the Cavs. Unbelievable!

We frequently have to adjust our ongoing behavior in order to stay aligned with our goals, because of encounters with behaviorally relevant events. But what happens to our attention and memory systems during such moments? Nowadays, Game 5 between Cleveland and Chicago is considered a classic, the shot is remembered as "The Shot", and it is one of the greatest clutch moments in Jordan's career. Odds are that shot is etched in his memory. But behaviorally relevant events do not need to carry as much weight as the final seconds of Game 5 to impact our attention and memory. More commonplace events can also have an impact on how our attention and memory systems function, if those events require a response of some sort in order for us to stay on track to meet our goals: detours on our way home forcing us to reroute, linguistic or non-linguistic cues that necessitate a change in the trajectory of a conversation, or work-related notifications popping up on our phone or computer about updates on a project.

You may think that these events tax our attention and memory systems more than other moments in time. After all, we are now faced with splitting our attention between keeping our current behavior going, qualifying the relevance and meaning of the event, and swiftly updating relevant mental representations to adjust our behavior for the new context if the event was behaviorally relevant. And yet, despite the limitations and fallibility of our attention and memory, we are able to manage the occurrence of many such events every day, even when such events occur close together in time. Better yet, as we will see in this dissertation, instead of negatively impacting attention and memory, acting on behaviorally relevant moments can actually enhance the functioning of those two systems during those moments.

This memory enhancement is observed in paradigms where people are instructed to memorize a series of sequentially presented images, while simultaneously responding to the appearance of predefined target cues in a concurrent stream of stimuli. So, whenever a target appears, they are required to act on them in some fashion, such as press a button, otherwise they don't stay on track to meet the task goals. Although non-target cues don't require a response and therefore offer opportunity to allocate more cognitive resources to memorizing the concurrent image, it is actually images that appeared concurrently with target cues that are subsequently remembered better. This is known as the *attentional boost effect*: the difference in memory between target-paired images and non-target-paired (also known as distractor-paired) images.

Why does this happen? This dissertation investigates cognitive, computational, and neural aspects of how behaviorally relevant events are handled by attention and memory systems to result in an attentional boost effect. My aim in this dissertation is to demonstrate that the attentional boost effect enhances more information than previously thought: not just the image concurrent to the target, but also various incidental relational features about the cue itself. Next, through computational modeling, I argue that these results cannot be accounted for by response bias. I also show that splitting attention even further, by asking people to memorize both the images and the concurrent cues, actually magnifies the attentional boost effect further. After this, I turn my attention to what the underlying neural mechanisms may be that produce this effect and hope to convince you that, currently, the most likely candidate is the locus coeruleus neuromodulatory system.

The topic investigated and questions asked in this dissertation were born very naturally out of the alignment in research interests between myself and Prof. Khena Swallow. Prior to coming to Cornell University, I had the pleasure of studying at Leiden University in The Netherlands, where I first became interested in attention, action, and event cognition. Leiden University also offered me the opportunity to work with functional magnetic resonance imaging for the first time. After Leiden, I steeped myself in research on computational models of reinforcement learning, a process by which an agent incrementally adapts ongoing decision-making over time. In the brain, neuromodulatory systems appear to be implementing such a process. Next, I worked on spatial visual search, memory, and eye tracking, by researching how our visual system finds predefined target items in a large array and what we subsequently remember from that array.

Clearly, I was always meant to come to Cornell. It is the only place where I could have combined all of my interests and all of my experience to do this exciting research.

Hamid B. Turker
Ithaca, March 2022

CHAPTER 1

GENERAL INTRODUCTION

1.1 Behaviorally Relevant Events and their Implications for Attention and Memory

Throughout daily life, we frequently encounter events that signal to us that we must adjust our ongoing behavior if we are to stay on track to meet our behavioral goals. For instance, drivers must maintain focus on the road, their speed, and their route. But if they see a detour sign or a pedestrian suddenly stepping out into the street, they will need to quickly, flexibly, and safely adjust their driving. Two people conversing must be able to pick up on various linguistic and non-linguistic cues that signal a change in the trajectory of a conversation and adapt their speech on the fly accordingly. While shopping for groceries, we may unexpectedly see someone who looks familiar and will then need to rely on the richness and accuracy of our memory to decide how to acknowledge them, lest we commit a faux pas. Arguably, our ability to respond adequately to behaviorally relevant events lies at the heart of adaptive behavior. But what happens to our attention and memory systems during those moments in time when we encounter behaviorally relevant events that require us to act on them?

1.2 Attention and Memory are Limited and Fallible

A longstanding notion is that attention is limited and memory is fallible (Ballard, Hayhoe, & Pelz, 1995; Hamilton, 1859; Hayhoe, 2000; James, 1890; Kinchla, 1992). Thus, rapidly evaluating a behaviorally relevant event and responding to it is no easy feat. Seminal research on attention and action (e.g., Broadbent, 1958, 1971; Eriksen & Eriksen, 1974; Eriksen & Hoffman, 1974) has formed the foundation of proposals that information processing is limited

in its capacity, that information concurrently presented at a given moment in time competes for representational resources, and thus that selection needs to occur at various levels from sensory input to behavioral output (e.g., Allport, 1980, 1993; Deutsch & Deutsch 1963; Norman & Shallice, 1986; Mesulam, 1985, 1998). Thus, when cognitive and neural structures with finite capacity are preoccupied with representing and processing a given stimulus, they will be unavailable to represent or process other information (Hirst & Kalmar, 1987). Performance on tasks should, therefore, be better when incoming information can rely on different structures or some information is selected at the expense of other information. In order to produce goal-directed behavior, competition for representation can be biased towards attending and responding to the information that is behaviorally relevant (Desimone & Duncan, 1995), such as items of a certain color, shape, or in a certain location.

In behavioral, cognitive, and brain sciences, the most commonly studied form of attention is spatial in nature: orienting attention in space and visual search for a predefined target item located somewhere in an array (Posner, 1980; Treisman & Gelade, 1980). Participants in such paradigms may be cued ahead of time to orient themselves to a certain quadrant in the array or to look out for certain perceptual features that may co-occur with the target feature. Using these instructions, they can then filter out information that is irrelevant given their ongoing task goals and thereby improve their performance by speeding up visual search (Wolfe, 2015). With the advent of non-invasive human neuroimaging, a great deal of research has been conducted on visuospatial attention and biased competition in the brain (for a review, see Buschman & Kastner, 2015). Visuospatial attention increases neural sensitivity (Reynolds, Pasternak, & Desimone, 2000), response gain (Williford & Maunsell, 2006), sharpens tuning curves to certain perceptual features (David, Hayden, Mazer, & Gallant, 2008), and even suppresses activity in

neurons with response selectivity to information that is currently irrelevant (Martinez-Trujillo & Treue, 2004). All of this is likely accomplished by long-distance neural projections from frontal areas onto the visual cortex (Zhang et al., 2014) which bias competition and thereby gate what information enters into working memory (for a review, see Gazzaley, 2011). Thus, attentional control over what information gets selected in sensory cortices during a visuospatial task is dependent on structures spread out across the brain, which has been referred to as a dorsal fronto-parietal attention network (Hazeltine, Poldrack, & Gabrieli, 2000; Kastner & Ungerleider, 2000). Notably, this work has generally implicated neocortical regions and networks in these attention and control processes, with limited work on the role of subcortical areas and brainstem neuromodulatory systems (but see, e.g., Corbetta & Shulman, 2002).

1.3 Temporal Attention, Selection, & Dual-Tasking

Attention can be allocated to spatial locations and perceptual features (Carrasco, 2011), but also to moments in time (Nobre & Van Ede, 2018). As time unfolds and situations change, attention will fluctuate, and cognitive processes are impacted in varying ways. Temporal attention is often studied under dual-task conditions, where behaviorally relevant stimuli appear at different moments and affect ongoing performance on a concurrent task. Similar to how dividing attention across space is possible to some extent, but can results in poorer performance (Hogendoorn, Carlson, Van Rullen, & Verstraten, 2010; Pashler, 1994), these dual-task scenarios can be managed but nevertheless result in interference, because the appearance of a behaviorally relevant event increases attentional demands (Chun & Potter, 1995; Duncan, 1980; Raymond, Shapiro, & Arnell, 1992). Given well-documented dual-task interference effects on attention, memory, and behavioral performance (e.g., Janczyk & Kunde, 2020; Jolicoeur, 1999; Kiesel,

Steinhauser, Wendt, Falkenstein, Jost, Philipp, & Koch, 2010; Monsell, 2003; Rubinstein, Meyer, & Evans, 2001; Wylie & Allport, 2000), how does that impact what is and is not remembered about the moment in time when the behaviorally relevant event occurred?

It would seem that memory for behaviorally relevant events must be worse than memory for other moments in time when no such event occurred. After all, there should be interference from dividing attention across multiple streams of information (one's ongoing task and simultaneous the qualifying, processing of, and responding to the behaviorally relevant event) and briefly increasing attention to one task will interfere with performance on the other task (Duncan, 1980; Kinchla, 1992; Troyer & Craik, 2000). However, this isn't necessarily the case.

1.3.1 The Attentional Boost Effect & Memory for Behaviorally Relevant Events

In the attentional boost effect paradigm (Lin, Pype, Murray, & Boynton, 2010; Swallow & Jiang, 2010), participants are instructed to memorize a series of images, briefly presented one after another, while simultaneously performing a target detection task on concurrent, but otherwise unrelated, cues. Thus, in addition to having to memorize images, they are instructed to respond each time a cue appears with a predefined feature (*targets*; for instance, a red circle, as opposed to yellow). Cues without the target-feature thus require no response (*distractors*) and cognitive resources can be allocated to primarily memorizing the image. Note that the required "response" to the behaviorally relevant event (i.e., the appearance of a target) can come in many forms. Typically, participants are instructed to press a button for each target (e.g., Swallow & Jiang, 2010), but they can also be instructed to covertly count the number of targets or instructed to withhold button presses for targets (Makovski, Jiang, & Swallow, 2013). Thus, the "acting on"

or “responding to” the behaviorally relevant event is critically defined by what is in the instructions and task set and not by, for instance, needing it to be a motor response (Robinson, Clevenger, & Irwin, 2018). Despite the fact that target-detection and processing is more demanding that distractor-rejection (Chun & Potter, 1995; Duncan, 1980), memory for images is better for those that were previously shown concurrently with target cues, compared to scenes shown with distractor cues. This is the *attentional boost effect* (ABE): the difference in memory between target-paired images and distractor-paired images. Critically, the ABE results from the occurrence of a behaviorally relevant event, the policy in the task set on what to do when that happens, and the actual execution of that policy. It is insufficient to simply detect a target – something has to be done now that it has appeared if one is to stay on track to meet task goals (Toh & Lee, 2022). It is the confluence of all of these characteristics that produces the ABE

The ABE has been demonstrated under different task scenarios, with covert and overt responses to targets, across sensory modalities (e.g., auditory targets enhancing memory for visual information), with a variety of visual and linguistic materials, and is not the result of target rarity (e.g., Au & Cheung, 2020; Broitman & Swallow, 2020; Makovski, Swallow, & Jiang, 2012; Schonberg et al., 2014; Smith & Mulligan, 2018; Swallow & Jiang, 2012). Moreover, the boost does not appear to benefit information that did not temporally overlap with the target, even if that information appeared close in time to it (Swallow & Jiang, 2011). It also enhances perceptual processing of non-fixated parts of the visual display (Leclercq, Le Dantec, & Seitz, 2014; Mulligan, Spataro, & Picklesimer, 2014).

At first glance, the ABE seems to contradict the perspectives in classic research on attention and memory. However, that literature has traditionally concerned itself with searching for and selectively processing stimuli in certain locations in space (visuospatial attention) or the

prioritizing of one task at the expense of another (dual-task interference). The ABE should be seen as a tradeoff between attentional competition and facilitation, depending on the circumstances, over time. The ABE is a critical characteristic of temporal selection, which is the attention system selecting a moment in time, and so fundamentally different from selection based on stimulus location, features, or modality – and not merely the transient application of spatial selection (for a review, see Swallow & Jiang, 2013). Its critical function is not to resolve competition for resources between spatially distributed, concurrent information. Rather, it resolves competition for information over time, by ensuring that incoming information relevant to ongoing behavior, and its context, is preferentially processed before being overwritten by new information.

1.3.2 Neural Underpinnings of Temporal Selection

What could be the neural mechanism that manages the tradeoff between attentional competition and facilitation in a way that results in an ABE? Although seemingly at odds with research on visuospatial attention and dual-task interference, the ABE was actually predictable from the research on event cognition. As time unfolds, we segment our continuous experience into discrete units (e.g., Zacks & Swallow, 2007). As we segment, our attention and memory systems must transition from their current configuration – reflecting the state of the world up until a moment ago – into a new one. The new configuration, with accompanying updated mental models, must reflect the new state of the world and help guide us through the upcoming moments in time. For instance, as we enter a restaurant, we need to update our mental models by retrieving any information in memory that will help guide us through the upcoming experience. Thus, this process depends on the interaction between attention and memory (e.g., Chun,

Golomb, & Turk-Browne, 2011; Turk-Browne, Golomb, & Chun, 2013). Importantly, boundaries in experience enjoy an encoding advantage, in that information presented as attention and memory systems transition from one configuration to the next is subsequently better remembered (e.g., Newtson & Engquist, 1976; Swallow, Zacks, & Abrams, 2009).

Research on event cognition proposes that input into working memory is gated by a control mechanism that increases bottom-up sensory information if predictions from our mental models about the current state of the world start to fail (e.g., Kurby & Zacks, 2008; Zacks, Speer, Swallow, Braver, & Reynolds, 2007). Thus, if one is to bring themselves back into alignment with 'what one wishes to accomplish', this requires a reconfiguration of the current cognitive state based on 'what is currently happening' by transiently boosting perceptual information.

Cognitive state transitions and the 'resetting' of neural networks has implicated brainstem neuromodulatory systems as being critical in facilitating that process (e.g., Bouret & Sara, 2005). Furthermore, these systems are theorized to modulate brain-wide network dynamics to optimize processing of, learning about, and responding to stimuli that carry behavioral relevance (for a review, see Briand, Gritton, Howe, Young, & Sarter, 2007). One particular neuromodulatory system – with well-established research indicating its involvement in vigilance, surprisal, resetting of network dynamics, and alerting and orienting to salient stimuli such as targets in a detection task – is the locus coeruleus system (e.g., Aston-Jones & Cohen, 2005; Bouret & Sara, 2005). Being the primary site for synthesis of norepinephrine, the locus coeruleus regulates task engagement by modulating the signal-to-noise ratio in brain regions involved in perceptual processing (Mather, Clewett, Sakaki, & Harley, 2016; Sokolov, Nezlina, Polyanskii, & Evtikhin, 2002). Importantly, because the locus coeruleus has widespread projections throughout the brain,

it could generate the variety of effects that have been seen at the behavioral level following temporal selection (Swallow & Jiang, 2013).

1.4 Dissertation Overview

In addition to the current introductory chapter, this dissertation consists of chapters based on empirical articles and a forward-looking conclusion chapter.

Chapter 2 asks what exactly gets caught up in the ABE. Is it exclusive to the image participants are instructed to memorize or do they, incidentally, learn about features of the concurrent detection task cue, as well? If so, is that exclusive to the task-relevant feature (e.g., color of the cue, if targets are defined by color) or task-irrelevant features, too (such as shape of the cue, if targets are defined by color)? If task-irrelevant information does also get enhanced, what kinds of task-irrelevant information – shape, location, unique identity of a specific target cue? By adjusting the typical attentional boost paradigm, the chapter demonstrates the extensive impact on memory that acting on behaviorally relevant events has. In fact, all of the aforementioned kinds of task-irrelevant information get caught up in the ABE. The chapter is adapted from Turker & Swallow (2019), with some minimal revision for fluency.

Chapter 3 expands on the experiments introduced in the previous chapter by applying cognitive modeling to its findings, along with data from two new experiments (Turker & Swallow, under review). Two questions are of importance here. First, the behavioral evidence put forth in the previous chapter leaves open, to some extent, the possibility of people employing metacognitive strategies to give correct responses on the memory task simply through response bias. Second, through the two new experiments, I ask what happens if participants are instructed to memorize the images as well as the cues? Thus, does instructing them to divide attention even

further eliminate the ABE? Using diffusion decision modeling (Ratcliff, Smith, Brown, & McKoon, 2016), I show that behaviorally relevant events during encoding are subsequently characterized by higher evidence accumulation during the memory test. Importantly, response bias is shown to be a minimal factor in producing the ABE findings in Chapter 1. Furthermore, instead of reducing or eliminating the ABE, instructing participants to memorize both the images and the cues actually enhances the ABE.

Then, turning to investigating the underlying neural mechanism, Chapter 4 opens with an evaluation of the current state of human fMRI research on the locus coeruleus neuromodulatory system. For brevity and profluence, the chapter is a condensed version of Turker, Riley, Luh, Colcombe, & Swallow (2021). This chapter highlights the importance of careful methodology in imaging of the locus coeruleus and also characterizes, to some extent, which regions in the brain are functionally correlated with locus coeruleus activity. Its main goal is to demonstrate that human neuroimaging of this difficult-to-scan neuromodulatory system is possible, that its functional characterization is improved with multi-echo fMRI and neuromelanin scans, and that functionally connected brain regions are important for perception and memory.

Chapter 5 analyzes publicly available human neuroimaging data to characterize where in the brain the locus coeruleus norepinephrine system elicits its effects compared to the ventral tegmental dopamine system, another area often implicated in processing salient events such as reward encounters (Turker, Colcombe, & Swallow, under review). Indeed, the proposed theoretical functions of the locus coeruleus system are similar to those of another: the ventral tegmental dopamine system. There are proposals of dopamine-based gating of working memory, goal-maintenance, and cognitive control (Botvinick, Braver, Barch, Carter, & Cohen, 2001; Frank, Loughry, & O'Reilly, 2001; Miller & Cohen, 2001; O'Reilly, Braver, & Cohen, 1999), as

well as empirical evidence that this system also responds to various behaviorally relevant events (Briand et al., 2007). I argue that the locus coeruleus, in particular, uniquely accounts for activity in areas of the brain that are important for perceptual processing. In doing so, this particular system could be critical in boosting the encoding of perceptual information during behaviorally relevant moments in time.

Chapter 6 concludes the dissertation by reviewing its advances and contributions. Naturally, not all questions can be answered within a single dissertation. And so, the chapter outlines several further avenues of research warranted by the findings presented herein which now have a foundation to be built upon.

References

Allport, D. A. (1980). Attention and performance. *Cognitive psychology: New directions*, *1*, 12-153.

Allport, A. (1993). Attention and control: Have we been asking the wrong questions? A critical review of twenty-five years. In D. E. Meyer & S. Kornblum (Eds.), *Attention and performance 14: Synergies in experimental psychology, artificial intelligence, and cognitive neuroscience* (pp. 183–218). The MIT Press.

Aston-Jones, G., & Cohen, J. D. (2005). An integrative theory of locus coeruleus-norepinephrine function: adaptive gain and optimal performance. *Annual Review of Neuroscience*, *28*, 403-450.

Au, R. K., & Cheung, C. N. (2020). The role of attention level in the attentional boost effect. *Journal of Cognitive Psychology*, *32*(3), 255-277.

Ballard, D. H., Hayhoe, M. M., & Pelz, J. B. (1995). Memory Representations in Natural Tasks. Journal of Cognitive Neuroscience, 7(1), 66–80. https://doi.org/10.1162/jocn.1995.7.1.66

Botvinick, M. M., Braver, T. S., Barch, D. M., Carter, C. S., & Cohen, J. D. (2001). Conflict monitoring and cognitive control. *Psychological review*, *108*(3), 624.

Bouret, S., & Sara, S. J. (2005). Network reset: a simplified overarching theory of locus coeruleus noradrenaline function. *Trends in neurosciences*, *28*(11), 574-582.

Briand, L. A., Gritton, H., Howe, W. M., Young, D. A., & Sarter, M. (2007). Modulators in concert for cognition: modulator interactions in the prefrontal cortex. *Progress in neurobiology*, *83*(2), 69-91.

Broadbent, D. E. (1958). The effects of noise on behaviour. In D. E. Broadbent, *Perception and communication* (pp. 81–107). Pergamon Press.

Broadbent, D. E. (1971). *Decision and stress*. Academic Press.

Broitman, A. W., & Swallow, K. M. (2020). The effects of encoding instruction and opportunity on the recollection of behaviourally relevant events. *Quarterly Journal of Experimental Psychology*, *73*(5), 711-725.

Buschman, T. J., & Kastner, S. (2015). From behavior to neural dynamics: an integrated theory of attention. *Neuron*, *88*(1), 127-144.

Carrasco, M. (2011). Visual attention: The past 25 years. *Vision research*, *51*(13), 1484-1525.

Chun, M. M., Golomb, J. D., & Turk-Browne, N. B. (2011). A taxonomy of external and internal attention. Annual review of psychology, 62, 73-101.

Chun, M. M., & Potter, M. C. (1995). A two-stage model for multiple target detection in rapid serial visual presentation. Journal of Experimental psychology: *Human perception and performance*, *21*(1), 109.

Corbetta, M., & Shulman, G. L. (2002). Control of goal-directed and stimulus-driven attention in the brain. *Nature reviews neuroscience*, *3*(3), 201-215.

David, S. V., Hayden, B. Y., Mazer, J. A., & Gallant, J. L. (2008). Attention to stimulus features shifts spectral tuning of V4 neurons during natural vision. *Neuron*, *59*(3), 509-521.

Deutsch, J. A., & Deutsch, D. (1963). Attention: Some theoretical considerations. *Psychological review*, *70*(1), 80.

Desimone, R., & Duncan, J. (1995). Neural mechanisms of selective visual attention. *Annual review of neuroscience*, *18*(1), 193-222.

Duncan, J. (1980). The locus of interference in the perception of simultaneous stimuli. Psychological Review, 87(3), 272–300.

Eriksen, B. A., & Eriksen, C. W. (1974). Effects of noise letters upon the identification of a target letter in a nonsearch task. *Perception & psychophysics*, *16*(1), 143-149.

Eriksen, C. W., & Hoffman, J. E. (1974). Selective attention: Noise suppression or signal enhancement? *Bulletin of the Psychonomic Society*, *4*(6), 587-589.

Frank, M. J., Loughry, B., & O'Reilly, R. C. (2001). Interactions between frontal cortex and basal ganglia in working memory: a computational model. *Cognitive, Affective, & Behavioral Neuroscience*, *1*(2), 137-160.

Gazzaley, A. (2011). Influence of early attentional modulation on working memory. *Neuropsychologia*, *49*(6), 1410-1424.

Hamilton, W. (1859). Lecture XIV. Consciousness--Attention in general (H. L. Mansel & J. Veitch, Eds.). In W. Hamilton & H. L. Mansel, J. Veitch (Eds.), Lectures on metaphysics and logic, Vol. 1. Metaphysics (pp. 171–182). Gould and Lincoln.

Hazeltine, E., Poldrack, R., & Gabrieli, J. D. (2000). Neural activation during response competition. *Journal of cognitive neuroscience*, *12*(2), 118-129.

Hirst, W., & Kalmar, D. (1987). Characterizing attentional resources. *Journal of Experimental Psychology: General*, *116*(1), 68.

Hayhoe, M. (2000). Vision Using Routines: A Functional Account of Vision. Visual Cognition, 7(1–3), 43–64. https://doi.org/10.1080/135062800394676

Hogendoorn, H., Carlson, T. A., Vanrullen, R., & Verstraten, F. A. (2010). Timing divided attention. *Attention, Perception, & Psychophysics*, *72*(8), 2059-2068.

James, W. (1890). The Principles of Psychology. Dover Publications.

Janczyk, M., & Kunde, W. (2020). Dual tasking from a goal perspective. Psychological Review, 127(6), 1079.

Jolicoeur, P. (1999). Dual-task interference and visual encoding. Journal of Experimental psychology: Human perception and performance, 25(3), 596.

Kastner, S., & Ungerleider, L. G. (2000). Mechanisms of visual attention in the human cortex. *Annual Review of Neuroscience*. *23*(1), 315-341.

Kiesel, A., Steinhauser, M., Wendt, M., Falkenstein, M., Jost, K., Philipp, A. M., & Koch, I. (2010). Control and interference in task switching—A review. Psychological bulletin, 136(5), 849.

Kinchla, R. A. (1992). Attention. *Annual Review of Psychology*, *43*, 711-742.

Kurby, C. A., & Zacks, J. M. (2008). Segmentation in the perception and memory of events. *Trends in cognitive sciences*, *12*(2), 72-79.

Leclercq, V., Le Dantec, C. C., & Seitz, A. R. (2014). Encoding of episodic information through fast task-irrelevant perceptual learning. *Vision research*, *99*, 5-11.

Lin, J. Y., Pype, A. D., Murray, S. O., & Boynton, G. M. (2010). Enhanced memory for scenes presented at behaviorally relevant points in time. *PLoS biology*, *8*(3), e1000337.

Makovski, T., Jiang, Y. V., & Swallow, K. M. (2013). How do observer's responses affect visual long-term memory? *Journal of Experimental Psychology: Learning, Memory, and Cognition*, *39*(4), 1097.

Mather, M., Clewett, D., Sakaki, M., & Harley, C. W. (2016). Norepinephrine ignites local hotspots of neuronal excitation: How arousal amplifies selectivity in perception and memory. *Behavioral and Brain Sciences*, *39*.

Mesulam, M.-M. 1985 Attention, confusional states and neglect. In M.-M. Mesulam (Ed.). *Principles of behavioral neurology*, pp. 125-168. Philadelphia, PA: F. A. Davis.

Mesulam, M. M. (1998). From sensation to cognition. *Brain: a journal of neurology*, 121(6), 1013-1052.

Miller, E. K., & Cohen, J. D. (2001). An integrative theory of prefrontal cortex function. *Annual Review of Neuroscience*, *24*(1), 167-202.

Monsell, S. (2003). Task switching. Trends in cognitive sciences, 7(3), 134-140.

Mulligan, N. W., Spataro, P., & Picklesimer, M. (2014). The attentional boost effect with verbal materials. *Journal of Experimental Psychology: Learning, Memory, and Cognition*, *40*(4), 1049.

Newtson, D., & Engquist, G. (1976). The perceptual organization of ongoing behavior. *Journal of Experimental Social Psychology*, *12*(5), 436-450.

Nobre, A. C., & Van Ede, F. (2018). Anticipated moments: temporal structure in attention. *Nature Reviews Neuroscience*, *19*(1), 34-48.

Norman, D. A., & Shallice, T. (1986). Attention to action. *In Consciousness and self-regulation* (pp. 1-18). Springer, Boston, MA.

O'Reilly, R. C., Braver, T. S., & Cohen, J. D. (1999). A biologically based computational model of working memory. In Miyake, A. & Shah, P. (Eds) *Models of Working Memory: Mechanisms of Active Maintenance and Executive Control*. New York: Cambridge University Press.

Pashler, H. (1994). Dual-task interference in simple tasks: data and theory. Psychological bulletin, 116(2), 220.

Posner, M. I. (1980). Orienting of attention. *Quarterly journal of experimental psychology*, *32*(1), 3-25.

Ratcliff, R., Smith, P. L., Brown, S. D., & McKoon, G. (2016). Diffusion decision model: Current issues and history. *Trends in cognitive sciences*, *20*(4), 260-281.

Raymond, J. E., Shapiro, K. L., & Arnell, K. M. (1992). Temporary suppression of visual processing in an RSVP task: An attentional blink? Journal of Experimental Psychology: Human Perception and Performance, 18(3), 849–860.

Reynolds, J. H., Pasternak, T., & Desimone, R. (2000). Attention increases sensitivity of V4 neurons. *Neuron*, *26*(3), 703-714.

Robinson, M. M., Clevenger, J., & Irwin, D. E. (2018). The action is in the task set, not in the action. *Cognitive psychology*, *100*, 17-42.

Rubinstein, J. S., Meyer, D. E., & Evans, J. E. (2001). Executive control of cognitive processes in task switching. Journal of experimental psychology: human perception and performance, 27(4), 763.

Schonberg, T., Bakkour, A., Hover, A. M., Mumford, J. A., Nagar, L., Perez, J., & Poldrack, R. A. (2014). Changing value through cued approach: an automatic mechanism of behavior change. *Nature neuroscience*, *17*(4), 625-630.

Smith, S. A., & Mulligan, N. W. (2018). Distinctiveness and the attentional boost effect. *Journal of Experimental Psychology: Learning, Memory, and Cognition*, *44*(9), 1464.

Sokolov, E. N., Nezlina, N. I., Polyanskii, V. B., & Evtikhin, D. V. (2002). The orientating reflex: the "targeting reaction" and "searchlight of attention". *Neuroscience and Behavioral Physiology*, *32*(4), 347-362.

Swallow, K. M., & Jiang, Y. V. (2010). The attentional boost effect: Transient increases in attention to one task enhance performance in a second task. *Cognition*, *115*(1), 118-132.

Swallow, K. M., & Jiang, Y. V. (2011). The role of timing in the attentional boost effect. *Attention, Perception, & Psychophysics*, *73*(2), 389-404.

Swallow, K. M., & Jiang, Y. V. (2012). Goal-relevant events need not be rare to boost memory for concurrent images. *Attention, Perception, & Psychophysics*, *74*(1), 70-82.

Swallow, K. M., & Jiang, Y. V. (2013). Attentional load and attentional boost: A review of data and theory. *Frontiers in Psychology*, *4*, 274.

Swallow, K. M., Makovski, T., & Jiang, Y. V. (2012). Selection of events in time enhances activity throughout early visual cortex. Journal of Neurophysiology, 108(12), 3239-3252.

Swallow, K. M., Zacks, J. M., & Abrams, R. A. (2009). Event boundaries in perception affect memory encoding and updating. *Journal of Experimental Psychology: General*, *138*(2), 236.

Toh, Y. N., & Lee, V. G. (2022). Response, rather than target detection, triggers the attentional boost effect in visual search. Journal of Experimental Psychology: *Human Perception And Performance*, *48*(1), 77.

Treisman, A. M., & Gelade, G. (1980). A feature-integration theory of attention. *Cognitive psychology*, *12*(1), 97-136.

Troyer, A. K., & Craik, F. I. (2000). The effect of divided attention on memory for items and their context. *Canadian Journal of Experimental Psychology*, *54*(3), 161.

Turk-Browne, N. B., Golomb, J. D., & Chun, M. M. (2013). Complementary attentional components of successful memory encoding. *NeuroImage*, 66, 553-562.

Turker, H. B., Riley, E., Luh, W. M., Colcombe, S. J., & Swallow, K. M. (2021). Estimates of locus coeruleus function with functional magnetic resonance imaging are influenced by localization approaches and the use of multi-echo data. *Neuroimage*, *236*, 118047.

Turker, H. B., & Swallow, K. M. (2019). Attending to behaviorally relevant moments enhances incidental relational memory. *Memory & cognition*, *47*(1), 1-16.

Williford, T., & Maunsell, J. H. (2006). Effects of spatial attention on contrast response functions in macaque area V4. *Journal of neurophysiology*, *96*(1), 40-54.

Wolfe, J. M. (2015). Visual search. In J. M. Fawcett, E. F. Risko, & A. Kingstone (Eds.), *The handbook of attention* (pp. 27–56). Boston Review.

Wylie, G., & Allport, A. (2000). Task switching and the measurement of "switch costs". Psychological research, 63(3), 212-233.

Zacks, J. M., Speer, N. K., Swallow, K. M., Braver, T. S., & Reynolds, J. R. (2007). Event perception: a mind-brain perspective. *Psychological bulletin*, *133*(2), 273.

Zacks, J. M., & Swallow, K. M. (2007). Event segmentation. *Current directions in psychological science*, *16*(2), 80-84.

Zhang, S., Xu, M., Kamigaki, T., Hoang Do, J. P., Chang, W. C., Jenvay, S., ... & Dan, Y. (2014). Long-range and local circuits for top-down modulation of visual cortex processing. *Science*, *345*(6197), 660-665.

CHAPTER 2
ATTENDING TO BEHAVIORALLY RELEVANT MOMENTS ENHANCES INCIDENTAL RELATIONAL MEMORY[1]

Why do people remember some moments better than others? You might easily recall having breakfast this morning – your kitchen, the taste of your toast, the smell of your coffee – but barely remember traveling to work afterwards. Although many factors play important roles in episodic memory formation (e.g., Chun & Turk-Browne, 2007; Craik & Tulving, 1975; Kelley & Jacoby, 2000), the exact contributions of attention are still being explored.

2.1 Episodic Encoding and Memory

Episodic memories are memories for events that occurred at specific times and locations (Conway, 2009; Tulving, 1972). Memory for an event (e.g., having breakfast) is therefore more than memory for an individual item (e.g., your coffee): it involves the recollection of perceptual, conceptual, and affective details of the situation in which that item was previously encountered (Baddeley, 1982; Mandler, 1980; Eichenbaum, 2004), allowing for vivid recollection (Ranganath, Yonelinas, Cohen, Dy, Tom, & D'Esposito, 2004; Tulving, 1985; Wheeler, Stuss, & Tulving, 1997). The information defining an event may be presented in a relational memory framework, which binds together individual elements of an experience to represent the event as a whole (Eichenbaum, 2004; Rubin & Umanath, 2015). As a result, systems that support episodic memories are important for representing arbitrary combinations of items, item features, and their social, affective, task, semantic, temporal, and spatial context (Davachi, 2006; Hannula &

[1] This chapter is an abridged version of the article originally published as *Turker, H. B., & Swallow, K. M. (2019). Attending to behaviorally relevant moments enhances incidental relational memory. Memory & Cognition, 47(1), 1-16*. Thus, the chapter is not the copy of record. Please do not copy or cite this chapter without the authors' permission and refer to the authoritative document published in Memory & Cognition instead.

Ranganath, 2008; Lee, Yeung, & Barense, 2012; Polyn, Norman, & Kahana, 2009; Wang, Cohen & Voss, 2015).

The systems involved in representing events exist alongside fundamental limitations in the mind's ability to represent perceptual information as it is encountered, both over space and over time (Ballard, Hayhoe, & Pelz, 1995; Hayhoe, 2000). It is therefore important to understand the extent to which attention mediates the encoding of items, their features, and their relationships as they appear over space and time. Some aspects of an event may be represented with minimal attention. People can extract and remember some conceptual and perceptual information from scenes that are viewed for as little as 150 ms (for a review, see Oliva, 2005; Potter, Staub, & O'Connor, 2004). In addition, memory for the spatiotemporal relationships between items can sometimes be formed in the absence of attention. For example, memory for relational information in a scene is similar when people are directed to attend to it or and when they are not (Ryan, Althoff, Whitlow, & Cohen, 2000). People can implicitly learn spatial configurations of unattended items (Chun & Jiang, 1998; Jiang & Leung, 2005) and these configurations may support memory for the locations and perceptual details of items in a scene (Hollingworth, 2007; Robin, Buchsbaum, & Moscovitch, 2018). Furthermore, incidental memory for fixated items and their orientation in visual scenes may be similar to what is observed under intentional encoding instructions (Castelhano & Henderson, 2005). Such findings suggest that memory for spatial configurations and gist may not require attention or the intention to remember during encoding.

Other data demonstrate that attention influences episodic memory. Change blindness and online task performance studies (Ballard et al., 1995; Hayhoe, 2000; Levin & Saylor, 2008), suggest that memory for scenes is limited to recently attended items and rapidly degrades once

attention is removed (Brady, et al., 2013). In addition, task-relevant features of scenes are better represented in episodic memory systems than irrelevant features, particularly the hippocampus (Aly & Turk-Browne, 2016). Divided attention during encoding also impairs explicit memory (e.g., item recognition or cued recall; Mulligan, 1998), subsequent recollection, but not familiarity judgments (Baddeley, Lewis, Eldridge, & Thomson, 1984; Craik, Govoni, Naveh-Benjamin, & Anderson, 1996; Jacoby, Woloshyn, & Kelley, 1989), and source memory (Johnson, Hashtroudi, & Lindsay, 1993; Troyer, Winocur, Craik, & Moscovitch, 1999). Divided attention also affects visual long-term memory, which is impaired when participants perform simultaneous detection tasks or search for visual targets that are overlaid on the images (Cohen, Alvarez, & Nakayama, 2011; Swallow & Jiang, 2010; Wolfe, Horowitz & Michod, 2007).

2.1.1 Does Attending to Behaviorally Relevant Events Enhance Relational Memory?

Just as attention can prioritize the encoding of some objects or spatial locations, attention can vary over time to enhance memory for information presented during behaviorally relevant moments (Nobre & Van Ede, 2018). Frames and objects from a film, for example, are better remembered if they come from time periods in which an event changed than if they come from the middle of an event (Newtson & Engquist, 1976; Schwan, Garsoffky, & Hesse, 2000; Swallow, Zacks, & Abrams, 2009). Similarly, in the *attentional boost effect* (ABE), pictures that are presented during behaviorally relevant moments are better remembered than those presented at other moments, even when they are equally frequent (Swallow & Jiang, 2012; Swallow & Jiang, 2014a; Swallow & Jiang, 2014b). In these experiments participants perform a target detection task as they encode a second stream of unrelated images into memory (Lin, Pype, Murray, & Boynton, 2010; Swallow & Jiang, 2010). On a later recognition memory test,

participants can better recognize images that appeared at the same time as a target than those that appeared before or after a target (Swallow & Jiang, 2011), despite increased attentional demands of target detection (Duncan, 1980; Raymond, Shapiro, & Arnell, 1992). Attending to a briefly presented target thus appears to enhance processing of multiple sources of information presented at that time, including sensory information (Pascucci & Turatto, 2013; Seitz & Watanabe, 2009; Spataro, Mulligan, & Rossi-Arnaud, 2013; Swallow, Makovski, & Jiang, 2012). Attending to briefly-presented targets in these tasks enhances the processing of other, concurrently presented information. We refer to the process that enhances information presented at these times as temporal selection (cf. Swallow, et al., 2012; Swallow & Jiang, 2013; Jiang & Swallow, 2014).

Though attending to targets enhances the encoding of and subsequent memory for background items, its effect on memory for the spatiotemporal relationship between items and their features is unclear. Four recent studies provide conflicting data. In one study, detecting a target increased the rate at which participants reported remembering, as opposed to knowing, that a scene was recently presented (Leclercq, Le Dantec, & Seitz, 2014). In another study, participants were better able to report which pictures appeared with a target item than which pictures appeared with a distractor item during encoding (Swallow & Atir, 2018). In contrast, a recent experiment found no effect of target detection on memory for the context of concurrently presented words, such as their font, modality, or whether the words were presented during the first or second half of the encoding task (Mulligan, Smith, & Spataro, 2016). Differences in the effect of target detection on category cued recall and exemplar generation also suggest primarily item-based effects of target detection on memory (Spataro, Mulligan, Bechi Gabrielli, & Rossi-Arnaud, 2017).

The current study examined the effect of temporal selection on relational memory encoding, specifically the spatiotemporal relationships between stimuli. We adapted the ABE paradigm by testing memory for the background scene and the detection task item it appeared with during encoding. We also examined the effects of target detection on the inclusion of relevant and irrelevant item features in relational memory. Targets and distractors varied along multiple dimensions (i.e., color, shape, location, gender, and identity), that were either relevant or irrelevant for the detection task, and memory for both types of features was tested. In these experiments, we refer to memory for the background item as scene memory, memory for the detection task item (*target/distractor*) as item memory, memory for the features of that item as either relevant or irrelevant feature memory, and memory for the association between a scene and the features of the detection task item as relational memory. If target detection enhances incidental relational memory, then participants should be able to report both relevant and irrelevant features of target items better than those of distractor items. To preview the results, target detection enhanced memory for all three types of information, indicating that it facilitated relational memory.

2.2 Experiment 1

Experiment 1 examined the effect of target detection on memory for the relationship between scenes and the features of the detection task items they appeared with during encoding. Participants memorized visual scenes while they monitored an unrelated stream of items which varied in color and shape. They pressed the spacebar each time the item was in the predefined target color (*task-relevant feature*). The other feature, shape, was not important for the encoding or detection task (*task-irrelevant feature*). Participants were told they only needed to remember

the scenes, but were tested on their memory for the scenes as well as the relevant and irrelevant features of the detection task item it appeared with.

In addition to replicating the ABE (*scene memory*), this experiment addressed two questions. Does detecting a target also facilitate memory for which item a scene appeared with (*relational memory*)? And, if it does, do these benefits extend to irrelevant features of that item (*irrelevant feature memory*)? The answers to these questions are important for two reasons.

First, explicit memory for the relevant and irrelevant features of attended items is sometimes used as a measure of context memory (e.g. Troyer & Craik, 2000). However, previous findings demonstrating relational memory advantage for items presented on target trials (Swallow & Atir, 2018) could reflect memory for the motor response, the status of the square as a target or distractor, or memory for the color of the square itself. In addition, because participants show no memory advantage for the features of words that appeared with targets rather than distractors (Mulligan, et al., 2016), the degree to which earlier findings reflect an effect of target detection on relational memory remains uncertain.

Second, the effect of attention on encoding an item's irrelevant features is unclear. There is some evidence that irrelevant features are encoded when an item is attended (Gajewski & Brockmole, 2006; Marshall & Bays, 2013; O'Craven, Downing, & Kanwisher, 1999; Schoenfeld, Hopf, Merkel, Heinze, & Hillyard, 2014) and the ability to remember the conjunctions of multiple object features may mediate episodic memory (Erez, Cusack, Kendall, & Barense, 2016). However, feature dimensions of the same item may be encoded and stored independently in memory (Brady, Konkle, Alvarez, & Oliva, 2013; Fougnie & Alvarez, 2011). In addition, a growing literature suggests that irrelevant features are not always maintained in

memory (Chen, Swan, & Wyble, 2016; Marshall & Bays, 2013; Serences, Ester, Vogel, & Awh, 2009; Woodman & Vogel, 2008), particularly when perceptual load is high (Xu, 2010).

We expected memory to be better for scenes that appeared with a target during encoding. If target detection facilitates relational memory, then participants also should more accurately report that target-paired scenes appeared with the relevant feature. In addition, if the effects of target detection on relational memory are limited to relevant features then memory for irrelevant features of target and distractor items should be similar. Alternatively, target detection may enhance processing more globally, boosting relational memory for a scene and the concurrent item's relevant and irrelevant features. Finally, irrelevant features may be encoded whenever relevant features are attended. If so, irrelevant features should be remembered well whenever relevant features are accurately reported, regardless of whether they were part of a target.

2.2.1 Methods

2.2.1.1 Participants

Participants for all experiments were recruited from the Cornell University community and received $10 or course credit. They had normal or corrected-to-normal vision. Normal color vision was verified with the Hardy Rand & Ritler pseudoisochromatic color blindness test (Richmond Products, Albuquerque, NM, USA). Experimental procedures were approved by Cornell's Institutional Review Board. All participants provided informed consent and were debriefed about the nature of the study afterwards.

For all experiments, sample sizes were determined a priori with G*Power 3.1 (Faul, Erdfelder, Lang, & Buchner, 2007). For Experiments 1 and 3 (which were conducted first), a target sample size of 32 was selected to provide a power (1-β) of .8 to detect an effect of $f =$

0.256 (equivalent to η_p^2 = .062). A conservative estimate of the size of the standard ABE was used to ensure adequate power to detect potentially smaller effects on relevant and irrelevant feature memory (Button et al., 2013). Because performance was near chance in some conditions in Experiment 1, and Experiment 2 included a test with four options, a larger target sample size of 48 was used for Experiment 2. This resulted in a power (1-β) of .8 to detect an effect of size f = 0.207 (equivalent to η_p^2 = .041), with α = 0.05 in a repeated-measures ANOVA. Participants were excluded from the analyses if they responded to fewer than 80% of the target items (hits) or responded to more than 10% of distractor items (false alarms) during the encoding task. Participants were recruited until data from enough participants who met these criteria were acquired. Because multiple participants were recruited at once, sample sizes were sometimes larger than the a priori target.

For Experiment 1, a total of 36 participants (29 female; 18-22 years old; age M = 19.89, SD = 1.17) were recruited. All met the performance criteria.

2.2.1.2 Materials and Equipment

Participants sat unconstrained in a normally lit room, approximately 50 cm away from a ViewSonic E70fB 17" CRT monitor (1024×768 pixels, 75 Hz refresh rate) and responded on a keyboard. All experiments were programmed using Psychtoolbox 3 (Brainard, 1997; Pelli, 1997) for MATLAB 2015a.

We acquired 650 color images of indoor and outdoor scenes (e.g., beaches, forests, mountains, cities, etc.) from personal collections and online databases, all used in previous studies (Swallow & Jiang, 2010). To strengthen generalizability, 200 scenes were randomly selected for each participant. A separate set of 22 scenes was used for the practice session (20

trials) and during instructions (2 examples). Items for the detection task (colored circles and stars) were generated in Psychtoolbox 3. For each participant, two colors were selected (counterbalanced) from a set of four (red: [255 0 0], green: [0 255 0], lilac: [255 0 255], yellow: [255 255 0]) to increase generalizability.

2.2.1.3 Procedure and Task Design

2.2.1.3.1 Encoding and Detection Task

For each participant 100 scenes were randomly selected for use in the encoding and detection task (*old scenes*). Old scenes were assigned to appear with one, and only one, of four items defined by the two shapes and two colors (e.g., red circle, red star, yellow circle, yellow star). Each of the four items was assigned to 25 old scenes. Half of the scenes were paired with an item in the target color and half were paired with an item in the distractor color. Pairings were maintained throughout the encoding and detection task. A second set of 100 scenes acted as *foil scenes* in the recognition phase.

Figure 2.1a provides an example of trials in the encoding and detection task in Experiment 1. On each trial, a scene (10.3°×10.3° visual angle) appeared for 1000 ms in the center of the screen. The item (circle, 1.15°×1.15°; star, 2.9°×2.9°) paired with that scene was initially overlaid on the scene, but disappeared after 200 ms (0 ms stimulus onset asynchrony). Trials were presented continuously, with no inter-trial interval. All 100 scene-item pairs were presented 10 times, for a total of 1000 trials. Trial order was pseudo-random: the full set of scene-item pairs was presented for each repetition and there were no more than four consecutive targets or distractors. The task paused every 200 trials for feedback and a self-paced break.

Participants were instructed to remember all the scenes for a subsequent memory task. They were told that an item would be superimposed in the center of each scene and to press the spacebar when the item was the predefined target color (e.g., yellow) but not the distractor color (e.g., red). Target color was counterbalanced across participants. Participants were told the item's shape was irrelevant and no mention of the association between scenes and items was made. Prior to beginning the main task, participants completed sets of 20 practice trials until performance requirements were met (≥80% hits, ≤10% false alarms).

2.2.1.3.2 Recognition Memory Task

The recognition memory task is illustrated in Figure 2.1b. On every trial, three two-alternative forced-choice questions tested participants' memory for the scene and the paired item. First, one old scene and one foil scene were presented on either side of the screen. Participants selected the scene they believed was old. Second, the old scene was displayed in the center of the screen and the two colors (relevant feature) were presented in a neutral shape (square) on either side. Participants selected the color of the item paired with the scene during encoding. Third, the correct old scene and the correct color (in the neutral shape) were displayed in the center of the screen. The circle and star (irrelevant feature) were presented in the correct color on either side. Participants selected the shape of the item paired with the scene during encoding. The second and third questions were included regardless of the accuracy of prior answers. Participants were informed they were viewing the actual old scene or old scene and color pair during those questions. For all questions, the side of the correct choice was counterbalanced and participants responded by pressing a key corresponding to the left or right option. Each question remained on screen for 10 seconds or until a response was given.

Feedback was provided by displaying the scene and the item at the end of each trial, as they appeared during the encoding task.

Prior to the recognition task participants were informed, for the first time, they would also be answering questions about relevant and irrelevant features of the paired item. They then practiced the 2AFC for the first question with two otherwise unused scenes to learn the response keys.

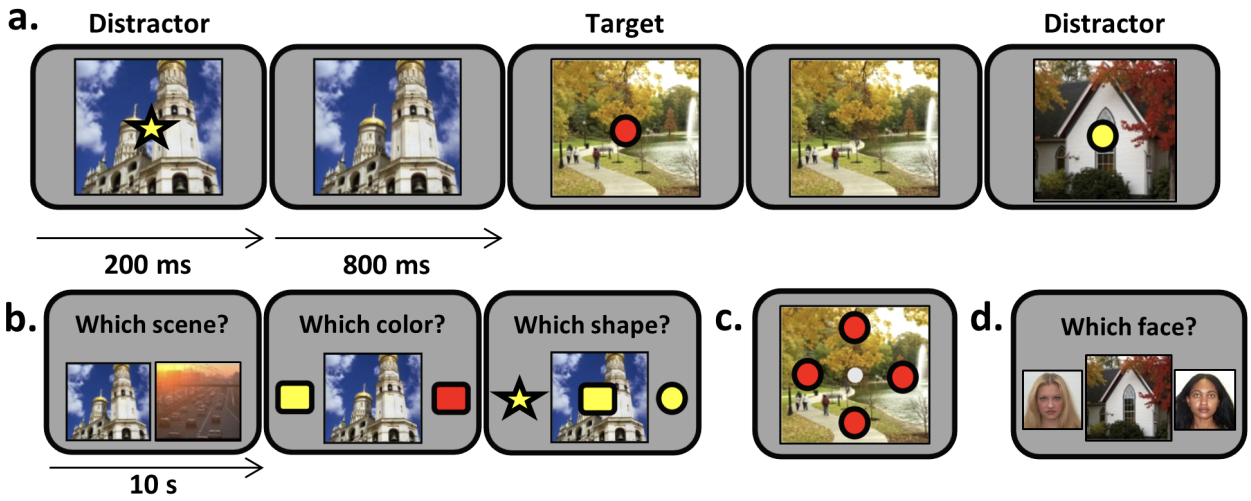

Figure 2.1 Task design experiments 1-3. *(a) Each trial of the encoding and detection task of Exp. 1 consisted of a scene and a superimposed item. Participants pressed the button when the item was a target (defined by color in Exp. 1 and 2 and by gender in Exp. 3). (b) During the recognition test of Exp. 1, participants were first tested on memory for the scene, then memory for the task-relevant color of the item it appeared with, and finally memory for the task-irrelevant shape. (c) In Exp. 2, the relevant feature was the color, but the item could appear in one of the four displayed locations around the central fixation point. The test of irrelevant location memory displayed the item in all four locations in the correct color with the central fixation dot. (d) In Exp. 3, after being asked about the background scene, participants chose which of two faces of the same gender (two targets or two distractors) from the encoding task had been paired with the scene. The on screen instructions have been simplified for this figure.*

2.2.2 Results

2.2.2.1 Encoding and Detection Task

Participants correctly responded to most of the target colors and to few of the distractor colors (Table 2.1).

Table 2.1
Encoding and detecting dual-task performance in Experiments 1-3

	Target		Distractor	
Experiment	**Hits (%)**	**RT (ms)**	**False Alarms (%)**	**RT (ms)**
Exp. 1	98.9 (1.1)	352.6 (81.6)	3.5 (2.0)	321.8 (160.6)
Exp. 2	98.83 (1.59)	355.1 (76.2)	3.95 (2.49)	332.6 (139.5)
Exp. 3	97.2 (2.72)	533.9 (95.0)	6.49 (2.18)	442.1 (176.3)

Note: Means and standard deviations (in parentheses) of response percentages and reaction times in milliseconds, on the encoding and detecting dual-tasks for each experiment.

2.2.2.2 Scene Recognition and Relational Memory

Recognition analyses were performed on sensitivity (Macmillan & Creelman, 2005) obtained with the psyphy package in R (Knoblauch, 2014). Accuracy is reported in Table 2.2. Planned analyses contrasted memory for scenes paired with a target or with a distractor during encoding in a paired t-test. Replicating the ABE (Figure 2.2a), participants better recognized target-paired scenes than distractor-paired scenes, $t(35) = 4.226$, $p < .001$, $d = 0.736$. Response time (RT) was shorter for tests of information encountered on target trials rather than distractor trials, providing no evidence of a speed accuracy trade-off in recognition memory.

Table 2.2
Recognition test performance in Experiments 1-3

Experiment	Scene	Relevant Feature	Irrelevant Feature	Irrelevant | Relevant & Scene
Exp. 1				
Target	86.22 (11.25)	67.57 (12.12)	54.85 (11.85)	58.03 (15.58)
Distractor	79.33 (9.93)	61.33 (12.87)	48.55 (12.81)	45.83 (15.72)
Exp. 2				
Target	87.54 (10.12)	68.30 (12.85)	37.78 (8.56)	41.81 (10.83)
Distractor	78.69 (12.20)	59.87 (16.87)	27.65 (7.20)	27.93 (10.08)
Exp. 3				
Target	83.06 (11.25)	N/A	70.99 (13.63)	N/A
Distractor	77.47 (10.21)	N/A	61.42 (10.99)	N/A

Note: Means and standard deviations (in parentheses) of the percentage of correct responses during the recognition test of Experiments 1-3.

Table 2.3
Recognition response times for accurate responses in Experiments 1-3

Experiment	Scene	Relevant Feature	Irrelevant Feature	Irrelevant | Relevant & Scene
Exp. 1				
Target	1.94 (1.02)	1.16 (0.97)	1.12 (0.95)	1.07 (0.84)
Distractor	2.17 (1.15)	1.40 (1.14)	1.15 (1.00)	1.18 (1.04)
Exp. 2				
Target	1.60 (0.95)	1.11 (1.05)	1.07 (1.02)	1.04 (1.04)
Distractor	1.80 (1.05)	1.31 (1.11)	1.15 (0.99)	1.19 (1.01)
Exp. 3				
Target	1.79 (0.97)	N/A	1.74 (1.10)	N/A
Distractor	1.92 (0.98)	N/A	1.77 (1.12)	N/A

Note: Means and standard deviations (in parentheses) of response times in seconds during the recognition test of Experiments 1-3 for accurate responses.

Because relational memory is demonstrated only when the scene is accurately remembered and paired with the item it was encoded with, relational memory analyses were restricted to trials on which the scene was correctly recognized. Sensitivity for the item features on these trials was entered into a 2x2 (encoding condition x relevance) repeated-measures ANOVA (Figure 2.2b). If target detection improves relational memory as well as scene memory, participants should better identify the item that a scene appeared with, if that item was previously a target rather than a distractor. Consistent with this possibility, participants more accurately identified the features of an item that appeared with a scene, when the item was a target rather than a distractor, main effect of encoding condition, $F(1,35) = 9.691$, $p = .004$, $\eta_p^2 = .217$. Encoding condition had a similar effect on relevant and irrelevant features, resulting in a nonsignificant interaction between these factors, $F(1,35) = 0.017$, $p = 0.898$. Overall, relevant features were more accurately recognized than irrelevant features, main effect of relevance, $F(1,35) = 24.22$, $p < .001$, $\eta_p^2 = 0.409$. Post hoc analyses indicated that sensitivity was greater than 0 for the irrelevant feature of target items, $t(35) = 2.446$, $p = .020$, $d = 0.408$, but not distractor items, $t(35) = -0.604$, $p = .55$.

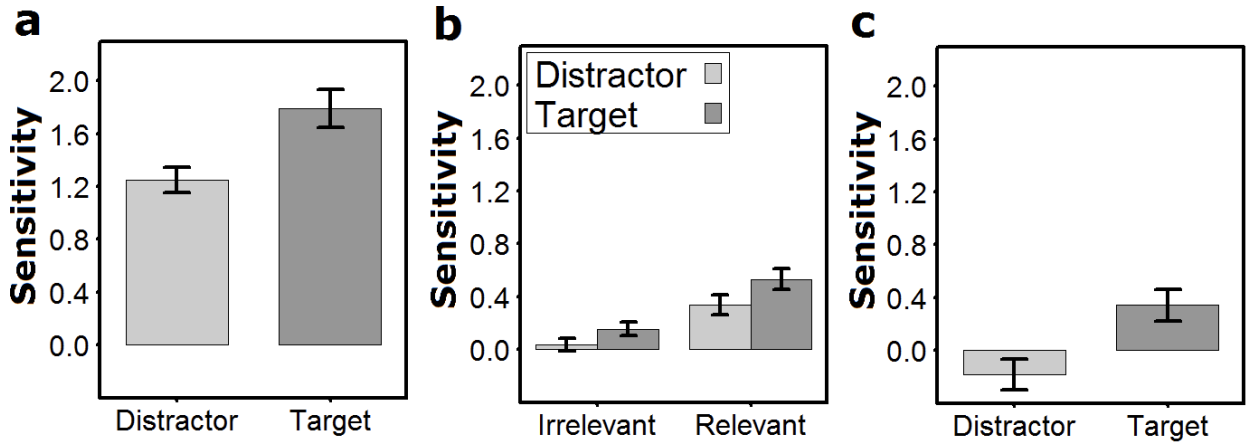

Figure 2.2 Sensitivity scores in Experiment 1. *(a) Scene memory, (b) relational memory of item features questions across conditions (given scene recognition), and (c) for task-irrelevant shape (given accurate recognition of scene and task-relevant color). Error bars represent +/- 1 standard error of the mean.*

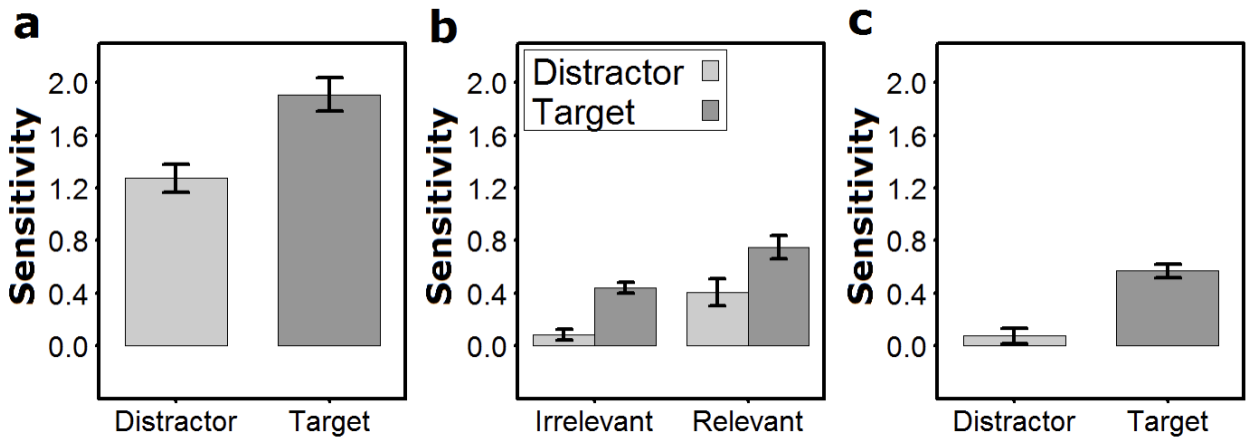

Figure 2.3 Sensitivity scores in Experiment 2. *(a) Scene memory, (b) relational memory of the paired features (given scene recognition), and (c) for the task-irrelevant location (given accurate recognition of scene and task-relevant color). Error bars represent +/- 1 standard error of the mean. Chance-level performance for scene memory was 50% (2AFC) for relevant features (panels a, b) and 25% (4AFC) for the irrelevant location (panels b, c).*

Target detection may have its strongest effects on irrelevant feature encoding if the scene and its paired relevant feature were also successfully encoded. Alternatively, all features of an attended item could be encoded into memory, whether they are relevant or not (e.g., O'Craven, et al., 1999; Schoenfeld, et al., 2014). If so, irrelevant features may be remembered equally well for

target and distractor items when the relevant item feature is correctly paired with the scene. Planned analyses examined memory for irrelevant features when both scene and the relevant feature were correctly recognized. Results indicated that memory for irrelevant features was still influenced by target detection: irrelevant features were more accurately reported for target items than for distractor items (Figure 2.2c), $t(35) = 2.569$, $p = .015$, $d = 0.752$. Follow-up analyses indicated that memory for the irrelevant feature was better than chance for target items, $t(35) = 2.902$, $p = .006$, $d = 0.484$, but not distractor items, $t(35) = -1.601$, $p = .118$.

2.2.3 Experiment 1: Discussion

Experiment 1 examined whether target detection facilitates relational memory for a scene and a concurrently presented item. Results replicated the ABE for scene memory. In a novel finding, participants were better able to match the irrelevant feature (shape) of an item, as well as the relevant feature (color) to correctly recognized target-paired scenes. Relational memory between a scene and both the relevant and irrelevant features of an item it was encoded with was therefore boosted when that item was a target. The memory advantage for the irrelevant features of items paired with scenes cannot be attributed to learning the association between either a scene and the motor response or between the scene and the presence of a target. It also cannot be easily attributed to a response bias. Because both irrelevant feature values were equally likely to occur with target or distractor items, any bias in selecting a particular irrelevant feature would apply to target and distractor conditions. The data suggest that temporal selection modulates relational memory encoding as well as memory for the irrelevant features of items. However, chance recognition of irrelevant features of distractor items precludes conclusions about whether the magnitude of this advantage depends on the relevance of the feature.

A key characteristic of relational memory is that it often includes information about spatial relationships between items. Because the target and distractor items always appeared at the same location – centered on the scene – the data from Experiment 1 do not address this critical component of relational memory.

2.3 Experiment 2

Experiment 2 examined whether memory for an item's location is enhanced on target trials. Items were assigned to target or distractor conditions based on their color (relevant feature) and could appear in any of four locations (irrelevant feature; Figure 2.1c). There were several reasons for examining the effect of target detection on memory for spatial location. First, the spatial configuration of items appears to be preferentially encoded by episodic memory systems (Burgess, Maguire, & O'Keefe, 2002; Chen & Wyble, 2015; Epstein, 2008; Hannula & Ranganath, 2008; Jiang, Olsen, & Chun, 2000). In addition, though there is abundant evidence that the ABE includes item information, relatively little is known about its effect on memory for spatial locations and configurations. Two previous experiments suggest that target detection may allow participants to better distinguish original from mirror reversed images (Swallow & Jiang, 2010) or to indicate whether an image appeared on the left or right side of a screen (Leclercq, Le Dantec, & Seitz, 2014). However, the effects were weak or only present in a small subset of the data. In Experiment 2, we also increased the number of response options to bring chance performance to 25%. By varying the spatial location of the target and distractor items, Experiment 2 offered an opportunity to replicate the relational memory effects observed in Experiment 1, while testing whether they extend to a critical feature of event memory.

2.3.1 Methods

2.3.1.1 Participants

Of the 52 participants recruited, 50 met performance criteria (32 female; 18-22 years old; age M = 19.5, SD = 1.18). Two participants were excluded for high false alarm rates.

2.3.1.2 Procedure and Task Design

2.3.1.2.1 Encoding and Detection Task

The task was identical to Experiment 1, with a few exceptions. As in Experiment 1, items varied in color (relevant feature). However, rather than varying in shape, the location of the items changed from trial to trial (irrelevant feature). Items could appear 3.04° above, below, left, or right of the center of the scene for the first 200 ms of scene presentation. Participants were instructed to maintain fixation on a white fixation dot (0.15°) that was continuously presented at the center of the scene. A total of 104 scenes were presented 10 times for 1040 trials. Scenes were assigned to always appear with the same type of item (target/distractor) in the same location. Participants were instructed to memorize the background scenes, respond to items of the predefined target color, and told that the item's location on the screen was irrelevant to their task.

2.3.1.2.2 Recognition Memory Task

As in Experiment 1, participants' memory for the scene and the relevant and irrelevant features of the target and distractor items was tested, and feedback was provided. Following the test of scene memory and the color of the item that it appeared with (2AFC; like Experiment 1, except the items appeared in the correct shape), participants reported where the item was located

in a four alternative forced choice (4AFC). For this question, the item appeared in the correct color in all four possible locations, with the fixation dot in the center. Participants selected a location with the arrow keys. The correct configuration of the scene, item color, and item location were displayed at the end of each trial as feedback.

2.3.2 Results

2.3.2.1 Encoding and Detection Task

Participants accurately discriminated between the targets and distractors with similar response times as in Experiment 1 (Table 2.2).

2.3.2.2 Scene Recognition and Relational Memory

As expected, participants better recognized target-paired scenes than distractor-paired scenes (Figure 2.3a), $t(49) = 6.634$, $p < .001$, $d = 0.779$. There was no evidence of a speed-accuracy trade-off (Table 2.1).

As in Experiment 1, planned analyses of memory for item features were limited to trials on which the scene was accurately recognized. Although chance level performance differed for relevant and irrelevant features, sensitivity could be directly compared in a 2x2 repeated-measures ANOVA with encoding condition and feature relevance as factors (MacMillan & Creelman, 2005). As expected, participants more accurately reported the relevant color of the item that appeared with a scene than its irrelevant location (Figure 3b), main effect of relevance, $F(1,49) = 22.368$, $p < .001$, $\eta_p^2 = 0.313$. Importantly, participants also more accurately reported the item's features if it was a target rather than a distractor, main effect of encoding condition, $F(1,49) = 25.37$, $p < .001$, $\eta_p^2 = 0.341$. The interaction was not significant,

$F(1,49) = 0.019$, $p = 0.891$. Unlike Experiment 1, sensitivity in memory for the irrelevant location of both targets and distractors was better than chance, $t(49) = 10.924$, $p < .001$, $d = 1.545$, for targets and $t(49) = 2.126$, $p = .039$, $d = 0.301$, for distractors.

When both the scene and its associated item color were accurately reported, participants also better reported the location of a target than the location of a distractor (Figure 2.1c), $t(49) = 6.596$, $p < .001$, $d = 1.294$. Sensitivity for the irrelevant locations of the items on these trials was better than chance for targets, $t(49) = 11.141$, $p < .001$, $d = 1.576$, but not distractors, $t(49) = 1.307$, $p = .197$.

2.3.3 Experiment 2: Discussion

Experiment 2 demonstrated that the ABE pattern is present in tests of the spatial relationship between an item and the background scene and when the location of the target or distractor varies across trials. This finding further supports the claim that a temporal selection mechanism, underlying the ABE, facilitates memory for the spatiotemporal relationship between items, as well as memory for the items themselves.

Prior data suggest that the spatial locations of items may be incidentally and rapidly encoded (Golomb, Kupitz, & Thiemann, 2014; Huang, 2010), scaffolding events in episodic memory (Robin, et al., 2018). In fact, the spatial location of an item can be accurately reported under conditions that lead to rapid forgetting of the irrelevant features of an item, such as its color or identity (Chen & Wyble, 2015). However, Experiment 2 demonstrates that temporal selection enhances memory for the location of an item as well as its color, even when it is task-irrelevant.

In Experiments 1 and 2 the irrelevant features of the items were predictable and varied little from item to item (having two or four potential values). As a result, they did not address the detail with which the irrelevant features are encoded and later recognized. Experiment 3 begins to address this issue by testing whether the ABE extends to the relationship between scenes and specific faces.

2.4 Experiment 3

Experiment 3 investigated the effect of target detection on relational memory for the identity of an item that was paired with a scene during the encoding task. The task was identical to Experiment 1 except the items were replaced with male and female faces. Participants pressed the space bar whenever the face was a pre-specified gender, making gender relevant and face identity irrelevant to the detection task. For the relational memory test, participants were presented with two faces of the same gender that were both used in the detection task. Thus, to demonstrate relational memory, participants had to remember which of two equally familiar faces from the same gender had been paired with the scene. This experiment only tested memory for the irrelevant item feature for two reasons. First, the ABE for relevant item features has been repeatedly demonstrated (present chapter; 3 experiments in Swallow & Atir, 2018), making a strong test of relational memory for irrelevant features most important. Second, testing gender requires some form of recoding (e.g., into verbal descriptors), which can influence visual recognition (Nakabayashi, Burton, Brandimonte, & Lloyd-Jones, 2012). As with the first two experiments, participants were not informed ahead of time that they needed to remember anything other than the scene. If target detection boosts relational memory for scenes and paired

faces, participants should more accurately report which face appeared with a scene when choosing between faces of the target gender than faces of the distractor gender.

2.4.1 Methods

2.4.1.1 Participants

Thirty-four participants (23 female; 18-26 years old; age M = 20.44, SD = 2.0) met all performance criteria, out of 43 recruited. Nine participants were excluded due to high false alarm rates (false alarm rate M = 14.71%, SD = 3.84%). All analyses were repeated with the full sample but this did not substantively change the results.

2.4.1.2 Materials

A total of 113 faces were acquired from an online database (Minear & Park, 2004). They were emotionally neutral, color portraits with a white background (100 x 100 pixels). Of the 113 faces, 12 faces were used exclusively in the practice session and 1 face exclusively for instruction. The remaining 100 faces consisted of five individual faces in each of 20 categories defined by crossing gender (male/female), age (young adult/old adult), and ethnicity (East Asian/South Asian/Black/Hispanic/White).

2.4.1.3 Procedure and Task Design

The procedure was identical to Experiment 1 except that the superimposed items were male and female faces (2.9°×2.9°). Whenever the face was of the target gender (e.g., male) but not the other (e.g., female), participants pressed the spacebar as quickly as they could. The gender assigned to the target condition was counterbalanced across participants.

For the recognition test participants were first asked to indicate which of two scenes was presented during the encoding and detection task. Next, the correct scene was presented in the center of the screen and two faces, one that had appeared with that scene (*matched face*) and one that had appeared with another scene (*foil face*), were presented on the left and right (Figure 2.1d). The faces were of the same gender and were both presented 10 times during the encoding and detection task. Participants identified the matched face that went with that scene. Each face was presented once as the matched face and once as a foil. Results did not change when the data were limited to the first presentation of each face (first half of the memory task). There was no feedback.

2.4.2 Results

2.4.2.1 Encoding and Detection Task

For the 34 participants who met the performance criteria, hit rates were similar to those observed in the previous experiments. However, Welch's two-sample t-tests indicated that false alarm rates were slightly higher (Table 2.1) in Experiment 3 than in Experiment 1, $t(66.644) = 5.972$, $p = < .001$, $d = 1.430$, and Experiment 2, $t(76.929) = 4.951$, $p < .001$, $d = 1.086$. Target RT (Table 2.1) was longer than in Experiment 1, $t(63.43) = 19.273$, $p < .001$, $d = 2.047$, and Experiment 2, $t(59.909) = 20.204$, $p < .001$, $d = 2.084$. These data, combined with the greater number of participants that did not meet the performance criteria, suggest that the detection task was more difficult when it was based on the gender of a face than on color.

2.4.2.2 Scene Recognition and Relational Memory

Though the target detection task was more difficult, participants better recognized target-paired scenes than distractor-paired scenes (Figure 2.4a), $t(33) = 3.584$, $p = .001$, $d = 0.606$.

Analysis of relational memory for the faces was again restricted to those trials on which the scene had been correctly recognized. If target detection facilitates relational memory for stimuli that differ along multiple dimensions, participants should more accurately pair a face to a scene when the face was of the target gender. Consistent with this prediction, participants more frequently selected the matched face than the foil face, if they were targets rather than distractors (Figure 2.4b), $t(33) = 4.653$, $p < .001$, $d = 0.806$.

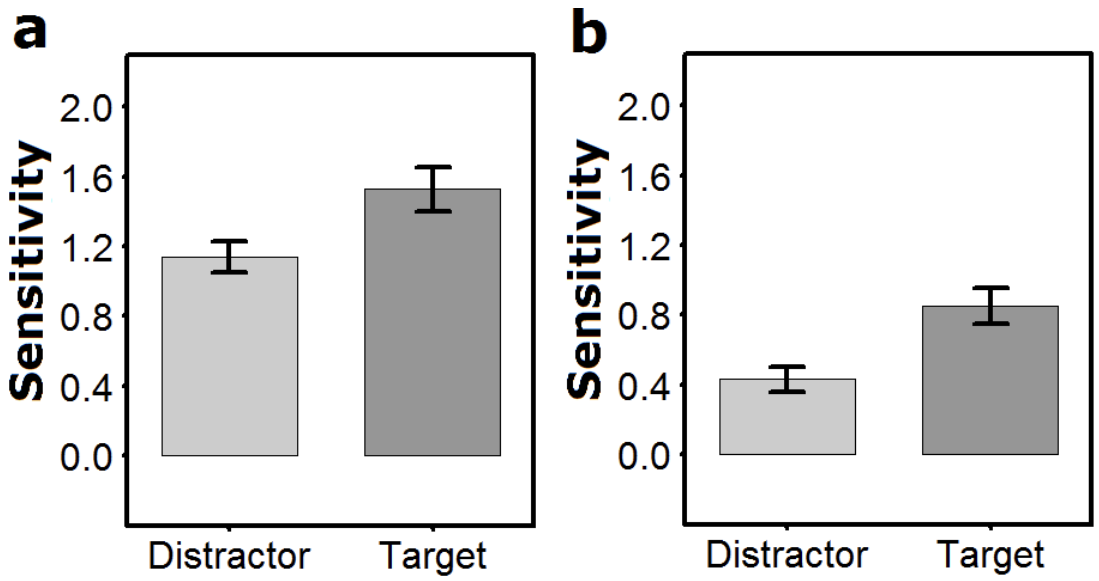

Figure 2.4 Sensitivity scores in Experiment 3. *(a) Scene memory and (b) relational memory of face identities given correct scene recognition. Error bars represent +/- 1 standard error of the mean.*

2.4.3 Experiment 3: Discussion

As in previous experiments, participants in Experiment 3 incidentally encoded the association between background scenes and otherwise unrelated stimuli – this time faces – presented for a detection task. Relational memory was affected by the status of the face as a target or distractor: Participants more accurately paired the specific face that appeared with a scene when it was the target gender rather than the distractor gender.

This relational memory advantage demonstrates two critical points. First, although dividing attention negatively affects relational memory (e.g., Kim & Giovanello, 2011), relational encoding is enhanced by attention to behaviorally relevant moments. This advantage extended to irrelevant information that, in this case, distinguished one face from other faces of the same gender. Second, target detection resulted in representations sufficiently detailed to support individual differentiation within gender. Unlike the first two experiments in which the items differed from each other along only two dimensions (color and shape or color and location), the faces in Experiment 3 differed in their identity, including gender, age, ethnicity, and the facial features that distinguish one face from another, such as second order configural information and texture (Burton, Schweinberger, Jenkins, & Kaufmann, 2015; Taubert, Apthorp, Aagten-Murphy, & Alais, 2011). They were therefore more perceptually rich and complex than the shapes used in Experiments 1 and 2. Importantly, the effect was incidental. Participants were never informed they would be asked about the faces. Experiment 3 extends the findings of the first two experiments to complex items differing along multiple visual dimensions and uniquely associated with a single scene. An outstanding question, however, is which facial features contributed to relational memory in this task. Because the faces differed in age and ethnicity, participants could have relied on this information to pair the matched face with the scene. Future

research should examine specific facial features such as second-order configurations and textures (Burton, et al., 2015; Taubert, et al., 2011).

These findings further demonstrate that the relational memory advantage for targets over distractors is not due to response bias (see also Swallow & Atir, 2018). Memory for encoding condition (target/distractor), association between scene and a motor response, gender (male/female) of the face, or familiarity with the face that was presented with a scene was not sufficient to accurately perform the recognition task. Therefore, these data provide the strongest evidence yet that target detection facilitates relational memory formation.

2.5 General Discussion

If attending to behaviorally relevant moments influences the encoding of an event, it must do so via its constituent items, their features, and their relationship to one another. Multiple studies have already demonstrated that such temporal selection enhances memory for items (e.g., Lin, et al., 2010; Makovski, Jiang & Swallow, 2013; Mulligan et al., 2016; Swallow & Jiang, 2010). The current study supports this conclusion. Across all experiments, attending to targets facilitated scene memory. More importantly, it also enhanced memory for the relationship between those scenes and detection task items, their features, and their locations.

Several key findings suggest that temporal selection facilitates memory for the perceptual and spatial details of an event. First, target detection enhanced relational memory for the visual scene and the relevant feature of a consistently paired and concurrently presented item. Second, target detection facilitated memory for features of the paired item that were not explicitly required for task performance. Because this advantage was also present on those trials in which the relevant feature was accurately reported, it could not be due to the automatic encoding of

irrelevant features of attended items (cf. Marshall & Bays, 2013; Wheeler & Treisman, 2002; Xu, 2010). Instead, the effects of target detection on encoding extended beyond the information explicitly needed for task performance. Third, target detection boosted memory for the spatial relationship between items and the scene on which they appeared, permitting participants to more accurately report the location of a target than the location of a distractor. Finally, target detection facilitated relational memory for the perceptual features of items with enough detail to distinguish between individuals that vary along multiple dimensions. Therefore, target detection enhances memory for the features of items that appear with a scene even when they are not explicitly relevant.

These findings cannot be explained by better memory for the individual items in isolation. For example, in Experiment 3, better memory for items would help participants recognize old faces as well as old scenes, and both of these should be enhanced by target detection (Makovski et al., 2013; Swallow & Jiang, 2010). However, for the relational memory test, participants had to determine which of two old faces had been presented with a particular old scene. Better memory for the individual items – the scene, the old face that was paired with it, or the old face that was not paired with it – would not be sufficient to perform well on this task. Participants must be able to accurately pair the correct old face with that particular scene. The beneficial effects of target detection on encoding therefore include relational memory.

Current views of relational memory suggest that any effects of attention reflect the shaping of input into the hippocampus by goal-based or salience based orienting mechanisms, likely subserved by prefrontal cortex (Rubin, et al., 2017; Wang, et al., 2015). However, it is unclear whether similar mechanisms explain the effects of temporal selection on relational memory. An important feature of the tasks used to examine the ABE is that the background

scenes (or words) are all intentionally encoded (or intentionally ignored, as in Swallow & Jiang, 2014a). Goal-based orienting mechanisms should prioritize all images during encoding, while also maintaining and implementing procedures for responding to targets. Because responding to targets demands attention (Duncan, 1980; Raymond, et al., 1992) the finding that divided attention impairs relational memory implies that it should be worse for target-paired scenes (e.g., Troyer & Craik, 2000). Yet, the opposite effect was observed in Experiments 1-3. The relational memory advantage for items presented on target trials represents a qualitatively different effect of attention on relational memory. Rather than the redistribution of limited processing resources, the data point to a mechanism that boosts the encoding of relational information encountered at behaviorally relevant moments.

The findings are consistent with prior studies that examined the effects of target detection on subjective judgments of remembering a scene (Leclerq et al., 2014) and on the ability to remember whether a scene was presented with a target or distractor (Swallow & Atir, 2018). Experiments 1-3 additionally establish a reliable effect of target detection on relational memory that extends to relevant and irrelevant features of detection task items. However, these data differ from two other studies that examined whether the ABE facilitates memory for the semantic or perceptual context in which words were encoded (Mulligan et al., 2016; Spataro et al., 2017). Though there are many ways in which these experiments differed from the ones presented here, we will focus on several factors that might explain differences in the results and warrant further investigation.

The first critical difference is the nature of the encoded item: words versus images. Whereas words were memorized in the experiments reported by Mulligan and colleagues (2016), pictures were encoded in Experiments 1-3 (and in Swallow & Atir, 2018). Source memory for

words may be poorer than it is for scenes, even with the same participants, encoding conditions, and test conditions (e.g., Onyper, Zhang, & Howard, 2010). Differences in memory for words and pictures could arise as a consequence of how participants approach the encoding task (cf., Intraub & Nicklos, 1985; Paivio & Csapo, 1973; Weldon, Roediger, Beitel, & Johnston, 1995). For example, when visual features are seemingly irrelevant, participants may focus on the abstract, semantic content of words, improving later recall and recognition of the words but not explicit incidental memory for visual features (e.g., Rajaram, Srinivas, & Roediger, 1998; Graf & Ryan, 1990; Smith & Vela, 2001; Weldon et al., 1995). For visual scenes, categorical information is rapidly assessed and persists in memory longer than visual features (Oliva, 2005; Potter et al., 2004). However, when participants memorize scenes from similar categories, they would do best by also focusing on information that distinguishes one scene from another, including subordinate categories and visual details (Anderson & Reder, 1999; Konkle, Brady, Alvarez, & Oliva, 2010; Nairne, 2002). Additional research is needed to evaluate the interaction between target detection and memory for different types of information, particularly as it relates to the ability to distinguish items from each other. Second, in Experiments 1-3, relational memory was examined by testing whether participants could report features of targets and distractors that appeared with a particular scene. Mulligan and colleagues (2016) tested memory for a word and its context by asking participants to indicate whether a given word was new, old and presented in one font/color combination, or old and presented in a different font/color combination. This procedure differs from that used in Experiments 1-3 in two potentially important ways. First, Experiments 1-3 tested memory for the perceptual features of the detection task items rather than the background items. It is possible that the beneficial effects of target detection are limited to the features of the detection targets or spatial locations, with little advantage for the perceptual

details of the background item or the scene's temporal context. This may be particularly true for irrelevant perceptual features, which may not always be encoded and remembered (e.g., Marshall & Bays, 2013; Xu, 2010). Second, rather than simultaneously testing memory for the item and spatiotemporal context (as in Mulligan, et al. 2016), Experiments 1-3 first tested scene memory, then showed the old scene during the test of memory for the paired item's relevant and irrelevant features (providing feedback for each question). This may have reduced participants' uncertainty and allowed for a better match between the retrieval cue and the memory trace (Hollingworth, 2006; Nairne, 2002; Reder, Donavos, & Erickson, 2002). However, a relational memory benefit for target paired images also has been observed in experiments where participants first indicated whether an image was old or new, and then selected the color of the square it appeared with (e.g., blue, orange, or no-square) before receiving feedback on their response (Swallow & Atir, 2018). It is therefore unlikely that the availability of more reliable retrieval cues in Experiments 1-3 is the sole source of the difference in findings from those of Mulligan and colleagues (2016).

In Experiments 1-3, the items were presented multiple times rather than once (the ABE can occur with a single presentation, cf. Lin, et al., 2010; Makovski, Swallow, & Jiang, 2012; Mulligan, et al., 2016; Spataro, et al., 2013). Participants therefore had multiple opportunities to learn the association between a scene and the item it was paired with. With repeated presentations, participants could learn scenes that predict the presence of target features, or the need to generate a motor response. However, because images that precede targets by 100 or 500 ms are not better remembered than those that precede distractors, it is unlikely that the ability to use a scene to predict the presence of a target is enough to boost memory (Swallow & Jiang, 2010; 2011). The ability to use a scene to predict the presence of task-relevant features also cannot account for the relational memory advantage for irrelevant features. Another possibility is

that participants first encode the background items and then add in relational and visual detail in subsequent presentations. If so, memory for the perceptual features of an item (as tested in Mulligan et al., 2016) may be weaker and more susceptible to interference than memory for the item's meaning (Anderson & Reder, 1999; Potter et al., 2004). Alternatively, memory for relational information may strengthen with additional presentations, though this effect is stronger when the items are presented over multiple days (Litman & Davachi, 2008).

The use of multiple presentations in Experiments 1-3 limits their applicability to memory for a single episode (Tulving, 1972). Instead, these experiments may relate more directly to event memory: the mental construction of a scene that takes place at one time, but integrates information encountered across multiple encoding episodes (Rubin & Umanath, 2015). This information may be represented across multiple systems, including basal ganglia, neocortex, and hippocampus. Indeed, previous research has demonstrated that damage to the hippocampus impairs relational memory even when scene-face pairs have been presented multiple times (Hannula, Ryan, Tranel, & Cohen, 2007). Future research should consider how the ABE is affected by the repetition of events with overlapping constituents.

Finally, it is important to note that targets were rare in Mulligan, et al., (2016), but as frequent as distractors in Experiments 1-3 (and in Swallow & Atir, 2018). Several lines of evidence indicate that distinctiveness, resulting from either the frequency or perceptual salience of targets relative to distractors, has little if any effect on the ABE for background images (Swallow & Jiang, 2012; 2014a; 2014b). However, distinctiveness manipulations that increase item related processing may reduce memory for irrelevant item features (Hunt & McDaniel, 1993; Mulligan, 2011). Therefore, the role of distinctiveness in modulating the effects of target detection on relational memory, and context more broadly, will be important to explore.

A related concern comes from the fact that target trials always included a motor response, but distractor trials did not. Motor productions can facilitate memory. For example, participants better remember words they have read aloud than words they have read silently (MacLeod, Gopie, Hourihan, Neary, & Ozubko, 2010). However, this effect disappears when uniform responses are made to half the words (e.g., pressing the same button, rather than reading the word aloud; MacLeod, et al., 2010). In addition, other work has shown that faces paired with no motor response are sometimes better remembered than faces paired with a motor response (Makovski, et al., 2013). This suggests that uniform motor responses like the ones in Experiments 1-3 are not sufficient to boost memory in these tasks.

To accommodate the current data, it is necessary to modify views on the effects of attention on memory. Current understanding of the ABE suggests that it occurs during encoding. In addition, there is substantial evidence that target detection affects the processing of low-level visual or auditory item features (e.g., Pascucci & Turatto, 2013; Spataro et al., 2013; Swallow, Makovski, & Jiang, 2012). However, the ABE in explicit memory tests of words does not appear to depend on matching visual or auditory features (e.g., word modality, font, or color) of the word during encoding and test (Mulligan, Spataro, & Picklesimer, 2014; Mulligan et al., 2016). This may mean that the ABE in explicit memory tests reflects a memory advantage for more abstract information, such as concepts and categories (Mulligan et al., 2016; Weldon et al., 1995). One might also claim that the ABE in explicit visual long-term memory results from better conceptual encoding (Konkle et al., 2010). However, data from Experiments 1-3 argue that, just as enhanced encoding of low-level perceptual features cannot be the whole story, neither can enhanced encoding of abstract, conceptual information.

A potential solution may be to extend an earlier account of the ABE, the dual-task interaction model, in two ways. The dual-task interaction model claims that well characterized mechanisms of attentional selection over space, objects, and features operate alongside a mechanism that globally boosts perceptual processing at behaviorally relevant moments (Swallow & Jiang, 2013). This model could readily incorporate effects of temporal selection on spatiotemporal context and abstract, amodal information, which were not explicitly considered when the account was first described. Indeed, the neurophysiological mechanism that was proposed to produce the ABE – the locus coeruleus norepinephrine system (LC-NE) – projects to nearly every region of the brain including the hippocampus (Sara, 2009). Because NE increases the signal-to-noise ratio of activity in afferent areas of the brain as well as long-term potentiation in the dentate gyrus of the hippocampus (Sara, 2009), phasic LC-NE activity in response to targets (Aston-Jones & Cohen, 2005) would have widespread facilitative effects on encoding such as the ones seen in this and similar studies.

The effects of goals and tasks on the way the current situation is processed should be more thoroughly considered in the dual-task interaction model. Independent effects of temporal selection (perhaps mediated by subcortical mechanisms) and the selection of task-relevant information, including features and locations (perhaps mediated by prefrontal cortex) might be sufficient to account for some data. For example, the ABE is present, but less reliable when background scenes are ignored during encoding (Swallow & Jiang, 2011; Swallow & Jiang, 2014a). In addition, expectations about the importance of distinguishing low-level perceptual features for a subsequent memory test may vary across scene and word encoding, changing the type of information that is facilitated by target detection (cf. Intraub & Nicklos, 1985). In a similar vein, the way a stimulus is processed during encoding could influence the conditions

under which the ABE is best measured (as in transfer appropriate processing; Graf & Ryan, 1990; Weldon et al., 1995).

2.6 Conclusion

Target detection can trigger the selection of a behaviorally relevant moment, boosting the encoding of concurrently presented items. It also enhances memory for the relationship between one item and relevant and irrelevant features of other items that appeared with it during encoding. As a result, increasing attention to behaviorally relevant moments, such as when a target appears in a stream of distractors, boosts memory for the event as a whole. Such a mechanism is well positioned to influence what people remember about their experiences, how they represent that information in memory, and how they envision the future.

References

Aly, M., & Turk-Browne, N. B. (2016).Attention promotes episodic encoding by stabilizing hippocampal representations. *Proceedings of the National Academy of Sciences*, *113*(4), E420-E429.

Anderson, J. R., & Reder, L. M. (1999). The fan effect: New results and new theories. *Journal of Experimental Psychology: General*, *128*(2), 186–197. https://doi.org/10.1037/0096-3445.128.2.186

Aston-Jones, G., & Cohen, J. D. (2005). An integrative theory of locus coeruleus-norepinephrine function: adaptive gain and optimal performance. *Annual Reviews of Neuroscience*, *28*, 403-450. https://doi.org/10.1146/annurev.neuro.28.061604.135709

Baddeley, A. D. (1982). Domains of recollection. *Psychological Review*, *89*(6), 708–729. https://doi.org/10.1037/0033-295X.89.6.708

Baddeley, A., Lewis, V., Eldridge, M., & Thomson, N. (1984). Attention and retrieval from long-term memory. *Journal of Experimental Psychology: General*, *113*(4), 518–540. https://doi.org/10.1037/0096-3445.113.4.518

Ballard, D. H., Hayhoe, M. M., & Pelz, J. B. (1995). Memory Representations in Natural Tasks. *Journal of Cognitive Neuroscience*, *7*(1), 66–80. https://doi.org/10.1162/jocn.1995.7.1.66

Brady, T. F., Konkle, T., Alvarez, G. A., & Oliva, A. (2013). Real-world objects are not represented as bound units: Independent forgetting of different object details from visual memory. *Journal of Experimental Psychology: General*, *142*(3), 791–808. https://doi.org/10.1037/a0029649

Brainard, D. H. (1997). The psychophysics toolbox. *Spatial Vision*, *10*(4), 433-436.

Burgess, N., Maguire, E. A., & O'Keefe, J. (2002). The human hippocampus and spatial and episodic memory. *Neuron*, *35*(4), 625-641.

Burton, A. M., Schweinberger, S. R., Jenkins, R., & Kaufmann, J. M. (2015). Arguments against a configural processing account of familiar face recognition. *Perspectives on Psychological Science*, *10*(4), 482-496.

Button, K. S., Ionnidis, J. P., Mokrysz, C., Nosek, B. A., Flint, J., Robinson, E. S., & Munafò, M. R. (2013). Power failure : why small sample size undermines the reliability of neuroscience. *Nature Reviews Neuroscience*, *14*(5), 365-376.

Castelhano, M. S., & Henderson, J. M. (2007). Initial scene representations facilitate eye movement guidance in visual search. *Journal of Experimental Psychology: Human Perception and Performance*, *33*(4), 753–763. https://doi.org/10.1037/0096-1523.33.4.753

Chen, H., Swan, G., & Wyble, B. (2016). Prolonged focal attention without binding: Tracking a ball for half a minute without remembering its color. *Cognition*, *147*, 144–148. https://doi.org/10.1016/j.cognition.2015.11.014

Chen, H., & Wyble, B. (2015). The location but not the attributes of visual cues are automatically encoded into working memory. *Vision Research*, *107*, 76-85.

Chun, M. M., & Jiang, Y. (1998). Contextual Cueing: Implicit Learning and Memory of Visual Context Guides Spatial Attention. *Cognitive Psychology*, *36*(1), 28–71. https://doi.org/10.1006/cogp.1998.0681

Chun, M. M., & Turk-Browne, N. B. (2007). Interactions between attention and memory. *Current opinion in neurobiology*, *17*(2), 177-184.

Cohen, M. A., Alvarez, G. A., & Nakayama, K. (2011). Natural-Scene Perception Requires Attention. *Psychological Science*, *22*(9), 1165–1172. https://doi.org/10.1177/0956797611419168

Conway, M. A. (2009). Episodic memories. *Neuropsychologia*, *47*(11), 2305–2313. https://doi.org/10.1016/j.neuropsychologia.2009.02.003

Craik, F. I. M., Govoni, R., Naveh-Benjamin, M., & Anderson, N. D. (1996). The effects of divided attention on encoding and retrieval processes in human memory. *Journal of Experimental Psychology: General*, *125*(2), 159–180. https://doi.org/10.1037/0096-3445.125.2.159

Craik, F. I. M., & Tulving, E. (1975). Depth of processing and the retention of words in episodic memory. *Journal of Experimental Psychology: General*, *104*(3), 268–294. https://doi.org/10.1037/0096-3445.104.3.268

Davachi, L. (2006). Item, context and relational episodic encoding in humans. *Current Opinion in Neurobiology*, *16*(6), 693–700. https://doi.org/10.1016/j.conb.2006.10.012

Duncan, J. (1980). The locus of interference in the perception of simultaneous stimuli. *Psychological Review*, *87*(3), 272–300. https://doi.org/10.1037/0033-295X.87.3.272

Eichenbaum, H. (2004). Hippocampus: Cognitive Processes and Neural Representations that Underlie Declarative Memory. *Neuron*, *44*(1), 109–120. https://doi.org/10.1016/j.neuron.2004.08.028

Epstein, R. A. (2008). Parahippocampal and retrosplenial contributions to human spatial navigation. *Trends in Cognitive Sciences*, *12*(10), 388-396.

Erez, J., Cusack, R., Kendall, W., & Barense, M. D. (2016). Conjunctive Coding of Complex Object Features. *Cerebral Cortex*, *26*(5), 2271–2282. https://doi.org/10.1093/cercor/bhv081

Faul, F., Erdfelder, E., Lang, A.-G., & Buchner, A. (2007). G*Power 3: A flexible statistical power analysis program for the social, behavioral, and biomedical sciences. *Behavior Research Methods*, *39*(2), 175–191. https://doi.org/10.3758/BF03193146

Fougnie, D., & Alvarez, G. A. (2011). Object features fail independently in visual working memory: Evidence for a probabilistic feature-store model. *Journal of Vision*, *11*(12), 3, https://doi.org/10.1167/11.12.3

Gajewski, D. A., & Brockmole, J. R. (2006). Feature bindings endure without attention: Evidence from an explicit recall task. *Psychonomic Bulletin & Review*, *13*(4), 581–587. https://doi.org/10.3758/BF03193966

Golomb, J. D., Kupitz, C. N., & Thiemann, C. T. (2014). The influence of object location on identity: A "spatial congruency bias". *Journal of Experimental Psychology: General*, *143*(6), 2262-2278.

Graf, P., & Ryan, L. (1990). Transfer-appropriate processing for implicit and explicit memory. *Journal of Experimental Psychology: Learning, Memory, and Cognition*, *16*(6), 978–992. https://doi.org/10.1037/0278-7393.16.6.978

Hannula, D. E., & Ranganath, C. (2008). Medial Temporal Lobe Activity Predicts Successful Relational Memory Binding. *Journal of Neuroscience*, *28*(1), 116–124. https://doi.org/10.1523/JNEUROSCI.3086-07.2008

Hannula, D. E., Ryan, J. D., Tranel, D., & Cohen, N. J. (2007). Rapid onset relational memory effects are evident in eye movement behavior, but not in hippocampal amnesia. *Journal of Cognitive Neuroscience*, *19*(10), 1690-1705. https://doi.org/10.1162/jocn.2007.19.10.1690

Hayhoe, M. (2000). Vision Using Routines: A Functional Account of Vision. *Visual Cognition*, *7*(1–3), 43–64. https://doi.org/10.1080/135062800394676

Hollingworth, A. (2006). Visual memory for natural scenes: Evidence from change detection and visual search. *Visual Cognition*, *14*(4–8), 781–807. https://doi.org/10.1080/13506280500193818

Hollingworth, A. (2007). Object-position binding in visual memory for natural scenes and object arrays. *Journal of Experimental Psychology: Human Perception and Performance*, *33*(1), 31–46.

Huang, L. (2010). Characterizing the nature of visual conscious access: The distinction between features and location. *Journal of Vision*, *10*(10), 24, doi:10.1167/10.10.24

Hunt, R. R., & McDaniel, M. A. (1993). The Enigma of Organization and Distinctiveness. *Journal of Memory and Language*, *32*(4), 421–445. https://doi.org/10.1006/jmla.1993.1023

Intraub, H., & Nicklos, S. (1985). Levels of processing and picture memory: The physical superiority effect. *Journal of Experimental Psychology: Learning, Memory, and Cognition*, *11*(2), 284–298. https://doi.org/10.1037/0278-7393.11.2.284

Jacoby, L. L., Woloshyn, V., & Kelley, C. (1989). Becoming famous without being recognized: Unconscious influences of memory produced by dividing attention. *Journal of Experimental Psychology: General*, *118*(2), 115–125. https://doi.org/10.1037/0096-3445.118.2.115

Jiang, Y., & Leung, A. W. (2005). Implicit learning of ignored visual context. *Psychonomic Bulletin & Review*, *12*(1), 100–106. https://doi.org/10.3758/BF03196353

Jiang, Y., Olson, I. R., & Chun, M. M. (2000). Organization of visual short-term memory. *Journal of Experimental Psychology: Learning, Memory, and Cognition*, *26*(3), 683-702.

Jiang, Y. V., & Swallow, K. M. (2014). Temporal yoking in continuous multitasking. *Journal of Experimental Psychology: Human Perception and Performance*, *40*(6), 2348–2360. https://doi.org/10.1037/a0038286

Johnson, M. K., Hashtroudi, S., & Lindsay, D. S. (1993). Source monitoring. *Psychological bulletin*, *114*(1), 3-28.

Kelley, C. M., & Jacoby, L. L. (2000). Recollection and familiarity. In E. Tulving (Ed.), *The Oxford Handbook of Memory*(pp. 215–228). Oxford University Press.

Kim, S.-Y., & Giovanello, K. S. (2011). The effects of attention on age-related relational memory deficits: Evidence from a novel attentional manipulation. *Psychology and Aging*, *26*(3), 678–688. https://doi.org/10.1037/a0022326

Knoblauch, K. (2014). psyphy: Functions for analyzing psychophysical data in R (Version 0.1-9). Retrieved from https://CRAN.R-project.org/package=psyphy

Konkle, T., Brady, T. F., Alvarez, G. A., & Oliva, A. (2010). Conceptual distinctiveness supports detailed visual long-term memory for real-world objects. *Journal of Experimental Psychology: General*, *139*(3), 558–578. https://doi.org/10.1037/a0019165

Lee, A. C., Yeung, L. K., & Barense, M. D. (2012). The hippocampus and visual perception. *Frontiers in human neuroscience*, *6*, 91. https://doi.org/10.3389/fnhum.2012.00091

Leclercq, V., Le Dantec, C. C., & Seitz, A. R. (2014). Encoding of episodic information through fast task-irrelevant perceptual learning. *Vision Research*, *99*(Supplement C), 5–11. https://doi.org/10.1016/j.visres.2013.09.006

Levin, D. T., & Saylor, M. M. (2008). Shining spotlights, zooming lenses, grabbing hands, and pecking chickens: the ebb and flow of attention during events. In T. F. Shipley & J. M. Zacks, *Understanding Events: From Perception to Action* (pp. 522–554). Oxford University Press.

Lin, J. Y., Pype, A. D., Murray, S. O., & Boynton, G. M. (2010). Enhanced Memory for Scenes Presented at Behaviorally Relevant Points in Time. *PLOS Biology*, *8*(3), e1000337. https://doi.org/10.1371/journal.pbio.1000337

Litman, L., & Davachi, L. (2008). Distributed learning enhances relational memory consolidation. *Learning & Memory*, *15*(9), 711–716. https://doi.org/10.1101/lm.1132008

MacLeod, C. M., Gopie, N., Hourihan, K. L., Neary, K. R., & Ozubko, J. D. (2010). The production effect: Delineation of a phenomenon. *Journal of Experimental Psychology: Learning, Memory, and Cognition*, *36*(3), 671-685. https://doi.org/10.1037/a0018785

Macmillan, N. A., & Creelman, C. D. (2004). *Detection theory: A user's guide*. Psychology press.

Makovski, T., Jiang, Y. V., & Swallow, K. M. (2013). How do observer's responses affect visual long-term memory? *Journal of Experimental Psychology: Learning, Memory, and Cognition*, *39*(4), 1097–1105. https://doi.org/10.1037/a0030908

Mandler, G. (1980). Recognizing: The judgment of previous occurrence. *Psychological Review*, *87*(3), 252–271. https://doi.org/10.1037/0033-295X.87.3.252

Marshall, L., & Bays, P. M. (2013). Obligatory encoding of task-irrelevant features depletes working memory resources. *Journal of vision*, *13*(2), 21-21. http://doi.org/10.1167/13.2.21

Minear, M., & Park, D. C. (2004). A lifespan database of adult facial stimuli. *Behavior Research Methods, Instruments, & Computers*, *36*(4), 630–633. https://doi.org/10.3758/BF03206543

Moscovitch, M., Cabeza, R., Winocur, G., & Nadel, L. (2016). Episodic Memory and Beyond: The Hippocampus and Neocortex in Transformation. *Annual Review of Psychology*, *67*(1), 105–134. https://doi.org/10.1146/annurev-psych-113011-143733

Mulligan, N. W. (1998). The role of attention during encoding in implicit and explicit memory. *Journal of Experimental Psychology: Learning, Memory, and Cognition*, *24*(1), 27–47. https://doi.org/10.1037/0278-7393.24.1.27

Mulligan, N. W. (2011). Generation disrupts memory for intrinsic context but not extrinsic context. *The Quarterly Journal of Experimental Psychology*, *64*(8), 1543-1562. https://doi.org/10.1080/17470218.2011.562980

Mulligan, N. W., Smith, S. A., & Spataro, P. (2016). The attentional boost effect and context memory. *Journal of Experimental Psychology: Learning, Memory, and Cognition*, *42*(4), 598–607. https://doi.org/10.1037/xlm0000183

Mulligan, N. W., Spataro, P., & Picklesimer, M. (2014). The attentional boost effect with verbal materials. *Journal of Experimental Psychology: Learning, Memory, and Cognition*, *40*(4), 1049-1069. https://doi.org/10.1037/a0036163

Nairne, J. S. (2002). The myth of the encoding-retrieval match. *Memory*, *10*(5–6), 389–395. https://doi.org/10.1080/09658210244000216

Nakabayashi, K., Burton, A. M., Brandimonte, M. A., & Lloyd-Jones, T. J. (2012). Dissociating positive and negative influences of verbal processing on the recognition of pictures of faces and objects. *Journal of Experimental Psychology: Learning, Memory, and Cognition*, *38*(2), 376-390. https://doi.org/10.1037/a0025782

Newtson, D., & Engquist, G. (1976). The perceptual organization of ongoing behavior. *Journal of Experimental Social Psychology*, *12*(5), 436-450.

Nobre, A. C., & Van Ede, F. (2018). Anticipated moments: temporal structure in attention. *Nature Reviews Neuroscience*, *19*(1), 34-48.

O'Craven, K. M., Downing, P. E., & Kanwisher, N. (1999). fMRI evidence for objects as the units of attentional selection. *Nature*, *401*(6753), 584-587. https:/doi.org/10.1038/44134

Oliva, A. (2005). Gist of the scene. In: L. Itti, G. Rees, & J.K. Tsotsos (Eds.), *Neurobiology of attention* (pp. 251–256). San Diego, CA: Elsevier

Onyper, S. V., Zhang, Y., & Howard, M. W. (2010). Some-or-none recollection: Evidence from item and source memory. *Journal of Experimental Psychology. General*, *139*(2), 341–364. https://doi.org/10.1037/a0018926

Paivio, A., & Csapo, K. (1973). Picture superiority in free recall: Imagery or dual coding? *Cognitive Psychology*, *5*(2), 176–206. https://doi.org/10.1016/0010-0285(73)90032-7

Pascucci, D., & Turatto, M. (2013). Immediate Effect of Internal Reward on Visual Adaptation. *Psychological Science*, *24*(7), 1317–1322. https://doi.org/10.1177/0956797612469211

Pelli, D. G. (1997). The VideoToolbox software for visual psychophysics: transforming numbers into movies. *Spatial Vision*, *10*(4), 437–442. https://doi.org/10.1163/156856897X00366

Polyn, S. M., Norman, K. A., & Kahana, M. J. (2009). A context maintenance and retrieval model of organizational processes in free recall. *Psychological review*, *116*(1), 129-156.

Potter, M. C., Staub, A., & O'Connor, D. H. (2004). Pictorial and Conceptual Representation of Glimpsed Pictures. *Journal of Experimental Psychology: Human Perception and Performance*, *30*(3), 478–489. https://doi.org/10.1037/0096-1523.30.3.478

Rajaram, S., Srinivas, K., & Roediger III, H. L. (1998). A transfer-appropriate processing account of context effects in word-fragment completion. *Journal of Experimental Psychology: Learning, Memory, and Cognition*, *24*(4), 993–1004. https://doi.org/10.1037/0278-7393.24.4.993

Ranganath, C., Yonelinas, A. P., Cohen, M. X., Dy, C. J., Tom, S. M., & D'Esposito, M. (2004). Dissociable correlates of recollection and familiarity within the medial temporal lobes. *Neuropsychologia*, *42*(1), 2–13. https://doi.org/10.1016/j.neuropsychologia.2003.07.006

Raymond, J. E., Shapiro, K. L., & Arnell, K. M. (1992). Temporary suppression of visual processing in an RSVP task: An attentional blink? *Journal of Experimental Psychology: Human Perception and Performance*, *18*(3), 849–860. https://doi.org/10.1037/0096-1523.18.3.849

Reder, L. M., Donavos, D. K., & Erickson, M. A. (2002). Perceptual match effects in direct tests of memory: The role of contextual fan. *Memory & Cognition*, *30*(2), 312–323. https://doi.org/10.3758/BF03195292

Robin, J., Buchsbaum, B. R., & Moscovitch, M. (2018). The primacy of spatial context in the neural representation of events. *Journal of Neuroscience*, 1638-17. https://doi.org/10.1523/JNEUROSCI.1638-17.2018

Rubin, R. D., Schwarb, H., Lucas, H. D., Dulas, M., R., & Cohen, N. J. (2017). Dynamic hippocampal and prefrontal contributions to memory processes and representations blur the boundaries of traditional cognitive domains. *Brain sciences*, *7*(7), 82-98. https://doi.org/10.3390/brainsci7070082

Rubin, D. C., & Umanath, S. (2015). Event memory: A theory of memory for laboratory, autobiographical, and fictional events. *Psychological Review*, *122*(1), 1-23.

Ryan, J. D., Althoff, R. R., Whitlow, S., & Cohen, N. J. (2000). Amnesia is a Deficit in Relational Memory. *Psychological Science*, *11*(6), 454–461. https://doi.org/10.1111/1467-9280.00288

Sara, S.J. (2009). The locus coeruleus and noradrenergic modulation of cognition. *Nature Reviews Neuroscience*, *10*(3), 211–223.

Schoenfeld, M. A., Hopf, J. M., Merkel, C., Heinze, H. J., & Hillyard, S. A. (2014). Object-based attention involves the sequential activation of feature-specific cortical modules. *Nature neuroscience*, *17*(4), 619-624. https://doi.org/10.1038/nn.3656

Schwan, S., Garsoffky, & Hesse, F. W. (2000). Do film cuts facilitate the perceptual and cognitive organization of activity sequences? *Memory and Cognition*, *28*(2), 214-223.

Seitz, A. R., & Watanabe, T. (2009). The phenomenon of task-irrelevant perceptual learning. *Vision Research*, *49*(21), 2604–2610. https://doi.org/10.1016/j.visres.2009.08.003

Serences, J. T., Ester, E. F., Vogel, E. K., & Awh, E. (2009). Stimulus-Specific Delay Activity in Human Primary Visual Cortex. *Psychological Science*, *20*(2), 207–214. https://doi.org/10.1111/j.1467-9280.2009.02276.x

Smith, S. M., & Vela, E. (2001). Environmental context-dependent memory: A review and meta-analysis. *Psychonomic Bulletin & Review*, *8*(2), 203–220. https://doi.org/10.3758/BF03196157

Spataro, P., Mulligan, N. W., Bechi Gabrielli, G., & Rossi-Arnaud, C. (2017). Divided attention enhances explicit but not implicit conceptual memory: an item-specific account of the attentional boost effect. *Memory*, *25*(2), 170-175.

Spataro, P., Mulligan, N. W., & Rossi-Arnaud, C. (2013). Divided attention can enhance memory encoding: The attentional boost effect in implicit memory. *Journal of Experimental Psychology: Learning, Memory, and Cognition*, *39*(4), 1123-1231.

Swallow, K. M., & Atir, S. (2018). The role of value in the attentional boost effect. *Quarterly Journal of Experimental Psychology*, https://doi.org/10.1177/1747021818760791.

Swallow, K. M., & Jiang, Y. V. (2010). The Attentional Boost Effect: Transient Increases in Attention to One Task Enhance Performance in a Second Task. *Cognition*, *115*(1), 118–132. https://doi.org/10.1016/j.cognition.2009.12.003

Swallow, K. M., & Jiang, Y. V. (2011). The role of timing in the attentional boost effect. *Attention, Perception, & Psychophysics*, *73*(2), 389–404. https://doi.org/10.3758/s13414-010-0045-y

Swallow, K. M., & Jiang, Y. V. (2012). Goal-relevant events need not be rare to boost memory for concurrent images. *Attention, Perception, & Psychophysics*, *74*(1), 70-82.

Swallow, K. M., & Jiang, Y. V. (2013). Attentional Load and Attentional Boost: A Review of Data and Theory. *Frontiers in Psychology*, *4*. https://doi.org/10.3389/fpsyg.2013.00274

Swallow, K. M., & Jiang, Y. V. (2014a). Perceptual load and attentional boost: A study of their interaction. *Journal of Experimental Psychology: Human Perception and Performance*, *40*(3), 1034–1045. https://doi.org/10.1037/a0035312

Swallow, K. M., & Jiang, Y. V. (2014b). The attentional boost effect really is a boost: Evidence from a new baseline. *Attention, Perception, & Psychophysics*, 1–10. https://doi.org/10.3758/s13414-014-0677-4

Swallow, K. M., Makovski, T., & Jiang, Y. V. (2012). Selection of events in time enhances activity throughout early visual cortex. *Journal of Neurophysiology*, *108*(12), 3239–3252. https://doi.org/10.1152/jn.00472.2012

Swallow, K. M., Zacks, J. M., & Abrams, R. A. (2009). Event boundaries in perception affect memory encoding and updating. *Journal of Experimental Psychology: General*, *138*(2), 236–257. https://doi.org/10.1037/a0015631

Taubert, J., Apthorp, D., Aagten-Murphy, D., & Alais, D. (2011). The role of holistic processing in face perception: Evidence from the face inversion effect. *Vision Research*, *51*(11), 1273-1278.

Troyer, A. K., & Craik, F. I. M. (2000). The effect of divided attention on memory for items and their context. *Canadian Journal of Experimental Psychology/Revue Canadienne de Psychologie Expérimentale*, *54*(3), 161–171. https://doi.org/10.1037/h0087338

Troyer, A. K., Winocur, G., Craik, F. I. M., & Moscovitch, M. (1999). Source memory and divided attention: Reciprocal costs to primary and secondary tasks. *Neuropsychology*, *13*(4), 467–474. https://doi.org/10.1037/0894-4105.13.4.467

Tulving, E. (1972). Episodic and semantic memory. In E. Tulving & W. Donaldson (Eds.), *Organization of memory* (pp. 381-402). New York, NY: Academic Press.

Tulving, E. (1985). Memory and consciousness. *Canadian Psychology/Psychologie Canadienne*, *26*(1), 1–12. https://doi.org/10.1037/h0080017

Weldon, M. S., Roediger, H. L., Beitel, D. A., & Johnston, T. R. (1995). Perceptual and Conceptual Processes in Implicit and Explicit Tests with Picture Fragment and Word Fragment Cues. *Journal of Memory and Language*, *34*(2), 268–285. https://doi.org/10.1006/jmla.1995.1012

Wang, J. X., Cohen, N. J., & Voss, J. L. (2015). Covert rapid action-memory simulation (CRAMS): A hypothesis of hippocampal-prefrontal interactions for adaptive behavior. *Neurobiology of learning and memory*, *117*, 22-33. https:doi.org/10.1016/j.nlm.2014.04.003

Wheeler, M. A., Stuss, D. T., & Tulving, E. (1997). Toward a theory of episodic memory: The frontal lobes and autonoetic consciousness. *Psychological Bulletin*, *121*(3), 331–354. https://doi.org/10.1037/0033-2909.121.3.331

Wheeler, M. E., & Treisman, A. M. (2002). Binding in short-term visual memory. *Journal of Experimental Psychology: General*, *131*(1), 48–64. https://doi.org/10.1037/0096-3445.131.1.48

Wolfe, J. M., Horowitz, T. S., & Michod, K. O. (2007). Is visual attention required for robust picture memory? *Vision Research*, *47*(7), 955–964. https://doi.org/10.1016/j.visres.2006.11.025

Woodman, G. F., & Vogel, E. K. (2008). Selective storage and maintenance of an object's features in visual working memory. *Psychonomic Bulletin & Review*, *15*(1), 223–229. https://doi.org/10.3758/PBR.15.1.223

Xu, Y. (2010). The Neural Fate of Task-Irrelevant Features in Object-Based Processing. *Journal of Neuroscience*, *30*(42), 14020–14028. https://doi.org/10.1523/JNEUROSCI.3011-10.2010

CHAPTER 3

DIFFUSION DECISION MODELING OF RETRIEVAL FOLLOWING THE TEMPORAL SELECTION OF BEHAVIORALLY RELEVANT MOMENTS [2]

On a daily basis, people are faced with decisions relying on memory. For instance, walking by a person on the street, one has to decide whether that person is an acquaintance and, if so, what one might say to them based on what happened the last time they met. For a memory to adequately contribute to such decision making, it must be rich, accurate, and rapidly retrievable. The quality of a memory is influenced by attention during its encoding and, as evidenced by dual-task interference studies, scenarios where attention must be divided across multiple ongoing tasks will typically result in memory representations of lower quality, less depth, and with worse binding of information that was present at the time (e.g., Chun & Turk-Browne, 2007; Mulligan, 2008). Yet, one kind of dual-task paradigm enhances memory for some items by transiently increasing attention. This is known as the *attentional boost effect* (ABE; Au & Cheung, 2020; Broitman & Swallow, 2020; Lin, Pype, Murray, & Boynton, 2010; Makovski, Jiang, & Swallow, 2013; Mulligan, Spataro, & Picklesimer, 2014; Schonberg et al., 2014; Sisk & Lee, 2022; Smith & Mulligan, 2018; Spataro, Mulligan, Rossi-Arnaud, 2013; Swallow & Jiang, 2010, 2012; Toh & Lee, 2022).

This broad boost to memory is selective over time, with no apparent benefit for information presented immediately before or after the cue (Swallow & Jiang, 2011), having led to the proposal that the ABE is a prominent feature of the selection of information presented at a specific time (*temporal selection*). In this account, information presented at moments carrying

[2] This chapter is an abridged version of the manuscript under review at time of defense of this dissertation, Turker & Swallow (submitted). Thus, please do not copy or cite this chapter without the authors' permission.

behavioral relevance, such as during the appearance of a target in a detection task, is enhanced during encoding and this mechanism is, therefore, fundamentally different from selection based on stimulus location, features, or modality (for a review, see Swallow & Jiang, 2013).

3.1 Incidental Relational Memory Findings and the ABE: Issues Raised

This characterization of the ABE suggests that target detection may also be enhancing the processing of information outside the current focus of goal-oriented attention. Consistent with this idea, recent work suggests it is possible to boost memory for the momentary context in which that cue appeared (Broitman & Swallow, 2020; Leclercq, Le Dantec, & Seitz, 2014; see also Spataro, Saraulli, Cestari, Mulligan, Santirocchi, Borowiecki, & Rossi-Arnaud, 2020) and its relationship with the image being memorized (Swallow & Atir, 2018; Turker & Swallow, 2019). The boost to memory for the relationships between various features of a given trial was incidental, as participants were not instructed to intentionally memorize anything other than the image. However, other work has raised concerns that these prior studies may not reflect incidental memory, and instead are due to decision-related factors (Mulligan, Spataro, Rossi-Arnaud, & Wall, 2021) or the availability of excess resources for encoding and the specifics of task instructions (Hutmacher & Kuhbandner, 2020). The current paper aims to provide additional insight into these concerns by modeling the latent cognitive processes involved in recognition and by manipulating task instructions for the encoding task.

3.1.1 The Possibility of a Response Bias

Memory of events consists of items, their perceptual features, and their spatiotemporal relationships to each other (e.g., Cohen & Eichenbaum, 1993; Davachi, 2006; Rubin & Umanath,

2015). While there is broad agreement that the ABE boosts item memory (for a review, see Swallow & Jiang, 2013), the extent to which it affects memory for relationships between items presented during a trial is still debated. Consistent with the latter possibility, temporal selection can increase remembering, as opposed to knowing, of images presented concurrently with targets (Broitman & Swallow, 2020; Meng, Lin, & Lin, 2019; Yebra, Galarza-Vallejo, Soto-Leon, Gonzalez-Rosa, De Berker, Bestmann, Oliviero, Kroes, & Strange, 2019) as well as whether those scenes were presented on the left or right side of the screen (Leclercq et al., 2014). In Swallow & Atir (2018), participants more accurately reported which images had been paired with a target than which images had been paired with a distractor during encoding, even though they were not instructed to attend to that relationship. Turker & Swallow (2019) investigated the effect of target detection on incidental relational memory for both task-relevant features of the detection task cues (*task-relevant cue features*; i.e., those that defined it as a target or distractor, such as their color) and task-irrelevant features (*task-irrelevant cue features*; i.e., not target-defining, such as their shape or location). Participants were told to expect a memory test on the images, but also got surprise questions on the task-relevant and task-irrelevant features. Both task-relevant and irrelevant features were remembered more accurately and faster under target conditions than under distractor conditions. In another study participants were better able to identify the relationship between a given word and target cues relative to distractor cues (Mulligan et al., 2021).

However, other studies suggest that temporal selection does not necessarily enhance memory for anything more than the to-be-memorized item. For instance, target detection during word encoding does not produce a boost in memory for perceptual features of word itself (e.g., font or modality), nor for whether the word was presented early or late in the encoding task

(Mulligan, Smith, & Spataro, 2016). Greater access to the semantic relationships between words is also not influenced by target detection during word list encoding (Spataro, Mulligan, Cestari, Santirocchi, Saraulli, & Rossi-Arnaud, 2021; Spataro et al., 2013).

These mixed results may reflect the different ways that context memory has been defined and tested. However, it is also possible that some of the findings reflect a metacognitive decision-making strategy rather than a boost to relational memory. In Swallow & Atir (2018) and for some parts of Turker & Swallow (2019), relational memory for task-relevant cue features was tested by asking participants to report whether an image appeared with a target or distractor cue during encoding. Mulligan et al. (2021) suggest that participants may have inferred that the images they remembered better were paired with a target and that images they remembered poorly or forgot were paired with a distractor, resulting in response bias changing with memory strength. Not all demonstrations of relational memory benefits in the ABE allow for such a response bias (cf. Experiment 3 in Chapter 2, Turker & Swallow, 2019), because they test aspects of relational memory that are independent of the status of the cue as a target or distractor. The concern about potential contributions from response biases is nonetheless valid when participants report whether an item appeared with a target or distractor cue. The current paper therefore uses cognitive modeling to parameterize response bias and other latent cognitive factors in recognition memory test performance.

3.1.2 The Possibility of Uninstructed Memorization

A second concern is whether the ABE is exclusive to information that is intentionally encoded or whether it also incorporates information incidental to the task, such as a to-be-ignored background image and task-irrelevant features of the cues. To investigate this,

several studies have instructed participants to either encode or ignore the background images. These studies have also produced mixed results (e.g., Broitman & Swallow, 2020; Dewald, Sinnet, & Doumas, 2011, 2013; Spataro et al., 2020; Swallow & Jiang, 2011, 2014; Leclercq & Seitz, 2012; Mulligan et al., 2021; Walker, Ciraolo, Dewald, & Sinnett, 2017), leading to the suggestion that the ABE for background images may be present, but difficult to detect under incidental encoding instructions (Swallow & Jiang, 2014). Fewer studies have examined incidental memory for the relationship between elements presented during a trial. Those that have suggest that a relational memory benefit for target-paired information is possible, whether participants were explicitly instructed to also pay attention to relational features (Experiment 3 in Mulligan et al., 2021) or not (Experiments 1 & 2 in Mulligan et al., 2021; Swallow & Atir, 2018; Turker & Swallow, 2019). However, Mulligan et al. (2021) suggest that these effects may be driven by inferential decision-making biases.

Hutmacher & Kuhbandner (2020) separately argue that participants in these studies may be attending to task-irrelevant features of trials despite instructions. They also suggest that the extent to which participants can or do adhere to instructions depends on characteristics of the task. If task demands are relatively low, attention may be used to intentionally memorize other information presented during a trial. In support of this claim, they illustrated that reducing trial duration and the number of times an image is presented eliminates the ABE for incidentally encoded images. However, this procedure also resulted in a relatively small ABE under intentional encoding conditions. Furthermore, brief trial durations were insufficient for generating the ABE in recollection estimates (Broitman & Swallow, 2020), suggesting that decreasing trial duration may have effects beyond simply preventing participants from attending to the background image. It is also possible that increasing the image presentation rate weakened

the ABE overall, making an ABE in incidental memory simply more difficult to detect. Thus, it remains unclear to what extent previously reported relational memory findings would differ between encoding instructions.

3.1.3 Diffusion Decision Modeling of Temporal Selection Effects on Memory

The aforementioned concerns regarding recent ABE findings can be addressed with cognitive modeling. The possibility of a response bias affecting ABE findings can be investigated through its parameterization in these models. Modeling also affords a closer look at how task instructions impact various parameters underpinning the ABE. Mulligan et al. (2021) used multinomial modeling to argue that the ABE in relational memory reflects response bias. However, these models do not capture multiple cognitive processes involved in decision making (Gold & Shadlen, 2007; Ratcliff & McKoon, 2008). The utility of these discrete-state models also remains unclear, with increasing evidence favoring continuous models such as those based on signal detection theory (Dube, Starns, Rotello, & Ratcliff, 2012; Pazzaglia, Dube, & Rotello, 2013). A type of model that is conceptually similar to signal detection models (e.g., Griffith, Baker, & Lepora, 2021; Ratcliff, Smith, Brown, & McKoon, 2016), but which captures latent cognitive processes relevant to the current paper, are evidence accumulation models (for a recent review, see Evans & Wagenmakers, 2019). These models formalize rapid decisions between two options in recognition tests as a choice that is made by continuous sampling of noisy evidence over time until a decision threshold is reached (Donkin, Brown, & Heathcote, 2009; Forstmann, Ratcliff, & Wagenmakers, 2016; Gold & Shadlen, 2007; Ratcliff & McKoon, 2008; Ratcliff & Rouder, 1998; Smith & Ratcliff, 2004).

In a specific kind of evidence accumulation model, the diffusion decision model (DDM; Ratcliff, 1978), several aspects of the decision process are commonly parameterized (Fig. 3.1e; Heathcote, Lin, Reynolds, Strickland, Gretton, & Matzke, 2019). First, evidence is accumulated at a certain rate, known as the *drift rate* (*v*). Second, evidence accumulates toward one of two decision boundaries, each reflecting one of two response options. The distance between the two boundaries is referred to as *boundary separation* (*a*). Third, evidence accumulation can start closer to one boundary than the other or halfway between the two boundaries. This starting point is known as the *bias* (*z*). The period during which evidence is accumulated is known as the *decision time*. A final parameter captures latent processes that occur before and after the evidence accumulation period to account for perceptual and motor contributions to response time. Together, they are known as *non-decision time* (*t0*). Faster response times on a recognition test could result from faster drift, smaller boundary separation, or lower non-decision time.

The DDM has been used to examine latent mechanisms involved in tasks that investigate factors involved in the ABE paradigm, including temporal attention, dual-task interference, and relational memory (Wagenmakers, 2009; Ratcliff et al., 2016). For instance, in Jepma, Wagenmakers, & Nieuwenhuis (2012), temporal cueing reduced non-decision time, suggesting that temporal cueing may promote noisy, premature sampling of sensory information. Other work examining the effects of cognitive load or time pressure on target detection has suggested that they can increase the amount of information required to make a response (reflected in boundary separation; Tillman, Strayer, Eidels, & Heathcote, 2017), or increase the rate at which information is acquired (reflected in drift rate) if secondary task demands are intermittent (e.g., Castro, Strayer, Matzke, & Heathcote, 2019; Palada, Neal, Strayer, Ballard, & Heathcote, 2019). Most pertinent to the effects examined in this paper, drift diffusion models have provided insight

into the effects of attentional manipulations during encoding on subsequent performance on episodic and relational memory tests. For instance, in Yazin, Das, Banerjee, & Roy (2021), improved memory for temporal sequences that violated expectations was associated with lower decision boundaries.

We are aware of no research that applies DDMs to subsequent memory data for stimuli presented during an attentional boost paradigm, with its counterintuitive dual-task memory enhancement. Therefore, DDMs offer an opportunity to uncover processes underlying the ABE which otherwise could remain hidden. Accordingly, we used DDM as a framework for addressing concerns about response biases and intentional encoding contributing to the relational memory findings in the ABE. We analyzed data from three experiments previously published in Turker & Swallow (2019) as well as two new experiments that manipulate encoding instructions to provide additional insight into these two issues.

3.2 Section I: Using DDM to estimate response bias in Turker & Swallow (2019)

As a first step in addressing concerns about response bias, we reanalyzed the data previously reported in Turker & Swallow (T&S; 2019, Chapter 2 in the current dissertation) using DDMs. Consistent with the suggestion that temporal selection facilitates the encoding of the relationships between items present at behaviorally relevant moments, in T&S target detection resulted in better recognition sensitivity to intentionally memorized scenes as well as for other incidental features of the trial, including task-irrelevant perceptual and relational features of the concurrent cue. These findings were subsequently questioned by Mulligan et al. (2021), who suggested that the original analyses may not have adequately accounted for response bias resulting from inferential processes during the recognition test. Therefore this DDM analysis

evaluated whether response bias and other parameters that influence recognition test performance varied across encoding conditions.

We expected the behavioral findings reported in T&S to be reflected in several DDM parameter estimates. First, if target detection enhances episodic encoding and relational memory, retrieval of that information may result in higher drift for information that had been presented on target, rather than distractor, trials. Furthermore, models that keep drift fixed should more poorly fit the data than those that allow it to vary across target and distractor conditions. An effect on non-decision time may also be observed if images that were paired with a target during encoding are more rapidly processed or responded to during recognition (cf. Pascucci & Turatto, 2013; Spataro et al., 2013). If the effects of target detection on relational memory reflect a decision bias, then correct recognition of the scene should increase bias toward target-paired responses on subsequent relational memory questions. If, however, the relational memory findings of the ABE are not due to response bias, models that estimate bias should place it at a neutral distance between boundaries. Additionally, models which keep bias fixed across encoding conditions should better fit the data than models that allow it to vary across conditions.

3.2.1 Methods

Experimental methods are summarized here, but with details that are relevant to the new experiments presented in Section II (for more information, see Turker & Swallow, 2019 or Chapter 2).

3.2.1.1 Participants

Participants were recruited from the Cornell University community and the procedures were approved by Cornell's Institutional Review Board.

3.2.1.2 Procedure and Task Design

3.2.1.2.1 Encoding and Detection Task

The procedure was similar across the three experiments. In the first half of the experiment, participants performed a continuous dual-task (Fig. 3.1a). For the encoding task, participants memorized images of visual scenes (*old scenes*), such as landscapes or cities. A second set of the same size of randomly selected, different scenes functioned as foils on the recognition task (*foil scenes*). Participants were always instructed to memorize the scenes.

At the same time that they memorized the scenes, participants also performed a target detection task on concurrent, superimposed, but otherwise unrelated, cues, based on a predefined target feature like the color of a shape (Experiments 1 and 2) or gender of a face (Experiment 3). This is the *task-relevant feature*. The exact shape of the cue or unique identity of the face were incidental and thus *task-irrelevant* features.

3.2.1.2.2 Recognition Memory Task

Each trial of the recognition task consisted of either three (Experiments 1-2) or two (Experiment 3) n-alternative forced-choice questions (Fig. 3.1b), concerning the visual scene, the task-relevant feature of the cue paired with that scene (Experiments 1 & 2 only), and the task-irrelevant feature of that cue. There was one trial for each scene shown during encoding. Thus, in Experiment 1, the recognition task consisted of 300 questions (100 scene-cue pairings x

3 questions: regarding the scene, the task-relevant color of the paired cue, and the task-irrelevant shape of the paired cue). There were 312 questions on Experiment 2 (104 scenes, 3 questions per scene) and 200 on Experiment 3 (100 scenes, 2 questions per scene). Participants proceeded through all three questions on a given trial, even if they got one of the questions wrong.

Each trial started with a 2AFC *scene recognition question*. An old scene and a foil were presented side-by-side with the text *"Which of these two images were you shown in the first part of the experiment?"*. Participants indicated their choice with either the f-key or j-key on the keyboard, mapping onto the left and right options. Once a response was made, the old (not necessarily correctly chosen) scene was shown in the center of the screen to provide feedback. For Experiments 1 and 2, the *task-relevant feature question* was also presented. The text *"This was the correct image. Do you remember what the color of the figure was that was shown with it?"* appeared above the scene. Two squares (a shape that was not used as a task-irrelevant feature during encoding), each in one of the two possible cue colors, flanked the scene. The final question was the *task-irrelevant feature question*. The correct scene and correct task-relevant feature (whether chosen previously or not) were shown on screen. Participants had to respond which task-irrelevant feature was paired with the scene-cue combination: e.g., on Experiment 1, *"This was the correct image and color. Do you remember what the shape of the figure was?"*, and on Experiment 2, *"Do you remember at which of the 4 locations the cue appeared?"* (Fig. 1c). In Experiment 3, the second question was regarding the task-irrelevant face identity. Participants chose between two faces of the same gender (thus, of the same task-relevant feature category), each of which had been paired with a scene during encoding and was shown to them the same number of times (Fig. 3.1d). As a consequence, the entire display as shown during encoding was never fully reproduced until final feedback after the three recognition questions.

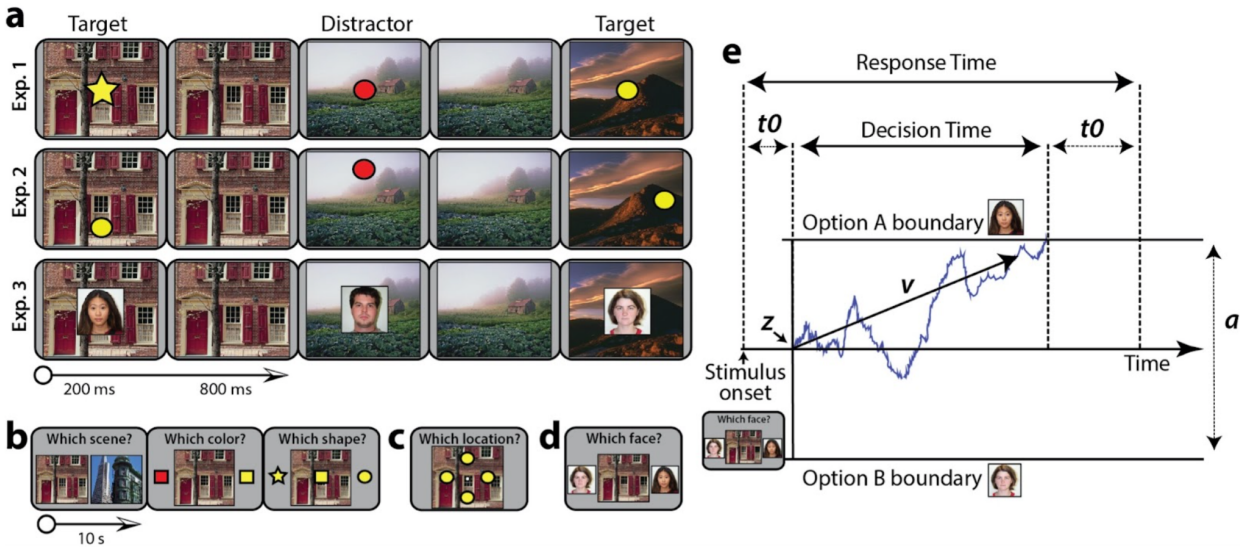

Figure 3.1 T&S task design & DDMs. *(a) Examples of trials in the encoding/detection tasks. Each trial consisted of a visual scene and a superimposed detection task cue (i.e., a colored shape or face). Participants pressed the button when the cue was the predefined target feature (color in Experiment 1 and 2, gender in Experiment 3; task-relevant feature). They were always instructed to memorize the scenes, but not the cues. The shape (Experiment 1, circle or star), location (Experiment 2, one of four locations), or unique identity (Experiment 3) was incidental to the task (task-irrelevant feature). (b, c) Participants were tested on the scenes, as they expected, but also received surprise questions about the task-relevant and task-irrelevant features of the cue that was paired with the scene. They were required to respond to each question within 10 s and the display disappeared as soon as a response was made. (d) For the task-irrelevant feature question in Experiment 3, participants chose which of two faces of the same gender had been paired with that particular scene. (e) A visualization of the diffusion decision process following the onset of the task-irrelevant feature question, with evidence accumulating in favor of one of the options. The DDM estimates the various parameters that constitute reaction times for correct and incorrect answers for that process (v = drift; z = bias; a = boundary separation; t0 = non-decision time). N.B.: Panels a-d of this figure have been adapted from Turker & Swallow (2019). Panel e is adapted from Murata, Hamada, Shimokawa, Tanifuji, & Yanigada (2014).*

3.2.2 Modeling Specifications

Using the open-source software Dynamic Models of Choice (DMC; Heathcote et al., 2019) in R (R Core Team, 2019), we obtained estimates for four parameters (*v*, *a*, *z*, and *t0*) for

both cue conditions for each 2AFC question answered by each participant in each experiment. Because Question 3 of Experiment 2 had four response options, we did not fit the DDM to those data. Data for questions following scene recognition were conditioned on the participant getting the scene question correct by removing trials where the scene was not recognized, because a demonstration of relational memory necessitates that both the scene and (some feature of) the paired cue is recognized, not merely one or the other.

Three types of models were fit to the data from each question and each experiment. First, a *full model* estimated all four parameters, within the context of priors. Reduced models were also estimated for model comparison. These models fixed either bias or drift to a specific value for all conditions (*bias-fixed*, z=0.5; *drift-fixed*, v=1.0). The model fitting procedure was otherwise the same for all models. Priors were truncated normal distributions based on reasonable values found in the literature (for a review, see Tran, Van Maanen, Heathcote, & Matzke, 2021; Supplementary Figure 1) and did not differ between cue conditions. For the bias parameter, the prior distribution offered a broad search space for investigating the possibility of response bias. Parameter estimation was performed in a hierarchical Bayesian manner in multiple steps, as implemented by DMC, through Markov Chain Monte-Carlo sampling with differential evolution (Turner, Sederberg, Brown, & Steyvers, 2013). First, 250 chains were used to generate starting points for each participant to subsequently perform sampling. Then, sampling was performed for the hierarchical model with a 5% migration probability, with only the crossover steps being used after burn-in. Sampling continued until all convergence criteria were met and the Gelman diagnostic was below 1.10 for all participants (Brooks & Gelman, 1998). Next, another 1000 samples were generated per chain for another round of sampling. Final

chains were well-mixed upon visual inspection. Posterior predictives showed good fits for the fully-estimated model presented here, as evidenced by the cumulative distribution functions.

For each recognition question, the parameters were estimated separately for target trials and distractor trials with the same priors for the given parameter. Thus, we allowed for the possibility that temporal selection during encoding would influence the parameters during the subsequent memory task, but made no assumptions as to what that difference might be.

For most models, response options were coded as a left or right button press (*button-coded models*). However, to test for response bias as outlined by Mulligan et al. (2021), the data were recoded for an alternative set of models (*feature-coded models*). First, rather than conditioning on initial scene accuracy as described above, scene accuracy was treated as a binary factor with no subsetting of the data. This way, we could test response bias parameters on subsequent questions following successful and unsuccessful scene recognition. Second, responses were coded for features that participants selected for the relational memory questions rather than the button that was pressed, where possible. For these, response options were mapped onto the two cue features that were tested on that question (this coding is not appropriate for those questions in which face identity was tested, as it was unique across trials). For instance, on Experiment 1's task-relevant feature question, responses were recoded to reflect the participant's choice that a target or distractor cue had appeared with the scene, regardless of that choice being presented on the left or right of the screen. On the task-irrelevant feature question, this meant a choice for a given shape rather than the left or right option. Combined, this allowed for testing of the possibility that participants strategically favored a certain cue feature in their answers based on how well they recognized the scene.

3.2.3 Results

3.2.3.1 Encoding and Detection Task

Descriptive statistics for the encoding and detection task are presented in Table 1. Participants performed the detection task well, responding to nearly all targets, with limited false alarms to distractors. Across the three experiments, 11 participants were excluded due to a high number of false alarms.

Table 3.1
Encoding and detecting dual-task performance in Experiments 1-4ab

		Target		Distractor	
Experiment	**N (excluded)**	**Hits (%)**	**RT (ms)**	**False Alarms (%)**	**RT (ms)**
Exp. 1	36 (0)	98.9 (1.1)	352.6 (81.6)	3.5 (2.0)	321.8 (160.6)
Exp. 2	50 (2)	98.8 (1.6)	355.1 (76.2)	4.0 (2.5)	332.6 (139.5)
Exp. 3	34 (9)	97.2 (2.7)	533.9 (95.0)	6.5 (2.2)	442.1 (176.3)
Exp. 4a	32 (10)	93.9 (4.5)	496.1 (53.8)	9.8 (4.3)	446.1 (66.4)
Exp. 4b	43 (13)	96.6 (3.5)	476.3 (72.6)	9.0 (3.2)	448.1 (95.5)

Note. Final sample size (with number of excluded participants in parentheses), means and standard deviations (in parentheses) of reaction times in milliseconds to targets (hits) and distractors (false alarms) in the detection task for each experiment. Data presented here are only for those participants who passed minimal performance criteria for inclusion in further analyses (≥ 80% hits, ≤ 10% false alarms on the detection task). Inclusion criteria were loosened for Experiment 4a and 4b (≤ 15% false alarms) to ensure a minimum of 32 participants in both experiments. This table is a modified and expanded version of Table 2.1 in Chapter 2.

3.2.3.2 Recognition Memory Task: Performance

Sensitivity based (d'; Macmillan & Creelman, 2004; generated with psyphy; Knoblauch, 2014) recognition analyses were presented in Chapter 2 but are summarized here, in Fig. 3.2, for convenience and comparison to Experiments 4a and 4b.

Briefly, participants were better able to recognize scenes that had been paired with target cues than those paired with distractor cues. Moreover, they were also better able to recognize task-relevant and task-irrelevant features of target cues compared to distractor cues, despite not having been instructed to actively memorize those.

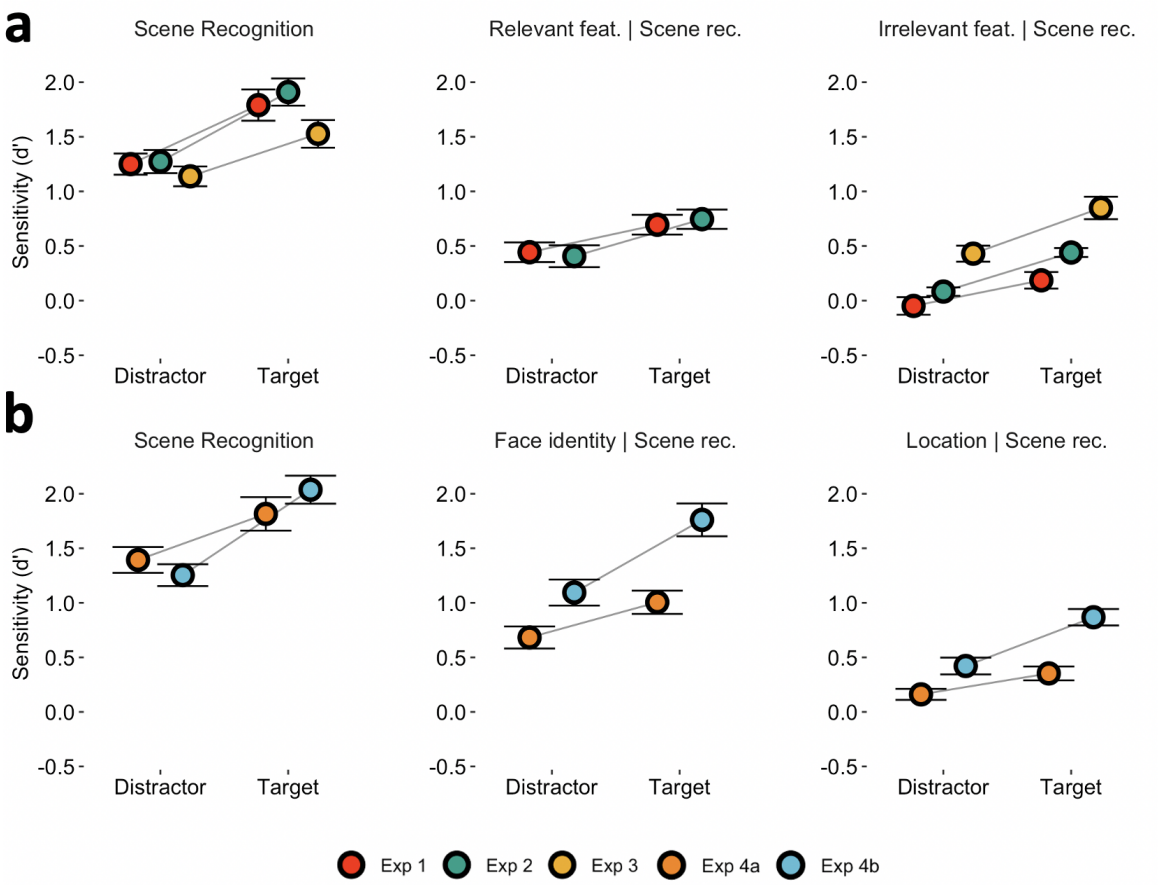

Figure 3.2 Sensitivity scores on all Experiments. *(a) Means and standard errors of memory performance (d') for the three experiments in T&S (Exp 1-3), split by the three recognition questions. The task-relevant feature in Experiment 3 (gender) was not tested. Values are replotted from T&S. (b) Memory performance in the new, instruction-manipulation experiments (Experiments 4a-b). Participants were instructed to memorize the faces in addition to the scenes in Experiment 4b (task-relevant) but not 4a (task-irrelevant). In both experiments, the location of the face varied across trials and was task-irrelevant. Error bars represent ±1 standard error of the mean.*

3.2.3.3 Recognition Memory Task: DDM Posterior Parameter Estimates

Analyses on posterior estimates (t-tests) are presented by question rather than by experiment to provide a more cohesive overview of which factors drove recognition test performance for different features of the trials (Tables 3.2-4; Fig. 3.3; contrast tests performed with DMC's compare.p are consistent with those reported here).

Scene Recognition. For the scene recognition test, drift rate was greater for target-paired scenes than distractor-paired scenes in all three experiments. Target detection during encoding also decreased non-decision time for subsequent scene recognition. There was no effect on bias and marginal evidence of greater boundary separation for target-paired scenes in Experiment 1.

Table 3.2
Analyses of posterior parameter estimates for scene recognition

Parameter	Experiment	*t*	*p*	*Cohen's d*
Drift (v)	*Exp. 1*	4.213	< .001	0.711
	Exp. 2	6.109	< .001	0.766
	Exp. 3	3.941	< .001	0.612
Bias (z)	*Exp. 1*	0.462	.646	0.098
	Exp. 2	-0.002	.999	< 0.001
	Exp. 3	-1.279	.210	0.297
Boundary (a)	*Exp. 1*	1.817	.078	0.193
	Exp. 2	1.000	.325	0.107
	Exp. 3	1.350	.187	0.157
Non-Decision Time (t0)	*Exp. 1*	-4.027	< .001	0.642
	Exp. 2	-2.517	.015	0.292
	Exp. 3	- 2.600	.014	0.339

Note. Inferential statistics for the difference in parameter estimates across cue conditions from models of scene recognition. Degrees of freedom for the t-statistics were 35, 48, and 33 for Experiments 1, 2, and 3, respectively.

Task-Relevant Feature Recognition. When asked to match the correct task-relevant feature of the cue to a correctly recognized scene, participants had higher drift rates in

Experiment 1 and 2. Evidence for a difference in non-decision time or boundary separation was mixed. Boundary separation was marginally larger for target conditions in Experiment 1 and significantly larger in Experiment 2. Non-decision time was lower for target conditions only in Experiment 1. Finally, there was no difference in bias.

Table 3.3
Analyses of posterior parameter estimates for task-relevant feature recognition

Parameter	**Experiment**	***t***	***p***	***Cohen's d***
Drift (v)	*Exp. 1*	2.280	.029	0.369
	Exp. 2	2.825	.007	0.463
Bias (z)	*Exp. 1*	0.656	.516	0.156
	Exp. 2	-0.635	.528	0.131
Boundary (a)	*Exp. 1*	-1.730	.093	0.178
	Exp. 2	-2.158	.036	0.278
Non-Decision Time (t0)	*Exp. 1*	-2.970	.005	0.359
	Exp. 2	-0.361	.720	0.045

Note. Inferential statistics for the difference in parameter estimates across cue conditions from models of recognition of the task-relevant feature of the cue. Degrees of freedom for the t-statistics were 35, 48, and 33 for Experiments 1, 2, and 3, respectively.

Task-Irrelevant Feature Recognition. The task-irrelevant feature was recognized with higher drift rates when that feature belonged to a target cue rather than a distractor cue during encoding (though the effect was weaker in Experiment 1). As with the task-relevant feature question, there was mixed evidence for a difference in non-decision time and boundary

separation. Neither were impacted in Experiment 1, but there was lower non-decision time and greater boundary separation for targets in Experiment 3. No differences were observed in bias.

Table 3.4
Analyses of posterior parameter estimates for task-irrelevant feature recognition

Parameter	Experiment	*t*	*p*	*Cohen's d*
Drift (v)	*Exp. 1*	1.942	.060	0.323
	Exp. 3	4.333	< .001	0.749
Bias (z)	*Exp. 1*	-0.885	.382	0.176
	Exp. 3	-0.959	.345	0.220
Boundary (a)	*Exp. 1*	-0.299	.766	0.031
	Exp. 3	3.106	.004	0.351
Non-Decision Time (t0)	*Exp. 1*	0.083	.935	0.014
	Exp. 3	-2.482	.018	0.402

Note. Inferential statistics for the difference in parameter estimates across cue conditions from models of recognition of the task-irrelevant feature of the cue. Degrees of freedom for the t-statistics were 35, 48, and 33 for Experiments 1, 2, and 3, respectively.

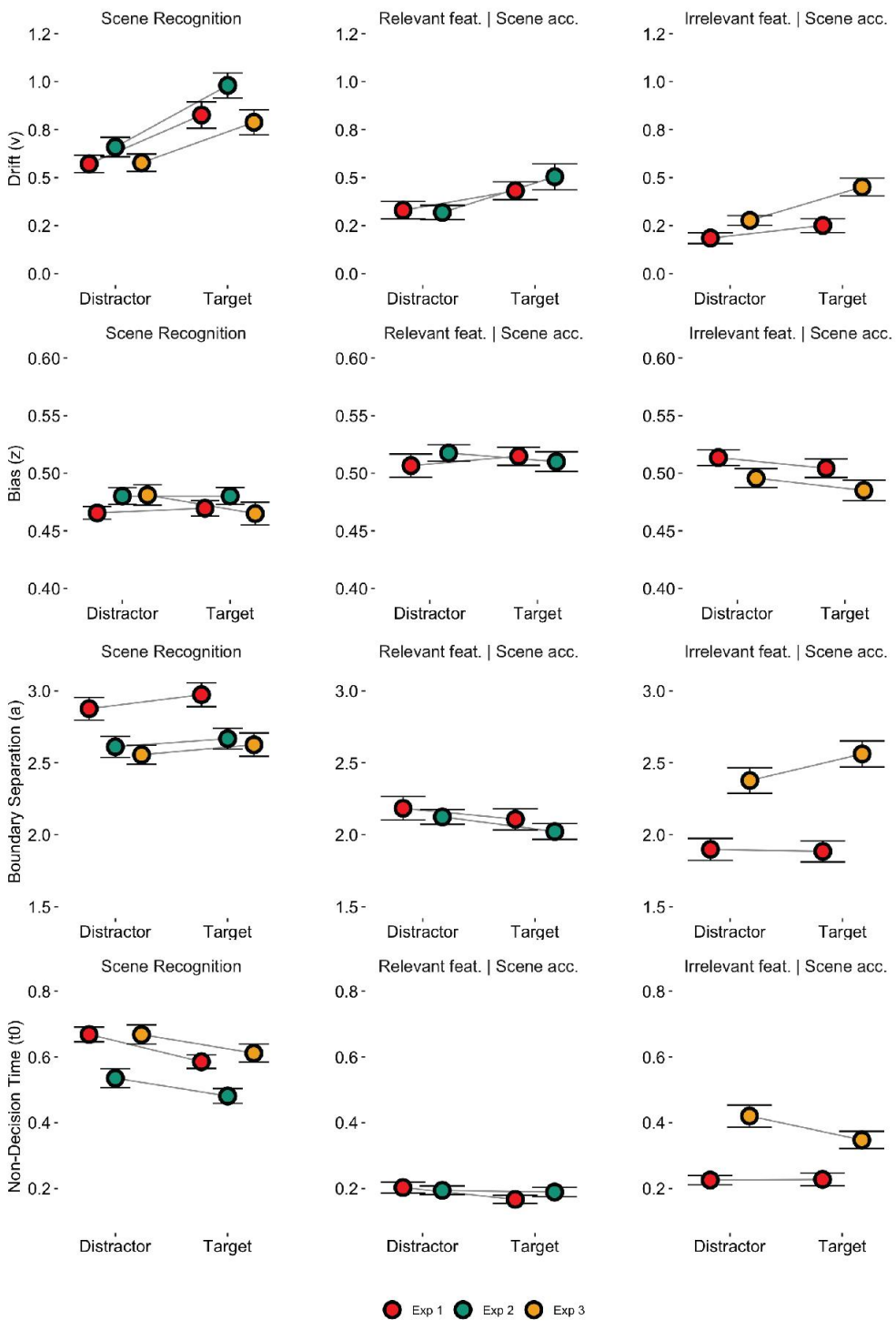

Figure 3.3 DDM parameter estimates in the recognition tasks in T&S. *Mean parameter estimates for each cue condition, recognition question, and experiment. Error bars represent ±1 standard error of the mean.*

3.2.3.4 Response Bias

A central concern raised about the findings in T&S is that they reflect an inference that scenes that are remembered well will be inferred to have been paired with a target, whereas scenes that are not remembered well will be inferred to have been paired with a distractor cue (Mulligan et al., 2021). This suggests that participants may be biased toward responding that a scene was paired with a target cue after they correctly recognized the scene, and a distractor cue when they were incorrect.

To address this issue, feature-coded models were fit to the relational memory questions for Experiments 1 and 2, with responses mapped to the specific feature indicated by the response rather than the button press. This was done for Question 2, in which participants were asked to report whether the scene appeared with the target cue or distractor cue (where response bias is of concern). It was also done for Question 3 of Experiment 1, where participants reported the feature of the cue that was irrelevant to the detection task. The data from Experiment 3 could not be fit to such a model, since all faces – and therefore all choices – were unique. If a response bias influences performance on the relevant feature questions, then bias estimates should shift away from 0.5 towards 1.0 (indicating a bias toward the target-cue option) following accurate scene recognition. They should move towards 0.0 (indicating a bias toward the distractor-cue option) following inaccurate scene recognition.

Parameter estimates provided evidence in favor of response bias changing with scene recognition accuracy in both Experiment 1 and 2 (Fig. 4; for drift, see Supplemental Information): bias shifted toward responses for the target color following correct recognition relative to incorrect recognition, $F(1,83) = 7.749$, $p = .007$, $\eta_p^2 = .09$. There was no effect of experiment, $F(1,83) = 0.714$, $p = .401$, $\eta_p^2 = .008$. As theorized by Mulligan et al. (2021), bias

following correct scene recognition increased above chance (z=.5) to .539 in Experiment 1, $t(35) = 3.985$, $p < .001$, $d = .664$ and to .541 in Experiment 2, $t(35) = 4.915$, $p < .001$, $d = .702$. However, bias following incorrect scene recognition remained at chance in both Experiment 1, $t(35) = .001$, $p = .999$, $d < .001$ and Experiment 2, $t(35) = 1.383$, p = .173, $d = .198$. This change in bias following correct scene recognition was relatively small and observed only for the relational memory question asking participants to report whether the scene was presented with a target or distractor cue. It was not present for the question regarding the irrelevant feature question in Experiment 1, $t(35) = -0.795$, $p = .432$, $d = .133$.

The effect of scene recognition on response bias for the relevant features supports the claim that bias could play a role in how participants answer these questions. However, because drift estimates also varied across target and distractor conditions in the button-coded models, the modeling shows that response bias is only one of several factors driving the ABE for relational memory of task-relevant features. This possibility is also exclusive to those questions where a response bias strategy was possible, which was not the case for most recognition memory questions in T&S for which it logically could play no role. Furthermore, the small magnitude of this response bias effect raises the question to what extent bias needs to be estimated to characterize the data well. This is investigated next.

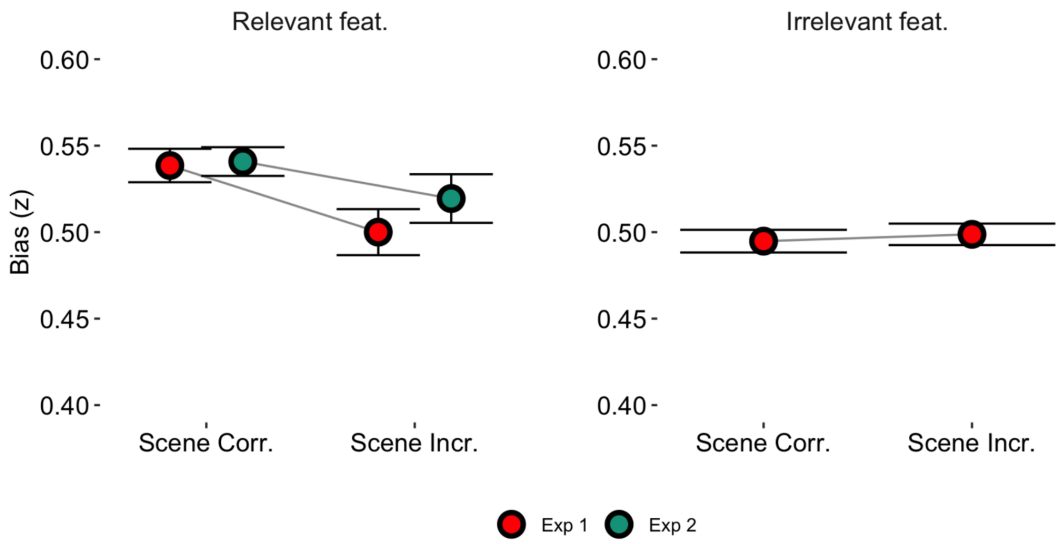

Figure 3.4 Estimates of bias from the feature-coded models. *Means of response bias estimates from the feature-coded models for the relevant feature and irrelevant feature questions in Experiments 1 and 2. Error bars represent ±1 standard error of the mean.*

3.2.3.5 Model Comparison

Parameter estimates from evidence-accumulation models, such as the DDM, may exhibit trade-offs, such that a change in one parameter can be compensated for by a change in another (Heathcote et al., 2019). This increases uncertainty about the reliability of estimates or the necessity of estimating certain parameters. Therefore, we compared the full models to simpler models in which either bias or drift was fixed across conditions. If drift or bias differ across conditions, then models in which they are fixed should produce poorer fits to the data than the full model. Conversely, bias-fixed or drift-fixed models should produce better fits to the data if that parameter is comparable across conditions. Therefore, if relational memory is enhanced in the ABE, then keeping drift fixed should produce a worse fit than the full model. If bias plays a role in accounting for these effects, then keeping bias fixed should also produce a worse fit. If

either drift or bias do not meaningfully differ across conditions, then keeping them fixed should improve model fit compared to the full model.

Models were evaluated using the Deviance Information Criterion (DIC), which penalizes models that have more free parameters (Spiegelhalter, Best, Carlin, & Van Der Linde, 2002). Bias-fixed models consistently performed better than the full model. When responses were coded based on the button press, the bias-fixed model (where z=0.5 for both cue conditions) produced a lower DIC than the full model for 58% of the participants on the scene recognition question (across all three experiments, N=120), 74% of participants for the task-relevant feature question, and 83% on the task-irrelevant feature model. Additionally, the feature-coded bias-fixed model also outperformed the feature-coded full model for 62% of participants on the three memory questions where feature-coding was possible. Model comparisons thus provided converging evidence that bias did not contribute meaningfully to responses on relational memory questions that tested memory for the task-relevant feature.

Drift-fixed button-coded models performed more poorly than the full model, despite the full model being penalized for having more parameters. On scene recognition questions, keeping drift fixed (v=1.0) produced a better model fit for only 8% of participants across all three experiments. Fixing drift resulted in a better fit for 7% of participants for the task-relevant feature question and 3% of participants for the task-irrelevant feature question. Similarly, drift-fixed feature-coded models outperformed the full feature-coded model for only 3.9% of participants, corroborating the proposal that drift during recognition is critically modulated by temporal selection during encoding.

In short, parameter estimates from the full model adequately captured the effects of encoding condition on drift during recognition memory task performance. They also capture bias

reasonably, given that the feature-coded model estimated it close to 0.5 and produced worse fits to the data than the bias-fixed feature-coded model. Thus, the small effect of scene recognition accuracy on bias in the feature-coded models appears to play a minor role in relational memory for task-relevant features.

3.2.4 Section I – T&S: Interim Discussion

The reanalysis of the data reported in T&S suggests that target detection during encoding increased drift rate during recognition. This was true whether participants were asked about the scene they were instructed to memorize or were asked about the task-relevant and task-irrelevant features of the detection task cue paired with that scene. There was also mixed evidence that boundary separation was higher and non-decision time was lower for tests of information presented on target trials rather than distractor trials.

Thus, DDM modeling of the three experiments in T&S supports the claim that temporal selection facilitates the encoding of information presented at behaviorally relevant moments (those when a target cue appears), and captures the spatial context in which the selected information appears (Broitman & Swallow, 2020; Swallow & Jiang, 2013; Turker & Swallow, 2019). In this way, temporal selection may result in higher quality memory representations that subsequently facilitate decision-making processes in the memory task.

The results from the DDMs also revealed that response bias may have had a small contribution to the subset of questions where inferential processes may have contributed to decision-making. However, employing different model instantiations suggested that the best fitting models were ones that kept bias fixed. Further, the relatively small difference in bias when the scene was correctly vs incorrectly recognized occurred in the presence of strong effects of

encoding condition on drift rate. Thus, although a role for bias, as outlined by Mulligan et al. (2021), was supported by these analyses, it cannot account for the overall relational memory effects reported in T&S.

3.3 Section II: Drift and bias for intentionally versus incidentally encoded information

The reanalysis of the data from T&S with DDM showed that the relational memory effects are primarily due to changes in drift rather than response bias. Though these findings are consistent with the ABE reflecting enhanced encoding on target trials, it is important to verify that the effects are replicable in a new sample of participants and that they are present for relational memory for the location of the cue presented with the scene. We therefore ran two new experiments to replicate and extend the findings from T&S. Like Experiment 3, participants intentionally encoded scenes while performing the detection task on faces that were uniquely paired with a scene. However, the faces could appear in one of two locations. Furthermore, like Experiment 3, participants were never tested on whether the scene was presented with a target or distractor cue. The relational memory questions instead asked about face identity and location. By design, these questions are not subject to contributions from biases to report that scenes that are better remembered are paired with a target.

Experiments 4a and 4b also provided an opportunity to examine whether the ABE for the background scene and for relational memory are influenced by the intentionality of encoding. Like other studies examining intentionality during encoding (e.g., Evans & Baddeley, 2018), instructions to participants were manipulated across the two experiments. Participants in Experiment 4a were instructed to memorize only the scene, while those in Experiment 4b were

instructed to memorize both the scene and the face. Participants were not instructed to memorize any conjunction of the scene, face, or the face's location.

In this way, Experiments 4a and 4b use a different approach than in prior studies: rather than manipulating instructions to memorize the background scene (or even its relationship to the detection task cue, see Mulligan et al., 2021), instructions in Experiment 4b directed participants to pay more attention to the cue. The primary result of this manipulation should be to increase attention to features of the cue that distinguish it from other faces. There are two potential consequences of doing so: First, it could increase interference with the scene encoding task. Therefore, if the ABE for the background image decreases when the ability to process and attend to the background scene is reduced (Hutmacher & Kuhbandner, 2020), then it should be smaller in Experiment 4b than in Experiment 4a. Second, by increasing attention to face identity, this manipulation may also result in a richer face representation that can be associated with the face's location and the background scene for both target and distractor trials, leading to overall better performance on the relational memory tests. However, if the ability to encode the faces and incidental relational information is boosted in the ABE, then these advantages should be even greater for target trials than for distractor trials.

Figure 3.5 Task design for Experiments 4a and 4b. *(a) Each trial of the encoding and detection task consisted of a scene and a superimposed face. The face and scene appeared simultaneously, but the face disappeared after 400 ms, leaving the scene on screen for another 600 ms. (b) During the recognition task, on each trial, participants were first tested on memory for the scene (always task-relevant), then on the identity of the face (task-irrelevant feature in Experiment 4a, but task-relevant in 4b) that appeared with the scene, and finally on the location of the face (always task-irrelevant) that appeared with the scene. The on-screen instructions have been simplified for this figure.*

3.3.1 Methods

All methods were identical to those described in Section I, except as indicated below.

3.3.1.1 Participants

Pilot data indicated that changing the face's location increased task difficulty. Participants also had more difficulty accurately performing the gender based detection task than the color based detection task in T&S (see Table 3.1, Experiment 3). Therefore, more participants were recruited for Experiments 4a and 4b to ensure that at least 32 participants in each study would meet performance-based inclusion criteria (target sample size was based on power calculations detailed in T&S). Participants were recruited in large batches (but run individually), resulting in 42 new participants being recruited for Experiment 4a and 56 being recruited for Experiment 4b.

However, consistent with our expectations that task difficulty would be greater in these experiments, after data collection was complete we found that many participants were unable to meet the performance criteria established for the earlier studies (⩾80% hits and ⩽10% false alarms) and using these criteria would result in a too small sample for Experiment 4a. Thus, to ensure a minimal sample size of 32 in both experiments, inclusion criteria were adjusted post hoc to ⩾80% hits and ⩽15% false alarms. This resulted in a sample of 32 participants in Experiment 4a (18 female; 18–22 years old; age M = 19.75, SD = 1.05) and 43 participants in Experiment 4b (21 female; 18–25 years old; age M = 20.30, SD = 1.46).

3.3.1.2 Procedures and Task Design

3.3.1.2.1 Encoding and Detection Task

The encoding/detection task was identical to T&S Experiment 3, with a few exceptions (Fig. 3.5). The visual angle, at 50 cm from the screen, for the faces was approximately 3 degrees to either the left or right half of the scene's center. A given face was always presented in the same location on the scene. In addition, half of the faces in each condition were presented on the left, while the other half were presented on the right. The location was orthogonal to the detection task. In addition, the duration of the cue was increased to 400 ms because a pilot sample indicated that participants needed longer to perform the task when the face appeared in variable locations. Scene duration was unchanged, however. The encoding/detection task took approximately 30 minutes.

The relevance of the face's identity was manipulated across experiments In Experiment 4a, participants were told they would only be tested on the scenes. In Experiment 4b, participants were informed they would be tested on both the scenes and the faces. No mention was made of

the pairing between a given scene, face, or the face's location on the scene to either group of participants.

3.3.1.2.2 Recognition Memory Task

As in prior experiments, participants completed 100 trials (Fig. 3.5b). Each trial included three questions, one for each scene-face-location conjunction in the encoding/detection task. First, participants chose between a scene shown during encoding (the old scene) and a novel foil. The old scene was then displayed in the center of the screen, whether correctly chosen or not, and two faces from the detection task of the same gender were displayed (one on each side). Note that participants chose between two faces used in the encoding/detection task, making it a true test of relational memory. As in most recognition task questions in Section I, this meant that they could not rely on some form of response bias to infer the correct response. Participants selected the face paired with that scene. Finally, the correct scene and face were shown, with the face superimposed on the scene at both locations. Participants indicated whether the face appeared on the left or right. The recognition task took approximately 30 minutes to complete.

3.3.2 Results

3.3.2.1 Encoding and Detection Task

Descriptive statistics of detection task performance for those participants who met the inclusion criteria are reported in Table 1. False alarm rates were closer to 10%, and were higher than those in Experiment 3, $t(45.637) = 3.771$, $p < .001$, $d = .946$ for Exp 4a and $t(73.629) = 3.861$, $p < .001$, $d = .849$ for Experiment 4b.

In Experiment 4a, among those 10 participants excluded from further analyses, the mean hit percentage was still high, 93.5% (SD = 3.6%), but so were false alarms, M = 17.1% (SD = 3.5%). Similarly, in Experiment 4b, for those 13 participants excluded from analyses, average hits were high, 95.6% (SD = 3.5%), and false alarms averaged 17.5% (SD = 2.1%), Thus, those excluded from further analyses were done so primarily on the basis of responding erroneously to distractor cues, rather than missing target cues, despite performance criteria being loosened to include participants with up to 15% false alarms.

The higher false alarm rates in Experiments 4a and 4b as well as the increased number of excluded participants (despite the more liberal inclusion criteria) suggests that Experiment 4a and 4b were more difficult than the experiments in Section I. Among participants who met performance criteria, instructing participants to memorize the face's identity in Experiment 4b did not appear to interfere with performance on the gender-based detection task compared to 4a, $t(55.208) = .376$, $d = .217$.

3.3.2.2 Recognition Memory Task: Performance

The effect of cue condition, experiment, and their interaction on sensitivity was evaluated in linear mixed effects models fit to data for each question using lmer (Bates, Maechler, & Bolker, 2012; Brown, 2021; Westfall, Kenny, & Judd, 2014), and Holm corrected contrast tests to characterize significant effects (emmeans; Lenth, 2019). In both experiments, recognition accuracy was better for stimuli presented on target trials than distractor trials (Fig. 3.2b; Table 3.5). Response times across the three questions did not significantly differ across conditions, indicating no speed-accuracy tradeoff (Table 3.6).

Table 3.5
ANOVA table of recognition performance in Experiments 4a-b

Question	Effect	*F*	*p*	η_p^2
Scene Recognition	*Exp*	0.069	.794	< .01
	Cue	48.807	< .001	.40
	*Exp*Cue*	4.396	.039	.06
Face Identity | Scene	*Exp*	12.557	< .001	.15
	Cue	42.954	< .001	.37
	*Exp*Cue*	5.194	.026	.07
Location | Scene	*Exp*	18.904	< .001	.21
	Cue	43.141	< .001	.37
	*Exp*Cue*	6.848	.011	.09

Note. Analysis of sensitivity scores on the recognition task in Experiments 4a and 4b. For Scene Recognition, degrees of freedom are $F(1,72.998)$ for Cue and the interaction, $F(1,73.003)$ for Experiment. For matching of face identity, degrees of freedom are $F(1,73)$. For location recognition, degrees of freedom are $F(1,73.003)$ for Exp, $F(1,72.998)$ for Cue, and $F(1,73)$ for the interaction.

Table 3.6
ANOVA table of response times for recognition in Experiments 4a-b

Question	Effect	*F*	*p*	η_p^2
Scene Recognition	*Exp*	1.442	.234	.02
	Cue	40.361	< .001	.35
	*Exp*Cue*	7.449	.008	.09
Face Identity | Scene	*Exp*	0.465	.497	< .01
	Cue	23.174	< .001	.24
	*Exp*Cue*	1.082	.302	.01
Location | Scene	*Exp*	8.808	.004	.11
	Cue	0.237	.628	< .01
	*Exp*Cue*	2.758	.101	.04

Note. Analysis of response times on the recognition task in Experiments 4a and 4b. For scene recognition, degrees of freedom are $F(1,73)$ for all effects. For matching face identity, degrees of freedom are $F(1,73.103)$ for Exp and $F(1,72.271)$ for Cue and the interaction. For location recognition, degrees of freedom are $F(1,73.015)$ for Exp and $F(1,72.152)$ for Cue and the interaction.

Scene Recognition. A linear-mixed-effects model of sensitivity scores, with experiment and cue condition as fixed effects and participant as a random effect, revealed a main effect of cue, no effect of experiment, and a significant interaction (Table 3.5). Holm corrected post-hoc comparisons showed sensitivity was higher for scenes presented on target trials than on distractor trials in Experiment 4a, $t(73) = 3.229$, $p = .002$, $d = .807$ and Experiment 4b, $t(73) = 6.953$, $p < .001$, $d = 1.499$, replicating the ABE in each experiment. There were no effects of experiment on performance within each cue condition, $t(114) < 1.243$, $p > .216$. Thus, the interaction suggests that the ABE was present, but larger in Experiment 4b than in Experiment 4a (Fig. 3.2b).

In response times, there was a main effect of cue, not for experiment, and a significant interaction. Post-hoc comparisons revealed that responses were faster in Experiment 4a for target-paired scenes (M = 1.36 s, SD = .29 s) than for distractor-paired scenes (M = 1.45 s, SD = .31 s), $t(72) = -2.379$, $p = .020$, $d = .595$. In Experiment 4b, responses were also faster for target-paired scenes (M = 1.38 s, SD = .34 s) than distractor-paired scenes (M = 1.61 s, SD = .41 s), $t(72.3) = -6.801$, $p < .001$, $d = 1.483$. Responses to distractor-paired scenes were marginally faster in Experiment 4a than in Experiment 4b, $t(88.2) = 1.984$, $p = .050$, $d = 1.054$. This suggests that, although instructing participants to memorize the face did not appear to interfere with accurate scene recognition, it may have had a small, negative effect on the accessibility or quality of these memory traces.

Relational Memory for Face Identity. For sensitivity, there was a significant main effect of cue, experiment, and an interaction (Table 3.5). Holm corrected comparisons showed that sensitivity to the identity of the face paired with a scene was higher in Experiment 4b than in Experiment 4a, both when the face was a target cue, $t(102) = 4.171$, $p < .001$, $d = .485$ and when the face was a distractor cue, $t(102) = 2.273$, $p = .025$, $d = .306$. Importantly, sensitivity for which of two faces was paired with a scene was greater for target relative to distractor trials in Experiment 4a, $t(73) = 2.823$, $p = .006$, $d = .923$, and in Exp 4b, $t(73) = 6.761$, $p < .001$, $d = 1.714$. Thus, the interaction suggests that the ABE was present in both experiments (replicating Experiment 3, Chapter 2), but that it was larger when participants were instructed to memorize the face (in Experiment 4b) than when they were not (in Experiment 4a; Fig. 3.2).

As for response times, a significant main effect of cue (Table 3.6) indicated that responses were faster for reporting which of two faces appeared with a scene when the faces

were target, rather than distractor, cues. Post-hoc comparisons showed that in Experiment 4a, responses were faster for target faces (M = 1.41 s, SD = .36 s) than distractor faces (M = 1.51 s, SD = .37 s), $t(72) = 2.503$, $p = .015$, $d = .626$. This was also the case in Experiment 4b (M = 1.33 s, SD = .43 s for target faces; M = 1.48 s, SD = .37 s for distractor faces), $t(72.3) = 4.453$, $p < .001$, $d = .971$.

Relational Memory for Face Location. There were main effects of cue, experiment, and an interaction on sensitivity to the face's location (Table 3.5). Post-hoc comparisons revealed accuracy was higher for target-cue locations relative to distractor-cue locations in Experiment 4a, $t(73) = 2.609$ $p = .011$, $d = .652$, and Experiment 4b, $t(73) = 7.031$, $p < .001$, $d = 1.516$. Across experiments, target-cue locations were better recognized when participants were instructed to memorize the face (in Experiment 4b), $t(113) = 5.070$, $p < .001$, $d = 1.747$, as were distractor-cue locations, $t(113) = 2.563$, $p = .012$, $d = .883$.

Linear mixed effects models of response times indicated a significant main effect of experiment, but no significant main effect of cue condition or interaction (Table 3.6). Holm corrected post-hoc comparisons revealed that face location was recognized faster in Experiment 4b than in 4a, both for target trials (Exp 4a.: M = 1.22 s, SD = .45 s; Exp 4b: M = .90 s, SD = .40 s), $t(84) = 3.299$, $p = .001$, $d = 2.072$, and for distractor trials (Experiment 4a: M = 1.16 s, SD = .41 s; Experiment 4b: M = .92 s, SD = .42 s), $t(83.7) = 2.425$, $p = .017$, $d = 1.521$.

3.3.2.3 Recognition Memory Task: DDM Posterior Parameter Estimates

Results for linear mixed effects models of the full DDM model are again presented by question rather than by experiment to provide a more cohesive overview of the factors that drove

recognition test performance for different components of the trials (Fig. 3.6; Table 3.7-9). Generally, the ABE for scenes was most reflected in estimates of drift in both experiments. However, the effect on drift was larger when the face was intentionally encoded. The same was the case for recognition of face identity and location. The evidence for effects on boundary separation or non-decision time were mixed in Experiment 4a, but clearer in Experiment 4b.

Scene Recognition. When participants were asked to indicate which of two scenes was presented in the encoding task, drift rates were significantly influenced by cue condition, experiment, and their interaction (Table 3.7; Fig. 3.6). Post-hoc Holm corrected comparisons revealed that drift estimates were higher for target paired scenes than distractor paired scenes in both Experiment 4a, $t(73) = 3.609$, $p = .001$, $d = .902$, and Experiment 4b, $t(73) = 7.934$, $p < .001$, $d = 1.711$. Drift estimates did not differ significantly across experiments for target-paired scenes, $t(99.8) = 1.058$, $p = .292$), or for distractor-paired scenes, $t(99.8) = .899$, $p = .371$. Boundary separation and non-decision time (but not bias) also differed across cue conditions, but this effect did not interact with the experiment.

Table 3.7
ANOVA table of posterior parameter estimates on scene recognition

Parameter	Effect	*F*	*p*	η_p^2
Drift (v)	*Exp*	0.008	.931	< .001
	Cue	62.651	< .001	.46
	*Exp*Cue*	6.000	0.017	.08
Bias (z)	*Exp*	0.177	.675	< .01
	Cue	1.044	.310	.01
	*Exp*Cue*	0.147	.702	< .01
Boundary (a)	*Exp*	1.851	.178	.02
	Cue	8.775	.004	.11
	*Exp*Cue*	2.069	.155	.03
Non-Decision Time (t0)	*Exp*	0.281	.598	< .01
	Cue	10.496	.002	.13
	*Exp*Cue*	2.654	.108	.04

Note. Degrees of freedom were $F(1,73)$.

Relational Memory for Face Identity Matching. When participants had to report which of two faces appeared with a scene, drift rates were impacted by cue condition, experiment, and their interaction (Table 3.8). Holm corrected comparisons indicated that drift was faster for reporting which target face appeared with a scene than they were for distractor faces in both Experiment 4a, $t(73) = 2.715$, $p = .008$, $d = .679$, and Experiment 4b, $t(73) = 6.508$, $p < .001$, $d = 1.404$. Drift was also faster for pairing a target face with its background scene when participants memorized face identity (Experiment 4b) than when they did not (Experiment 4a), $t(101) = 3.492$, $p = .001$, $d = 1.414$. This difference was not significant for distractor trials, $t(101) = 1.702$,

p = .092, suggesting that the ABE for relational memory was larger in Experiment 4b primarily because of a larger advantage for information presented on target trials relative to distractor trials. Boundary separation and non-decision time (but not bias) were also impacted by cue condition (Table 3.8): boundary separation was greater and non-decision time was reduced for target trials relative to distractor trials (Fig. 3.6). Boundary separation was greater for Experiment 4b than for Experiment 4a.

Table 3.8
ANOVA table of posterior parameter estimates on face identity matching

Parameter	**Effect**	***F***	***p***	η_p^2
Drift (v)	*Exp*	8.087	.006	.10
	Cue	39.779	< .001	.35
	*Exp*Cue*	4.821	.031	.06
Bias (z)	*Exp*	.099	.754	< .001
	Cue	.209	.648	< .01
	*Exp*Cue*	.533	.467	< .01
Boundary (a)	*Exp*	6.034	.016	.08
	Cue	12.391	< .001	.15
	*Exp*Cue*	0.641	.426	< .01
Non-Decision Time (t0)	*Exp*	1.340	.251	.02
	Cue	23.410	< .001	.24
	*Exp*Cue*	.500	.482	< .01

Note. Degrees of freedom were $F(1,73)$.

Relational Memory for Face Location. When participants were asked to report where the face appeared on the scene, drift rates significantly depended on experiment, cue condition, and

their interaction (Table 3.9). Post-hoc comparisons showed that drift rates were higher for the locations of target faces relative to distractor faces in Experiment 4b, $t(73) = 6.002$, $p < .001$, $d = 1.294$, but the difference was marginal in Experiment 4a, $t(73) = 1.687$, $p = .096$. Bias additionally showed a main effect of cue (participants were more likely to respond with the right key on distractor trials, with bias near .5 on target trials), though none of the post-hoc comparisons were significant, largest $t(73) = 1.941$, $p = .056$ for Experiment 4b.

Boundary separation was larger for target trials than distractor trials and was lower when faces were intentionally encoded (Experiment 4b) than when they were not (Experiment 4a). Non-decision time also differed across cue conditions and experiments. However, a trend toward a cue condition x experiment interaction reflected faster non-decision times for face location on target trials than on distractor trials in Experiment 4b, $t(73) = -3.437$, $p = .001$, $d = .741$, but not Exp 4a, $t(73) = .526$, $p = .601$, $d = .131$. Non-decision times for target trials also were faster in Experiment 4b than in Experiment 4a, $t(102) = 3.180$, $p = .002$, $d = .665$.

Table 3.9
ANOVA table of posterior parameter estimates on location recognition

Parameter	Effect	*F*	*p*	η_p^2
Drift (v)	*Exp*	19.898	< .001	.21
	Cue	27.014	< .001	.27
	*Exp*Cue*	6.986	.010	.09
Bias (z)	*Exp*	0.019	.890	< .001
	Cue	6.026	.016	.08
	*Exp*Cue*	0.007	.934	< .001
Boundary (a)	*Exp*	3.170	.079	.04
	Cue	7.606	.007	.09
	*Exp*Cue*	0.334	.565	< .01
Non-Decision Time (t0)	*Exp*	7.051	.010	.09
	Cue	6.987	.010	.09
	*Exp*Cue*	3.410	.067	.04

Note. Degrees of freedom were $F(1,73)$.

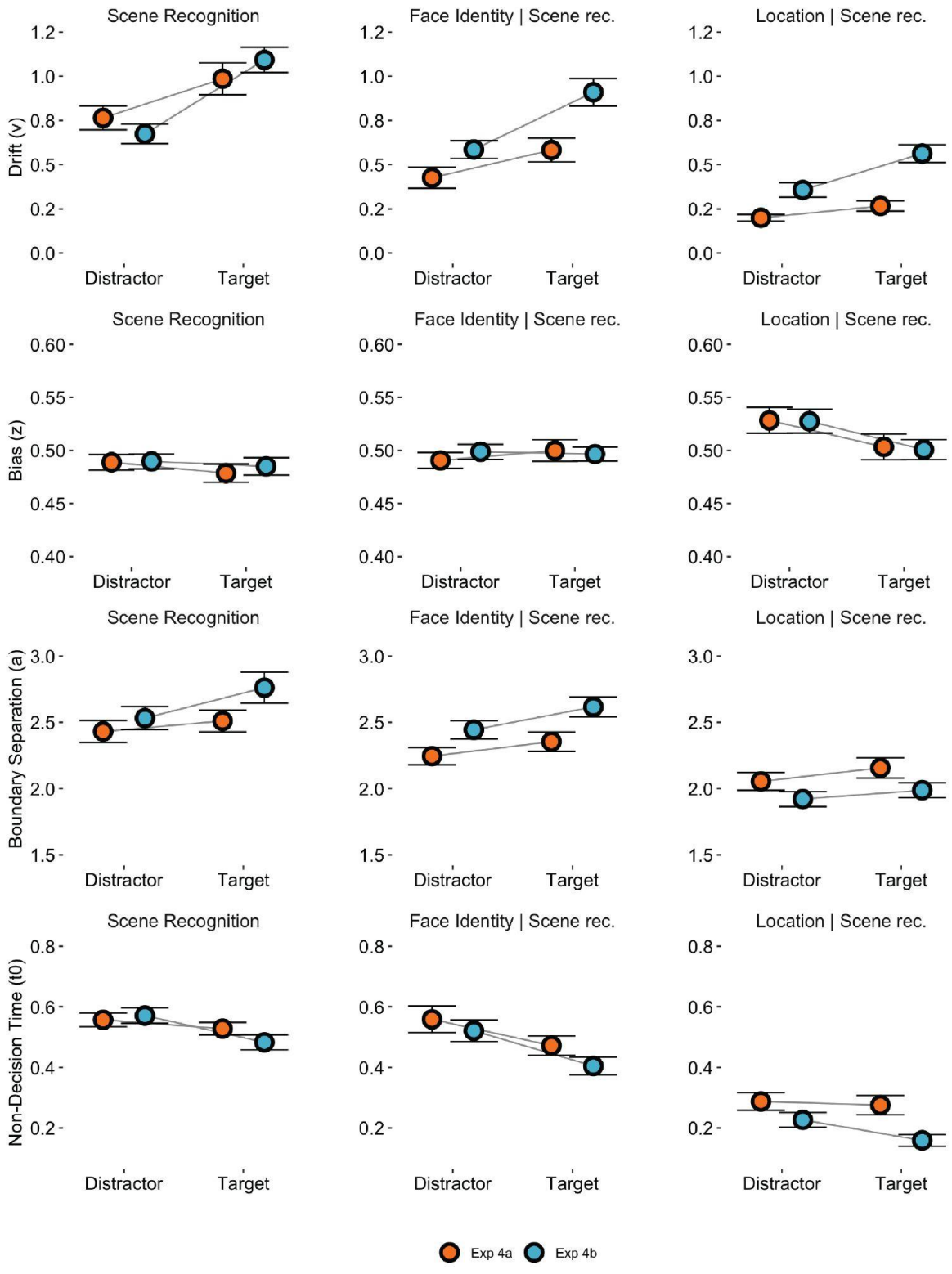

Figure 3.6 DDM parameter estimates in the recognition tasks in Exp 4a-b. *Means and standard error for drift, bias, boundary separation, and non-decision time, calculated for each participant and split by cue condition. Error bars represent ±1 standard error of the mean.*

3.3.3 Section II – Experiments 4a-b: Interim Discussion

Both new experiments broadly replicated the findings from Chapter 2: information presented on target trials is better remembered than information presented on distractor trials, even when it is incidental to the ongoing task. These effects can be observed in sensitivity and in the rate at which evidence is accumulated during recognition. The design of the new experiments also allowed modeling of the task-irrelevant location, which was not possible in Experiment 2. Here too, the drift rates were higher for the locations of target faces than for distractor faces, with a larger effect in Experiment 4b.

Bias did not significantly differ across cue conditions for the scene recognition and face identity questions. Indeed, for button-coded responses, the bias-fixed model outperformed the full model 63% of the time (N=75; 60% across all five experiments with N=195) on scene recognition. It outperformed the full model 78% of the time on the question where participants had to match face identity to the scene (76% across all five experiments regarding the task-relevant feature). Although there was a bias toward indicating that the face appeared on the right when the face was a distractor, the button-coded bias-fixed model specification produced a better fit for 64% of all participants in Experiments 4a and 4b for this question (83% across all experiments with a task-irrelevant feature question). Keeping drift fixed again resulted in poor fit compared to the full model which allowed it to vary between cue conditions. That drift-fixed model outperformed the full model only 17% of the time on scene recognition (11% across all experiments), 12% on matching face identity (8% across all task-relevant feature questions), and 14% on location recognition (6% across all task-irrelevant feature questions in this study). There

are no feature-coded models for Experiments 4a and 4b. Thus, the ABE incorporates relational memory between the cues, their location, as well as the background scene itself.

In Experiment 4b, participants were additionally instructed to memorize the identity of the face. This manipulation both changes the intentionality of face memory and also requires participants to do more in a task that already produces a significant amount of dual-task interference (Spataro et al., 2013; Swallow & Jiang, 2010). In Experiment 4b, instructing participants to attend to the identity of all the faces led to numerically poorer and significantly slower scene recognition in the distractor condition than when face identity was incidental to the task. This suggests that attention to the background scenes was comparable across conditions, if not worse when the face was intentionally encoded. Yet, the magnitude of the ABE for the background scene was significantly greater when the face was intentionally, rather than incidentally, encoded.

These findings contrast with the suggestion that incidental memory for the background scene reflects a failure of the detection task to prevent excess attention from being directed toward it (Hutmacher & Kuhbandner, 2020). This implies that the ABE should be smaller when the detection task is more difficult and requires more attention. However, if this were the case, then the ABE should have been weaker or comparable in magnitude, not larger, in Experiment 4b than in Experiment 4a.

In contrast to the minimal evidence that instructions to memorize the face increased interference with scene encoding, the manipulation was clearly effective in raising overall levels of relational memory. Importantly, the effect of target detection on relational memory interacted with encoding instructions: the impact that target detection had on memory was larger and more consistent when the face was intentionally, rather than incidentally, encoded. This occurred

despite task demands being higher when having to intentionally encode both scenes and faces instead of only the scenes. Consistent with previous findings (e.g., Broitman & Swallow 2020; Dewald, Sinnet, & Doumas, 2011, 2013; Hutmacher & Kuhbandner, 2020; Sisk & Lee, 2022; Swallow & Jiang, 2011, 2014; Walker et al., 2017; but see Mulligan et al., 2021), these data further demonstrate that the ABE is modulated by goal-directed attention: directing participants to attend to more of the display increases the benefit from target detection for those elements as well as their momentary configural relationship.

3.4 General Discussion

Recent work on the ABE claims that it extends to incidental relational information (Turker & Swallow, 2019). However, these relational memory effects have been challenged, warranting a deeper investigation into how they arise and establishing their robustness and replicability. Specifically, it remained unclear to what extent intentionality during encoding and response bias during recognition contributed to previously reported incidental relational memory effects. Those questions were addressed here by using diffusion-decision modeling (Ratcliff, 1978) of previously reported data and two new experiments to characterize how the ABE influences the latent cognitive processes involved in recognition. Previously reported effects of target detection on incidental relational memory were replicated in the new experiments and shown to be associated with higher drift rates in all cases. The advantage for information presented on target trials was repeatedly demonstrated for relational memory questions where response bias could not have contributed to the target trial advantage. Moreover, instructing participants to intentionally encode more items from each trial resulted in an increased, rather

than decreased, ABE for both the intentionally encoded background scene and incidental relational memory.

3.4.1 DDMs reveal that the ABE is present in evidence accumulation rates

Across all five experiments and for each of the memory questions, evidence accumulation was higher for target-paired information than for distractor-paired information. The effect of target detection on drift rates was strongest for the scene memory questions, weaker for the task-relevant relational memory questions, and weakest, but still present, for the task-irrelevant relational memory questions. Drift rates should be higher when the information presented at test provides a better match to the information stored in memory (Ratcliff & McKoon, 2007). Thus, higher drift rates on questions about target trials relative to distractor trials imply that target detection during encoding results in higher quality memory representations. These higher quality representations then allow for more accurate and faster comparisons to the options in the 2AFC recognition task.

A critical question addressed in this study was whether performance on the relational memory questions reflects a true memory advantage or is instead due to a response bias. The target-associated advantage in drift rates observed here, for both task-relevant and task-irrelevant relational memory, provides a clear answer. Not only were drift rates higher for relational memory for target trials than distractor trials, more parsimonious models that kept drift fixed performed more poorly than those that allowed it to vary across conditions. This was not the case for models that fixed response bias, which performed as well as or better than models that allowed bias to vary across target and distractor conditions. Feature-coded models provided some evidence of a shift in bias that conforms to the pattern described by Mulligan et al. (2021). That

study demonstrated that participants were more likely to report that items with a weak or no memory trace were presented with a distractor during encoding. However, with DDM modeling and comparison to a bias-fixed model, the current data suggest that bias is unlikely to account for all the relational memory effects. This conclusion is strongly supported by Experiments 3, 4a, and 4b, where a memory strength-based response bias was not possible by design, yet relational memory effects were still observed.

Moreover, Experiment 4a tested relational memory for two features of the detection task cue that were incidental to the detection and encoding task: identity of the unique face paired with the scene and the location at which that face had been presented. Results demonstrated that the advantage in drift rates and sensitivity can occur for multiple task-irrelevant features at once. Turker & Swallow (2019) had previously demonstrated this possibility for only one task-irrelevant feature. Accordingly, relational memory is enhanced by temporal selection during encoding, such that multiple constituent features of a given trial, immediately relevant to one's ongoing behavior or not, enjoy this encoding benefit.

The observation that the ABE extends to incidental relational memory does not necessarily contradict findings that suggest that it does not incorporate all aspects of context. Different experiments operationalize context memory differently, focusing on temporal relationships (i.e., whether a word was presented early versus late in a list; Mulligan et al., 2016), perceptual features of to-be-encoded words (i.e., color, font, modality; Mulligan et al., 2016), subjective reports of memory quality (i.e., remember/know judgments or confidence ratings; Broitman & Swallow, 2020; Leclercq et al., 2014; Meng et al., 2019), semantic features of words (Spataro et al., 2021), or the association between concurrent items and features of the detection task cues (as in this study). While the "relational memory" construct (Cohen & Eichenbaum,

1993) captures the types of associations examined in the present study, it does not necessarily incorporate all of these features of context memory. Evidence that one aspect of context memory is enhanced in the ABE is not evidence that it will also be enhanced for other aspects of context memory. Our results show clearly that incidental relational memory for pictures is boosted by target detection, demonstrating that information about "what appeared with what else, and where" is captured by temporal selection. Based on the available evidence, it seems unlikely that this translates into a boost for "what appeared when".

Further, it remains possible that differences in the materials participants are asked to memorize may result in different effects. Studies that have reported no advantage for context memory in the ABE have used words (Mulligan et al., 2016; Mulligan et al., 2021; Spataro et al., 2021), while those that have found an effect have used pictures (Leclercq et al., 2014; Swallow & Atir, 2019; Turker & Swallow, 2019). Intentional memorization of verbal and visual materials may lead participants to process these items differently, with greater emphasis on meaning for words and fine grained detail in visual scenes, particularly when the visual materials are categorically similar (Evans & Baddeley, 2018). Consistent with this possibility, compared to verbal stimuli, pictures benefit less from deeper levels of processing and instructions to memorize (Baddeley & Hitch, 2017; Craik & Lockhart, 1972), and memory for where an item appeared during encoding may be worse for words than for pictures (Onyper, Zhang, & Howard, 2010). This could mean that, in a study using verbal materials, manipulating encoding instructions may have different effects than those observed here.

3.4.2 The ABE is present in other factors contributing to decisions

Target detection also occasionally resulted in greater boundary separation and lower non-decision time. Higher boundary separation reflects more cautious responding, whereas lower non-decision time reflects faster stimulus processing or response execution once a decision is reached (Heathcote et al., 2019). The pattern was most clear in Experiment 3 when participants were asked to indicate which of two faces appeared with a scene. Because the question required participants to decide between two faces from the same condition and that were both presented in the encoding task, increased boundary separation for target faces could reflect greater response caution when both faces are remembered well, even in light of a higher drift rate. In contrast, lower non-decision times could reflect faster fluency of encoding the target faces in the 2AFC, faster retrieval prior to matching the correct face to its scene, or faster response execution once the decision was made. These possibilities cannot be arbitrated with these data and will require further research.

In Experiments 4a and 4b, there was also greater boundary separation and lower non-decision for the question regarding which face appeared with a scene when the face was a target rather than a distractor. Although this effect did not differ across experiments, boundary separation was higher overall in Experiment 4b. This indicates that when participants are asked to decide which of two familiar faces appeared with a given scene, response caution was greater for the faces that were intentionally encoded. Moreover, intentionally encoding the faces also increased the magnitude of the ABE on non-decision time for the face's location. This supports the idea that goal-directed encoding of a face enhances the ABE for scene-face pairs.

3.4.3 The ABE is stronger when more attention is paid to the detection task cue

A second question addressed in this study was whether the ABE is modulated by intentionality during encoding (Broitman & Swallow, 2020; Hutmacher & Kuhbandner, 2020; Mulligan et al., 2021). The current study provides additional evidence that the intention to encode modulates the ABE. Despite instructions directing more attention to the faces in Experiment 4b than in 4a, the memory advantage for target-paired scenes relative to distractor-paired scenes was larger. Furthermore, the magnitude of the ABE was also larger for matching the face to its paired scene and for indicating where that face appeared. Thus, the intention to encode the identity of the face increased the magnitude of the ABE on memory for background scenes and on relational memory for task-relevant and task-irrelevant information.

The matter of intentionality reflects a broader ongoing debate about the necessity of (goal-directed) attention and intention for memory. When it comes to visual scenes, the intention to encode an item for an expected memory test will most strongly benefit scenes that have few unique details (Evans & Baddeley, 2018). In the current study, all participants intentionally encoded scenes that varied widely in type and in perceptual detail (e.g., cities with buildings, houses, various kinds of landscapes). Within category, however, many scenes were visually similar, though this was more true for some types of scenes (beaches) than others (houses). It is therefore possible that the instruction to memorize the scenes in this study may be stronger for some categories of scenes than for others. Faces were either intentionally or incidentally encoded and they are rich in unique detail (Burton, Schweinberger, Jenkins, & Kaufmann, 2015; Taubert, Apthorp, Aagten-Murphy, & Alais, 2011). Yet, instructing participants to memorize the faces also resulted in better overall relational memory. All in all, the current findings represent a robust

and replicable exception to the observation that visual encoding is not strongly influenced by the instruction to memorize an image (Baddeley & Hitch, 2017).

3.4.4 Implications for mechanisms that generate the ABE

This study suggests that the interaction of task demands with the ABE may be more complicated than previously assumed and that, since response bias cannot account for all findings, intentional and incidental relational memory is indeed being enhanced. Significant dual-task interference has previously been reported in the continuous detection task (Swallow & Jiang, 2010) and target detection interferes with the ability to process other concurrent stimuli (Duncan, 1980). It is therefore unclear why instructing participants to intentionally encode another, unrelated image produces a larger memory benefit for scenes presented with a target. The possibility of the ABE extending to incidentally encoded information (e.g., Dewald et al., 2013; Swallow & Jiang, 2014) also contrasts with work suggesting that incidental, task-irrelevant information may be inhibited during encoding (e.g., Choi, Seitz, & Watanabe, 2009; Leclercq et al., 2014; Walker, Ciraolo, Dewald, & Sinnett, 2017). Resolving these remaining issues will require a better understanding of the neural mechanisms involved in the ABE. Regardless, however, the data show that whatever mechanism produces the ABE, it is modulated by goal-directed attention.

One account of the ABE (Swallow & Jiang, 2013) suggests that it reflects a transient enhancement of encoding through temporal selection, and that temporal selection occurs when an event requires a response, whether that is pressing a button (e.g., the current study), incrementing an internal counter (Swallow & Jiang, 2012), or withholding from repetitive button pressing (Makovski et al., 2013; also see Toh & Lee, 2022). Temporal selection may occur via

the phasic engagement of neuromodulatory systems that respond to behaviorally relevant events (Briand, Gritton, Howe, Young, & Sarter, 2007). The locus coeruleus system, in particular, may be an important contributor to the mechanism that underpins the ABE (Hoffing & Seitz, 2015; Moyal et al., preprint; Swallow, Jiang, & Riley, 2019; Swallow, Makovski, & Jiang, 2012; Yebra et al., 2019): the locus coeruleus is involved in decision-making processes preceding responses to Go cues in Go-NoGo tasks (Clayton, Rajkowski, Cohen, & Aston-Jones, 2004; Rajkowski, Majczynski, Clayton, & Aston-Jones, 2004; Aston-Jones & Waterhouse, 2016; Berridge & Waterhouse, 2003), modulating task engagement (e.g., Gilzenrat, Nieuwenhuis, Jepma, & Cohen, 2010), and modulating broader brain-wide network dynamics (e.g. Bouret & Sara, 2005; Shine, 2019; Turker, Riley, Luh, Colcombe, & Swallow, 2021) as well as more localized representations in areas critical for relational memory, such as the hippocampus (e.g., Cohen & Eichenbaum, 1993; Kempadoo, Mosharov, Choi, Sulzer, & Kandel, 2016; Konkel & Cohen, 2009). Furthermore, the locus coeruleus also amplifies the effects of goal-directed attention on visual processing via positive feedback loops between local norepinephrine release and glutamate in perceptual processing areas (Mather, Clewett, Sakaki, & Harley, 2016), meaning that it may contribute critically to the impact of task-instructions observed here. In sum, in order to ground the current study's findings better in cognitive and neural mechanisms, further investigation into this neuromodulatory system's direct effects on regions supporting goal-directed attention and perception as well as memory is warranted.

3.4.5 Limitations

Several limitations to this study may impact the ability to generalize the results to other intentionality manipulations and stimuli. Experiments 4a and 4b manipulated intentionality and

task demands in novel ways. Unlike previous studies (Broitman & Swallow, 2020; Hutmacher & Kuhbandner, 2020; Mulligan et al., 2021), Experiment 4b directed participants to memorize the detection task cue as well as the background scene. This approach demonstrated that instructing participants to memorize one image, rather than just process it for predefined features, can generate an even larger boost for other, concurrently presented images presented at that time, as well as for relational memory. However, this also means that the results are not directly comparable to earlier studies that manipulated the intention to encode the scene itself.

In Experiment 4b there was also never a test of memory for the face itself, outside the context of the scene that appeared with it. As a result, we do not know whether faces presented in Experiment 4b would have been better remembered than the faces in Experiment 4b, only that they were more accurately paired with the concurrently presented scene. Memory for the relationship between faces and scenes, as well as their locations was always therefore incidental to the instructed tasks. The current study also did not look at the influence of instructions to ignore the scene, nor at instructions to memorize the relationship between a given face and scene, or its location. Future research will need to consider these manipulations and evaluate whether effects can be observed in a wider variety of tasks and with different operationalizations of spatiotemporal context.

This study also did not address all of the concerns raised by Hutmacher & Kuhbandner (2020). They argue that the only way to ensure that excess attentional resources are not used for uninstructed encoding of task-irrelevant information is by presenting trials at a faster pace and only once. Though a surprising amount of information can be extracted from briefly presented images (e.g., category information, Greene & Oliva, 2009; Potter, 2012), this may not be sufficient for the robust encoding of complex images (Liu & Jiang, 2005). The importance of

giving participants sufficient opportunity to encode items into memory was demonstrated in Broitman & Swallow (2020). This study showed that the boost to recollection estimates required up to two seconds to emerge, regardless of whether that time was distributed across multiple trials or aggregated within a single trial. In all of the experiments reported here, participants had a total of 10 s to encode the scenes and other information that was presented with them and DDM parameterization could therefore change when the trials are presented fewer times and for less time.

Another limitation of these studies is that the task used in Experiments 4a and 4b was too difficult for several participants to perform at sufficiently accurate levels. As a result, more participants were excluded from these experiments, particularly in Experiment 4a, and inclusion criteria needed to be loosened to meet minimal sample size goals. Both factors could have impacted the results. One consequence of increased difficulty of the tasks in Experiments 4a and 4b could be that the difference between target and distractor trials was reduced: false alarms to distractors were higher in these experiments, and were the primary reason for excluding participants in these two experiments.

Finally, evidence accumulation models may not adequately capture all of the mechanisms involved in the ABE or in decision making more generally. Despite their ability to provide insights into decision-making, the application of DDMs is often limited to the kinds of paradigms like those investigated here (for a review, see Evans & Wagenmakers, preprint). Specifically, in these paradigms trial onset is clear, no more than 2AFC options are used, and behavioral measures consist of response times with binary accuracy scores. Indeed, the particular DDM used here could not be applied to Experiment 3's 4AFC question, nor to response data with graded accuracy (e.g. precision of a memory representation for a color as reported on a

color wheel), nor would it be easily applied to paradigms making use of free recall (e.g., Mulligan et al., 2014), where it may be unclear how to model decision-processes without an objective starting point for evidence accumulation. DDMs also assume that the cognitive mechanisms involved in decision-making are engaged sequentially. However, it has become widely accepted that many of the processes involved in attention, perception, and cognition occur in parallel (e.g., Cisek, 2007; Lisman, 2015). Therefore, although the DDM results provide a basis for further investigation into the ABE, its sequential conceptualization of the decision process may not provide a full account of the actual mechanism involved. The use of DDMs in this study also relies on conceptually translating the estimated parameters to processes that may be impacted in the ABE. Indeed, the manipulation that produces the ABE paradigm occurs during encoding but the DDM models were fit to recognition data. As a result, differences in parameter estimates when information presented on target versus distractor trials is tested provide an indirect assessment of the effects of target detection on how the information is encoded.

3.5 Conclusion

Diffusion decision modeling of recognition test performance indicates that temporal selection during encoding enhances intentional and incidental relational memory through a boost in representational quality and accessibility. Analyses of data from five experiments revealed that the ABE primarily influenced evidence accumulation rates during subsequent tests of scene and relational memory. These effects interacted with the intention to encode images presented during the detection task. Importantly, response bias cannot account for the consistent and robust relational memory effects observed across all five experiments. Taken together, this study

strengthens the claim that responding to a target can boost the encoding of incidental relational features appearing at the same time. More broadly, it demonstrates that temporal selection during encoding, when cognitive resources are transiently mobilized to respond to a behaviorally relevant stimulus enhances memory encoding.

References

Aston-Jones, G., & Waterhouse, B. (2016). Locus coeruleus: from global projection system to adaptive regulation of behavior. *Brain research*, *1645*, 75-78.

Au, R. K., & Cheung, C. N. (2020). The role of attention level in the attentional boost effect. *Journal of Cognitive Psychology*, *32*(3), 255-277.

Baddeley, A. D., & Hitch, G. J. (2017). Is the levels of processing effect language-limited?. *Journal of Memory and Language*, *92*, 1-13.

Bates, D., Maechler, M., & Bolker, B. (2012). lme4: Linear mixed-effects models using Eigen and S4.

Berridge, C. W., & Waterhouse, B. D. (2003). The locus coeruleus–noradrenergic system: modulation of behavioral state and state-dependent cognitive processes. *Brain research reviews*, *42*(1), 33-84.

Bouret, S., & Sara, S. J. (2005). Network reset: a simplified overarching theory of locus coeruleus noradrenaline function. *Trends in neurosciences*, *28*(11), 574-582.

Briand, L. A., Gritton, H., Howe, W. M., Young, D. A., & Sarter, M. (2007). Modulators in concert for cognition: modulator interactions in the prefrontal cortex. *Progress in neurobiology*, *83*(2), 69-91.

Broitman, A. W., & Swallow, K. M. (2020). The effects of encoding instruction and opportunity on the recollection of behaviourally relevant events. *Quarterly Journal of Experimental Psychology*, *73*(5), 711-725.

Brooks, S. P., & Gelman, A. (1998). General methods for monitoring convergence of iterative simulations. *Journal of computational and graphical statistics*, *7*(4), 434-455.

Brown, V. A. (2021). An introduction to linear mixed-effects modeling in R. Advances in *Methods and Practices in Psychological Science*, *4*(1), 2515245920960351.

Burton, A. M., Schweinberger, S. R., Jenkins, R., & Kaufmann, J. M. (2015). Arguments against a configural processing account of familiar face recognition. *Perspectives on Psychological Science*, *10*(4), 482-496.

Castro, S. C., Strayer, D. L., Matzke, D., & Heathcote, A. (2019). Cognitive workload measurement and modeling under divided attention. *Journal of experimental psychology: human perception and performance*, *45*(6), 826.

Choi, H., Seitz, A. R., & Watanabe, T. (2009). When attention interrupts learning: inhibitory effects of attention on TIPL. *Vision research*, *49*(21), 2586-2590.

Craik, F. I., & Lockhart, R. S. (1972). Levels of processing: A framework for memory research. *Journal of verbal learning and verbal behavior*, *11*(6), 671-684.

Chun, M. M., & Turk-Browne, N. B. (2007). Interactions between attention and memory. *Current opinion in neurobiology*, *17*(2), 177-184.

Cisek, P. (2007). A parallel framework for interactive behavior. *Progress in brain research*, *165*, 475-492.

Clayton, E. C., Rajkowski, J., Cohen, J. D., & Aston-Jones, G. (2004). Phasic activation of monkey locus ceruleus neurons by simple decisions in a forced-choice task. *Journal of Neuroscience*, *24*(44), 9914-9920.

Cohen, N. J., & Eichenbaum, H. (1993). *Memory, amnesia, and the hippocampal system*. The MIT Press.

Davachi, L. (2006). Item, context and relational episodic encoding in humans. *Current opinion in neurobiology*, *16*(6), 693-700.

Dewald, A. D., Sinnett, S., & Doumas, L. A. (2011). Conditions of directed attention inhibit recognition performance for explicitly presented target-aligned irrelevant stimuli. *Acta psychologica*, *138*(1), 60-67.

Dewald, A. D., Sinnett, S., & Doumas, L. A. (2013). A window of perception when diverting attention? Enhancing recognition for explicitly presented, unattended, and irrelevant stimuli by target alignment. *Journal of experimental psychology: human perception and performance*, *39*(5), 1304.

Donkin, C., Brown, S. D., & Heathcote, A. (2009). The overconstraint of response time models: Rethinking the scaling problem. *Psychonomic Bulletin & Review*, *16*(6), 1129-1135.

Dube, C., Starns, J. J., Rotello, C. M., & Ratcliff, R. (2012). Beyond ROC curvature: Strength effects and response time data support continuous-evidence models of recognition memory. *Journal of Memory and language*, *67*(3), 389-406.

Duncan, J. (1980). The locus of interference in the perception of simultaneous stimuli. *Psychological review*, *87*(3), 272.

Evans, K. K., & Baddeley, A. (2018). Intention, attention and long-term memory for visual scenes: It all depends on the scenes. *Cognition*, 180, 24-37.

Evans, N. J., & Wagenmakers, E. J. (2019). Evidence accumulation models: Current limitations and future directions. PsyArXiv. doi:10.31234/osf.io/74df9

Forstmann, B. U., Ratcliff, R., & Wagenmakers, E. J. (2016). Sequential sampling models in cognitive neuroscience: Advantages, applications, and extensions. *Annual review of psychology*, *67*, 641-666.

Gilzenrat, M. S., Nieuwenhuis, S., Jepma, M., & Cohen, J. D. (2010). Pupil diameter tracks changes in control state predicted by the adaptive gain theory of locus coeruleus function. *Cognitive, Affective, & Behavioral Neuroscience*, *10*(2), 252-269.

Gold, J. I., & Shadlen, M. N. (2007). The neural basis of decision making. *Annu. Rev. Neurosci.*, *30*, 535-574.

Greene, M. R., & Oliva, A. (2009). Recognition of natural scenes from global properties: Seeing the forest without representing the trees. *Cognitive psychology*, *58*(2), 137-176.

Griffith, T., Baker, S. A., & Lepora, N. F. (2021). The statistics of optimal decision making: Exploring the relationship between signal detection theory and sequential analysis. *Journal of Mathematical Psychology*, *103*, 102544.

Heathcote, A., Lin, Y. S., Reynolds, A., Strickland, L., Gretton, M., & Matzke, D. (2019). Dynamic models of choice. *Behavior research methods*, *51*(2), 961-985.

Hutmacher, F., & Kuhbandner, C. (2020). Detailed long-term memory for unattended, irrelevant, and incidentally encoded auditory information. *Journal of Experimental Psychology: General*, *149*(2), 222.

Hoffing, R., & Seitz, A. R. (2015). Pupillometry as a glimpse into the neurochemical basis of human memory encoding. *Journal of cognitive neuroscience*, *27*(4), 765-774.

Jepma, M., Wagenmakers, E. J., & Nieuwenhuis, S. (2012). Temporal expectation and information processing: A model-based analysis. *Cognition*, *122*(3), 426-441.

Kempadoo, K. A., Mosharov, E. V., Choi, S. J., Sulzer, D., & Kandel, E. R. (2016). Dopamine release from the locus coeruleus to the dorsal hippocampus promotes spatial learning and memory. *Proceedings of the National Academy of Sciences*, *113*(51), 14835-14840.

Knoblauch, K. (2014). psyphy: Functions for analyzing psychophysical data in R. R package version 0.1-9.

Konkel, A., & Cohen, N. J. (2009). Relational memory and the hippocampus: representations and methods. *Frontiers in neuroscience*, *3*, 23.

Leclercq, V., Le Dantec, C. C., & Seitz, A. R. (2014). Encoding of episodic information through fast task-irrelevant perceptual learning. *Vision research*, *99*, 5-11.

Leclercq, V., & Seitz, A. R. (2012). The impact of orienting attention in fast task-irrelevant perceptual learning. *Attention, Perception, & Psychophysics*, *74*(4), 648-660.

Lenth, R. (2019). Emmeans: Estimated Marginal Means, aka Least-Squares Means. R package version 1.7.2.

Lin, J. Y., Pype, A. D., Murray, S. O., & Boynton, G. M. (2010). Enhanced memory for scenes presented at behaviorally relevant points in time. *PLoS biology*, *8*(3), e1000337.

Lisman, J. (2015). The challenge of understanding the brain: where we stand in 2015. *Neuron*, *86*(4), 864-882.

Liu, K., & Jiang, Y. (2005). Visual working memory for briefly presented scenes. *Journal of Vision*, *5*(7), 650–658. doi:10.1167/5.7.5

Macmillan, N. A., & Creelman, C. D. (2004). *Detection theory: A user's guide*. Psychology press.

Makovski, T., Jiang, Y. V., & Swallow, K. M. (2013). How do observer's responses affect visual long-term memory? *Journal of Experimental Psychology: Learning, Memory, and Cognition*, *39*(4), 1097.

Mather, M., Clewett, D., Sakaki, M., & Harley, C. W. (2016). Norepinephrine ignites local hotspots of neuronal excitation: How arousal amplifies selectivity in perception and memory. *Behavioral and Brain Sciences*, 39.

Meng, Y., Lin, G., & Lin, H. (2019). The role of distractor inhibition in the attentional boost effect: Evidence from the R/K paradigm. *Memory*, *27*(6), 750-757.

Mulligan, N. W. (2008). Attention and memory. In H. L. Roediger (Ed.), *Learning & Memory: A comprehensive reference*, (pp. 7–22). Elsevier. doi: 10.1016/B978-012370509-9.00134-0

Mulligan, N. W., Smith, S. A., & Spataro, P. (2016). The attentional boost effect and context memory. *Journal of Experimental Psychology: Learning, Memory, and Cognition*, *42*(4), 598.

Mulligan, N. W., Spataro, P., & Picklesimer, M. (2014). The attentional boost effect with verbal materials. *Journal of Experimental Psychology: Learning, Memory, and Cognition*, *40*(4), 1049.

Mulligan, N. W., Spataro, P., Rossi-Arnaud, C., & Wall, A. R. (2021). The attentional boost effect and source memory. *Journal of Experimental Psychology: Learning, Memory, and Cognition*.

Murata, T., Hamada, T., Shimokawa, T., Tanifuji, M., & Yanagida, T. (2014). Stochastic process underlying emergent recognition of visual objects hidden in degraded images. *PLoS One*, *9*(12), e115658.

Onyper, S. V., Zhang, Y. X., & Howard, M. W. (2010). Some-or-none recollection: Evidence from item and source memory. *Journal of Experimental Psychology: General*, *139*(2), 341.

Palada, H., Neal, A., Strayer, D., Ballard, T., & Heathcote, A. (2019). Using response time modeling to understand the sources of dual-task interference in a dynamic environment. *Journal of Experimental Psychology: Human Perception and Performance*, *45*(10), 1331.

Pascucci, D., & Turatto, M. (2013). Immediate effect of internal reward on visual adaptation. *Psychological Science*, *24*(7), 1317-1322.

Pazzaglia, A. M., Dube, C., & Rotello, C. M. (2013). A critical comparison of discrete-state and continuous models of recognition memory: implications for recognition and beyond. *Psychological Bulletin*, *139*(6), 1173.

Potter, M. C. (2012). Recognition and memory for briefly presented scenes. *Frontiers in psychology, 3*, 32.

R Core Team (2019). R: A language and environment for statistical computing. Vienna, Austria: R Foundation for Statistical Computing. Retrieved from https://www.R-project.org/

Rajkowski, J., Majczynski, H., Clayton, E., & Aston-Jones, G. (2004). Activation of monkey locus coeruleus neurons varies with difficulty and performance in a target detection task. *Journal of neurophysiology*, *92*(1), 361-371.

Ratcliff, R. (1978). A theory of memory retrieval. *Psychological review*, *85*(2), 59.

Ratcliff, R., & McKoon, G. (2008). The diffusion decision model: theory and data for two-choice decision tasks. *Neural computation*, *20*(4), 873-922.

Ratcliff, R., & Rouder, J. N. (1998). Modeling response times for two-choice decisions. *Psychological science*, *9*(5), 347-356.

Ratcliff, R., Smith, P. L., Brown, S. D., & McKoon, G. (2016). Diffusion decision model: Current issues and history. *Trends in cognitive sciences*, *20*(4), 260-281.

Rubin, D. C., & Umanath, S. (2015). Event memory: A theory of memory for laboratory, autobiographical, and fictional events. *Psychological review*, *122*(1), 1.

Schonberg, T., Bakkour, A., Hover, A. M., Mumford, J. A., Nagar, L., Perez, J., & Poldrack, R. A. (2014). Changing value through cued approach: an automatic mechanism of behavior change. *Nature neuroscience*, *17*(4), 625-630.

Shine, J. M. (2019). Neuromodulatory influences on integration and segregation in the brain. *Trends in cognitive sciences*, *23*(7), 572-583.

Sisk, C. A., & Lee, V. G. (2022). Concurrent target detection is associated with better memory for object exemplars. *Psychonomic Bulletin & Review*, *29*(1), 159-168.

Smith, S. A., & Mulligan, N. W. (2018). Distinctiveness and the attentional boost effect. *Journal of Experimental Psychology: Learning, Memory, and Cognition*, *44*(9), 1464.

Smith, P. L., & Ratcliff, R. (2004). Psychology and neurobiology of simple decisions. *Trends in neurosciences*, *27*(3), 161-168.

Spataro, P., Mulligan, N. W., Cestari, V., Santirocchi, A., Saraulli, D., & Rossi-Arnaud, C. (2021). The attentional boost effect enhances the item-specific, but not the relational, encoding of verbal material: Evidence from multiple recall tests with related and unrelated lists. *Journal of Experimental Psychology: Learning, Memory, and Cognition*.

Spataro, P., Mulligan, N. W., & Rossi-Arnaud, C. (2013). Divided attention can enhance memory encoding: The attentional boost effect in implicit memory. *Journal of Experimental Psychology: Learning, Memory, and Cognition*, *39*(4), 1223.

Spataro, P., Saraulli, D., Cestari, V., Mulligan, N. W., Santirocchi, A., Borowiecki, O., & Rossi-Arnaud, C. (2020). The attentional boost effect enhances the recognition of bound features in short-term memory. *Memory*, *28*(7), 926-937.

Spiegelhalter, D. J., Best, N. G., Carlin, B. P., & Van Der Linde, A. (2002). Bayesian measures of model complexity and fit. *Journal of the royal statistical society: Series b (statistical methodology)*, *64*(4), 583-639.

Swallow, K. M., & Atir, S. (2019). The role of value in the attentional boost effect. *Quarterly Journal of Experimental Psychology*, *72*(3), 523-542.

Swallow, K. M., & Jiang, Y. V. (2010). The attentional boost effect: Transient increases in attention to one task enhance performance in a second task. *Cognition*, *115*(1), 118-132.

Swallow, K. M., & Jiang, Y. V. (2011). The role of timing in the attentional boost effect. *Attention, Perception, & Psychophysics*, *73*(2), 389-404.

Swallow, K. M., & Jiang, Y. V. (2012). Goal-relevant events need not be rare to boost memory for concurrent images. *Attention, Perception, & Psychophysics*, *74*(1), 70-82.

Swallow, K. M., & Jiang, Y. V. (2013). Attentional load and attentional boost: A review of data and theory. *Frontiers in Psychology*, *4*, 274.

Swallow, K. M., & Jiang, Y. V. (2014). The attentional boost effect really is a boost: Evidence from a new baseline. *Attention, Perception, & Psychophysics*, *76*(5), 1298-1307.

Swallow, K. M., Jiang, Y. V., & Riley, E. B. (2019). Target detection increases pupil diameter and enhances memory for background scenes during multi-tasking. *Scientific reports*, *9*(1), 1-13.

Swallow, K. M., Makovski, T., & Jiang, Y. V. (2012). Selection of events in time enhances activity throughout early visual cortex. *Journal of Neurophysiology*, *108*(12), 3239-3252.

Taubert, J., Apthorp, D., Aagten-Murphy, D., & Alais, D. (2011). The role of holistic processing in face perception: Evidence from the face inversion effect. *Vision Research*, *51*(11), 1273-1278.

Tillman, G., Strayer, D., Eidels, A., & Heathcote, A. (2017). Modeling cognitive load effects of conversation between a passenger and driver. *Attention, Perception, & Psychophysics*, *79*(6), 1795-1803.

Tran, N., Van Maanen, L., Heathcote, A., & Matzke, D. (2021). Systematic parameter reviews in cognitive modeling: towards a robust and cumulative characterization of psychological processes in the diffusion decision model. *Frontiers in Psychology*, 3922.

Toh, Y. N., & Lee, V. G. (2022). Response, rather than target detection, triggers the attentional boost effect in visual search. *Journal of Experimental Psychology: Human Perception and Performance*, *48*(1), 77.

Turker, H. B., Riley, E., Luh, W. M., Colcombe, S. J., & Swallow, K. M. (2021). Estimates of locus coeruleus function with functional magnetic resonance imaging are influenced by localization approaches and the use of multi-echo data. *Neuroimage*, *236*, 118047.

Turker, H. B., & Swallow, K. M. (2019). Attending to behaviorally relevant moments enhances incidental relational memory. *Memory & cognition*, *47*(1), 1-16.

Turner, B. M., Sederberg, P. B., Brown, S. D., & Steyvers, M. (2013). A method for efficiently sampling from distributions with correlated dimensions. *Psychological methods*, *18*(3), 368.

Wagenmakers, E. J. (2009). Methodological and empirical developments for the Ratcliff diffusion model of response times and accuracy. *European Journal of Cognitive Psychology*, *21*(5), 641-671.

Walker, M., Ciraolo, M., Dewald, A., & Sinnett, S. (2017). Differential processing for actively ignored pictures and words. *PloS one*, *12*(1), e0170520.

Westfall, J., Kenny, D. A., & Judd, C. M. (2014). Statistical power and optimal design in experiments in which samples of participants respond to samples of stimuli. *Journal of Experimental Psychology: General*, *143*(5), 2020.

Yazin, F., Das, M., Banerjee, A., & Roy, D. (2021). Contextual prediction errors reorganize naturalistic episodic memories in time. *Scientific reports*, *11*(1), 1-17.

Yebra, M., Galarza-Vallejo, A., Soto-Leon, V., Gonzalez-Rosa, J. J., de Berker, A. O., Bestmann, S., ... & Strange, B. A. (2019). Action boosts episodic memory encoding in humans via engagement of a noradrenergic system. *Nature communications*, *10*(1), 1-12.

CHAPTER 4

ESTIMATES OF LOCUS COERULEUS FUNCTION WITH FUNCTIONAL MAGNETIC RESONANCE IMAGING[3]

Accurately characterizing functions of neuromodulatory systems with functional magnetic resonance imaging (fMRI) can be a difficult task, especially for one of the neuromodulatory systems of interest in this dissertation: the locus coeruleus norepinephrine (LC-NE) system. The LC is a pair of small, cylindrical nuclei located in the brainstem near the fourth ventricle (4V). As the main site for the synthesis of the neuromodulator NE, the LC influences many aspects of cognition and autonomic regulation (e.g., Aston-Jones, Gonzalez, & Doran, 2007; Berridge & Waterhouse, 2003). Because of its small size and location, however, investigations of LC function in humans using fMRI face a unique set of challenges in confidently localizing and isolating signals associated with neural activity in the LC.

This chapter investigates the impact of two data acquisition and processing approaches on LC neuroimaging: neuromelanin-weighted T1 (nmT1) imaging to localize the LC, which is rich in neuromelanin, in each individual (Sasaki et al., 2006) as well as multi-echo functional magnetic resonance imaging (ME-fMRI) to increase blood oxygen level dependent (BOLD) contrast and reduce non-BOLD artifacts (Kundu, Inati, Evans, Luh, & Bandettini, 2012). To compare the impacts of using any of these different approaches, I characterize differences in estimates of the intrinsic functional connectivity (iFC) of the LC when these approaches are and are not used. In doing so, I demonstrate that the LC iFC impacts regions critical for

[3] This chapter is an abridged and modified version of the article originally published as *Turker, H. B., Riley, E., Luh, W. M., Colcombe, S. J., & Swallow, K. M. (2021). Estimates of locus coeruleus function with functional magnetic resonance imaging are influenced by localization approaches and the use of multi-echo data. NeuroImage, 236, 118047.* Thus, the chapter is not the copy of record. Please do not copy or cite this chapter without the authors' permission and refer to the authoritative document published in NeuroImage instead.

understanding how the mind and brain perceive, process, and respond to behaviorally relevant events.

4.1 Characterization of Locus Coeruleus Function

Despite its small size, the LC projects to most of the central nervous system, excluding the striatum (Jones & Moore, 1977; Jones & Yang, 1985; Samuels & Szabadi, 2008). It also contains sub-populations of cells that project to different regions of the brain, such as the brainstem, spinal cord, medial prefrontal cortex, hippocampus, septum, and amygdala (Chandler, Gao, & Waterhouse, 2014; Schwarz & Luo, 2015), and has particularly dense projections to sensory and motor regions (Loughlin, Foote, & Bloom, 1986; Schwarz & Luo, 2015). LC projections also show large amounts of branching along the anterior-posterior axis in the neocortex that may be driven by the shared function of target regions (Loughlin, Foote, & Fallon, 1982; Aston-Jones & Waterhouse, 2016). In turn, the LC receives input from the brainstem, hypothalamus, central nucleus of the amygdala, anterior cingulate cortex, and orbitofrontal cortex (Aston-Jones et al., 1991; Luppi, Aston-Jones, Akaoka, Chouvet, & Jouvet, 1995). This circuitry allows the LC to regulate autonomic states and task engagement to influence how neural systems respond to behaviorally relevant events (Aston-Jones, Rajkowski, & Cohen, 1999; Glennon et al., 2019; Greene, Bellgrove, Gill, & Robertson, 2009; Nieuwenhuis et al., 2007; Mohanty, Gitelman, Small, & Mesulam, 2008). Its activity may also be reflected in pupil dilation (e.g., Larsen & Waters, 2018).

Although the precise mechanisms by which LC activity accomplishes all this are still being investigated (Mather, Clewett, Sakaki, & Harley, 2016; Uematsu, Tan, & Johansen, 2015; Schwarz & Luo, 2015), NE is known to improve the signal-to-noise ratio in brain regions

involved in perceptual processing, including ventral visual cortex (Berridge & Waterhouse, 2003; Foote, Freedman, & Oliver, 1975; Warren et al., 2016). Important within the context of this dissertation, the LC-NE may influence the integration and segregation dynamics of networks across brain regions (Shine et al., 2016; Chapter 5) and promote memory consolidation and retrieval (Sara, 2009; Grella et al., 2019; Swallow, Jiang, & Riley, 2019; Chapters 2 & 3).

4.1.1 Localizing Human LC and Measuring its Neuromelanin Content Using MRI

The small size and location next to the 4V of the LC nuclei pose unique challenges to identifying them in both structural and functional MRI scans. In standard T1-weighted structural images, the LC and surrounding regions appear relatively homogenous, making identification of voxels that contain the LC difficult. This is further exacerbated by natural variability in exact location (Keren, Lozar, Harris, Morgan, & Eckert, 2009). As a consequence, once structural and functional scans are aligned, identifying voxels reflecting LC function is also hampered.

To help address the localization problem, neuroimaging sequences have been developed that increase the contrast for regions containing neuromelanin (nmT1 imaging), a pigment found in the LC (Sasaki et al., 2006). The paramagnetic, T1 shortening effects of neuromelanin can be leveraged by nmT1 imaging to increase the contrast of voxels containing neuromelanin to allow for the visualization and localization of the LC in structural MRI scans (Enochs et al., 1997; Keren et al., 2009; Sulzer et al., 2018; Wakamatsu, Tabuchi, Ojika, Zucca, Zecca, & Ito, 2015). Because regions that contain more neuromelanin appear brighter in nmT1 images, it also provides an in vivo measure of the amount of neuromelanin in the LC (e.g., Keren et al., 2009; Keren et al., 2015; Liu et al., 2019).

The majority of studies on LC function do not make use of nmT1 imaging to localize the LC. Instead, they rely either on previously published coordinates, probabilistic atlases (such as developed by Keren et al., 2009), or use exploratory whole-brain analyses (for a review, see Liu, Marijatta, Hämmerer, Acosta-Cabronero, Düzel, & Howard, 2017). But because the precise location and shape of a brain region can vary across individuals, defining regions of interest (ROIs) at the group level risks missing the region in a given individual and capturing signal from surrounding areas. This can result in group level ROIs producing less reliable findings than individually defined ROIs (e.g., Swallow, Braver, Snyder, Speer, & Zacks, 2003). Therefore, coordinates from other studies or probabilistic LC ROIs, while likely to capture the LC, may also capture other nearby brainstem structures such as the inferior colliculus, the nucleus incertus, or other parts of the ascending reticular activating system that also play a role in arousal, orienting, and learning (e.g., Ryan, Ma, Olucha-Bordonau, & Gundlach, 2011).

4.1.2 Estimating LC Activity: Multi-Echo Versus Single-Echo Functional MRI

Previous investigations of LC function have used single-echo functional magnetic resonance imaging (1E-fMRI), which measures the MR signal in each voxel once per volume acquisition. By measuring the MR signal two or more times per acquisition, multi-echo (ME) fMRI offers two potential advantages over 1E-fMRI that could be particularly effective at reducing the impacts of non-BOLD noise and signal drop-out on estimates of LC function: maximization of BOLD contrast through the optimal combination of echoes during data analysis and independent components analysis (ICA) denoising.

With 1E-fMRI, the time at which the signal is measured (echo time; TE) is selected to maximize BOLD contrast for the brain as a whole, balancing variability in the

susceptibility-weighted transverse relaxation (T2*) signal decay rates across the brain that arise from regional differences in tissue composition and signal drop-out (e.g., Cho & Ro, 1992; Park, Ro, & Cho, 1988). Because ME-fMRI measures the MR signal at multiple points during each acquisition, it can be used to estimate initial signal intensity and the rate at which the T2* signal decays at every voxel in the volume. This information can be used to create volumes that optimally weigh and combine the TEs for each individual voxel. Rather than choosing one TE for the entire brain, ME-fMRI can be used to effectively estimate the signal at the optimal TE for a given voxel and brain region after the data have been acquired (Kundu, Voon, Balchandani, Lombardo, Poser, & Bandettini, 2017). This approach has been used to improve BOLD contrast in regions of the brain that are subject to signal-dropout in typical 1E-fMRI, such as the ventromedial prefrontal cortex and nucleus basalis, without sacrificing contrast in other brain regions (Markello, Spreng, Luh, Anderson, & De Rosa, 2018).

Estimation of initial signal intensity and T2* decay also affords ME-fMRI data with a theoretically motivated approach to denoising BOLD data. Changes in BOLD activity are dependent on the TE, while artifactual effects on MR signal are TE-independent, and these can be algorithmically distinguished from each other (Kundu et al., 2012; Kundu et al., 2013). ME independent components analysis (ME-ICA) leverages these differences in order to identify and remove the contributions of non-BOLD signal components, such as head motion and physiological noise, from the data. Advantages of this process are that it is fully automated and requires no physiological measures, temporal noise models, or anatomical templates. It has been shown to significantly reduce the effects of head motion and other noise sources on BOLD data (Power et al., 2018). In contrast, denoising of 1E-fMRI data often requires removing observations that are likely to be contaminated by motion (e.g., by scrubbing) or by estimating

and regressing out noise from motion and physiology (e.g., Dipasquale et al., 2017). For example, with RETROICOR, variance associated with cardiac phase and respiration is removed from the data using regression (Glover, Li, & Ress, 2000). With 1E-fMRI, principle components and independent components analysis can also be used, for example, to identify and remove motion related components (e.g., ICA-AROMA; Pruim, Mennes, Van Rooij, Llera, Buitelaar, & Beckmann, 2015). These methods are sometimes employed in conjunction with the inclusion of first- and second-order motion regressors in the statistical analyses. Although, when directly compared to ME-ICA, these methods are less effective at reducing noise, they may nevertheless offer acceptable alternatives to ME-fMRI if only 1E-fMRI acquisition is possible. Previous studies investigating the iFC of the LC have not consistently accounted for cardiac and respiratory effects, and few have reported correcting for motion (Liu et al., 2017). Because physiological and motion-related noise can cause spurious correlations in iFC maps (Power et al., 2012), steps to reduce their impact on the data are needed to gain a better understanding of LC function. In fact, previous neuroimaging studies showing task-related activity in the vicinity of the LC have been called into question precisely because of this problem (Astafiev, Snyder, Shulman, & Corbetta, 2010).

4.2 The Current Study

Human neuroimaging of the LC has been hampered by several related issues: localizing the LC, isolating LC activity from other nearby regions, and removing the effects of noise from motion and physiology. In this study, we investigate whether using nmT1 images and ME-fMRI can offer appreciable advantages to one's efforts to characterize LC function. Previous work on

ME-ICA and small brain regions like the nucleus basalis of Meynert (Markello et al., 2018) suggests we should also see appreciable gains in signal-to-noise ratio of imaging data of the LC.

To investigate effects of ME-fMRI, our main analyses compared a pipeline that utilized all three echoes from an ME-fMRI acquisition to a pipeline that utilized only the second echo (E2) from the same acquisition. Because both pipelines utilized data from the same scan, this approach held state dependent brain activity constant and minimized concerns about inter-run reliability (Birn et al., 2013).

4.2.1 Methods

4.2.2 Participants

Twenty right-handed participants (14 female, 6 male; 19-40 years old, M = 21.05, SD = 4.57) completed one multi-echo resting state run. Participants were screened for non-MRI compatible medical devices or body modifications (e.g., piercings, implants), claustrophobia, movement disorders, pregnancy, mental illness, use of medication affecting cognition, and color blindness. All participants provided consent at the start of the session, were debriefed at the end, and all procedures were approved by the Cornell University Institutional Review Board.

4.2.3 MRI Acquisition

Magnetic resonance imaging was performed with a 3T GE Discovery MR750 MRI scanner and a 32-channel head coil at the Cornell Magnetic Resonance Imaging Facility in Ithaca, NY. Participants laid supine on the scanner bed with their head supported and immobilized. Ear plugs, headphones, and a microphone were used to reduce scanner noise, allow the participant to communicate with the experimenters, and to present auditory stimuli during the

tasks. Visual stimuli were presented with a 32” Nordic Neuro Lab liquid crystal display (1920 × 1080 pixels, 60 Hz, 6.5 ms g to g) located at the back of the scanner bore and viewed through a mirror attached to the head coil. Pulse oximetry and respiration were recorded throughout all scans.

Anatomical data were acquired with a T1-weighted MPRAGE sequence (TR = 7.7 ms; TE = 3.42 ms; 7° flip angle; 1.0 mm isotropic voxels, 176 slices). A second anatomical scan utilized a neuromelanin sensitive T1-weighted partial volume turbo spin echo (nmT1) sequence (TR = 700 ms; TE = 13 ms; 120° flip angle; 0.43 × 0.43 mm in-plane voxels, 10 interleaved 3.0 mm thick axial slices, 0 mm spacing; adapted from Keren et al., 2009). Slices for the nmT1 volume were oriented perpendicular to the brain stem to provide high resolution data in the axial plane, where the dimensions of the LC are smallest, and positioned to cover the most rostral portion of the pons.

Participants completed one resting state scan with eyes open and the lights on during multi-echo echo planar imaging (612s; TR = 3.0 s; TEs = 13, 30, 47 ms; 83° flip angle; 3.0 mm isotropic voxels; 46 interleaved slices). The display was set to a uniform light grey background throughout the scan. Participants were told to keep their eyes open and remain awake throughout the scan, but were free to move their eyes and blink as needed.

4.3 Region of Interest Identification

4.3.1 Anatomically Defined Regions

Anatomical data were submitted to FreeSurfer's segmentation and surface-based reconstruction software (recon-all; v 5.3; http://surfer.nmr.mgh.harvard.edu/; Dale, Fischl, & Sereno, 1999; Fischl, Sereno, & Dale, 1999) to label each individual's anatomy. Labels for

cortical gray matter (GM), ventral medial prefrontal cortex (vmPFC), fourth ventricle (4V), hippocampus (HPC), primary visual cortex (V1), brainstem, precentral gyrus (motor cortex, MC), and transverse temporal gyrus (auditory cortex, AC) were extracted and converted to volumetric ROIs using FreeSurfer and AFNI (Cox, 1996) tools. A white matter (WM) ROI was similarly created, but eroded using AFNI's 3dmask_tool (dilate_input -2) to ensure that the ROI did not extend into nearby regions.

4.3.2 Locus Coeruleus

Voxels that were likely to include the LC were identified in two ways: using the probabilistic Keren atlas and using individual nmT1 images. ROIs that were based on the Keren atlas were defined using the binary 1 SD and 2 SD masks, provided by those authors (referred to here as K1 and K2 ROIs, respectively; Keren et al., 2009) in the MNI152 atlas (T1 MNI-152 0.5 mm iso-voxel). To provide the most conservative comparison between the Keren atlas and the nmT1-based LC ROIs, analyses focused primarily on the K1 ROI. The Keren atlas is based on nmT1 images (3 × 0.4 × 0.4 mm axial slices) of 44, right-handed, healthy adults, aged 19–79. Their final probabilistic atlas was based on the group means and standard deviations of the highest intensity voxels on the left and right in each axial slice (for more details, see Keren et al., 2009).

Individual, hand-traced LC ROIs for each participant were defined using the nmT1 image, with the same scanning parameters as used for the Keren atlas. Tracing was performed on the un-transformed nmT1 image to take advantage of its high in-plane resolution and to avoid blurring the data when aligning and resampling to the participant's native MPRAGE. Prior to tracing the ROIs, the individual MPRAGE (with skull, for additional landmarks) and anatomical

parcellation from FreeSurfer were aligned to the nmT1 image using a 6 parameter affine transformation (AFNI's align_epi_anat.py; Cox & Jesmanowicz, 1999; Saad, Glen, Beauchamp, Desai, & Cox, 2009). Then, we extracted brainstem and 4V voxels from the nmT1 images. Each slice was mean centered by subtracting the mean signal intensity of voxels within the brainstem from all voxels in the slice (corrected nmT1 image).

The LC was manually defined in FreeView (https://surfer.nmr.mgh.harvard.edu) on the corrected nmT1 images by two independent raters using the following criteria (adapted from Tona et al., 2017; see Fig. 4.1):

1. The corrected nmT1 image was viewed in false color and overlaid on the aligned MPRAGE image. Brush size was 1 voxel.

2. Visual contrast was equated across participants using a predefined range for the false color palette (Jet - minimum: 10, maximum: 80). Pixel intensity threshold for inclusion in the LC (only green, yellow, orange and red pixels could be included; values roughly ≥ 40) was agreed upon prior to drawing the ROIs.

3. Two landmarks were used to locate the most rostral portion of the LC: the lower boundary of the inferior colliculus (seen in sagittal view) and the upper boundary of the 4V (seen in axial view). The rostral end of the LC was in the first axial slice caudal to the inferior colliculus in which two distinct hyperintensities on the edge of the 4V were visible in the nmT1 image.

4. The LC was defined starting on this slice and moving caudally through the pons. Hyperintensities in more caudal slices were included in the LC only if they were both sufficiently bright and connected to hyperintensities in the next most rostral slice, verified in sagittal and coronal views.

5. Tracing was informed by the assumption that each LC nucleus would appear as a roughly circular shape within each axial slice, resulting in bilateral, roughly cylindrical regions. In addition, the LC was assumed to be solid and contain no holes. If a voxel was surrounded in-plane by voxels included in the LC, then that voxel was also included.

6. In some cases, a second, more medial hyperintensity was found near the rostral part of the LC. This region was taken to be part of the trochlear nerve and was not included in the LC ROI. Avoiding this secondary hyperintensity prevented the LC ROI from having a very oblong shape or extending to the midline at any point.

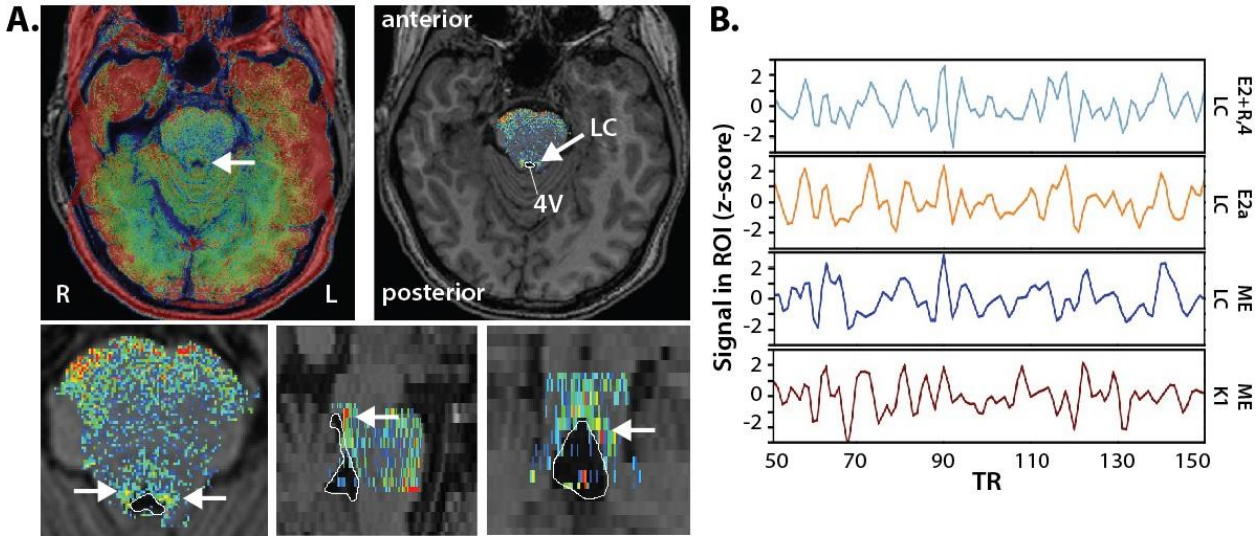

Fig. 4.1 Visualization of the ROI creation and seed extraction process. *A) Individual MPRAGE scans (including skull) were aligned to the normalized nmT1 image (arrow is pointing to one of the LC nuclei; top left) to preserve the higher in-plane spatial resolution of the nmT1 images. After extracting the brainstem from the nmT1, correcting image intensity, and setting the false color palette to the predefined range (low values in blue, high values in red, range = 10–80), potential LC voxels can now be visually distinguished from nearby regions (top right). Two researchers independently traced the LC according to the protocol described in the methods, by selecting voxels that appeared yellow or redder (corresponding roughly to intensity values ≥ 40). Candidate LC voxels are visible in the axial, sagittal, and coronal plane (bottom row), indicated with arrows. The 4V is encircled to emphasize its proximity to LC nuclei. B) Excerpts from one individual's seed time series (acquisition numbers 50 to 150; z-scored) following different denoising pipelines. LC and K1 seeds were always extracted in native space. ME = multi-echo, ME-ICA denoised data; E2+R,4 = second echo with RETROICOR and 4V regression; E2a = E2 pipeline including ICA-AROMA; LC = hand-traced LC ROI; K1 = 1 SD Keren ROI.*

An individual's final LC ROI consisted of voxels included in both raters' ROIs, after removing any voxels that overlapped with 4V. The 4V was defined starting from the most rostral axial slice in which the cerebral aqueduct began to widen, until the most caudal axial slice in which the ventricle appeared dark and had an inverted-U shape.

A probabilistic map illustrating the location and distribution of the LC ROIs in all participants was created by registering each person's LC ROI to MNI152 space. To do so, alignment parameters were calculated for each individual by combining the inverse of the

transformation that aligned the native MPRAGE and nmT1 images and the nonlinear transformation from the individual's native MPRAGE to MNI152 standard calculated with AFNI's 3dQwarp and then applied using 3dNwarpApply. Successful alignment of the brainstem to the individual MPRAGE and the MNI152 template was visually confirmed. Similar to previous findings (e.g., Tona et al., 2017), linear transformations were inadequate for registering a small brainstem ROI to the MNI152 space: with affine registration only, many LC ROIs overlapped the 4V or other parts of the pons. LC ROIs in MNI152 space were thresholded to remove scattered non-zero voxels introduced by the nonlinear warping process, by removing any voxels with values of 0.1 and below. Finally, each voxel value was divided by the number of participants to create the probabilistic map (Fig. 4.2).

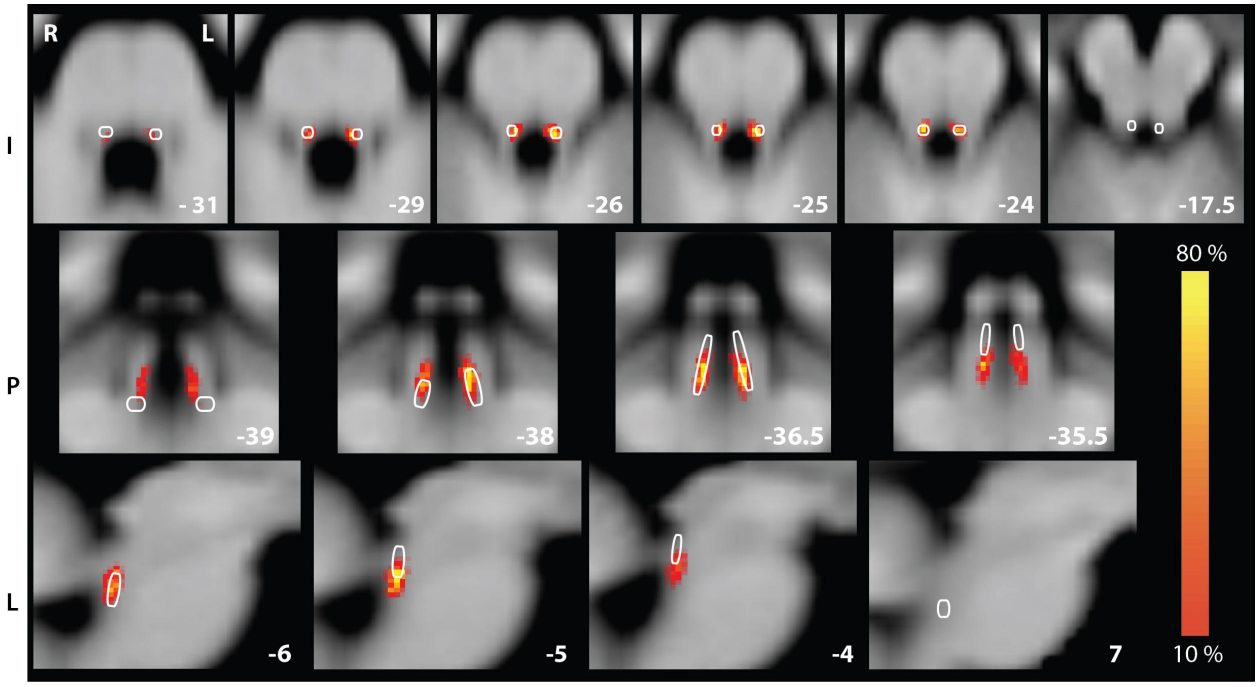

Fig. 4.2 Visualization of nmT1-based LC to atlas-based K1 ROIs. *Hand-traced LC atlas (heat; percentage of participant) and binary K1 atlas (white outline) overlayed on the MNI152 template. Slices were selected to best visualize similarities and differences between the LC heat map and K1 atlas. This figure is for illustrative purposes only: each LC and K1 ROI was applied to functional data aligned to the individual's native anatomy, but is being shown here aligned to MNI152 for aggregation and comparison to the Keren atlas as shown in Keren et al. (2009). Coordinates in LPI.*

4.3.3 Pontine Tegmentum

Within axial slices of the participant's MPRAGE (as aligned to the nmT1), the pontine tegmentum (PT) ROI was defined as a circular ROI 10 voxels in diameter centered at the midline of the brainstem, ventral to the fourth ventricle, and approximately equidistant from the left and right LC ROIs, to define the vertex of an equilateral triangle. The PT ROI was defined only in slices that also contained an LC ROI (see also Clewett, Lee, Greening, Ponzio, Margalit, & Mather, 2016).

4.3.4 Alignment of ROIs to Native Space

ROI statistics and seeds for time series and iFC analyses were acquired in native space after aligning the LC and PT ROIs (acquired in nmT1 space), the K1 ROIs (originally in MNI152 space), and functional data to the native MPRAGE for each individual. The LC and PT ROIs were aligned to native space by using the inverse of the transformation used to align the individual MPRAGE and nmT1 images. The K1 ROIs were transformed to each participant's native space using the inverse of the 3dQwarp transformation between MNI152 and the participant's native MPRAGE. They were then thresholded at 0.1 and resampled to the 3 mm isotropic grid. This approach minimized transformation of the EPI data and equated the number of transformations computed and applied to each of the ROIs.

4.3.5 MRI Data Pre-Processing

To evaluate the effects of different denoising procedures on data quality and the resulting iFC maps, two single-echo pre-processing pipelines and one multi-echo pre-processing pipeline were used. Pre-processing of ME data were modeled after the procedures outlined in Jo et al. (2013) and Markello et al. (2018). The E2 pipelines differed in amount and method of noise removal, but were otherwise matched as closely as possible to the ME pipeline. See Turker et al. (2021) for a flowchart illustrating all pipelines covered in this chapter as well as several more. We first describe the pipeline used for ME-ICA denoising, followed by the various E2 pipelines.

For the ME pipeline with ME-ICA-denoising, the standard ME-ICA pipeline (meica.py, Version 2.5, beta 9; tedana.py, Version 2.5 beta 9; t2smap.py, Version 2.5 beta 6; Kundu et al., 2012; Kundu et al., 2013) was implemented using the following steps. First, the MPRAGE volume was

skull stripped using FSL BET (b = 0.25). Second, the obliquity of the anatomical volume was matched to the EPI time series. Third, motion was estimated using the first echo time series using 3dvolreg with the third volume as the target. The parameters for deobliqueing the data and calculating motion were saved for use during motion correction and volume registration in Step 7. Fourth, all EPI data were despiked and slice time acquisition differences were corrected using 3dTshift. Fifth, for each echo time series, the first two volumes were dropped and the remaining EPI data were registered to the third volume. Sixth, the three echoes were concatenated and processed by t2smap.py to generate the baseline intensity volume (s0), the T2* relaxation map, and the optimal combination volume time series (OCV). Seventh, the OCV was used to calculate coregistration parameters to the anatomical image. These coregistration parameters and the previously calculated deobliqueing parameters were then applied to the EPI data in one step to align the data with the individual anatomical volume in its original acquisition space. Eighth, EPI data were denoised using ME-ICA to identify and separate BOLD components from non-BOLD components (tedana.py; Kundu et al., 2012; Kundu et al., 2013). This approach identifies BOLD components based on quantifying the T2* portion of the BOLD fMRI signal (see Kundu et al., 2013 for a complete description). BOLD components were selected automatically by identifying components that showed TE-dependent decay. These components were then recombined with thermal noise, to create the denoised EPI data. Ninth, because global signal regression was not used, nuisance regressors capturing unaccounted for physiological and motion related noise (Power et al., 2018) (demeaned motion) were then obtained by averaging the time series of each voxel within the WM and 4V ROIs. All regressors were obtained prior to blurring the data (native blur; nb), to avoid further contaminating the regressor with signal from neighboring areas (Jo et al., 2013). Tenth, to examine the effects of blurring on the analyses, a second data set was

created in which the data were incrementally blurred until the observed smoothness was 5mm FWHM and was uniform throughout the brain (b5; 3dBlurtoFWHM). Voxels from the 4V were masked during blurring. Eleventh, the nb and b5 data were bandpass filtered ($0.01 < f < 0.1$) and nuisance regressors were removed, in one step, with 3dTproject (cenmode NTRP). Bandpass filter thresholds were selected to reflect conventional values used in resting state analyses (e.g., Yan et al., 2013; Wu, Gu, Lu, Stein, Chen, & Yang, 2008; cf., Chen & Glover, 2015). Finally, alignment parameters to MNIa were computed using AFNI's @auto_tlrc on the MPRAGE and then applied to the cleaned b5 data. Once in MNIa space, the cleaned and blurred EPI data were used as the target volume for iFC. The target volume was always a blurred dataset. A copy of the nb and b5 EPI was kept in native space to extract the LC, K1, and other ROI seeds.

E2 data were denoised in two different ways: one pipeline that was based on commonly used regression approaches (referred to collectively as regression-based denoising) and one that used ICA-AROMA (collectively referred to, with ME-ICA, as components-based denoising). Except where noted, these pipelines were matched to the ME pipeline described in the previous paragraph.

For the E2+R,4 pipeline, pre-processing skipped Steps 6 and 8, coregistration parameters were calculated using the E2 EPI data, and nuisance regressors included RETROICOR and 4V regression, resulting in a typical regression-based denoising approach for 1E-fMRI data. To apply RETROICOR, respiration and pulse oximetry data were used to generate per slice regressors using AFNI's retroTS.py (Glover et al., 2000) and these were removed from the EPI data using AFNI's 3dREMLfit.

For the E2a pipeline, ICA-AROMA was introduced which employs ICA to identify noise components, similar to ME-ICA, although for motion. For this pipeline, we adapted the procedure from Pruim et al. (2015) into the E2+R,4 pipeline: linear registration parameters were computed with FSL-FLIRT and boundary-based registration (Jenkinson, Bannister, Brady, & Smith, 2002; Jenkinson & Smith, 2001; Greve & Fischl, 2009) and non-linear registration parameters with FSL-FNIRT (Andersson, Jenkinson, & Smith, 2007). Motion parameters were estimated with MCFLIRT (Jenkinson et al., 2002). This pipeline necessitated blurring the data (5mm FWHM) to keep it in line with the methods outlined in Pruim et al. (2015). Results with blurring at levels typically used with ICA-AROMA (6mm) as well as the effects of including blurring in other pipelines can be found in Turker et al. (2021). Because the effects of blurring on LC functional characterization were minimal, they are not covered in the current chapter. After blurring, ICA-AROMA was performed with automatic component selection through MELODIC (Beckmann & Smith, 2004) and non-aggressive denoising. Because ICA-AROMA removes noise related to motion, motion parameters and their derivatives were not included as nuisance regressors in Step 11.

4.3.6 Intrinsic Functional Connectivity Analyses

For first level functional connectivity analyses, seeds were created by averaging the time series of voxels within the ROIs in native space. The seed time series were then correlated with the timeseries of each voxel in the blurred data set in MNIa space for visualization (5mm FWHM, with AFNI's 3dBlurToFWHM). Thus, the blurring here refers to the target data upon which the seed is applied, not the blurring of the seed data itself. The Fisher r-to-z transform was then applied to the correlation maps to produce z-maps for the second level analysis. In the

second level analysis, voxel-wise t-tests (3dTtest++) were performed to test each pipeline against zero and the statistical maps were controlled for multiple comparisons using the false discovery rate (FDR; Genovese, Lazar, & Nichols, 2002). First and second level analyses were performed for each of the denoised data sets to produce functional connectivity maps that varied along several factors: E2 vs. ME (data type), LC vs K1 seeds (ROI), and blurring versus no blurring prior to seed extraction (although, for brevity, effects of blurring are not discussed here).

4.4 Results

4.4.1 Summary of Comparisons and Analyses

The aforementioned procedures allowed us to examine the effects of several data acquisition or pre-processing choices on data quality and functional connectivity maps of putative LC regions. Analyses were carried out in several phases. First, we focused on assessing changes to temporal signal-to-noise ratio (tSNR; the mean of a time series divided by its standard deviation) and delta variation signal (DVARS; the root of the square of the difference in the spatially averaged signal for two successive time points) following various forms of E2 denoising and ME-ICA on ME-fMRI data, reported in Turker et al. (2021). These measures are indicators of data quality. Generally speaking, higher tSNR and lower DVARS are preferred. These analyses indicated that among the E2 pipelines, E2+R,4 performed best in terms of tSNR and E2a performed best in terms of DVARS. ME-ICA was superior to both of these. We then assessed the specificity of the various seed time series that result from these three pipelines. Finally, we characterized the connectivity maps that result from those time series.

Because E2+R,4 and E2a were the best performing pipelines for either tSNR or DVARS, all subsequent analyses considered both those E2 pipelines against the ME pipeline. Recall that

for all the pipelines in this dataset, the underlying neural activity is the same because they come from the same scan. Further analyses comparing a different 1E-fMRI dataset (with shorter TR, optimized for our scanner and given certain scan parameters) to another ME-fMRI acquisition acquired in separate scans are reported in Turker et al. (2021).

4.4.2 T2 Relaxation Estimates*

ME-fMRI can be used to estimate T2* decay rates within each voxel to optimally combine the echoes for each voxel of the brain (Kundu et al., 2017). Variance in T2* decay rates across the brain and across individuals is normal, which is why this estimation with ME-fMRI is beneficial. Variance was examined by calculating the mean and the standard deviation of the individual T2* values generated by meica.py in native space (Fig. 4.3). As expected, these maps illustrate that T2* values vary across regions: values were relatively low in vmPFC (M = 19.899 ms, SD = 2.608), more moderate in medial occipital cortex (e.g., V1, M = 39.691 ms, SD = 4.317), and high in both auditory (M = 51.812 ms, SD = 2.756) and motor cortex (M = 52.208 ms, SD = 6.131). Echo times were moderate and similar for the LC (M = 47.385 ms, SD = 8.801) and K1 (M = 48.211 ms, SD = 6.697). Regions more susceptible to signal dropout due to field inhomogeneities, such as ventral temporal cortex, also showed greater variance across individuals. Therefore, at least part of the tSNR and DVARS advantage for ME-ICA denoising should reflect the optimal combination of echoes using the T2* values for each individual and voxel (Kundu et al., 2017).

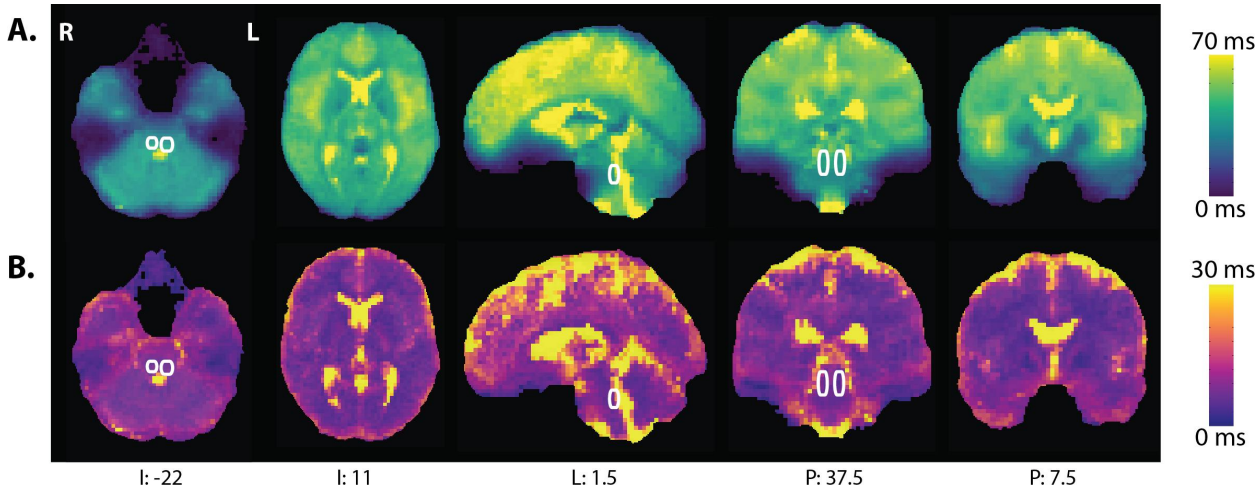

Fig. 4.3 T2* map computed with t2smap.py as part of the meica.py pipeline. *A) Mean observed T2* relaxation across participants. B) Standard deviation of observed T2* relaxation. The location of the LC, outlined in white, is based on the heat map of LC ROIs as illustrated in Figure 4.2. Data in MNIa, with coordinates in LPI. Descriptive statistics for various ROIs were calculated in native space*.

Table 4.1
Means and standard deviations of correlations in the brainstem

	$r_{K1, PT}$	$r_{K1, LC}$	$r_{LC, PT}$	$r_{K1,PT \cdot LC}$
E2+R,4	.233	.388	.161	.189
	(.175)	(.265)	(.171)	(.174)
E2a	.379	.684	.315	.239
	(.205)	(.312)	(.205)	(.175)
ME	.430	.658	.353	.278
	(.191)	(.274)	(.283)	(.225)

Note: Pearson's r values were Fisher transformed to compute the mean and standard deviation and then transformed back. Correlations are presented between nmT1-based LC, atlas-based K1, and PT ROIs for the E2+R,4, E2a, and ME pipelines, including a correlation between K1 and PT with LC partialled out.

4.4.3 Intrinsic Functional Connectivity Analysis

4.4.3.1 Specificity of Seeds

To examine whether estimates of LC function differ across data acquisition approaches and ROI definitions, we computed the correlation coefficients between time series of multiple brainstem regions (Table 4.1).

Correlations for PT with LC and K1 ROIs were used to evaluate whether each ROI captured patterns of activity that were present in other parts of the brainstem. Correlations with PT were greater for K1 than LC ROIs and for ME than E2+R,4 data. These differences were significant in an ANOVA on the Fisher-transformed correlations with PT: correlations with the PT time series significantly differed across K1 and LC ROIs, $F(1,19) = 6.452$, $p = .02$, $\eta_p^2 = .253$ (95% CI: .004–.505) and denoising pipeline, $F(1,19) = 8.271$, $p = .010$, $\eta_p^2 = .303$ (.021–.544). Thus, perhaps unsurprisingly, methods that reduced noise in the data (ME-ICA denoising and blurring) increased the correlations among regions. The benefits of blurring were smaller for ME, relative to E2+R,4, perhaps reflecting the improved tSNR and DVARS.

The moderate correlations between PT and K1, combined with the weaker correlations between LC and the PT, suggest that the LC ROI was less likely to capture activity from the surrounding pons than K1. To confirm this, we regressed out the LC signal from the K1 and PT ROIs and correlated their residuals to produce partial correlations between K1 and PT. These partial correlations remained relatively high, indicating that the atlas-based signal that correlates with the PT reflects substantial activity outside the individually defined LC ROIs.

4.4.3.2 Correlations Among Functional Connectivity Maps

Differences in the iFC maps generated by each method should lead to weaker correlations among maps, particularly if those maps have already been thresholded. Therefore, the effects of seed ROI and denoising approach on estimates of functional connectivity between the LC and the rest of the brain were characterized by determining the correlation and mutual information (Hausser, Strimmer, & Strimmer, 2012) of the resulting maps. For these analyses, only those voxels that were in the top 15% of either map and that were not in the K1 and LC ROIs were considered, because differences in high correlation voxels other than in those ROIs would be of more interest to researchers. Because voxels that survived thresholding in either iFC map were used, correlations will decrease as differences in voxel values increase and as the number of voxels that survive thresholding in one map do not survive thresholding in the other (overlap in thresholded maps is analyzed in the next section).

Voxel-to-voxel correlations across maps generated with E2 pipelines and ME data were small and often negative, and mutual information was low (Table 4.2; see also Fig. 4.4). Keeping pipeline constant and only differing in use of LC or K1, the correlations remain moderate, with mutual information in the same low range as for comparisons between E2 and ME (Table 4.3; Fig. 4.5). Thresholded functional connectivity maps generated from E2 rather than ME data, or from K1 rather than LC ROIs, therefore contained different information, despite all coming from the same scan and thus aiming to characterize connectivity with the same (putative) locus coeruleus signal. The differences between the E2 and ME maps could have resulted from the presence of spurious correlations in the data (Yarkoni, 2009), which may survive thresholding of one map but not the other. Spurious correlations are less likely for the ME data than the E2 data, as higher tSNR should reduce their likelihood (Yarkoni, 2009).

Table 4.2
Relationships between thresholded maps that differed in preprocessing

Map X	Map Y	Pearson's r_{xy}	Mutual Information
E2+R,4 K1	*ME K1*	-.164	0.107
E2+R,4 LC	*ME LC*	-.288	0.085
E2a K1	*ME K1*	.057	0.102
E2a LC	*ME LC*	-.128	0.040
E2a K1	*E2+R,4 K1*	.430	0.212
E2a LC	*E2+R,4 LC*	.139	0.117

Table 4.3
Relationships between thresholded maps that differed in seed ROI

Map X	Map Y	Pearson's r_{xy}	Mutual Information
ME LC	*ME K1*	.347	0.100
E2+R,4 LC	*E2+R,4 K1*	.117	0.097
E2a LC	*E2a K1*	.548	0.113

4.4.3.3 Characterizing the Effects of Seed ROI and Data Type on iFC Maps

To better characterize the extent to which different methods and preprocessing steps result in different LC connectivity maps, we visualized and quantified differences in map topography and correlation values for four central comparisons (Fig. 4.4): (i) ME LC vs E2a LC to evaluate the effects of data type and (ii) ME LC vs ME K1 to evaluate the effects of ROI type.

We also compared (iii) E2a LC to E2+R,4V to examine maps generated by regression-based versus ICA-based denoising approaches to single-echo data.

To quantitatively compare the topography of the functional correlation maps, the Euler characteristic (EC) was calculated with SPM12 (rev. 7487; Penny et al., 2011) for maps thresholded across a range of t-statistics (Fig. 4.5B). Negative ECs occur when voxels that survive the threshold form largely connected topographies with holes rather than disconnected clusters. EC increases and becomes positive as voxels that survive the threshold form disconnected clusters (Bowring et al., 2019; Brett, Penny, & Kiebel, 2003; Worsley, Marrett, Neelin, Vandal, Friston, & Evans, 1996). Therefore, each map was thresholded to the t-statistic that corresponded to the maximum EC to maximize the number of disconnected clusters in a map. ECs were highest for the E2+R,4 LC map (805). They were lower and similar for the E2a LC, ME K1, and ME LC (589, 581, and 578 respectively). However, the maximum ECs occurred at lowest t-statistics for the two E2 maps and at the highest t-statistic for the ME K1 map. The EC for ME K1 was negative around the peak ECs for the other maps, indicating that this functional correlation captured widespread, nonspecific activation (particularly along the midline).

Agreement in which voxels survive increasingly conservative thresholds was evaluated by calculating the Dice coefficient across thresholded maps. Percentile thresholds were used to equate the number of surviving voxels in each map. Consistent with the correlation analyses, Dice coefficients decreased rapidly when the E2a LC maps and ME LC map were compared (Fig. 4.4C-D). Decreases in the Dice coefficient for the ME LC and ME K1 comparison were less steep, but still indicated only modest overlap at high thresholds.

To investigate whether differences in the maps are systematic or reflect random variation across methods, Bland-Altman plots (Bland & Altman, 1999; Bowring et al., 2019) were created. These visualize differences in the estimated correlation coefficient in the two maps as a function of their mean values. Visual inspection of these plots indicates that values in the E2a LC map were higher than the E2+R,4 LC map (Fig. 4.4C), suggesting that ICA-AROMA can boost statistical power of 1E-fMRI data analyses. However, ME-fMRI remains advantageous, as ME LC had systematically higher values than did E2a LC (Fig. 4.4D). Utilizing the K1 ROI rather than the LC ROI produced large differences in the maps: the mean of the difference in estimated correlations was nearly 1.96 standard deviations above 0, with larger differences at more extreme mean values.

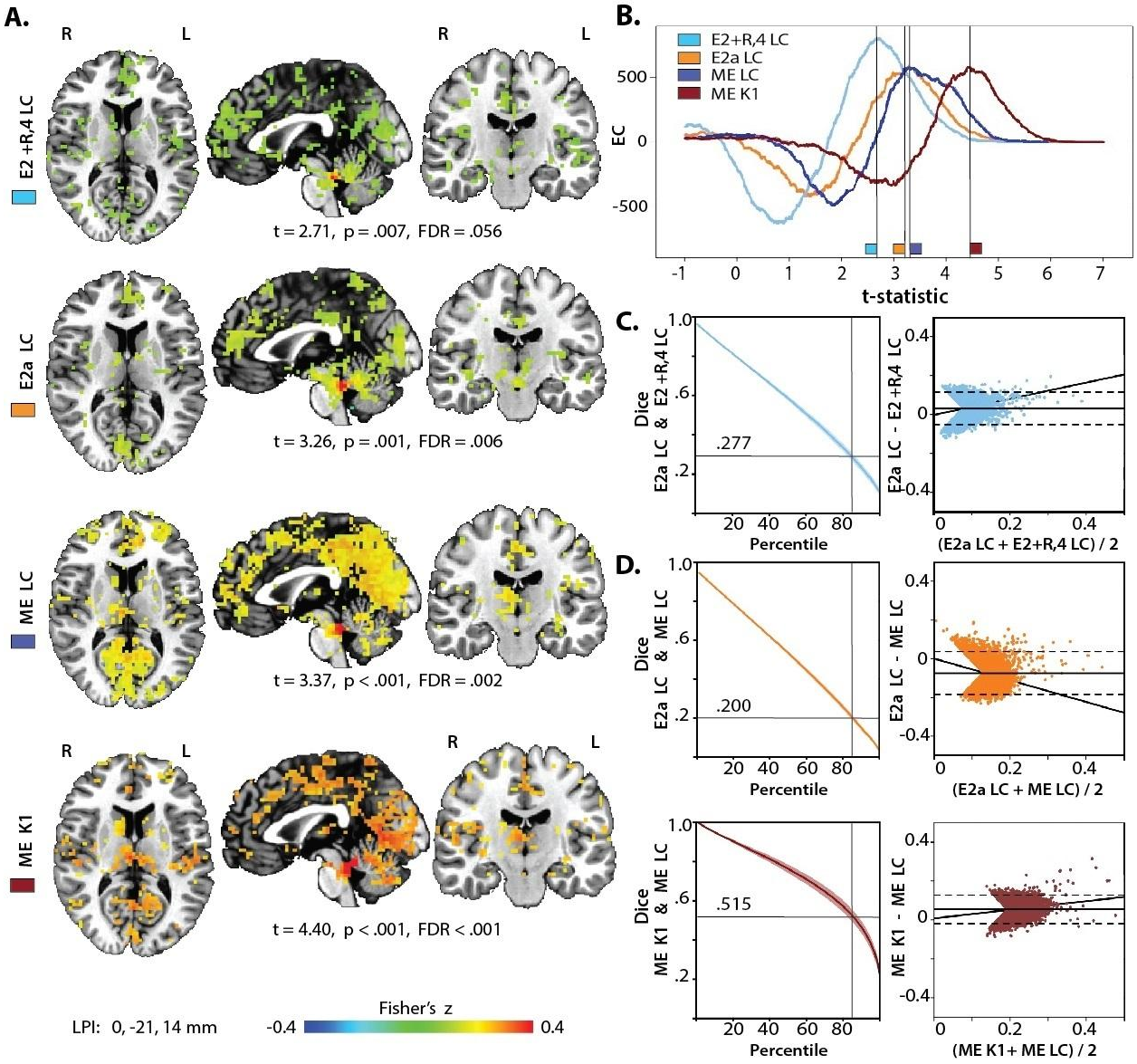

Fig. 4.4 Intrinsic functional connectivity maps. *A) iFC maps for the different LC seeds with various ME and E2 pipelines. Maps were thresholded at the t-statistic with the maximum EC. B) EC for all iFC maps as a function of the t-statistic. C) Dice coefficients across percentiles and Bland-Altman plots comparing the E2+R,4 pipeline to the E2a pipeline. Horizontal line indicates the 85th percentile. This served as the threshold for analyses reported in Table 4.2, Table 4.3, and for the Bland-Altman plots in the right column. Solid line: mean difference, dashed lines: +/-1.96 of the standard deviation of the differences. D) Dice coefficients and Bland-Altman plots to compare the ME LC iFC map against the E2a pipeline with nmT1-based LC ROIs and against the ME-ICA pipeline with atlas-based K1 ROIs.*

4.4.3.4 Characterization of LC Functional Connectivity with Other Brain Regions

To further characterize differences in the iFC maps, we investigated the proximity of the peaks in the ME LC map to peaks in each of the other maps. Twenty-five peaks were extracted from each map (using AFNI's 3dmaxima) with a minimal distance of 18 mm (6 voxels) between a given ranked peak and the next. This approach first finds the top peak in a given map and then excludes any other peaks within 18 mm before searching for the next highest peak. Table 2.4 lists the top 25 peaks for the ME LC map as well as the rank of the nearest peak in the comparison maps. Some caution is warranted in interpreting these data, since peaks that do not make it into the top 25 of one map may nevertheless fall close to a peak that did make it into the top peaks of another map. Consistent with the previous analyses, the percentage of peaks in the ME LC map that fell within 18 mm of a peak on another map was highest for the E2a LC map (17 peaks, 68%), second for the ME K1 map (16 peaks, 68%), and lowest for E2+R,4 LC (13 peaks, 52%).

Table 4.4
Ranked peaks in ME LC nb and their proximity to peaks in the other iFC maps

Rank	Area	Coordinates (LPI)	Fisher's Z (%-tile)	Rank of nearest peak in E2a LC (mm distance)	Rank of nearest peak in ME K1 (mm distance)
1	R. Locus coeruleus	4 -41 -19	0.562 (99.99)	1 (3)*	1 (9)*
2	R. Thalamus	4 -23 14	0.301 (99.95)	18 (13.4)*	3 (0)*
3	L. Precuneus	-2 -41 53	0.294 (99.95)	22 (13.4)*	20 (15)*
4	R. Visual cortex / BA 18	19 -77 -7	0.287 (99.94)	24 (9.9)*	4 (0)*
5	R. Anterior Cingulate	10 34 20	0.285 (99.94)	3 (8.5)*	25 (3)*
6	R. Hippocampus / Parahipp. gyrus	16 -38 -1	0.282 (99.93)	17 (12.4)*	7 (6.7)*
7	L. Anterior Cingulate	-11 37 14	0.275 (99.93)	7 (17.2)*	25 (19.2)
8	L. Precuneus	-2 -65 20	0.275 (99.90)	11 (19.4)	2 (16.4)*
9	L. Retrosplenial Cortex / BA 30	-5 -50 8	0.274 (99.89)	10 (11.2)*	21 (0)*
10	L. Hippocampus / Parahipp. gyrus	-29 -41 -10	0.273 (99.89)	2 (12.7)*	18 (9)*

11	R. Precuneus	16 -65 26	0.272 (99.89)	11 (7.3)*	2 (26.5)
12	L. Angular gyrus	-44 -59 41	0.271 (99.88)	4 (29.1)	5 (42.5)
13	L. Visual cortex / BA 17-18	-26 -89 -10	0.235 (99.85)	12 (13.1)*	12 (6)*
14	L. Precuneus	-2 -74 62	0.267 (99.84)	22 (21.2)	11 (21.2)
15	L. Hippocampus / Parahipp. gyrus	-11 -32 -1	0.266 (99.84)	2 (14.7)*	18 (15.6)*
16	L. Visual cortex / BA 19	-44 -77 -1	0.265 (99.84)	12 (23.6)	14 (7.3)*
17	R. Visual cortex / BA 17-18	1 -83 -4	0.265 (99.83)	9 (9)*	2 (15)*
18	R. Parieto-occip. fissure	10 -83 47	0.265 (99.83)	11 (21.4)	11 (0)*
19	L. Precuneus	-2 -59 47	0.263 (99.81)	22 (13.4)*	20 (20.1)
20	L. Posterior Cingulate	-23 -62 11	0.262 (99.80)	4 (23.6)	21 (21.8)
21	L. Precuneus	-5 -53 68	0.261 (99.79)	22 (9.5)*	20 (5.2)*
22	R. Dorsomedial Prefrontal Cortex / BA 9	28 43 20	0.260 (99.78)	3 (26.3)	25 (22.8)

23	R. Transverse gyrus / BA 42	46 -29 11	0.258 (99.75)	21 (17.5)*	16 (10.8)*
24	L. Medial Superior Frontal gyrus	-2 25 41	0.257 (99.73)	20 (15)*	25 (24.6)
25	Subcallosal (parolfactory) area / BA 25	1 10 -1	0.256 (99.72)	18 (27.3)	8 (25.8)

Note: *=peaks that were less than 18 mm apart and would be considered part of the same cluster by our peak finding algorithm. Labels for the area are based on the peak coordinates, center of mass for the peak's cluster, and anatomical plausibility.

4.5 General Discussion

A growing body of research on the functional and anatomical properties of the LC suggests that it plays a central role in a variety of cognitive processes and in neurodegenerative disease (Mather & Harley, 2016). However, characterizing LC function and anatomy in human fMRI has multiple challenges that have not been systematically investigated in the literature (Liu et al., 2017). This chapter addressed several of these challenges by comparing LC localization approaches and fMRI BOLD data acquisition and denoising approaches. The analyses suggest that alternatives in LC localization method, data acquisition, and denoising approaches are likely to lead to different interpretations of the same data. These results are especially important and timely given the broader conversation in fMRI literature on the effects of pipeline variability (Botvinik-Nezer et al., 2020).

4.5.1 Localization of LC with a Probabilistic Atlas or nmT1 Imaging

One purpose of this study was to investigate whether individually defining LC ROIs using nmT1 imaging produces substantially different results from using a probabilistic atlas. Probabilistic ROIs may not adequately account for variability in individual brainstem anatomy and LC shape and location (German et al., 1988; Keren et al., 2015). In addition, studies report a wide range of bilateral LC coordinates that sometimes go beyond the dimensions of the Keren atlas (Liu et al., 2017). The use of an ROI defined by coordinates or a group atlas, like the K1 ROIs used here, could therefore partially miss the LC, if not entirely, and capture activity from neighboring brainstem areas (e.g., the pontine tegmentum, medial cerebral peduncle, cranial nerve nuclei, and inferior colliculus; Neary, 2008). These neighboring areas play critical roles in processing motor and sensory information, which would confound analyses. Thus, despite the practical advantages of probabilistic atlases, the best way to isolate activity from the LC could still be to individually define ROIs using nmT1 imaging.

The results support this recommendation: the K1 ROIs were larger and tended to extend further rostrally and caudally than the individual LC ROIs, and there was only low to moderate overlap between the individually defined LC ROIs and K1 ROIs. Activity in the K1 ROIs was also more strongly correlated with activity and in the pontine tegmentum than was activity in the LC ROIs. These differences had consequences for estimates of LC connectivity: overlap between thresholded iFC maps generated by LC and K1 ROIs was moderate (.515 for the top 15% of voxels). The Keren atlas also produced stronger correlations overall, which caused less specific activity at thresholds used for the other maps, and the need for higher thresholds to isolate network clusters. In addition, although the LC and K1 ROIs produced maps with peaks that were near each other (i.e., thalamus, HPC, midline regions, and auditory and visual areas), the K1 iFC

maps also included highly ranked peaks in primary and supplementary motor areas. Thus, the final iFC maps produced by K1 showed more widespread associations that also differed in their spatial topography from those produced by the nmT1-based LC ROIs.

Ultimately, the choice to use either an atlas or manual tracing will depend on several factors. Although tracing may confer more confidence in one's localization of the LC in fMRI data, it necessitates an additional nmT1-based scan and subsequent time investment in individually tracing each ROI for each participant in the study. This may not be feasible for every study. In those cases, an atlas is practical and beneficial. Atlasses also offer the opportunity to analyze data from other studies in novel ways.

4.5.2 Use of ME-fMRI Versus 1E-fMRI

Because ME-ICA denoising may be particularly effective at reducing noise from motion and improving BOLD contrast (Power et al., 2018), another goal of this study was to characterize whether the resting state iFC maps differed between ME-fMRI and 1E-fMRI. Results suggested that ME and E2 data from the same run, thus reflecting the same brain activity, can result in different iFC maps. Overlap between ME and E2a iFC maps decreased rapidly as thresholds increased, correlations between the thresholded group level iFC maps were low, and only 68% of peaks in the ME LC map fell within 18 mm of the top peaks on the E2a LC map. Though our results suggest that ICA-AROMA should be used with single echo data, they nevertheless demonstrate that the maps that resulted from the ICA-AROMA and ME-ICA pipelines differed both quantitatively (Fig. 4.4) and qualitatively (Table 4.4). These differences could reflect the ability to accommodate different optimal echo times across the brain and to remove components of the signal with non-BOLD-like characteristics when using ME-fMRI (Kundu et al., 2012).

Indeed, ME-fMRI with ME-ICA was superior to 1E-fMRI in both tSNR and DVARS in every region examined, including the LC ROIs (Turker et al., 2021). Importantly, these differences are unlikely to be mitigated by using shorter TRs that are possible in a 1E-fMRI scan. Nearly identical patterns were observed when comparing ME-fMRI data to 1E-fMRI data acquired in a separate resting state scan and with a shorter TR (1.9 s; see Turker et al., 2021). Thus, the use of ME-fMRI is advantageous, particularly with small regions like the LC.

4.5.3 Functional connectivity of the LC in Typical Young Adults

Previous functional studies on the LC have exclusively been performed using 1E-fMRI and frequently used the Keren 2 SD atlas (analyses in this chapter focused on the more conservative 1 SD atlas). Across those studies, regions that typically emerge in iFC analyses are the prefrontal cortex, cerebellum, right supplementary motor area, cingulate cortex, thalamus, visual cortex, lingual and fusiform gyrus, insula, amygdala, and the hippocampus (e.g., Bär et al., 2016; Köhler, Wagner, & Bär, 2019; Kline et al., 2016; Murphy et al., 2014; Sterpenich et al., 2006). Nearly all these regions were ranked highly in our ME K1 map. The amygdala did not rank in the top of any of our maps, possibly because it was too close to peaks in the hippocampus to survive our peak selection procedure.

Other studies on LC iFC have not always identified the same regions. For example, Song et al. (2017) showed connectivity to the reticular formation, ventral tegmental area, and caudate. None of our pipelines ranked any peaks in the reticular formation highly (other than peaks constituting the LC), although these (or nearby) regions may have survived our Euler characteristic-based thresholding procedure. The ventral tegmental area was ranked 6th in the E2a LC and ME K1 map, however. Zhang, Hu, Chao, & Li (2016) found positive connectivity to

inferior temporal cortex, anterior parahippocampal gyrus, posterior insula, ventrolateral thalamus, and a large region in the cerebellum. Intriguingly, they found negative connectivity to several regions that were positively correlated with the LC in our maps (similar to others), including the bilateral visual cortex, middle and superior temporal cortex, precuneus, retrosplenial cortex, posterior parahippocampal cortex, frontopolar cortex, caudate, and dorsal and medial thalamus. An important methodological difference between our study and theirs, however, was the use of whole brain (global) signal regression, which can introduce negative correlations (Fox, Zhang, Snyder, & Raichle, 2009). We will return to this point below.

One intriguing peak found in our maps was a cluster in the basal forebrain (subcallosal area in Table 4.4). This cluster has not been widely reported in studies of LC iFC, perhaps because it is located in a part of the brain that is susceptible to field inhomogeneities and difficult to measure using 1E-fMRI. Previous work has demonstrated that ME-fMRI can effectively recover signal from this region during pre-processing (Markello et al., 2018). Relative to our 1E-fMRI maps, the clearer presence of this region in our ME maps is particularly important: studies on the basal forebrain's physiology and function suggest an important anatomical and functional relationship between these regions and the LC in the regulation of attention and memory (e.g., Mesulam, 2013; Ljubojevic, Luu, & De Rosa, 2014; Sarter, Hasselmo, Bruno, & Givens, 2005; Yu & Dayan, 2005).

4.5.4 Limitations and Further Considerations

There are several limitations to the results presented here. First, we did not explore several other denoising approaches for 1E or ME data (e.g., ANATICOR) and it is possible that these would have led to different outcomes (e.g., Dipasquale et al., 2017; Jo et al., 2010; for a

review of several common denoising procedures, see Caballero-Gaudes & Reynolds, 2017). Second, a common denoising strategy in resting state iFC analyses is to regress out the mean signal across the brain (global signal) to reduce the contributions of physiological and motion related artifacts (Liu, Nalci, & Falahpour, 2017). Although some argue that global signal regression is the most effective way to remove physiological noise (e.g. Power et al., 2018), it does contain functional signals (e.g., Schölvinck, Maier, Frank, Duyn, & Leopold, 2010), including those related to vigilance (e.g., Liu et al., 2017). This is of particular concern for studies of the LC because it is involved in regulating vigilance both on and off-task (e.g., Aston-Jones et al., 1994; Aston-Jones et al., 2007), and has widespread projections throughout the brain (e.g., Schwarz & Luo, 2015). To avoid removing LC related activity, we therefore utilized white matter nuisance regression and bandpass filtering (with a commonly applied range) to reduce the contributions of respiration, heart rate, and movement to the EPI data (Power et al., 2018). While this approach also could still remove meaningful LC-related signal as well as noise, it is less aggressive than global signal regression. In analyses that utilized global signal regression (Turker et al., 2021), correlations were weaker, included negative values (a common consequence of global signal regression; Fox et al., 2009; Zhang et al., 2016), and included only pontine areas centered on the respective seed when thresholded at $p = .05$. New approaches, such as temporal ICA (Glasser et al., 2018), may offer other ways to address physiological noise captured by the global signal and their application will require future investigation.

There are also pragmatic concerns associated with ME-fMRI, which requires longer TRs than 1E-fMRI and greater computational resources. Shorter TRs are sometimes needed to characterize the hemodynamic response or when tasks include events that are closely spaced.

Under these conditions, multi-echo multi-band techniques (MEMB; e.g., Olafsson, Kundu, Wong, Bandettini, & Liu, 2015) could be used. One systematic evaluation of ME-ICA with MEMB suggests that this approach may offer additional benefits by improving estimates of the hemodynamic response (Kundu et al., 2017). Although multi-band techniques were outside the scope of the current study, they certainly warrant separate investigation in combination with ME-fMRI. However, ME-fMRI also has higher computational costs than 1E-fMRI that would be exacerbated by combining it with multi-band imaging. Because acquiring three echoes triples the amount of data acquired during a scan, ME-fMRI requires more storage than 1E-fMRI. In addition, running ME-ICA adds substantial processing time to preprocessing. Similar to the choice between atlas-based and nmT1-based LC localization, depending on a given study's experimental goals, timeframe, and budget, these factors may reduce the utility of ME-fMRI with ME-ICA, despite the clear and well-established boost to data quality and power.

The ability to use nmT1 imaging may also be limited to particular scanners and populations. Neuromelanin levels change over the lifespan (Halliday, Fedorow, Rickert, Gerlach, Riederer, & Double, 2006) and differ between clinical and non-clinical populations (Braak, Thal, Ghebremedhin, & Del Tredici, 2011; Marien, Colpaert, & Rosenquist, 2004). Researchers interested in the effects of neuromelanin on cognitive decline in the elderly, cognitive development in childhood, or the mediating role of neuromelanin on cognitive differences between clinical and non-clinical populations, may therefore have to consider alternative ways of localizing the LC. Furthermore, nmT1 scanning may work best with 3T scanners, as it has a better signal to noise ratio than 1.5T (Uğurbil et al., 1993) but none of the unique challenges that come with human imaging at 7T or higher (Ladd et al., 2018). However, the exact benefits and

disadvantages that come with scanning pontine nuclei at different field strengths remain unexplored.

It will be important for future research to more extensively evaluate the contributions of different volume registration approaches for characterizing LC function. The small size of the LC (within-plane diameter of the LC is about 2.5 mm; Fernandes et al., 2012) and coarse spatial resolution of functional images (usually 2 or 3 mm isotropic voxels) also make it critically important to align the EPI data and the ROIs as accurately as possible. However, many registration algorithms are optimized for aligning the neocortex rather than the brainstem to an atlas. The brainstem may be best aligned to group data if it is separated from the rest of the brain and nonlinearly warped to the template (Tona et al., 2017). However, such algorithms are not widely used.

Finally, in-house algorithms that partially or fully automate LC segmentation are still in development, with no systematic comparison existing yet between manual and automated methods (e.g., Betts et al., 2019; Chen et al., 2014; Morris et al., 2020). As these algorithms become more widely adopted, it will be important for future research to compare their resultant LC characterization to those presented here.

4.6 Conclusion

fMRI studies of LC function and structure have been hampered by the difficulties involved in localizing the LC, isolating LC activity from other nearby regions, and removing the effects of noise from motion and physiology on BOLD data (Liu et al., 2017). By systematically investigating the benefits of using nmT1 images and ME-fMRI, this study has found that the

methods used to localize the LC, acquire BOLD data, and denoise it may have significant effects on how LC function is characterized. Although using nmT1 images to localize the LC necessitates additional scan time and manual tracing, these efforts may lead to greater specificity in the iFC maps. In addition, ME-fMRI with ME-ICA denoising protocols increased the quality of the data and revealed a cluster in the basal forebrain, a region that is otherwise susceptible to signal drop out (Park et al., 1988).

Although there is no ground truth for what the functional characterization of the LC must look like across various measures, our results do suggest that, when possible, the use of ME-fMRI data acquisition combined with nmT1-based localization should increase confidence in one's characterization of LC connectivity. These approaches, however, come at a cost that may render them unfeasible for certain studies. Ultimately, whatever methods are chosen, LC researchers must carefully consider their tradeoffs in their methodology and nuance findings accordingly.

References

Andersson, J. L., Jenkinson, M., & Smith, S. (2007). Non-linear registration aka Spatial normalisation FMRIB Technical Report TR07JA2. FMRIB Analysis Group of the University of Oxford, 1-22.

Astafiev, S. V., Snyder, A. Z., Shulman, G. L., & Corbetta, M. (2010). Comment on "Modafinil shifts human locus coeruleus to low-tonic, high-phasic activity during functional MRI" and "Homeostatic sleep pressure and responses to sustained attention in the suprachiasmatic area." *Science*, *328*(5976), 309-309. https://doi.org/10.1126/science.1177200

Aston-Jones, G., Shipley, M. T., Chouvet, G., Ennis, M., van Bockstaele, E., Pieribone, V., … Williams, J. T. (1991). Chapter 4 - Afferent regulation of locus coeruleus neurons: Anatomy, physiology and pharmacology. In C. D. Barnes & O. Pompeiano (Eds.), *Progress in Brain Research,* (Vol. 88, pp. 47–75). Elsevier Press. https://doi.org/10.1016/S0079-6123(08)63799-1

Aston-Jones, G., Gonzalez, M., & Doran, S. (2007). Role of the locus coeruleus-norepinephrine system in arousal and circadian regulation of the sleep-wake cycle. In *Brain norepinephrine: Neurobiology and therapeutics*(pp. 157–195). https://doi.org/10.1017/CBO9780511544156.007

Aston-Jones, G., Rajkowski, J., & Cohen, J. (1999). Role of locus coeruleus in attention and behavioral flexibility. *Biological Psychiatry*, *46*(9), 1309–1320. https://doi.org/10.1016/S0006-3223(99)00140-7

Aston-Jones, G., Rajkowski, J., Kubiak, P., & Alexinsky, T. (1994). Locus coeruleus neurons in monkey are selectively activated by attended cues in a vigilance task. *Journal of Neuroscience*, *14*(7), 4467-4480.

Aston-Jones, G., & Waterhouse, B. (2016). Locus Coeruleus: From Global Projection System to Adaptive Regulation of Behavior. *Brain Research*, *1645*, 75–78. https://doi.org/10.1016/j.brainres.2016.03.001

Bär, K.-J., de la Cruz, F., Schumann, A., Koehler, S., Sauer, H., Critchley, H., & Wagner, G. (2016). Functional connectivity and network analysis of midbrain and brainstem nuclei. *NeuroImage*, *134*, 53–63. https://doi.org/10.1016/j.neuroimage.2016.03.071

Beckmann, C. F., & Smith, S. M. (2004). Probabilistic independent component analysis for functional magnetic resonance imaging. *IEEE Transactions on Medical Imaging*, *23*(2), 137-152.

Berridge, C. W., & Waterhouse, B. D. (2003). The locus coeruleus–noradrenergic system: Modulation of behavioral state and state-dependent cognitive processes. *Brain Research Reviews*, *42*(1), 33–84. https://doi.org/10.1016/S0165-0173(03)00143-7

Betts, M. J., Kirilina, E., Otaduy, M. C., Ivanov, D., Acosta-Cabronero, J., Callaghan, M. F., ... & Loane, C. (2019). Locus coeruleus imaging as a biomarker for noradrenergic dysfunction in neurodegenerative diseases. *Brain*, *142*(9), 2558-2571.

https://doi.org/10.1093/brain/awz193
Birn, R. M., Molloy, E. K., Patriat, R., Parker, T., Meier, T. B., Kirk, G. R., ... & Prabhakaran, V. (2013). The effect of scan length on the reliability of resting-state fMRI connectivity estimates. *Neuroimage*, *83*, 550-558.
Biswal, B., Yetkin, F. Z., Haughton, V. M., & Hyde, J. S. (1995). Functional connectivity in the motor cortex of resting human brain using echo-planar mri. *Magnetic Resonance in Medicine*, *34*(4), 537–541. https://doi.org/10.1002/mrm.1910340409
Bland, J. M., & Altman, D. G. (1999). Measuring agreement in method comparison studies. *Statistical Methods in Medical Research*, *8*(2), 135–160. https://doi.org/10.1177/096228029900800204
Botvinik-Nezer, R., Holzmeister, F., Camerer, C. F. *et al.* (2020). Variability in the analysis of a single neuroimaging dataset by many teams. *Nature*, 582, 84-88. https://doi.org/10.1038/s41586-020-2314-9
Bowring, A., Maumet, C., & Nichols, T. E. (2019). Exploring the impact of analysis software on task fMRI results. *Human Brain Mapping*, *40*(11), 3362–3384. https://doi.org/10.1002/hbm.24603
Braak, H., Thal, D. R., Ghebremedhin, E., & Del Tredici, K. (2011). Stages of the Pathologic Process in Alzheimer Disease: Age Categories From 1 to 100 Years. *Journal of Neuropathology & Experimental Neurology*, *70*(11), 960–969. https://doi.org/10.1097/NEN.0b013e318232a379
Brett, M., Penny, W., & Kiebel, S. (2003). *An Introduction to Random Field Theory*. In R. Frackowiak, K. Friston, C. Frith, R. Dolan, C. Price, S. Zeki, J. Ashburner, & W. Penny (Eds.), *Human Brain Function II,* (Chapter 14). Academic Press.
Breton-Provencher, V., & Sur, M. (2019). Active control of arousal by a locus coeruleus GABAergic circuit. *Nature Neuroscience*, *22*(2), 218–228. doi:10.1038/s41593-018-0305-z
Caballero-Gaudes, C., & Reynolds, R. C. (2017). Methods for cleaning the BOLD fMRI signal. *NeuroImage*, *154*, 128-149.
Chandler, D. J., Gao, W.-J., & Waterhouse, B. D. (2014). Heterogeneous organization of the locus coeruleus projections to prefrontal and motor cortices. *Proceedings of the National Academy of Sciences of the United States of America*, *111*(18), 6816–6821. https://doi.org/10.1073/pnas.1320827111
Chen, J. E., & Glover, G. H. (2015). BOLD fractional contribution to resting-state functional connectivity above 0.1 Hz. *NeuroImage*, *107*, 207-218.
Chen, X., Huddleston, D. E., Langley, J., Ahn, S., Barnum, C. J., Factor, S. A., ... & Hu, X. (2014). Simultaneous imaging of locus coeruleus and substantia nigra with a quantitative neuromelanin MRI approach. Magnetic resonance imaging, 32(10), 1301-1306. https://doi.org/10.1016/j.mri.2014.07.003
Cho, Z. H., & Ro, Y. M. (1992). Reduction of susceptibility artifact in gradient-echo imaging. *Magnetic Resonance in Medicine*, *23*(1), 193–200.

https://doi.org/10.1002/mrm.1910230120
Clewett, D. V., Lee, T.-H., Greening, S., Ponzio, A., Margalit, E., & Mather, M. (2016). Neuromelanin marks the spot: Identifying a locus coeruleus biomarker of cognitive reserve in healthy aging. *Neurobiology of Aging*, *37*, 117–126. https://doi.org/10.1016/j.neurobiolaging.2015.09.019
Costa, V. D., & Rudebeck, P. H. (2016). More than Meets the Eye: The Relationship between Pupil Size and Locus Coeruleus Activity. *Neuron*, *89*(1), 8–10. https://doi.org/10.1016/j.neuron.2015.12.031
Cox, R. W. (1996). AFNI: Software for Analysis and Visualization of Functional Magnetic Resonance Neuroimages. *Computers and Biomedical Research*, *29*(3), 162–173. https://doi.org/10.1006/cbmr.1996.0014
Cox, R. W., & Jesmanowicz, A. (1999). Real-time 3D image registration for functional MRI. *Magnetic Resonance in Medicine*, *42*(6), 1014–1018. https://doi.org/10.1002/(SICI)1522-2594(199912)42:6<1014::AID-MRM4>3.0.CO;2-F
Dagli, M. S., Ingeholm, J. E., & Haxby, J. V. (1999). Localization of cardiac-induced signal change in fMRI. *NeuroImage*, *9*(4), 407–415. https://doi.org/10.1006/nimg.1998.0424
Dale, A. M., Fischl, B., & Sereno, M. I. (1999). Cortical Surface-Based Analysis: I. Segmentation and Surface Reconstruction. *NeuroImage*, *9*(2), 179–194. https://doi.org/10.1006/nimg.1998.0395
Dipasquale, O., Sethi, A., Laganà, M. M., Baglio, F., Baselli, G., Kundu, P., … Cercignani, M. (2017). Comparing resting state fMRI de-noising approaches using multi- and single-echo acquisitions. *PLoS ONE*, *12*(3), e0173289. https://doi.org/10.1371/journal.pone.0173289
Einhäuser, W., Stout, J., Koch, C., & Carter, O. (2008). Pupil dilation reflects perceptual selection and predicts subsequent stability in perceptual rivalry. *Proceedings of the National Academy of Sciences*, *105*(5), 1704–1709. https://doi.org/10.1073/pnas.0707727105
Eldar, E., Niv, Y., & Cohen, J. D. (2016). Do You See the Forest or the Tree? Neural Gain and Breadth Versus Focus in Perceptual Processing. *Psychological Science*, *27*(12), 1632–1643. https://doi.org/10.1177/0956797616665578
Enochs, W. S., Petherick, P., Bogdanova, A., Mohr, U., & Weissleder, R. (1997). Paramagnetic metal scavenging by melanin: MR imaging. *Radiology*, *204*(2), 417–423. https://doi.org/10.1148/radiology.204.2.9240529
Fernandes, P., Regala, J., Correia, F., & Gonçalves-Ferreira, A. J. (2012). The human locus coeruleus 3-D stereotactic anatomy. *Surgical and Radiologic Anatomy*, *34*(10), 879–885. https://doi.org/10.1007/s00276-012-0979-y
Fischl, B., Sereno, M. I., & Dale, A. M. (1999). Cortical Surface-Based Analysis: II: Inflation, Flattening, and a Surface-Based Coordinate System. *NeuroImage*, *9*(2), 195–207. https://doi.org/10.1006/nimg.1998.0396
Foote, S. L., Freedman, R., & Oliver, A. P. (1975). Effects of putative neurotransmitters on

neuronal activity in monkey auditory cortex. *Brain Research*, *86*(2), 229–242. https://doi.org/10.1016/0006-8993(75)90699-X

Fox, M. D., Zhang, D., Snyder, A. Z., & Raichle, M. E. (2009). The Global Signal and Observed Anticorrelated Resting State Brain Networks. *Journal of Neurophysiology*, *101*(6), 3270–3283. https://doi.org/10.1152/jn.90777.2008

Genovese, C. R., Lazar, N. A., & Nichols, T. (2002). Thresholding of statistical maps in functional neuroimaging using the false discovery rate. *NeuroImage*, *15*(4), 870–878. https://doi.org/10.1006/nimg.2001.1037

German, D. C., Walker, B. S., Manaye, K., Smith, W. K., Woodward, D. J., & North, A. J. (1988). The human locus coeruleus: Computer reconstruction of cellular distribution. *Journal of Neuroscience*, *8*(5), 1776–1788. https://doi.org/10.1523/JNEUROSCI.08-05-01776.1988

Gilzenrat, M. S., Nieuwenhuis, S., Jepma, M., & Cohen, J. D. (2010). Pupil diameter tracks changes in control state predicted by the adaptive gain theory of locus coeruleus function. *Cognitive, Affective & Behavioral Neuroscience*, *10*(2), 252–269. https://doi.org/10.3758/CABN.10.2.252

Glasser, M. F., Coalson, T. S., Bijsterbosch, J. D., Harrison, S. J., Harms, M. P., Anticevic, A., ... & Smith, S. M. (2018). Using temporal ICA to selectively remove global noise while preserving global signal in functional MRI data. *NeuroImage*, 181, 692-717. https://doi.org/10.1016/j.neuroimage.2018.04.076

Glennon, E., Carcea, I., Martins, A. R. O., Multani, J., Shehu, I., Svirsky, M. A., & Froemke, R. C. (2019). Locus coeruleus activation accelerates perceptual learning. *Brain Research*, *1709*, 39–49. https://doi.org/10.1016/j.brainres.2018.05.048

Glover, G. H., Li, T.-Q., & Ress, D. (2000). Image-based method for retrospective correction of physiological motion effects in fMRI: RETROICOR. *Magnetic Resonance in Medicine*, *44*(1), 162–167. https://doi.org/10.1002/1522-2594(200007)44:1<162::AID-MRM23>3.0.CO;2-E

Greene, C. M., Bellgrove, M. A., Gill, M., & Robertson, I. H. (2009). Noradrenergic genotype predicts lapses in sustained attention. *Neuropsychologia*, *47*(2), 591–594. https://doi.org/10.1016/j.neuropsychologia.2008.10.003

Grella, S. L., Neil, J. M., Edison, H. T., Strong, V. D., Odintsova, I. V., Walling, S. G., … Harley, C. W. (2019). Locus Coeruleus Phasic, But Not Tonic, Activation Initiates Global Remapping in a Familiar Environment. *Journal of Neuroscience*, *39*(3), 445–455. https://doi.org/10.1523/JNEUROSCI.1956-18.2018

Greve, D. N., & Fischl, B. (2009). Accurate and robust brain image alignment using boundary-based registration. *NeuroImage*, *48*(1), 63-72.

Halliday, G. M., Fedorow, H., Rickert, C. H., Gerlach, M., Riederer, P., & Double, K. L. (2006). Evidence for specific phases in the development of human neuromelanin. *Journal of Neural Transmission*, *113*(6), 721–728. https://doi.org/10.1007/s00702-006-0449-y

Hausser, J., Strimmer, K., & Strimmer, M. K. (2012). Package 'entropy' for R.

Jenkinson, M., Bannister, P., Brady, M., & Smith, S. (2002). Improved optimization for the robust and accurate linear registration and motion correction of brain images. *NeuroImage*, *17*(2), 825-841.

Jenkinson, M., & Smith, S. (2001). A global optimisation method for robust affine registration of brain images. *Medical Image Analysis*, *5*(2), 143-156.

Jepma, M., & Nieuwenhuis, S. (2010). Pupil Diameter Predicts Changes in the Exploration–Exploitation Trade-off: Evidence for the Adaptive Gain Theory. *Journal of Cognitive Neuroscience*, *23*(7), 1587–1596. https://doi.org/10.1162/jocn.2010.21548

Jo, H. J., Gotts, S. J., Reynolds, R. C., Bandettini, P. A., Martin, A., Cox, R. W., & Saad, Z. S. (2013). Effective preprocessing procedures virtually eliminate distance-dependent motion artifacts in resting state FMRI. *Journal of Applied Mathematics*, *2013*. https://doi.org/10.1155/2013/935154

Jo, H. J., Saad, Z. S., Simmons, W. K., Milbury, L. A., & Cox, R. W. (2010). Mapping Sources of Correlation in Resting State FMRI, with Artifact Detection and Removal. *NeuroImage*, *52*(2), 571–582. https://doi.org/10.1016/j.neuroimage.2010.04.246

Jones, B. E., & Moore, R. Y. (1977). Ascending projections of the locus coeruleus in the rat. II. Autoradiographic study. *Brain Research*, *127*(1), 23–53. https://doi.org/10.1016/0006-8993(77)90378-X

Jones, B. E., & Yang, T.-Z. (1985). The efferent projections from the reticular formation and the locus coeruleus studied by anterograde and retrograde axonal transport in the rat. *Journal of Comparative Neurology*, *242*(1), 56–92. https://doi.org/10.1002/cne.902420105

Joshi, S., Li, Y., Kalwani, R., & Gold, J. I. (2016). Relationships between pupil diameter and neuronal activity in the locus coeruleus, colliculi, and cingulate cortex. *Neuron*, *89*(1), 221–234. https://doi.org/10.1016/j.neuron.2015.11.028

Keren, N. I., Lozar, C. T., Harris, K. C., Morgan, P. S., & Eckert, M. A. (2009). In vivo mapping of the human locus coeruleus. *NeuroImage*, *47*(4), 1261–1267. https://doi.org/10.1016/j.neuroimage.2009.06.012

Keren, N. I., Taheri, S., Vazey, E. M., Morgan, P. S., Granholm, A.-C. E., Aston-Jones, G. S., & Eckert, M. A. (2015). Histologic validation of locus coeruleus MRI contrast in post-mortem tissue. *NeuroImage*, *113*, 235–245. https://doi.org/10.1016/j.neuroimage.2015.03.020

Kline, R. L., Zhang, S., Farr, O. M., Hu, S., Zaborszky, L., Samanez-Larkin, G. R., & Li, C.-S. R. (2016). The Effects of Methylphenidate on Resting-State Functional Connectivity of the Basal Nucleus of Meynert, Locus Coeruleus, and Ventral Tegmental Area in Healthy Adults. *Frontiers in Human Neuroscience*, *10*. https://doi.org/10.3389/fnhum.2016.00149

Knapen, T., de Gee, J. W., Brascamp, J., Nuiten, S., Hoppenbrouwers, S., & Theeuwes, J. (2016). Cognitive and ocular factors jointly determine pupil responses under equiluminance. *PloS one*, *11*(5). https://doi.org/10.1371/journal.pone.0155574

Köhler, S., Wagner, G., & Bär, K.-J. (2019). Activation of brainstem and midbrain nuclei during cognitive control in medicated patients with schizophrenia. *Human Brain Mapping*,

40(1), 202–213. https://doi.org/10.1002/hbm.24365

Krebs, R. M., Park, H. R., Bombeke, K., & Boehler, C. N. (2018). Modulation of locus coeruleus activity by novel oddball stimuli. *Brain Imaging and Behavior*, *12*(2), 577-584. http://doi.org/10.1007/s11682-017-9700-4

Kundu, P., Brenowitz, N. D., Voon, V., Worbe, Y., Vértes, P. E., Inati, S. J., … Bullmore, E. T. (2013). Integrated strategy for improving functional connectivity mapping using multiecho fMRI. *Proceedings of the National Academy of Sciences*, *110*(40), 16187–16192. https://doi.org/10.1073/pnas.1301725110

Kundu, P., Inati, S. J., Evans, J. W., Luh, W.-M., & Bandettini, P. A. (2012). Differentiating BOLD and Non-BOLD Signals in fMRI Time Series Using Multi-Echo EPI. *Neuroimage*, *60*(3), 1759–1770. https://doi.org/10.1016/j.neuroimage.2011.12.028

Kundu, P., Voon, V., Balchandani, P., Lombardo, M. V., Poser, B. A., & Bandettini, P. A. (2017). Multi-echo fMRI: A review of applications in fMRI denoising and analysis of BOLD signals. *NeuroImage*, *154*, 59–80. https://doi.org/10.1016/j.neuroimage.2017.03.033

Ladd, M. E., Bachert, P., Meyerspeer, M., Moser, E., Nagel, A. M., Norris, D. G., … Zaiss, M. (2018). Pros and cons of ultra-high-field MRI/MRS for human application. *Progress in Nuclear Magnetic Resonance Spectroscopy*, *109*, 1–50. https://doi.org/10.1016/j.pnmrs.2018.06.001

Larsen, R. S., & Waters, J. (2018). Neuromodulatory correlates of pupil dilation. *Frontiers in neural circuits*, *12*, 21.

Liu, K. Y., Acosta-Cabronero, J., Cardenas-Blanco, A., Loane, C., Berry, A. J., Betts, M. J., … Hämmerer, D. (2019). In vivo visualization of age-related differences in the locus coeruleus. *Neurobiology of Aging*, *74*, 101–111. https://doi.org/10.1016/j.neurobiolaging.2018.10.014

Liu, K. Y., Marijatta, F., Hämmerer, D., Acosta-Cabronero, J., Düzel, E., & Howard, R. J. (2017). Magnetic resonance imaging of the human locus coeruleus: A systematic review. *Neuroscience & Biobehavioral Reviews*, *83*, 325–355. https://doi.org/10.1016/j.neubiorev.2017.10.023

Liu, T. T., Nalci, A., & Falahpour, M. (2017). The Global Signal in fMRI: Nuisance or Information? *NeuroImage*, *150*, 213–229. https://doi.org/10.1016/j.neuroimage.2017.02.036

Ljubojevic, V., Luu, P., & Rosa, E. D. (2014). Cholinergic Contributions to Supramodal Attentional Processes in Rats. *Journal of Neuroscience*, *34*(6), 2264–2275. https://doi.org/10.1523/JNEUROSCI.1024-13.2014

Lombardo, M. V., Auyeung, B., Holt, R. J., Waldman, J., Ruigrok, A. N. V., Mooney, N., … Kundu, P. (2016). Improving effect size estimation and statistical power with multi-echo fMRI and its impact on understanding the neural systems supporting mentalizing. *Neuroimage*, *142*, 55–66. https://doi.org/10.1016/j.neuroimage.2016.07.022

Loughlin, S. E., Foote, S. L., & Bloom, F. E. (1986). Efferent projections of nucleus locus coeruleus: Topographic organization of cells of origin demonstrated by three-dimensional

reconstruction. *Neuroscience*, *18*(2), 291–306. https://doi.org/10.1016/0306-4522(86)90155-7

Loughlin, S. E., Foote, S. L., & Fallon, J. H. (1982). Locus coeruleus projections to cortex: Topography, morphology and collateralization. *Brain Research Bulletin*, *9*(1), 287–294. https://doi.org/10.1016/0361-9230(82)90142-3

Luppi, P.-H., Aston-Jones, G., Akaoka, H., Chouvet, G., & Jouvet, M. (1995). Afferent projections to the rat locus coeruleus demonstrated by retrograde and anterograde tracing with cholera-toxin B subunit and Phaseolus vulgaris leucoagglutinin. *Neuroscience*, *65*(1), 119–160. https://doi.org/10.1016/0306-4522(94)00481-J

Mann, D. M., Yates, P. O., & Hawkes, J. (1983). The pathology of the human locus ceruleus. *Clinical Neuropathology*, *2*(1), 1–7.

Marien, M. R., Colpaert, F. C., & Rosenquist, A. C. (2004). Noradrenergic mechanisms in neurodegenerative diseases: A theory. *Brain Research Reviews*, *45*(1), 38–78. https://doi.org/10.1016/j.brainresrev.2004.02.002

Markello, R. D., Spreng, R. N., Luh, W.-M., Anderson, A. K., & De Rosa, E. (2018). Segregation of the human basal forebrain using resting state functional MRI. *NeuroImage*, *173*, 287–297. https://doi.org/10.1016/j.neuroimage.2018.02.042

Mather, M., Clewett, D., Sakaki, M., & Harley, C. W. (2016). Norepinephrine ignites local hot spots of neuronal excitation: How arousal amplifies selectivity in perception and memory. *The Behavioral and Brain Sciences*, *39*, e200. https://doi.org/10.1017/S0140525X15000667

Mather, M., & Harley, C. W. (2016). The Locus Coeruleus: Essential for Maintaining Cognitive Function and the Aging Brain. *Trends in Cognitive Sciences*, *20*(3), 214–226. https://doi.org/10.1016/j.tics.2016.01.001

Mesulam, M.-M. (2013). Cholinergic Circuitry of the Human Nucleus Basalis and Its Fate in Alzheimer's Disease. *The Journal of Comparative Neurology*, *521*(18), 4124–4144. https://doi.org/10.1002/cne.23415

Mikl, M., Mareček, R., Hluštík, P., Pavlicová, M., Drastich, A., Chlebus, P., … Krupa, P. (2008). Effects of spatial smoothing on fMRI group inferences. *Magnetic Resonance Imaging*, *26*(4), 490–503. https://doi.org/10.1016/j.mri.2007.08.006

Mohanty, A., Gitelman, D. R., Small, D. M., & Mesulam, M. M. (2008). The Spatial Attention Network Interacts with Limbic and Monoaminergic Systems to Modulate Motivation-Induced Attention Shifts. *Cerebral Cortex (New York, NY)*, *18*(11), 2604–2613. https://doi.org/10.1093/cercor/bhn021

Morris, L. S., Tan, A., Smith, D. A., Grehl, M., Han-Huang, K., Naidich, T. P., ... & Murrough, J. W. (2020). Sub-millimeter variation in human locus coeruleus is associated with dimensional measures of psychopathology: An in vivo ultra-high field 7-Tesla MRI study. *NeuroImage: Clinical*, 102148. https://doi.org/10.1016/j.nicl.2019.102148

Mouton, P. R., Pakkenberg, B., Gundersen, H. J. G., & Price, D. L. (1994). Absolute number and

size of pigmented locus coeruleus neurons in young and aged individuals. *Journal of Chemical Neuroanatomy*, *7*(3), 185–190. https://doi.org/10.1016/0891-0618(94)90028-0

Murphy, P. R., O'Connell, R. G., O'Sullivan, M., Robertson, I. H., & Balsters, J. H. (2014). Pupil diameter covaries with BOLD activity in human locus coeruleus. *Human Brain Mapping*, *35*(8), 4140–4154. https://doi.org/10.1002/hbm.22466

Neary, D. (2008). Chapter 19 - Brain Stem. In S. Standring & A. R. Crossman (Eds.), *Gray's Anatomy*, (Ed. 40, pp. 275-296). Edinburgh: Churchill Livingstone.

Nieuwenhuis, S., van Nieuwpoort, I. C., Veltman, D. J., & Drent, M. L. (2007). Effects of the noradrenergic agonist clonidine on temporal and spatial attention. *Psychopharmacology*, *193*(2), 261–269. https://doi.org/10.1007/s00213-007-0770-7

Olafsson, V., Kundu, P., Wong, E. C., Bandettini, P. A., & Liu, T. T. (2015). Enhanced identification of BOLD-like components with multi-echo simultaneous multi-slice (MESMS) fMRI and multi-echo ICA. *Neuroimage*, *112*, 43-51.

Park, H. W., Ro, Y. M., & Cho, Z. H. (1988). Measurement of the magnetic susceptibility effect in high-field NMR imaging. *Physics in Medicine and Biology*, *33*(3), 339–349. https://doi.org/10.1088/0031-9155/33/3/003

Penny, W. D., Friston, K. J., Ashburner, J. T., Kiebel, S. J., & Nichols, T. E. (Eds.). (2011). Statistical parametric mapping: the analysis of functional brain images. Elsevier.

Power, J. D. (2017). A simple but useful way to assess fMRI scan qualities. *Neuroimage*, *154*, 150-158.

Power, J. D., Barnes, K. A., Snyder, A. Z., Schlaggar, B. L., & Petersen, S. E. (2012). Spurious but systematic correlations in functional connectivity MRI networks arise from subject motion. *Neuroimage*, *59*(3), 2142–2154. https://doi.org/10.1016/j.neuroimage.2011.10.018

Power, J. D., Plitt, M., Gotts, S. J., Kundu, P., Voon, V., Bandettini, P. A., & Martin, A. (2018). Ridding fMRI data of motion-related influences: Removal of signals with distinct spatial and physical bases in multiecho data. *Proceedings of the National Academy of Sciences*, *115*(9), E2105–E2114. https://doi.org/10.1073/pnas.1720985115

Pruim, R. H. R., Mennes, M., van Rooij, D., Llera, A., Buitelaar, J. K., & Beckmann, C. F. (2015). ICA-AROMA: A robust ICA-based strategy for removing motion artifacts from fMRI data. *NeuroImage*, *112*, 267–277. https://doi.org/10.1016/j.neuroimage.2015.02.064

R Core Team (2020). R: A language and environment for statistical computing. R Foundation for Statistical Computing, Vienna, Austria. https://www.R-project.org/

Ryan, P. J., Ma, S., Olucha-Bordonau, F. E., & Gundlach, A. L. (2011). Nucleus incertus—An emerging modulatory role in arousal, stress and memory. *Neuroscience & Biobehavioral Reviews*, *35*(6), 1326–1341. https://doi.org/10.1016/j.neubiorev.2011.02.004

Saad, Z. S., Glen, D. R., Chen, G., Beauchamp, M. S., Desai, R., & Cox, R. W. (2009). A New Method for Improving Functional-to-Structural MRI Alignment using Local Pearson Correlation. *NeuroImage*, *44*(3), 839–848. https://doi.org/10.1016/j.neuroimage.2008.09.037

Samuels, E. R., & Szabadi, E. (2008). Functional Neuroanatomy of the Noradrenergic Locus Coeruleus: Its Roles in the Regulation of Arousal and Autonomic Function Part I: Principles of Functional Organisation. *Current Neuropharmacology*, *6*(3), 235-253. http://doi.org/10.2174/157015908785777229

Sara. S. J. (2009). The locus coeruleus and noradrenergic modulation of cognition. *Nature Reviews Neuroscience*, *10*(3), 211-223.

Sarter, M., Hasselmo, M. E., Bruno, J. P., & Givens, B. (2005). Unraveling the attentional functions of cortical cholinergic inputs: Interactions between signal-driven and cognitive modulation of signal detection. *Brain Research Reviews*, *48*(1), 98–111. https://doi.org/10.1016/j.brainresrev.2004.08.006

Sasaki, M., Shibata, E., Tohyama, K., Takahashi, J., Otsuka, K., Tsuchiya, K., … Sakai, A. (2006). Neuromelanin magnetic resonance imaging of locus ceruleus and substantia nigra in Parkinson's disease. *NeuroReport*, *17*(11), 1215. https://doi.org/10.1097/01.wnr.0000227984.84927.a7

Scheinost, D., Papademetris, X., & Constable, R. T. (2014). The impact of image smoothness on intrinsic functional connectivity and head motion confounds. *Neuroimage*, *95*, 13-21.

Schölvinck, M. L., Maier, A., Frank, Q. Y., Duyn, J. H., & Leopold, D. A. (2010). Neural basis of global resting-state fMRI activity. *Proceedings of the National Academy of Sciences*, *107*(22), 10238-10243

Schwarz, L. A., & Luo, L. (2015). Organization of the Locus Coeruleus-Norepinephrine System. *Current Biology*, *25*(21), R1051–R1056. https://doi.org/10.1016/j.cub.2015.09.039

Shine, J. M., Bissett, P. G., Bell, P. T., Koyejo, O., Balsters, J. H., Gorgolewski, K. J., … Poldrack, R. A. (2016). The Dynamics of Functional Brain Networks: Integrated Network States during Cognitive Task Performance. *Neuron*, *92*(2), 544–554. https://doi.org/10.1016/j.neuron.2016.09.018

Song, A. H., Kucyi, A., Napadow, V., Brown, E. N., Loggia, M. L., & Akeju, O. (2017). Pharmacological Modulation of Noradrenergic Arousal Circuitry Disrupts Functional Connectivity of the Locus Ceruleus in Humans. *The Journal of Neuroscience, 37*(29), 6938–6945. https://doi.org/10.1523/JNEUROSCI.0446-17.2017

Sterpenich, V., D'Argembeau, A., Desseilles, M., Balteau, E., Albouy, G., Vandewalle, G., … Maquet, P. (2006). The Locus Ceruleus Is Involved in the Successful Retrieval of Emotional Memories in Humans. *Journal of Neuroscience*, *26*(28), 7416–7423. https://doi.org/10.1523/JNEUROSCI.1001-06.2006

Sulzer, D., Cassidy, C., Horga, G., Kang, U. J., Fahn, S., Casella, L., … Zecca, L. (2018). Neuromelanin detection by magnetic resonance imaging (MRI) and its promise as a biomarker for Parkinson's disease. *NPJ Parkinson's Disease*, *4*(1), 1–13. https://doi.org/10.1038/s41531-018-0047-3

Swallow, K. M., Braver, T. S., Snyder, A. Z., Speer, N. K., & Zacks, J. M. (2003). Reliability of functional localization using fMRI. *NeuroImage*, *20*(3), 1561–1577.

Swallow, K. M., Jiang, Y. V., & Riley, E. B. (2019). Target detection increases pupil diameter

and enhances memory for background scenes during multi-tasking. *Scientific Reports*, *9*(1), 1–13. https://doi.org/10.1038/s41598-019-41658-4

Szőnyi, A., Sos, K. E., Nyilas, R., Schlingloff, D., Domonkos, A., Takács, V. T., … Nyiri, G. (2019). Brainstem nucleus incertus controls contextual memory formation. *Science*, *364*(6442), eaaw0445. https://doi.org/10.1126/science.aaw0445

Tona, K.-D., Keuken, M. C., de Rover, M., Lakke, E., Forstmann, B. U., Nieuwenhuis, S., & van Osch, M. J. P. (2017). In vivo visualization of the locus coeruleus in humans: Quantifying the test–retest reliability. *Brain Structure and Function*, *222*(9), 4203–4217. https://doi.org/10.1007/s00429-017-1464-5

Uematsu, A., Tan, B. Z., & Johansen, J. P. (2015). Projection specificity in heterogeneous locus coeruleus cell populations: Implications for learning and memory. *Learning & Memory*, *22*(9), 444–451. https://doi.org/10.1101/lm.037283.114

Uğurbil, K., Garwood, M., Ellermann, J., Hendrich, K., Hinke, R., Hu, X., … Ogawa, S. (1993). Imaging at high magnetic fields: Initial experiences at 4 T. *Magnetic Resonance Quarterly*, *9*(4), 259–277.

Van den Heuvel, M. P., & Hulshoff Pol, H. E. (2010). Exploring the brain network: A review on resting-state fMRI functional connectivity. *European Neuropsychopharmacology: The Journal of the European College of Neuropsychopharmacology*, *20*(8), 519–534. https://doi.org/10.1016/j.euroneuro.2010.03.008

Wakamatsu, K., Tabuchi, K., Ojika, M., Zucca, F. A., Zecca, L., & Ito, S. (2015). Norepinephrine and its metabolites are involved in the synthesis of neuromelanin derived from the locus coeruleus. *Journal of Neurochemistry*, *135*(4), 768–776. https://doi.org/10.1111/jnc.13237

Warren, C. M., Eldar, E., van den Brink, R. L., Tona, K. D., van der Wee, N. J., Giltay, E. J., ... & Nieuwenhuis, S. (2016). Catecholamine-mediated increases in gain enhance the precision of cortical representations. *Journal of Neuroscience*, *36*(21), 5699-5708.

Windischberger, C., Langenberger, H., Sycha, T., Tschernko, E. M., Fuchsjäger-Mayerl, G., Schmetterer, L., & Moser, E. (2002). On the origin of respiratory artifacts in BOLD-EPI of the human brain. *Magnetic Resonance Imaging*, *20*(8), 575–582. https://doi.org/10.1016/S0730-725X(02)00563-5

Worsley, K. J., Marrett, S., Neelin, P., Vandal, A. C., Friston, K. J., & Evans, A. C. (1996). A unified statistical approach for determining significant signals in images of cerebral activation. *Human Brain Mapping*, *4*(1), 58–73. https://doi.org/10.1002/(SICI)1097-0193(1996)4:1<58::AID-HBM4>3.0.CO;2-O

Wu, C. W., Gu, H., Lu, H., Stein, E. A., Chen, J. H., & Yang, Y. (2008). Frequency specificity of functional connectivity in brain networks. *Neuroimage*, *42*(3), 1047-1055.

Yarkoni, T. (2009). Big Correlations in Little Studies: Inflated fMRI Correlations Reflect Low Statistical Power—Commentary on Vul et al. (2009). *Perspectives on Psychological Science*, *4*(3), 294–298. https://doi.org/10.1111/j.1745-6924.2009.01127.x

Yan, C. G., Cheung, B., Kelly, C., Colcombe, S., Craddock, R. C., Di Martino, A., ... & Milham,

M. P. (2013). A comprehensive assessment of regional variation in the impact of head micromovements on functional connectomics. *Neuroimage*, *76*, 183-201.

Yebra, M., Galarza-Vallejo, A., Soto-Leon, V., Gonzalez-Rosa, J. J., de Berker, A. O., Bestmann, S., ... & Strange, B. A. (2019). Action boosts episodic memory encoding in humans via engagement of a noradrenergic system. *Nature Communications*, *10*(1), 1-12.

Yu, A. J., & Dayan, P. (2005). Uncertainty, Neuromodulation, and Attention. *Neuron*, *46*(4), 681–692. https://doi.org/10.1016/j.neuron.2005.04.026

Zhang, S., Hu, S., Chao, H. H., & Li, C.-S. R. (2016). Resting-State Functional Connectivity of the Locus Coeruleus in Humans: In Comparison with the Ventral Tegmental Area/Substantia Nigra Pars Compacta and the Effects of Age. *Cerebral Cortex (New York, NY)*, *26*(8), 3413–3427. https://doi.org/10.1093/cercor/bhv172

CHAPTER 5

SHARED & UNSHARED CONTRIBUTIONS OF LC AND VTA TO STATIC FUNCTIONAL CONNECTIVITY NETWORKS[4]

The locus coeruleus (LC) and ventral tegmental area (VTA) neuromodulatory systems are implicated in many overlapping cognitive processes and project to overlapping regions throughout the brain (e.g., Chandler, Waterhouse, & Gao, 2014; Clark & Noudoost, 2014; Trutti, Mulder, Hommel, & Forstmann, 2019). These systems are theorized to modulate brain-wide network dynamics to optimize processing of, learning about, and responding to stimuli that carry behavioral relevance (Aston-Jones & Cohen, 2005; Aston-Jones, Rajkowski, & Cohen, 2000; Berridge & Waterhouse, 2003; Bouret & Sara, 2005; Mather, Clewett, Sakaki, & Harley, 2016; Servan-Schreiber, Printz, & Cohen, 1990). But whether these systems accomplish this modulation in concert or independently remains an ongoing line of inquiry (for a review, see Briand, Gritton, Howe, Young, & Sarter, 2007), in part because each system is typically studied in isolation. This study investigates the possibility that these systems account for those brain-wide dynamics in common and unique ways by differentially impacting neural networks.

5.1 Anatomical Characteristics of Locus Coeruleus and Ventral Tegmental Area

The LC is a pair of bilateral nuclei in the brainstem located along the fourth ventricle, below the inferior colliculi, and the main source of norepinephrine (NE) in the brain (e.g., Dahlström & Fuxe, 1964). The LC releases NE throughout much of the central nervous system, with branching along the anteroposterior axis of the neocortex (Aston-Jones & Waterhouse,

[4] This chapter is an abridged version of the manuscript Turker, Colcombe, & Swallow (under review). Thus, please do not copy or cite this chapter without the authors' permission.

2016; Loughlin, Foote, & Fallon, 1982). It modulates the surrounding brainstem, cerebellum, medial prefrontal cortex, cingulate thalamus, hippocampus (HPC), and amygdala, with notable exceptions being the basal ganglia and nucleus accumbens (NAcc) (e.g., Aston-Jones & Waterhouse, 2016; Berridge & Waterhouse, 2003; Chandler, Gao, & Waterhouse, 2014). It has reciprocal connections with anterior cingulate, orbitofrontal, prefrontal areas (e.g., Arnsten & Goldman-Rakic, 1984; Jodo, Chiang, & Aston-Jones, 1998), and also strongly innervates motor and sensory regions (Loughlin, Foote, & Bloom, 1986; Schwarz & Luo, 2015). The LC projects strongly to the HPC and recent data suggest that it is the primary source of NE and dopamine (DA) to this part of the brain in rodents, particularly the dorsal hippocampus (anatomically homologous to posterior hippocampus in humans; Kempadoo, Mosharov, Choi, Sulzer, & Kandel, 2016; Loughlin et al., 1986; McNamara & Dupret, 2017; Pickel, Segal, & Bloom, 1974; Swanson & Hartman, 1975; Takeuchi et al., 2016).

The VTA in the mesencephalon, at the level of the superior colliculi, is the primary source of DA for prefrontal cortex (e.g., Briand et al., 2007). Like the LC, the VTA projects to much of the cortex and subcortex, such as medial prefrontal cortex, cingulate, thalamus, HPC, and amygdala (e.g., Aransay, Rodriguez-López, García-Amado, Clascá, & Prens, 2015; Morales & Margolis, 2017; Tang, Kochubey, Kintscher, & Schneggenburger, 2020) and similarly has reciprocal connections with prefrontal cortex (Sesack & Grace, 2010). In contrast to the LC, however, the primary target of the VTA is the NAcc (Haber, 2014; Ikemoto, 2007). LC and VTA may also have similarities and differences in their projections to the HPC. Activity in a VTA-CA3 loop has previously been associated with salient changes in context (Bromberg-Martin, Matsumoto, & Hikosaka, 2010; Luo, Tahsili-Fahadan, Wise, Lupica, & Aston-Jones, 2011; Neunuebel, Yoganarasimha, Rao, & Nierim, 2013), although recent findings

suggest that this response in HPC to context changes and novelty may be driven by LC instead (Takeuchi et al., 2016; Wagatsuma, Okuyama, Sun, Smith, Abe, & Tonegawa, 2018). Furthermore, in contrast to dense LC innervation of the DG, the VTA has only minor, diffuse projections to the DG in rodents (Lisman & Grace, 2005).

In sum, both systems strongly and reciprocally innervate prefrontal regions, which are part of brain-wide neural networks that implement cognitive control and executive function (Friedman & Robbins, 2022; for a review, see Haber, Liu, Seidlitz, & Bullmore, 2022). However, the LC and VTA can also be differentiated by projections to many other areas, particularly in their projections to the striatum and HPC. Thus, this raises the question whether shared and unshared anatomical connectivity across the brain of LC and VTA will be reflected at the level of different functional cortical networks and subcortical structures.

5.2 Functional Characteristics of Locus Coeruleus and Ventral Tegmental Area

Neuromodulatory systems like the LC and VTA have tonic and phasic firing (e.g., Grace & Bunney, 1984a, 1984b; Devilbiss & Waterhouse, 2011). Tonic activity is a sustained, low frequency firing, whereas phasic activity is a transient, high frequency burst of activity against the tonic background firing. There are many similarities in the types of events that are likely to elicit phasic LC and VTA activity: both are active as a function of behavioral relevance, like Go cues in Go/NoGo tasks (e.g., Guitart-Masip, Chowdhury, Sharot, Dayan, Duzel, & Dolan, 2012; Krebs, Park, Bombeke, & Boehler, 2018; Rajkowski, Majczynski, Clayton, & Aston-Jones, 2004), novelty (Aston-Jones & Bloom, 1981; Bassareo, De Luca, & Di Chiara, 2002; Vankov, Hervé-Minvielle, & Sara, 1995), rewards in reinforcement learning scenarios (Bouret & Sara, 2004; Schultz, Dayan, & Montague, 1997), as well as uncertainty and changes in associative

contingencies (Dayan & Yu, 2002; Fouragnan, Retzler, & Philiastides, 2018). Much of this is thought to reflect an attention and orienting signal (e.g., Corbetta, Patel, & Shulman, 2008; Sara & Bouret, 2012; Solié et al., 2022), suggesting there should be overlapping functional connectivity from the LC and VTA to networks like the VSN, DAN, and the control network that regulate the deployment of cognitive resources.

There are also proposed differences in what elicits phasic activity in LC and VTA. For example, VTA may be signaling 'common novelty', which is the appearance of new exemplar within a familiar category, and thereby facilitating the encoding of semantic information, whereas LC may signal 'distinct novelty', which is the first encounter with an entirely novel category, producing highly episodic memories (Duszkiewicz, McNamara, Takeuchi, & Genzel, 2019). Moreover, different levels of cognitive demand will modulate functional connectivity of LC and VTA. In a Stroop task (Köhler, Bär, & Wagner, 2016), interference and the need for cognitive control strengthened functional connectivity between VTA and areas like NAcc, caudate, putamen, thalamus, and insula. Conversely, it strengthened LC connectivity with ventrolateral and dorsolateral prefrontal cortex, premotor cortex, occipital cortex, and the superior parietal cortex. Thus, there may also be unshared functional connectivity that differentiates LC and VTA in networks underpinning control, memory, and perceptual processing.

Tonic activity across systems may also show similarities and differences. Most prominently, tonic activity regulates the sleep-wake cycle (Hobson, McCarley, & Wyzinski, 1975) and tonic LC is correlated with vigilance and arousal when awake (Aston-Jones, Gonzalez, & Doran, 2007; Aston-Jones, Rajkowski, Kubiak, & Alexinsky, 1994). In the explore-exploit dilemma (Sutton & Barto, 1998; Wilson, Geana, White, Ludvig, & Cohen,

2014), exploration may be regulated by tonic LC (Aston-Jones & Cohen, 2005), whereas tonic VTA may track fluctuations in values of reward and motivation to acquire those rewards (Berridge & Robinson, 1998; Cagniard et al., 2006; Niv, Daw, Joel, & Dayan, 2007; Wang, Toyoshima, Kunimatsu, Yamada, & Matsumoto, 2021). In a recent fMRI study (Laureiro-Martínez, Brusoni, Canessa, & Zollo, 2015), exploration was indeed correlated with activity in reward regions, whereas exploitation was correlated with LC and regions important for controlling and orienting attention. Combined, research on phasic and tonic LC and VTA activity suggests they modulate a range of overlapping as well as complementary (e.g., facilitating the processing of salient or otherwise behaviorally relevant stimuli) or even opposing functions (e.g., tracking incentive value of stimuli and motivating approach behavior versus exploring broader context in which various stimuli appear and encoding the relevant information around them), implemented by overlapping or different brain areas. However, research on LC and VTA is limited in its simultaneous investigation of both of these systems and its qualifying of correlated brain areas within larger functional units like networks.

5.3 Simultaneous Investigation of LC and VTA and Their Impacts on Networks

Studies which investigated the function of LC and VTA simultaneously have produced seemingly mixed results. In two electrophysiology studies (Jahn, Varazzani, Sallet, Walton, & Bouret, 2020; Varazzani, San-Galli, Gilardeau, & Bouret, 2015), LC was implicated in task engagement and learning about reward contingencies, whereas VTA and an adjacent DA-producing nucleus, the substantia nigra pars compacta (SNc), drove evaluation of the reward. However, in a pharmacological study (Hauser, Eldar, Purg, Moutoussis, & Dolan, 2019), a DA-antagonist negatively impacted perceptual features of stimuli, whereas a NE-antagonist

reduced reward effects. From this, it may look unclear whether LC or VTA system should be expected to have effects on attention, reward, or perceptual networks. More likely, though, given their partially overlapping functions and physiology, is that these systems produce shared and unshared effects across all of these networks under different circumstances.

In a resting-state fMRI study (Van Den Brink et al., 2016), raising NE and DA levels with atomoxetine reduced, rather than increased, global correlation levels between visual, somatomotor, and frontoparietal networks. It also reduced specific interregional correlation: within posterior brain regions, such as visual cortex, but not more anterior regions like basal ganglia. These effects were subsequently shown to depend on the spatial distribution of catecholamine receptor gene expression (Van Den Brink, Nieuwenhuis, & Donner, 2018; Van Den Brink, Pfeffer, & Donner, 2019), further highlighting that neuromodulatory systems should not be expected to have homogeneous effects across the brain and that their influence may vary across networks.

Finally, one resting state fMRI study explicitly investigated shared and distinct LC and VTA/SNc functional connectivity using analyses that categorized voxels as being functionally associated with LC only, VTA only, or both (Zhang, Hu, Chao, & Li, 2016). Consistent with other research, LC and VTA/SNc showed shared positive connectivity to areas like putamen, posterior insula, thalamus, and cerebellum. However, they shared negative connectivity to visual cortex, precuneus, temporal cortex, cingulate cortex, and caudate, which is at odds with some previous findings (e.g., Turker, Riley, Luh, Colcombe, & Swallow, 2021). Compared to VTA/SNc, LC had less connectivity to visual, parietal, and somatomotor cortices. Moreover, bilateral amygdala and right anterior insula showed negative LC, but positive VTA/SNc, connectivity. Therefore, it remains unclear whether regions that show shared connectivity also

show independent connectivity and to what extent the findings relate to regions and networks implicated in functions that these two neuromodulatory systems are proposed to implement.

5.4 The Current Study: Shared and Unshared Functional Connectivity to Networks

Whole-brain functional connectivity research has established the existence of robust networks in the human brain (Power et al., 2011; Reineberg, Gustavson, Benca, Banich, & Friedman, 2018; Wig, Laumann, & Petersen, 2014). These functional connectivity (FC) networks (Fox & Raichle, 2007; Seeley et al., 2007) are sets of regions whose activity correlates during both task-based and task-free paradigms and map onto a range of domains (Laird et al., 2011; Smith et al., 2009), such as the control network, default mode network (DMN), dorsal attention network (DAN), limbic network, ventral salience network (VSN), somatomotor network (SMN), and the visual network (Schaefer et al., 2018; Yeo, Krienen, Chee, & Buckner, 2014). Opposing brain-behavior relationships have been reported for these networks. For instance, optimized behavioral performance is associated with high DMN activity, whereas lapses in attention and performance are correlated with high DAN and VSN activity (Esterman, Noonan, Rosenberg, & Degutis, 2013; Fortenbaugh, Rothlein, McGlinchey, DeGutis, & Esterman, 2018; Kucyi, Hove, Esterman, Hutchison, & Valera, 2017) and individuals with attention-deficit hyperactivity disorder spend more time in suboptimal network configurations (Yamashita, Rothlein, Kucyi, Valera, & Esterman, 2021). Thus, given that LC and VTA are well-positioned to modulate these FC networks (e.g., Bouret & Sara, 2005; Shine, 2019), a deeper understanding of their shared and unshared FC is warranted.

In the current study, we use rs-fMRI with task-free viewing of naturalistic stimuli, which are likely to elicit tonic and phasic LC and VTA activity in varying degrees. Our primary goal is

to pull apart the shared and unshared relationships between LC and VTA activity within each voxel and provide a finer-grained assessment of their associations to regional and network-level activity. This is not possible using techniques that examine conjunctions of thresholded maps (e.g., Zhang et al., 2016) or through pharmacological manipulations (e.g., Van Den Brink et al., 2016). To achieve this, we generate six functional connectivity maps, representing raw, shared variance, and unshared variance for LC and VTA. Given recent concerns about the contributions of vigilance or motivation to overall levels of brain activity, we utilize ICA-AROMA to denoise the data (Pruim, Mennes, Buitelaar, & Beckmann, 2015; Pruim, Mennes, Van Rooij, Llera, Buitelaar, & Beckmann, 2015), rather than global signal regression, which can result in anticorrelations (Fox, Zhang, Snyder, & Raichle, 2009), and because global signal can contain functional signals (Liu, Nalci, & Falahpour, 2017; Schölvinck, Maier, Frank, Duyn, & Leopold, 2010). To conclude, we frame our findings within the context of the commonly proposed functions of these neuromodulatory systems regarding broader network dynamics, cognition, and psychiatric disorders.

5.5 Methods

5.5.1 Dataset Description

Data consisted of a publicly available imaging dataset (https://openneuro.org/datasets/ds003338/versions/1.1.0). Twenty participants (6 female, 14 male, 18-35 years old), who self-reported having seen or played in over 50 basketball games, watched the last few minutes of nine varsity basketball games from the 2012 men's National Collegiate Athletic Association while undergoing fMRI scans. Video clips were between 5-8 minutes in length and segments were chosen to include events that could violate expectations,

such as sudden changes in ball possession. Participants viewed three clips in each of three scans in pseudo-random order. Movie viewing scans were alternated with scans in which participants recalled as much as they could about the three clips in the preceding scan. Recall scans and behavioral estimates of subjective surprise were not analyzed here.

Imaging data were acquired using a 3T Siemens Prisma scanner with 64-channel head coil (T2*-weighted echo planar imaging (EPI), simultaneous multislice factor 4, flip angle 59°, TR = 1 s, TE = 30 ms, whole-brain coverage with 56 slices of 2.5 mm thickness, in-plane isotropic resolution of 2.5 mm, FOV 195 mm). Anatomy was obtained with 1 mm isotropic T1-weighted scans. Additional detail can be found in Antony et al. (2021).

5.5.2 Region of Interest Identification

5.5.2.1 Individually Defined Anatomical Regions

The T1-weighted anatomical scans were segmented with FreeSurfer (7.2.0.; surfer.nmr.mgh.harvard.edu; Dale, Fischl, & Sereno, 1999; Fischl, Sereno, & Dale, 1999) and converted to volumetric regions of interest (ROIs) using FreeSurfer and AFNI (21.2.00; Cox, 1996; Cox & Hyde, 1997; Gold et al., 1998). These subject-level ROIs were created for fourth ventricle (4V), white matter (WM), parahippocampus, thalamus, putamen, caudate, precentral gyrus, transtemporal gyrus, amygdala, fusiform gyrus, ventral medial prefrontal cortex (vmPFC), and visual cortical areas V1 and V2. The WM ROI was eroded with AFNI's 3dmask_tool (dilate_input -2), to minimize chances of the ROI extending into gray matter after downsampling to the voxel dimensions of the EPI. Further segmentation was performed to create labels for subiculum, dentate gyrus (DG), CA1, and CA2/3 (Iglesias et al., 2015; Sämann et al., 2022). Finally, we also measure the gray matter (GM) and global signal (GS).

These subject-level anatomy-based ROIs complement the atlas-based ROIs, parcels, and networks which are described next. This is because the atlas-based ROIs primarily cover the cortical sheet and thereby miss important subcortical and non-cortical areas. Additionally, by including anatomy-based ROIs that partially overlap with some of the following atlas-based ROIs, we ensure that analyses are sensitive enough to catch FC that may be unique to a given individual's anatomical and functional characteristics.

5.5.2.2 Putative LC

LC was identified using the probabilistic Keren atlas (Keren, Lozar, Harris, Morgan, Eckert, 2009), which is based on neuromelanin-T1 weighted images of 44, right handed, healthy adults, aged 19-79. The atlas used here is based on the group mean and 1 SD of the voxel intensities in the left and right axial slice. As shown in Turker et al. (2021), estimates of LC are impacted by localization method. Therefore, care was taken to ensure that the putative LC ROI was well aligned to each individual's anatomy, with additional alignment steps performed as necessary: manual translation to improve EPI to anatomical alignment and removal of any LC ROI voxels that overlapped, in part or in full, with the 4V after resampling to the EPI grid.

5.5.2.3 Putative VTA

VTA was identified using the probabilistic Pauli atlas (Pauli et al., 2018). This atlas was built using high-resolution T1 and T2-weighted structural images from 168 typical adults, aged 22-35. The VTA is relatively larger than the LC and should therefore be less impacted by small misalignments. It also does not neighbor a source of noise the way the LC does. Accordingly, the VTA ROI was warped to the native space of each participant and applied without any trimming.

5.5.2.4 Additional Atlas-Based Anatomical Regions

We also used the probabilistic Pauli atlas to attain ROIs for NAcc, SNc, substantia nigra pars reticulata (SNr), and habenula, which are important DA-producing (SNc and SNr lie adjacent to the VTA) or DA-modulated and DA-modulating areas (NAcc and habenula receive input from VTA; Pauli, Nili, & Tyszka, 2018).

5.5.2.5 Schaefer Parcellation and Networks

The Schaefer parcellation was used to divide each individual's cortex into a set of 200 parcels covering the entire cortical sheet. This parcellation method uses a gradient-weighted Markov Random Field model to apply the same or a different label to neighboring voxels based on local resting-state FC gradients. Each of the 200 parcels falls into one of 7 networks in the Schaefer atlas: control, default mode network (DMN), dorsal attention network (DAN), limbic network, ventral salience network (VSN), somatomotor network (SMN), and the visual network (Schaefer et al., 2018; Yeo et al., 2014). Thus, to create the network ROIs, the corresponding parcels were combined. Parcels were also classified as anterior or posterior based on their center of mass falling anterior to the -23 mm anteroposterior coordinate in MNI152 space (1 mm grid, LPI coordinates), resulting in 100 anterior and 100 posterior parcels.

5.5.2.6 Transformation of Atlases to Individual Anatomy

All ROIs were applied in each participant's native space, oriented to their deobliqued anatomical scan, including the atlas-based ROIs described next, which were available in MNI space. These were aligned to each participant's anatomical scan using the inverse of AFNI's

3dQwarp transformation of each individual's native anatomical scan to the MNI152 template, so data could be extracted on an untransformed EPI (as in Turker et al., 2021).

5.5.3 MRI Data Processing

Our preprocessing pipeline was matched as much as possible to the ICA-AROMA pipeline described in Turker et al. (2021). First, the anatomical scan was skull-stripped (FSL BET, b = .25) and its obliquity was matched to the EPI. Next, motion was estimated with reference to the third volume of the EPI to identify volumes with more than .2 mm of differential motion in sequential TRs. The first two volumes of the EPI data were dropped, and the remaining TRs were despiked, slice time corrected, and scaled. Then, EPI data were registered to the new first volume with FSL's MCFLIRT (Jenkinson et al., 2002). We used FSL-FLIRT and boundary-based linear registration (Jenkinson, Bannister, Brady, & Smith, 2002; Jenkinson & Smith, 2001; Greve & Fischl, 2009) to generate parameters aligning the EPI data to the deobliqued anatomical and FSL-FLIRT alongside FSL-FNIRT non-linear registration (Andersson, Jenkinson, & Smith, 2007) to warp the anatomical to the MNI152 template. Additional visual inspection and manual alignment was performed on the EPI, where necessary, to improve accuracy after each scan's alignment to the deobliqued anatomical. Following this, 4th ventricle and an eroded WM ROI were applied to extract nuisance time courses. The 4th ventricle ROI was then used to mask out the ventricle prior to applying data blurring. Blurring was performed with AFNI's 3dBlurtoFWHM to bring blurring up to an estimated 5 mm, before submitting the EPI to ICA-AROMA (non-aggressive denoising). Next, the EPI was deconvolved with the previously acquired 4th ventricle and WM nuisance regressors as well as polynomial drift of an automatically set order by AFNI's 3dDeconvolve. We also included additional

nuisance regressors: onsets of each of the basketball clips were modeled as a canonical hemodynamic response function and each clip itself was modeled as a block of corresponding duration. Data were bandpass filtered ($0.01 < f < 0.15$). Following this denoising, the masks were applied in native space to the EPI to extract the critical functional data. Finally, the denoised data were warped to the MNI152 template for group-level analyses.

5.5.4 Static Functional Connectivity Analyses and Seed Types

For first-level FC maps, putative LC and VTA time series were created by averaging activity across voxels within the ROI at each TR. Maps of raw, shared, and unshared LC and VTA connectivity were then created from those maps in several steps. First, each participant's LC and VTA time courses were mean centered by subtracting the mean of the overall time course in the given scan (*raw LC, VTA seed*). Second, voxel-wise linear regression was used to predict LC activity using the centered VTA seed (*shared LC seed*) and to predict VTA activity using the centered LC seed (*shared VTA seed*). Thus, the shared maps for one neuromodulatory system are weighted versions of the raw map for the other neuromodulatory system, where the weight is determined by the correlation between the LC and VTA. Third, the residuals from the linear regressions were used to create unshared LC and VTA FC maps, reflecting the correlation between LC and activity in each voxel of the brain after partialing out variance explained by the VTA (*unshared LC seed*) and the correlation between VTA and the rest of the brain after partialing out variance explained by the LC (*unshared VTA seed*). The final time courses were then concatenated to create one seed for each of the six seed types, for both LC and VTA, per participant. The six seeds were correlated with the time series of each voxel in the EPI (in MNI152 space) that consisted of the three scan runs also concatenated together, to create six

first-level FC maps per participant. Each first level FC map was Fisher-transformed before group-level analyses.

Group-level analyses consisted of voxel-wise two-tailed one sample t-tests against zero (AFNI's 3dTtest++), with multiple comparisons controlled using the false discovery rate (FDR; Genovese, Lazar, & Nichols, 2002).

5.6 Results

5.6.1 Correlations Between Seed Types

4V and WM correlate with physiological factors like heartbeat and respiration and thus contaminate the fMRI signal in a non-random way (e.g., Jo, Saad, Simmons, Milbury, & Cox, 2010; Wowk, McIntyre, & Saunders, 1997). However, correlations for LC and VTA with 4V and WM were low, while retaining high correlations with GM, GS, and other ROIs, indicating that preprocessing measures to mitigate the impact of these sources of noise were successful (Table 1).

The LC seed remained correlated with the Keren 1SD probabilistic ROI that it was based on (Mean Pearson's $r_{raw\ LC,\ Keren\ 1SD}$ = .445, SD = .184), even after manual trimming of the Keren 1SD ROI when needed, suggesting both were capturing overlapping signal from putative LC. The VTA ROI was only weakly correlated with the Keren 1SD ROI (Mean $r_{raw\ VTA,\ Keren\ 1SD}$ = .149, SD = .191). Correlation between raw LC and VTA (Mean $r_{raw\ LC,\ raw\ VTA}$ = .399, SD = .165) indicated that both regions are indeed overlapping in how their activity fluctuates as a function of the task-free naturalistic videos participants were watching in the scanner. By scaling the raw LC seed with the raw VTA seed, and vice versa, correlation is increased ($r_{shared\ LC,\ shared\ VTA}$ = .461), whereas mutual partialing out of the seeds resulted, expectedly, in a negative correlation ($r_{unshared\ LC,\ unshared\ VTA}$ = -.434).

Table 5.1
Correlations between LC and VTA seeds with anatomical ROIs

	Raw FC		Shared FC		Unshared FC	
ROI	*LC*	*VTA*	*LC*	*VTA*	*LC*	*VTA*
4V	$-1.4\cdot10^{-6}$ ($2.4\cdot10^{-5}$)	$-1.3\cdot10^{-6}$ ($1.8\cdot10^{-5}$)	$-2.0\cdot10^{-6}$ ($1.7\cdot10^{-5}$)	$-4.0\cdot10^{-6}$ ($3.2\cdot10^{-5}$)	$5.8\cdot10^{-7}$ ($2.4\cdot10^{-5}$)	$-2.5\cdot10^{-7}$ ($1.8\cdot10^{-5}$)
WM	.150 (.20)	.084 (.19)	.084 (.19)	.149 (.20)	.135 (.12)	.214 (.11)
GM	.579 (.12)	.542 (.13)	.531 (.13)	.573 (.11)	.355 (.11)	.311 (.10)
GS	.600 (.11)	.557 (.13)	.544 (.13)	.591 (.11)	.369 (.11)	.318 (.10)
NAcc	.285 (.17)	.342 (.16)	.341 (.16)	.284 (.17)	.136 (.10)	.232 (.09)
SNc	.460 (.12)	.730 (.07)	.706 (.08)	.461 (.12)	.145 (.11)	.567 (.09)
SNr	.439 (.14)	.648 (.09)	.627 (.09)	.438 (.15)	.160 (.11)	.490 (.08)
Caudate	.435 (.14)	.478 (.12)	.472 (.12)	.436 (.13)	.232 (.11)	.308 (.08)
Putamen	.446 (.14)	.454 (.14)	.451 (.14)	.446 (.14)	.252 (.11)	.273 (.09)
Thalamus	.574 (.11)	.584 (.11)	.576 (.12)	.572 (.10)	.332 (.10)	.356 (.09)
Habenula	.390 (.19)	.405 (.18)	.397 (.18)	.388 (.18)	.223 (.13)	.250 (.12)
vmPFC	.289 (.15)	.305 (.16)	.301 (.16)	.292 (.14)	.149 (.09)	.190 (.10)
Precent.	.469 (.15)	.440 (.16)	.432 (.16)	.466 (.15)	.289 (.11)	.246 (.12)
Transt.	.421 (.14)	.405 (.14)	.402 (.14)	.417 (.14)	.248 (.10)	.234 (.08)
V1	.409 (.13)	.369 (.14)	.357 (.14)	.402 (.13)	.261 (.10)	.199 (.08)
V2	.427 (.13)	.382 (.15)	.372 (.15)	.420 (.14)	.272 (.10)	.204 (.10)
Amygdala	.365 (.13)	.334 (.15)	.335 (.15)	.363 (.13)	.221 (.08)	.185 (.10)
Fusiform	.431 (.12)	.388 (.15)	.376 (.15)	.424 (.13)	.273 (.09)	.211 (.11)
Parahipp.	.487 (.11)	.449 (.13)	.442 (.13)	.480 (.11)	.305 (.08)	.250 (.08)
Subiculum	.376 (.14)	.372 (.14)	.367 (.15)	.376 (.14)	.217 (.10)	.216 (.08)
CA1	.370 (.13)	.334 (.15)	.331 (.15)	.367 (.13)	.228 (.09)	.182 (.10)
CA23	.316 (.15)	.337 (.16)	.332 (.16)	.316 (.14)	.167 (.08)	.205 (.10)
DG	.381 (.15)	.367 (.15)	.364 (.14)	.380 (.14)	.221 (.11)	.212 (.08)

Note. Mean correlations (standard deviations in parentheses) between six LC and VTA seeds with ROIs defined on each participant's unique anatomy (with the exception of NAcc, SNc, SNr, and habenula, which were atlas-based). Values were first computed for each participant within each run (Pearson's r), Fisher z-scored, averaged across the three runs, averaged across participants, and then inverse z-scored.

5.6.2 Whole-Brain Raw, Shared, and Unshared Static Functional Connectivity Maps

Figure 5.1A shows the six group-level static FC maps. Maps are thresholded to view voxels in the top 20% of the z-score range, to highlight similarities and differences. Consistent with previous findings, raw LC correlated with many areas along the midline, such as the cingulate and precuneus, insula, thalamus, pons, cerebellum, basal ganglia, hippocampus, and perceptual, somatomotor, and parietal cortices. Raw VTA also showed correlations along the midline with the same regions, cingulate and precuneus. Furthermore, it was correlated with insula, thalamus, cerebellum, hippocampus, perceptual and somatomotor cortices. Relative to LC, correlations were stronger in the basal ganglia and anterior cingulate, but weaker in precuneus and occipital cortex, suggesting a potential anteroposterior difference along the midline.

Shared LC and VTA seeds produce FC maps where the given seed's map approximates the raw FC map of the other seed (e.g. the shared LC FC map is highly comparable to the raw VTA FC map). Dice coefficient plots confirm the substantial level of overlap between raw and shared FC LC and VTA FC maps, even when maps are thresholded at the z-score's 80th percentile (Fig. 1B-C).

Using the unshared LC and VTA seeds to make FC maps, LC still accounts for variance (that is unaccounted for by VTA) in primarily posterior regions, such as posterior cingulate cortex, precuneus, cerebellum, and parietal and occipital regions. Conversely, VTA strongly accounts for activity unaccounted for by LC in prefrontal cortex, anterior cingulate, thalamus, anterior cingulate, and basal ganglia.

Dice plots comparing raw to unshared FC showed the highest overlap (at the 80th percentile: $\text{Dice}_{\text{raw LC, unshared LC}} = 63\%$, $\text{Dice}_{\text{raw VTA, unshared VTA}} = 65\%$). This suggests that, despite the many regions that are correlated in the raw FC maps to both LC and VTA, raw LC and VTA still show differentiable strength in

how they connect to those overlapping regions. This difference is further highlighted when the other seed is regressed out to create unshared FC maps. When comparing overlap for unshared FC between LC and VTA, dice is lowest at the 80th percentile (Dice $_{\text{unshared LC, unshared VTA}}$ = 35%). Thus, LC activity can be scaled by VTA activity to resemble the raw VTA FC map, but this shared LC map is a poor reflection of the unshared LC FC map. Instead, raw maps show better overlap with their unshared FC counterparts.

Cortical surface maps of the unshared FC (Fig. 1D) emphasize the differential impact of LC and VTA across the cortical sheet. They suggest that LC and VTA may be accounting for unshared variance in different cortical parcels and networks, differently along the anteroposterior gradient of the brain, and for different regions not captured in the parcellation of the cortical sheet (e.g., subcortical ROIs or HPC subfields). These possibilities are investigated in the following sections, with the focus therefore primarily being on unshared LC and VTA connectivity.

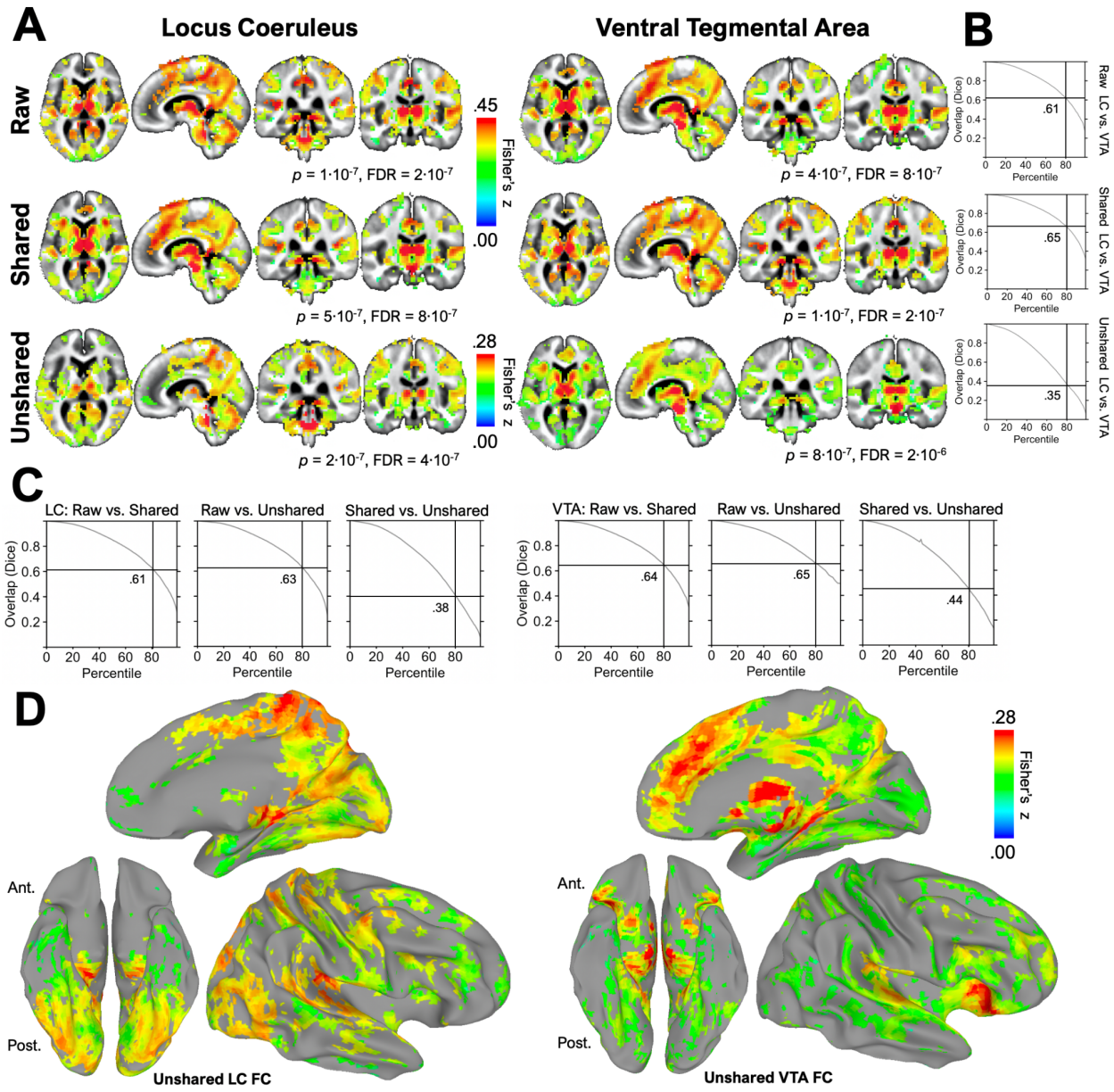

Figure 5.1 Comparisons of static IFC maps. *A) Group-level FC maps in MNI152 for LC and VTA for each seed type: raw, shared, and unshared FC. Maps are thresholded to show the top 20 percent of voxels, based on z-score. Note the smaller scale for the unshared FC maps. Coordinates for the brain slices: 6 mm (superior), 7 mm (right), 34 mm (posterior), 14 mm (posterior). B) Dice plots of the overlaps between LC and VTA maps created with the same seed type. C) Dice plots of the overlaps for maps created with different seed types within LC and within VTA maps. D) Surface maps of the unshared LC and VTA FC maps.*

5.6.3 Unique Connectivity Profiles to Parcels and Networks

To analyze unshared LC and VTA FC profiles across the cortical sheet, we first created a connectome that visualizes the edges from LC and VTA nodes to the top 20% of parcels in terms of correlation strength (i.e. 40 parcels per seed; Fig. 5.2A). Consistent with the static FC maps in the previous section, in the unshared FC connectome, the strongest LC edges connected more to posterior parcels while those for the VTA connected to more anterior ones. This difference is investigated in section 5.6.5.

Thresholded chord diagrams were then used to visualize network membership of those top 20% of seed-to-parcel edges in the connectome for unshared FC (Fig. 5.2B). LC edges were highly connected (relative to VTA edges) to the visual network, SMN, and DAN. Conversely, VTA's strongest edges showed an overrepresentation in the DMN and VSN, relative to LC.

Group-level correlations were strong from both raw and shared seeds to the different networks (Table 5.2). Unshared correlations were larger for LC with all networks except for the VSN. The broader VSN system consists of the regions on the cortical sheet captured by the VSN network ROI, but also areas like the amygdala, striatum, thalamus, and various other subcortical and brainstem nuclei (Seeley, 2019). This raises a shortcoming of the Schaeffer parcels and networks, which cover the cortical sheet, but not many other structures. In the next section, we investigate differences between LC and VTA with the individually defined anatomical ROIs and atlas-based subcortical ROIs.

Table 5.2
Correlations between LC and VTA seeds with the network ROIs

		Control	DMN	DAN	Limbic	VSN	SMN	Visual
Raw	*LC*	.502 (.12)	.511 (.12)	.507 (.14)	.449 (.12)	.518 (.13)	.495 (.14)	.459 (.13)
	VTA	.477 (.15)	.485 (.15)	.467 (.14)	.428 (.14)	.523 (.14)	.446 (.16)	.415 (.14)
Shared	*LC*	.467 (.15)	.480 (.15)	.453 (.14)	.421 (.14)	.517 (.14)	.441 (.16)	.403 (.15)
	VTA	.500 (.12)	.509 (.12)	.502 (.14)	.443 (.12)	.517 (.13)	.492 (.14)	.451 (.14)
Unshared	*LC*	.299 (.11)	.305 (.10)	.321 (.12)	.270 (.10)	.299 (.11)	.311 (.11)	.292 (.10)
	VTA	.280 (.11)	.282 (.10)	.256 (.11)	.249 (.10)	.315 (.10)	.241 (.11)	.225 (.10)

Note. Mean correlations (standard deviation in parentheses) between LC and VTA seed types and the 7 networks. They were first computed for each participant within each run (Pearson's r), Fisher z-scored, averaged across the three runs, averaged across participants, and then inverse z-scored to return to the typical range.

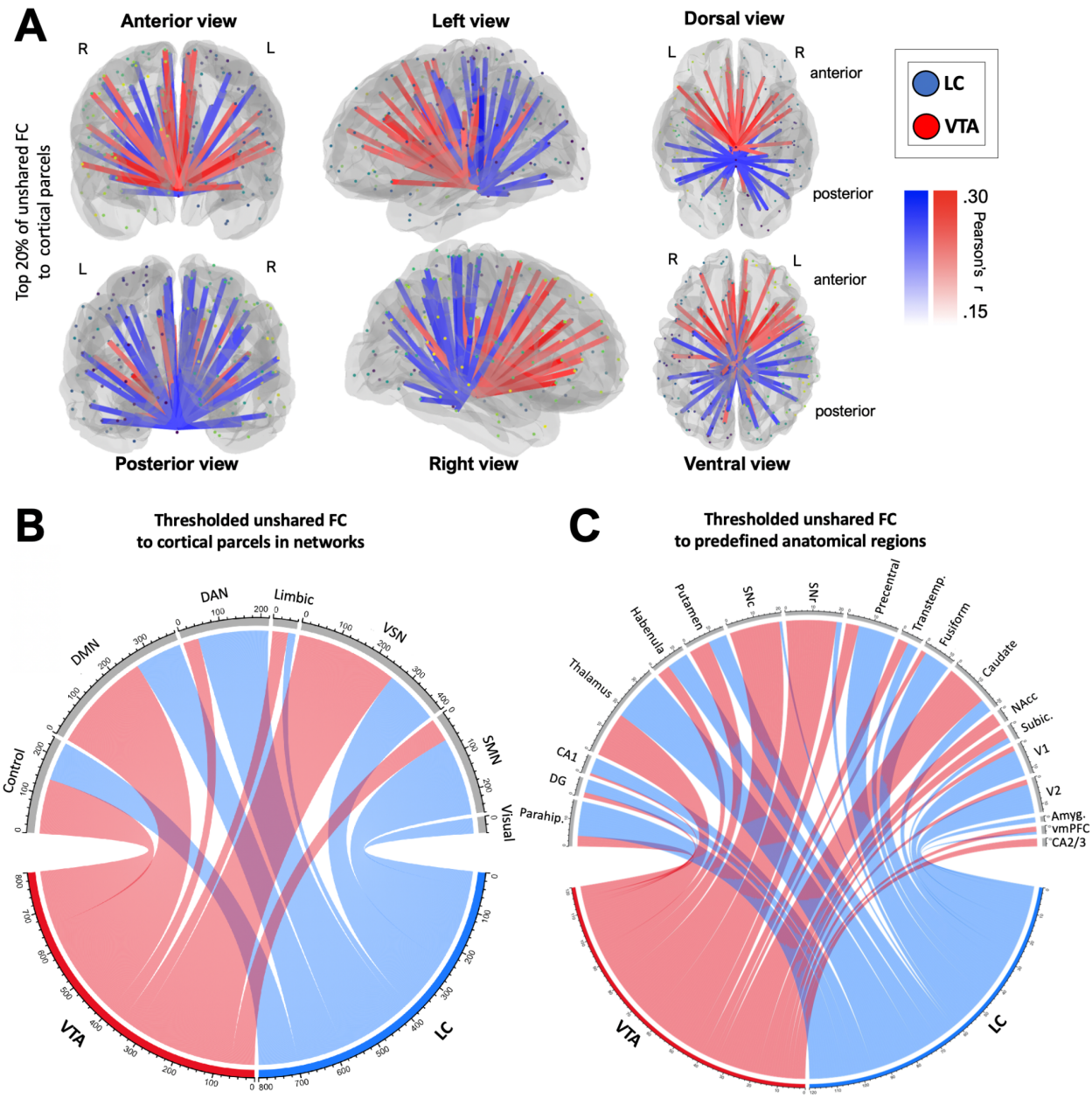

Figure 5.2 Connectome of unshared LC and VTA connectivity. *A) Thresholded group-level connectome of unshared FC for LC and VTA to the top 20% (40 per seed) of Schaefer parcels. B) Thresholded subject-level unshared FC of parcels grouped by network (top 20% of parcels, 40 parcels per each of 20 participants, 800 total chords per seed). C) Thresholded subject-level unshared FC connectivity to the other anatomical ROIs (top 6 regions per participant, 120 chords per seed).*

5.6.4 Unique Connectivity Profiles to Targeted Subcortical and Hippocampal ROIs

To investigate the unique profile of unshared LC and VTA FC to ROIs not included in the Schaefer parcellation, we also characterized FC to the individually defined ROIs, with a chord diagram (Fig. 5.2C). For each participant, we computed the correlation between their unshared LC and VTA seeds to each of the nineteen other ROIs. Then, to uncover the profile, we plotted a chord for only the top 6 correlated regions correlated with a given participant's LC and VTA. LC accounted for more unshared variance in parahippocampus, amygdala, DG, CA1, precentral gyrus, fusiform gyrus, V1, and V2. Conversely, the VTA's unshared variance seeds most strongly correlated with SNc, SNr, caudate, and CA2/3.

To better characterize these profiles, we fit linear mixed-effects models to Fisher transformed correlation coefficients, using lmer (Bates, Maechler, & Bolker, 2012; Brown, 2021; Westfall, Kenny, & Judd, 2014) and Holm corrected contrast tests (emmeans; Lenth, 2019). Models included seed (LC, VTA), ROI (amygdala, caudate, fusiform, habenula, NAcc, parahippocampus, precentral gyrus, transtemporal gyrus, putamen, thalamus, V1, V2, vmPFC, CA1, CA2/3, DG, and subiculum), and their interaction as fixed effects, and participant as a random effect. SNc and SNr were excluded because of their immediate adjacency to and high correlation with the VTA (Table 5.1), but including them in the model did not change results.

When predicting the raw FC correlations, the model revealed only a main effect of ROI, $F(16,627) = 18.951$, $p < .001$, $\eta_p^2 = .33$. However, when predicting the unshared FC correlations, there was a main effect of ROI, $F(16,627) = 7.436$, $p < .001$, $\eta_p^2 = .16$, as well as an interaction, $F(16,627) = 2.703$, $p < .001$, $\eta_p^2 = .06$, suggesting that LC and VTA had unshared FC in non-overlapping ROIs. With VTA accounting for variability over and above what is accounted for by LC, post-hoc Holm corrected contrasts revealed a significant difference in caudate, $t(627) = -2.442$, $p = .015$, and in NAcc, $t(627) = -3.180$, $p = .002$. LC accounted for more variance in fusiform gyrus, $t(627) = 2.021$, $p = .044$, in V1,

$t(627) = 2.022$, $p = .044$, and V2, $t(627) = 2.201$, $p = .028$. There was a marginal difference, with LC having a numerically higher correlation, in parahippocampus, $t(627) = 1.750$, $p = .081$.

5.6.5 Unique Contributions of LC and VTA along the Anteroposterior Axis

The static FC maps (Fig. 5.1A,D) and connectome (Fig. 5.2A) suggested a difference in how the LC and VTA account for unshared variance along the anteroposterior axis of the cortical sheet. Accordingly, we split up the seed-to-network chord diagram (Fig. 5.2B) based on whether the particular parcel fell in the anterior or posterior half of the brain (Fig. 5.3A). However, such thresholded representation in a static FC map and network membership considers only the correlation strength with reference to other correlations to the same seed, but not the entire range of correlation coefficients pooled together. We compare all correlation coefficients pooled together here.

The anteroposterior pattern is still evident when all edges were considered, rather than only the top 20%, in several networks (Fig. 5.3B). Considering all edges, rather than a thresholded subset, is done to avoid biasing the data a priori and support the previous thresholded analyses. A linear mixed-effects model of all 400 edges to cortical parcels (200 per seed), with seed (LC, VTA), location (anterior, posterior), and network (7 Schaeffer networks) as fixed effect predictors and participant as a random factor, revealed a main effect of seed, $F(1,7769) = 35.788$, $p < .001$, $\eta_p^2 < .01$, location, $F(1,188) = 5.108$, $p = .025$, $\eta_p^2 = .03$, and network, $F(6,188) = 3.579$, $p = .002$, $\eta_p^2 = .10$. There was no significant interaction between seed and location, but a significant interaction between seed, location, and network, $F(4,7933) = 3.704$, $p = .005$, $\eta_p^2 < .01$.

Post-hoc Holm corrected contrasts reveal stronger correlations for LC to anterior parcels of the control network, $t(7769) = 3.919$, $p < .001$, posterior parcels of the DAN, $t(7769) = 6.490$, $p < .001$, both anterior and posterior SMN, $t(7769) = 8.552$, $p < .001$ and $t(7769) = 5.180$, $p < .001$, respectively, and marginally in the posterior DMN, $t(7769) = 1.759$, $p = .079$. Unshared LC was also more strongly correlated, relative to unshared VTA FC, to the visual network, $t(7769) = 8.963$, $p < .001$, which lies fully

in the posterior part of the brain. Conversely, unshared VTA FC is expressed more strongly to the anterior parcels of the VSN, $t(7769) = -2.387$, $p = .017$.

We also computed the centers of mass (AFNI's 3dCM) for each seed at the whole-brain level as well as within each network (Fig. 5.3C). The center of mass reflects the mean location of a set of voxels that have been weighted by their Fisherized correlation coefficients. At the whole-brain level, in MNI152 space, the anteroposterior center of mass for unshared LC FC was located more towards to posterior (Mean coordinate = 24.04 mm, SD = 3.69) than the unshared VTA FC (Mean coordinate = 19.69 mm, SD = 3.48), $t(19) = 4.542$, $p < .001$, corroborating the anteroposterior gradient visualized in the static FC maps (Fig. 5.1). Within networks, unshared FC for LC was more posteriorly (and conversely, unshared FC for VTA more anteriorly) connected to the SMN, $t(19) = 4.926$, $p < .001$, DMN, $t(19) = 2.361$, $p = .029$, limbic network, $t(19) = 4.182$, $p < .001$, VSN, $t(19) = 2.694$, $p = .014$, control network, $t(19) = 2.909$, $p = .009$, marginally in the DAN, $t(19) = 1.968$, $p = .064$, and not different within the visual network, $t(19) = 0.697$, $p = .494$. Thus, within each network the weighted center of mass is generally more towards the posterior voxels for unshared LC FC compared to unshared VTA FC.

Finally, density plots of all the parcels and additional anatomical regions (Fig. 5.3D), corroborate that unshared LC FC is more strongly expressed in the outer cortical sheet, with a larger proportion of the LC-parcel correlations falling in the higher end of the range of correlations. The reverse is true for unshared VTA-parcel correlations, when the additional anatomical regions are considered instead, because subcortical areas like basal ganglia are included there. Splitting the non-thresholded, pooled LC-parcel and VTA-parcel correlations up by network (Fig. 5.3E) corroborates the results from the previous linear mixed-effects model, by still showing a differential impact on networks between the two seeds.

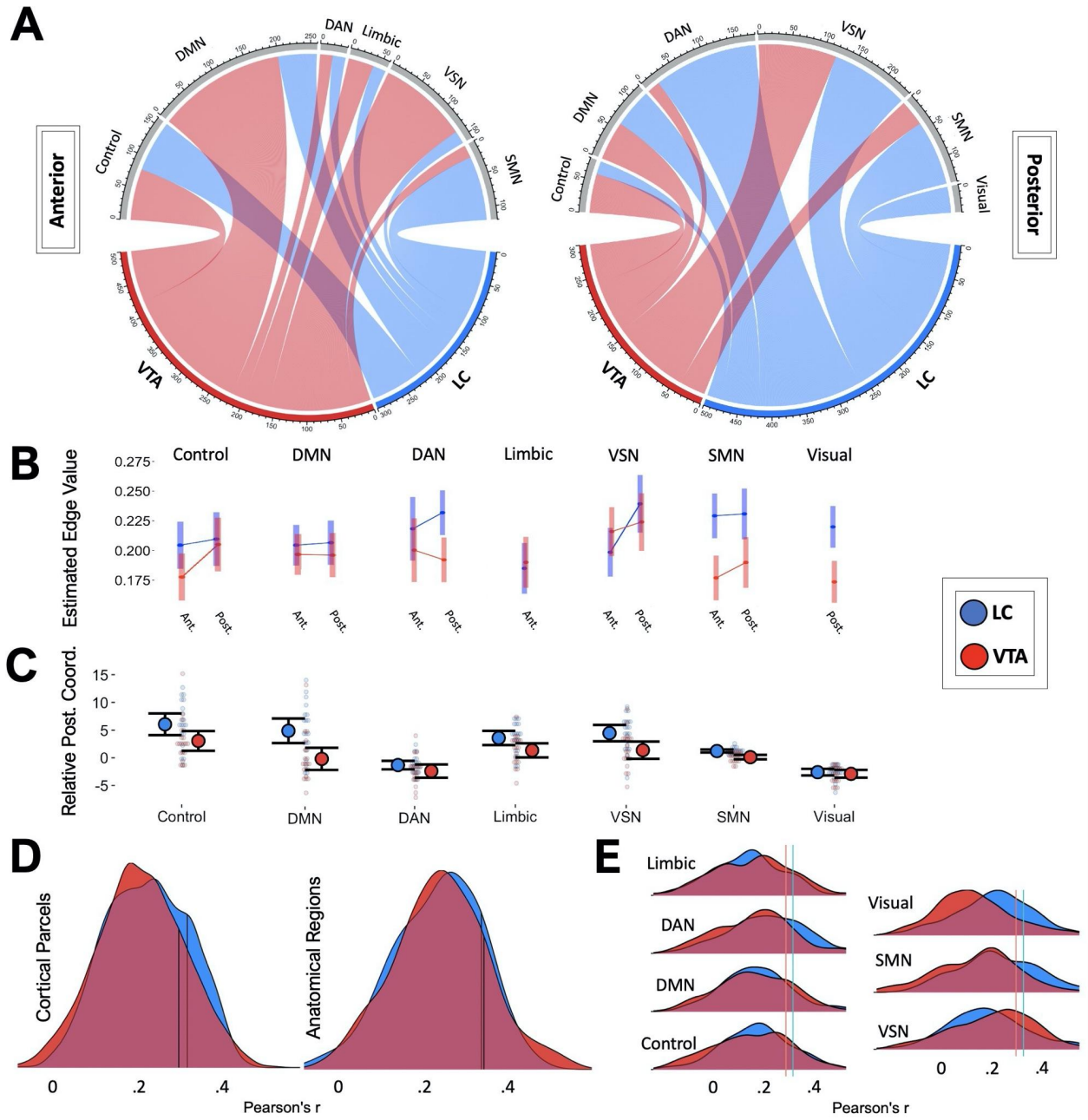

Figure 5.3 An anteroposterior split in unshared LC and VTA connectivity. *A) Connectomes of unshared LC and VTA connectivity split by anterior and posterior location of the parcel. B) Estimated marginal means of all the edge values for each network. CB) Relative posterior coordinates of the weighted center of mass for each seed's connectivity to a network. Center of mass coordinates for each seed was weighted by correlation coefficient in voxels falling within the network. The anteroposterior coordinate of the unweighted center of mass for each network was then subtracted from the weighted coordinate to produce the relative coordinate toward the posterior from the unweighted center of mass of the network itself. C) Estimated marginal means of all the edge values for each network. D) Density plots of the strength of all edges for all participants. E) Density plots of edges for all participants split by network. Vertical lines show the 80th quantile for correlation values per seed.*

5.7 General Discussion

Neuromodulatory systems have critical impacts on brain-wide FC networks. Among these systems, the LC and the VTA are two of the most widely investigated in cognitive neuroscience. They have broadly similar theoretical functions and overlapping neural projections, but also conceptual and anatomical differences (e.g., Briand et al., 2007). Although many characteristics of their static FC have been investigated, their shared and unshared contributions to functional networks remained unclear. Our study presents an important step forward in characterizing those contributions.

Complementing previous conjunction analyses (Zheng et al., 2016) and pharmacological manipulations (Van Den Brink et al., 2016, 2018), we compared multiple static FC maps based on their raw, shared variance, and unshared variance time courses. The raw FC maps were consistent with previous reports of LC and VTA FC (e.g., Liebe, Kaufman, Li, Skalej, Wagner, & Walter, 2020; Liu et al., 2021; Mäki-Marttunen & Espeseth, 2021; Song, Kucyi, Napadow, Brown, Loggia, & Akeju, 2017; Zheng et al., 2016). Both LC and VTA were strongly correlated to areas along the midline, basal ganglia, and prefrontal, motor, and perceptual cortices. The similarity of these maps was further evident in the Dice coefficient analyses, which suggested a high degree of overlap of voxels in the raw and shared LC and VTA FC maps. Critically, when variance is partialed out, the resultant unshared FC maps showed clearly distinguishable differences in LC and VTA brain-wide connectivity.

5.7.1 Unique Functional Connectivity Profiles of LC and VTA

Analyses showed different unshared FC profiles for LC and VTA. Across the cortical sheet, LC was shown to account primarily for variance in posterior parcels of the brain, once VTA-related variance was regressed out. Specifically, relative to VTA, unshared LC FC showed stronger connectivity to posterior DAN, SMN, and to the visual network, which is exclusively in the posterior half of the brain. It also showed stronger connectivity, relative to VTA, to the anterior half of the control network and SMN. Both NE and DA are critical in performing the theorized functions of these networks (e.g., Briand et al.,

2007; Laird et al., 2011; Schaefer et al., 2018; Smith et al., 2009). In turn, after removing variance accounted for by LC, unshared VTA FC was stronger in VSN, relative to LC, likely driven by VTA's strong unshared FC to the insula (Seeley, 2019). Therefore, this anteroposterior differentiation is not merely the result of the LC being inherently more posterior relative to VTA. Instead, LC connectivity strength is specific to certain networks and, in particular, to posterior parcels of those networks. Conversely, unshared FC VTA, has stronger connectivity to those VSN parcels that fall in the anterior half of the brain. Weighted centers of mass, which take the entire network ROI into account, confirmed this anteroposterior differentiation: across the entire network, voxel correlation coefficients were weighted towards posterior for the LC neuromodulatory system.

Because the Schaefer parcels and corresponding network ROIs (Schaefer et al., 2018; Yeo et al., 2014) only cover the cortical sheet and not subcortical areas or, for instance, HPC, we also measured FC to a set of additional anatomical areas. Although chord diagrams suggested that LC might be accounting for unshared variance in multiple regions, like parahippocampus, amygdala, DG, CA1, precentral gyrus, fusiform gyrus, V1, and V2, statistical analyses only showed a distinguishable difference in fusiform gyrus, V1, and V2. Notably, these are relatively posterior visual processing areas, likely to be important during the viewing of naturalistic video clips during the resting-state fMRI scan. Conversely, within HPC subfields, VTA appears strongly correlated with CA2/3, although this was also not statistically significant. Instead, unshared VTA FC was higher than LC to the caudate and NAcc. The lack of statistical significance in the HPC subfield contrasts may be because there is indeed no difference in accounting for unshared variance in those subfields. Alternatively, the current data may have been underpowered to adequately uncover those differences. Given the differences in receptor expression in HPC subfields (e.g. Lisman & Grace, 2005), one could expect there to be unshared variance that is accountable for by either one of the current neuromodulatory systems under investigation. Thus, because one of the proposed functions of these neuromodulatory systems is that they facilitate learning about behaviorally relevant stimuli, further investigation into unshared variance in these critical memory regions is warranted. Furthermore, LC and VTA share characteristics with other neuromodulatory systems, as well (e.g., Briand

et al., 2007). Therefore, similar research comparing raw, shared, and unshared variance among other such systems would help shed light on their individual unique functions and how they relate to the unshared FC of LC and VTA presented here. Finally, although outside of the scope of this study, the thresholded unshared FC maps and top parcels in the connectome cover areas with differing neuromodulator receptor expression (Gryglewski et al., 2018; Van Den Brink et al., 2019), with LC showing relatively strong unshared FC to areas of the brain dense in α_{1A}-receptors and VTA showing unshared FC to areas with strong D_5-receptor expression. However, despite nonhomogeneity of receptor distribution, there is still substantial overlap among all receptor types for all neuromodulators. Thus, further research here is also needed, to map unshared FC onto receptor expression.

The LC accounting for unshared variance in various networks across the cortical sheet and VTA primarily accounting for unshared variance in VSN may have clinical importance. Both neuromodulatory systems are strongly implicated in psychiatric disorders. LC and VTA modulate prefrontal regions in response to stress (Feenstra, 2000; Finlay, Zigmond, & Abercrombie, 1995). The LC is one of the earliest sites affected in the early stages of Alzheimer's disease (e.g., Theofilas et al., 2017) and disrupted VTA connectivity is a common marker of Alzheimer's disease (De Marco & Venneri, 2018). Schizophrenia is marked by anomalies in VTA (e.g., Rice, Roberts, Melendez-Ferro, & Perez-Costas, 2016) as well as LC (e.g., Craven, Priddle, Crow, & Esiri, 2005). Autism spectrum disorders are accompanied by atypical functional connectivity (Huang, Yu, Wilson, Park, Cheng, Kong, Lu, & Kong, 2021). In rodents, lesions in the VTA result in compulsive and perseverative behavior (Pioli, Meissner, Sohr, Gross, Bezard, & Bioulac, 2008) and dysregulated LC activity can result in obsessive compulsive disorder symptomatology (Lustberg, Iannitelli, Tillage, Pruitt, Liles, & Weinshenker, 2020). Administration of atomoxetine and methylphenidate, another DA and NE reuptake inhibitor, are common in the treatment of attention deficit-hyperactivity disorder in children and adolescents with similar efficacy (Hazell, Kohn, Dickson, Walton, Granger, & Van Wyk, 2011), although the prior blocks reuptake in thalamic and frontal areas where the latter impacts striatum (e.g., Cubillo, Smith, Barrett, Giampietro, Brammer, Simmons, & Rubia, 2014). DA is critical for proper functioning of the VSN, which is critically involved in evaluating

incentive salience of stimuli, motivation, and invigorating approach behaviors (e.g., Berridge & Robinson, 2016), and dysfunctional DA signaling to VSN is associated with schizophrenia (Gradin et al., 2013; McCutcheon, Abi-Dargham, & Howes, 2019), addictive behavior (Contreras, Ceric, & Torealba, 2007), and psychosis (Kapur, 2003; Palaniyappan & Liddle, 2012). When functioning normally, DA-modulated insula drives novelty-seeking (Suhara, Yasuno, Sudo, Yamamoto, Inoue, Okubo, & Suzuki, 2001). Accordingly, there is still a need for a better understanding of shared and unique effects of neuromodulatory systems on psychiatric disorders (Decker & McGaugh, 1991) and our study contributes to this research by presenting the unshared variance for LC and VTA within the context of well-established FC networks with clear theorized functions.

5.7.2 Strengths and Limitations

The differences in our approach to parsing out unique FC, compared to previous studies, have some important strengths. By combining unique subject-level ROIs with group-level ROIs in a standardized space, we ensured that analyses were sensitive enough to catch FC that may be unique to a given individual's anatomical and functional characteristics. Our approach of applying all ROIs in native space circumvented the need to warp the functional EPI, allowed for trimming where needed of the LC ROI once resampled to the EPI grid by using the native MPRAGE as reference (rather than a template based on averaged anatomical scans), and allowed for maintaining as much similarity as possible to the pipelines in Turker et al. (2021; Chapter 4).

One particular choice was to not apply global signal regression, which has been proposed to mitigate physiological noise (e.g., Power et al., 2018). However, GS can also contain functional signals, through correlation with attention and arousal driven by tonic LC activity (Aston-Jones et al., 1994, 2007; Liu et al., 2017; Schölvinck et al., 2010). Additionally, its removal may inadvertently lead to anticorrelations (Fox et al., 2009). Turker et al. (2021) indeed demonstrated that global signal regression can remove wide-spread functional connectivity with LC. However, in not applying global signal regression, the current study's findings may be difficult to directly compare to Zhang et al. (2016), who

did apply global signal regression. Indeed, in their study, LC and VTA/SNc shared negative connectivity to visual cortex, precuneus, temporal cortex, cingulate cortex, and caudate. Compared to VTA/SNc, LC had less connectivity to visual, parietal, and somatomotor cortices. Moreover, bilateral amygdala and right anterior insula showed negative LC but positive VTA/SNc connectivity. In the current study, however, visual cortex and precuneus were particularly strongly impacted by LC. It is possible that global signal regression removed true FC to those areas and indeed resulted in negative correlation. Alternatively, our approach may be retaining noise in the signal in those regions. Compared to Zhang et al. (2016), the current dataset had a limited sample size, did not contain older adults, nor did it make use of a second sample to examine impacts of physiological noise. Thus, future research will have to disentangle whether application of global signal regression is a step that must be taken or be avoided for these kinds of analyses, as they greatly impact final characterization of FC.

The current findings must also be nuanced in light of certain clear limitations. As demonstrated previously (Turker et al., 2021), functional characteristics of LC are impacted by the method chosen to localize the nuclei. Because no neuromelanin-weighted T1w scans were available for this dataset, the current study relied on a probabilistic atlas (Keren et al., 2009). However, an atlas cannot account for individual variability in anatomy in LC (German et al., 1988; Keren et al., 2015). It is therefore possible that neighboring pontine signal was introduced into our LC seeds. However, the low correlations between the various putative LC seeds and 4V argue that our mitigating measures, including trimming of the Keren atlas ROI as well as manual alignment where necessary, were successful. Nevertheless, future research should consider the use of neuromelanin-weighted T1w scans to localize LC more directly, potentially in combination with multi-echo fMRI to boost blood oxygen level dependent contrast and mitigate artifacts (Kundu, Inati, Evans, Luh, & Bandettini, 2012; Turker et al., 2020).

Similarly, it is also possible that voxels selected for VTA (partially) contained the neighboring SNc. This adjacent dopamine producing structure (Bär, De la Cruz, Schumann, Koehler, Sauer, Critchley, & Wagner, 2016) has related, but not the same, functions as the VTA – such as computing effort and reward signals (Hauser, Eldar, & Dolan, 2017) – and different developmental trajectories and morphology

(Fu, Paxinos, Watson, & Halliday, 2016). However, it is not necessarily the case that correlations here should or ought to be low, given their overlapping functions, neighboring location in the brain, and neighboring afferent projections. Thus, to partial out the unshared FC of these neighboring structures, future work may consider task-free rs-fMRI paradigms with stimuli that are likely to elicit activity in both structures to explore their unique impact on cortical and subcortical structures.

A final limitation is that the current study does not differentiate between phasic and tonic contributions to the rs-fMRI signal. Indeed, rs-fMRI FC cannot directly differentiate between these two (e.g., Minzenberg et al., 2008). Thus, differentiating between modes of firing would require a method to identify fast, transient fluctuations in putative LC or VTA voxels that are likely below the temporal resolution of fMRI, as well as a method to track dynamic changes in FC over time to investigate changes in FC following phasic time points. Importantly, dynamic tracking of unshared FC would allow for deeper insight into how LC and VTA contribute to fast-paced integration and segregation of FC between the various networks (Shine, 2019) and their resetting (Bouret & Sara, 2005).

5.8 Conclusion

Compared to previous fMRI investigations of the similarities and differences in functional connectivity between these two neuromodulatory systems, the current study offers a finer-grained, voxel-level characterization, as well as a coarser-grained, network-level characterization. We have demonstrated, for the first time, by partialing out variance accounted for by the other neuromodulatory system, that there is a prominent anteroposterior differentiation in LC and VTA FC across the cortical sheet. Importantly, this difference maps connectivity onto commonly observed neural networks, showing that LC accounts for variance above and beyond what is accounted for by VTA in networks implicated in perceiving, learning about, and responding to behaviorally relevant events, such as the visual network and posterior DAN and SMN. Conversely, the VTA accounts for unshared variance in the VSN, a network underpinning incentive salience, motivation, and invigorating approach behaviors.

References

Antony, J. W., Hartshorne, T. H., Pomeroy, K., Gureckis, T. M., Hasson, U., McDougle, S. D., & Norman, K. A. (2021). Behavioral, physiological, and neural signatures of surprise during naturalistic sports viewing. *Neuron*, *109*(2), 377-390.

Arnsten, A. F. T., & Goldman-Rakic, P. S. (1984). Selective prefrontal cortical projections to the region of the locus coeruleus and raphe nuclei in the rhesus monkey. *Brain research*, *306*(1-2), 9-18.

Aston-Jones, G., & Bloom, F. E. (1981). Nonrepinephrine-containing locus coeruleus neurons in behaving rats exhibit pronounced responses to non-noxious environmental stimuli. *Journal of Neuroscience*, *1*(8), 887-900.

Aston-Jones, G., & Cohen, J. D. (2005). An integrative theory of locus coeruleus-norepinephrine function: adaptive gain and optimal performance. *Annu. Rev. Neurosci.*, *28*, 403-450.

Aston-Jones, G., Gonzalez, M., & Doran, S. (2007). Role of the locus coeruleus-norepinephrine system in arousal and circadian regulation of the sleep-wake cycle. In G. A. Ordway, M. A. Schwartz, & A. Frazer (Eds.), *Brain norepinephrine: Neurobiology and therapeutics* (pp. 157–195). Cambridge University Press.

Aston-Jones, G., Rajkowski, J., & Cohen, J. (2000). Locus coeruleus and regulation of behavioral flexibility and attention. *Progress in Brain Research*, *126*, 165-182.

Aston-Jones, G., Rajkowski, J., Kubiak, P., & Alexinsky, T. (1994). Locus coeruleus neurons in monkey are selectively activated by attended cues in a vigilance task. *Journal of Neuroscience*, *14*(7), 4467-4480.

Aston-Jones, G., & Waterhouse, B. (2016). Locus coeruleus: from global projection system to adaptive regulation of behavior. Brain research, 1645, 75-78.

Bär, K. J., de la Cruz, F., Schumann, A., Koehler, S., Sauer, H., Critchley, H., & Wagner, G. (2016). Functional connectivity and network analysis of midbrain and brainstem nuclei. *Neuroimage*, *134*, 53-63.

Bassareo, V., De Luca, M. A., & Di Chiara, G. (2002). Differential expression of motivational stimulus properties by dopamine in nucleus accumbens shell versus core and prefrontal cortex. *Journal of neuroscience*, *22*(11), 4709-4719.

Bates, D., Maechler, M., & Bolker, B. (2012). lme4: Linear mixed-effects models using Eigen and S4.

Berridge, K. C., & Robinson, T. E. (1998). What is the role of dopamine in reward: hedonic impact, reward learning, or incentive salience? *Brain research reviews*, *28*(3), 309-369.

Berridge, C. W., & Waterhouse, B. D. (2003). The locus coeruleus–noradrenergic system: modulation of behavioral state and state-dependent cognitive processes. *Brain research reviews*, *42*(1), 33-84.

Bouret, S., & Sara, S. J. (2005). Network reset: a simplified overarching theory of locus Coeruleus noradrenaline function. *Trends in neurosciences*, *28*(11), 574-582.

Briand, L. A., Gritton, H., Howe, W. M., Young, D. A., & Sarter, M. (2007). Modulators in concert for cognition: modulator interactions in the prefrontal cortex. *Progress in*

neurobiology, *83*(2), 69-91
Bromberg-Martin, E. S., Matsumoto, M., & Hikosaka, O. (2010). Dopamine in motivational control: rewarding, aversive, and alerting. *Neuron*, *68*(5), 815-834.
Brown, V. A. (2021). An introduction to linear mixed-effects modeling in R. Advances in *Methods and Practices in Psychological Science*, *4*(1), 2515245920960351.
Cagniard, B., Balsam, P. D., Brunner, D., & Zhuang, X. (2006). Mice with chronically elevated dopamine exhibit enhanced motivation, but not learning, for a food reward. *Neuropsychopharmacology*, *31*(7), 1362-1370.
Chandler, D. J., Waterhouse, B. D., & Gao, W. J. (2014). New perspectives on catecholaminergic regulation of executive circuits: evidence for independent modulation of prefrontal functions by midbrain dopaminergic and noradrenergic neurons. *Frontiers in neural circuits*, *8*, 53.
Clark, K. L., & Noudoost, B. (2014). The role of prefrontal catecholamines in attention and working memory. *Frontiers in neural circuits*, *8*, 33.
Contreras, M., Ceric, F., & Torrealba, F. (2007). Inactivation of the interoceptive insula disrupts drug craving and malaise induced by lithium. *Science*, *318*(5850), 655-658.
Corbetta, M., Patel, G., & Shulman, G. L. (2008). The reorienting system of the human brain: from environment to theory of mind. *Neuron*, *58*(3), 306-324.
Cox, R. W. (1996). AFNI: software for analysis and visualization of functional magnetic resonance neuroimages. *Computers and Biomedical Research*, *29*(3), 162-173.
Cox, R. W., & Hyde, J. S. (1997). Software tools for analysis and visualization of fMRI data. *NMR in Biomedicine: An International Journal Devoted to the Development and Application of Magnetic Resonance In Vivo*, 10(4‐5), 171-178.
Craven, R. M., Priddle, T. H., Crow, T. J., & Esiri, M. M. (2005). The locus coeruleus in schizophrenia: a postmortem study of noradrenergic neurons. *Neuropathology and applied neurobiology*, *31*(2), 115-126.
Cubillo, A., Smith, A. B., Barrett, N., Giampietro, V., Brammer, M. J., Simmons, A., & Rubia, K. (2014). Shared and drug-specific effects of atomoxetine and methylphenidate on inhibitory brain dysfunction in medication-naive ADHD boys. *Cerebral Cortex*, *24*(1), 174-185.
Dahlström, A., & Fuxe, K. (1964). Localization of monoamines in the lower brain stem. *Experientia*, *20*(7), 398-399.
Dale, A. M., Fischl, B., & Sereno, M. I. (1999). Cortical surface-based analysis: I. Segmentation and surface reconstruction. *Neuroimage*, *9*(2), 179-194.
Dayan, P., & Yu, A. J. (2002). Expected and unexpected uncertainty: ACh and NE in the neocortex. *Advances in neural information processing systems*, *15*.
Decker, M. W., & McGaugh, J. L. (1991). The role of interactions between the cholinergic system and other neuromodulatory systems in learning and memory. *Synapse*, *7*(2), 151-168.

De Marco, M., & Venneri, A. (2018). Volume and connectivity of the ventral tegmental area are linked to neurocognitive signatures of Alzheimer's disease in humans. *Journal of Alzheimer's Disease*, *63*(1), 167-180.

Devilbiss, D. M., & Waterhouse, B. D. (2011). Phasic and tonic patterns of locus coeruleus output differentially modulate sensory network function in the awake rat. *Journal of neurophysiology*, *105*(1), 69-87.

Duszkiewicz, A. J., McNamara, C. G., Takeuchi, T., & Genzel, L. (2019). Novelty and dopaminergic modulation of memory persistence: a tale of two systems. *Trends in Neurosciences*, *42*(2), 102-114.

Esterman, M., Noonan, S. K., Rosenberg, M., & DeGutis, J. (2013). In the zone or zoning out? Tracking behavioral and neural fluctuations during sustained attention. *Cerebral Cortex*, *23*(11), 2712-2723.

Feenstra, M. G. (2000). Dopamine and noradrenaline release in the prefrontal cortex in relation to unconditioned and conditioned stress and reward. *Progress in brain research*, *126*, 133-163.

Finlay, J. M., Zigmond, M. J., & Abercrombie, E. D. (1995). Increased dopamine and norepinephrine release in medial prefrontal cortex induced by acute and chronic stress: effects of diazepam. *Neuroscience*, *64*(3), 619-628.

Fischl, B., Sereno, M. I., & Dale, A. M. (1999). Cortical surface-based analysis: II: inflation, flattening, and a surface-based coordinate system. *Neuroimage*, *9*(2), 195-207.

Fortenbaugh, F. C., Rothlein, D., McGlinchey, R., DeGutis, J., & Esterman, M. (2018). Tracking behavioral and neural fluctuations during sustained attention: A robust replication and extension. *Neuroimage*, *171*, 148-164.

Friedman, N. P., & Robbins, T. W. (2022). The role of prefrontal cortex in cognitive control and executive function. *Neuropsychopharmacology*, *47*(1), 72-89.

Fouragnan, E., Retzler, C., & Philiastides, M. G. (2018). Separate neural representations of prediction error valence and surprise: Evidence from an fMRI meta‐analysis. *Human Brain Mapping*, *39*(7), 2887-2906.

Fox, M. D., & Raichle, M. E. (2007). Spontaneous fluctuations in brain activity observed with functional magnetic resonance imaging. *Nature reviews neuroscience*, *8*(9), 700-711.

Fox, M. D., Zhang, D., Snyder, A. Z., & Raichle, M. E. (2009). The global signal and observed anticorrelated resting state brain networks. *Journal of Neurophysiology*, *101*(6), 3270-3283.

Fu, Y., Paxinos, G., Watson, C., & Halliday, G. M. (2016). The substantia nigra and ventral tegmental dopaminergic neurons from development to degeneration. *Journal of chemical neuroanatomy*, *76*, 98-107.

German, D. C., Walker, B. S., Manaye, K., Smith, W. K., Woodward, D. J., & North, A. J. (1988). The human locus coeruleus: computer reconstruction of cellular distribution. *Journal of Neuroscience*, *8*(5), 1776-1788.

Gold, S., Christian, B., Arndt, S., Zeien, G., Cizadlo, T., Johnson, D. L., ... & Andreasen, N. C. (1998). Functional MRI statistical software packages: a comparative analysis. *Human brain mapping*, *6*(2), 73-84.

Grace, A. A., & Bunney, B. S. (1984a). The control of firing pattern in nigral dopamine neurons: single spike firing. *Journal of neuroscience*, *4*(11), 2866-2876.

Grace, A. A., & Bunney, B. S. (1984b). The control of firing pattern in nigral dopamine neurons: burst firing. *Journal of neuroscience*, *4*(11), 2877-2890.

Gradin, V. B., Waiter, G., O'Connor, A., Romaniuk, L., Stickle, C., Matthews, K., ... & Steele, J. D. (2013). Salience network-midbrain dysconnectivity and blunted reward signals in schizophrenia. *Psychiatry Research: Neuroimaging*, *211*(2), 104-111.

Gryglewski, G., Seiger, R., James, G. M., Godbersen, G. M., Komorowski, A., Unterholzner, J., ... & Lanzenberger, R. (2018). Spatial analysis and high resolution mapping of the human whole-brain transcriptome for integrative analysis in neuroimaging. *Neuroimage*, *176*, 259-267.

Guitart-Masip, M., Chowdhury, R., Sharot, T., Dayan, P., Duzel, E., & Dolan, R. J. (2012). Action controls dopaminergic enhancement of reward representations. *Proceedings of the National Academy of Sciences*, 109(19), 7511-7516.

Haber, S. N. (2014). The place of dopamine in the cortico-basal ganglia circuit. *Neuroscience*, *282*, 248-257.

Haber, S. N., Liu, H., Seidlitz, J., & Bullmore, E. (2022). Prefrontal connectomics: from anatomy to human imaging. *Neuropsychopharmacology*, *47*(1), 20-40.

Hauser, T. U., Eldar, E., & Dolan, R. J. (2017). Separate mesocortical and mesolimbic pathways encode effort and reward learning signals. *Proceedings of the National Academy of Sciences*, *114*(35), E7395-E7404.

Hauser, T. U., Eldar, E., Purg, N., Moutoussis, M., & Dolan, R. J. (2019). Distinct roles of dopamine and noradrenaline in incidental memory. *Journal of Neuroscience*, *39*(39), 7715-7721.

Hazell, P. L., Kohn, M. R., Dickson, R., Walton, R. J., Granger, R. E., & van Wyk, G. W. (2011). Core ADHD symptom improvement with atomoxetine versus methylphenidate: a direct comparison meta-analysis. *Journal of Attention Disorders*, *15*(8), 674-683.

Hobson, J. A., McCarley, R. W., & Wyzinski, P. W. (1975). Sleep cycle oscillation: reciprocal discharge by two brainstem neuronal groups. *Science*, *189*(4196), 55-58.

Huang, Y., Yu, S., Wilson, G., Park, J., Cheng, M., Kong, X., ... & Kong, J. (2021). Altered extended locus coeruleus and ventral tegmental area networks in boys with autism spectrum disorders: a resting-state functional connectivity study. *Neuropsychiatric disease and treatment*, *17*, 1207.

Iglesias, J. E., Augustinack, J. C., Nguyen, K., Player, C. M., Player, A., Wright, M., ... & Alzheimer's Disease Neuroimaging Initiative. (2015). A computational atlas of the hippocampal formation using ex vivo, ultra-high resolution MRI: application to adaptive

segmentation of in vivo MRI. *Neuroimage*, *115*, 117-137.
Ikemoto, S. (2007). Dopamine reward circuitry: two projection systems from the ventral midbrain to the nucleus accumbens–olfactory tubercle complex. *Brain research reviews*, *56*(1), 27-78.
Jahn, C. I., Varazzani, C., Sallet, J., Walton, M. E., & Bouret, S. (2020). Noradrenergic but not dopaminergic neurons signal task state changes and predict reengagement after a failure. *Cerebral Cortex*, *30*(9), 4979-4994.
Jo, H. J., Saad, Z. S., Simmons, W. K., Milbury, L. A., & Cox, R. W. (2010). Mapping sources of correlation in resting state FMRI, with artifact detection and removal. *Neuroimage*, *52*(2), 571-582.
Jodoj, E., Chiang, C., & Aston-Jones, G. (1998). Potent excitatory influence of prefrontal cortex activity on noradrenergic locus coeruleus neurons. *Neuroscience*, *83*(1), 63-79.
Kapur, S. (2003). Psychosis as a state of aberrant salience: a framework linking biology, phenomenology, and pharmacology in schizophrenia. *American Journal of Psychiatry*, *160*(1), 13-23.
Kempadoo, K. A., Mosharov, E. V., Choi, S. J., Sulzer, D., & Kandel, E. R. (2016). Dopamine release from the locus coeruleus to the dorsal hippocampus promotes spatial learning and memory. *Proceedings of the National Academy of Sciences*, *113*(51), 14835-14840.
Keren, N. I., Lozar, C. T., Harris, K. C., Morgan, P. S., & Eckert, M. A. (2009). In vivo mapping of the human locus coeruleus. *Neuroimage*, *47*(4), 1261-1267.
Keren, N. I., Taheri, S., Vazey, E. M., Morgan, P. S., Granholm, A. C. E., Aston-Jones, G. S., & Eckert, M. A. (2015). Histologic validation of locus coeruleus MRI contrast in post-mortem tissue. *Neuroimage*, *113*, 235-245.
Köhler, S., Bär, K. J., & Wagner, G. (2016). Differential involvement of brainstem noradrenergic and midbrain dopaminergic nuclei in cognitive control. *Human Brain Mapping*, *37*(6), 2305-2318.
Krebs, R. M., Park, H. R., Bombeke, K., & Boehler, C. N. (2018). Modulation of locus coeruleus activity by novel oddball stimuli. *Brain imaging and behavior*, *12*(2), 577-584.
Kucyi, A., Hove, M. J., Esterman, M., Hutchison, R. M., & Valera, E. M. (2017). Dynamic brain network correlates of spontaneous fluctuations in attention. *Cerebral Cortex*, *27*(3), 1831-1840.
Kundu, P., Inati, S. J., Evans, J. W., Luh, W. M., & Bandettini, P. A. (2012). Differentiating BOLD and non-BOLD signals in fMRI time series using multi-echo EPI. *Neuroimage*, *60*(3), 1759-1770.
Laird, A. R., Fox, P. M., Eickhoff, S. B., Turner, J. A., Ray, K. L., McKay, D. R., ... & Fox, P. T. (2011). Behavioral interpretations of intrinsic connectivity networks. *Journal of cognitive neuroscience*, *23*(12), 4022-4037.
Laureiro‐Martínez, D., Brusoni, S., Canessa, N., & Zollo, M. (2015). Understanding the exploration–exploitation dilemma: An fMRI study of attention control and decision‐making performance. *Strategic Management Journal*, *36*(3), 319-338.

Lenth, R. (2019). Emmeans: Estimated Marginal Means, aka Least-Squares Means. R package version 1.7.2.

Liebe, T., Kaufmann, J., Li, M., Skalej, M., Wagner, G., & Walter, M. (2020). In vivo anatomical mapping of human locus coeruleus functional connectivity at 3 T MRI. *Human Brain Mapping*, *41*(8), 2136-2151.

Lisman, J. E., & Grace, A. A. (2005). The hippocampal-VTA loop: controlling the entry of information into long-term memory. *Neuron*, *46*(5), 703-713.

Liu, T. T., Nalci, A., & Falahpour, M. (2017). The global signal in fMRI: Nuisance or Information? *Neuroimage*, *150*, 213-229.

Liu, J., Tao, J., Xia, R., Li, M., Huang, M., Li, S., ... & Kong, J. (2021). Mind-body exercise modulates locus coeruleus and ventral tegmental area functional connectivity in individuals with mild cognitive impairment. *Frontiers in aging neuroscience*, 295.

Loughlin, S. E., Foote, S. L., & Bloom, F. E. (1986). Efferent projections of nucleus locus coeruleus: topographic organization of cells of origin demonstrated by three-dimensional reconstruction. *Neuroscience*, *18*(2), 291-306.

Loughlin, S. E., Foote, S. L., & Fallon, J. H. (1982). Locus coeruleus projections to cortex: topography, morphology and collateralization. *Brain research bulletin*, *9*(1-6), 287-294.

Luo, A. H., Tahsili-Fahadan, P., Wise, R. A., Lupica, C. R., & Aston-Jones, G. (2011). Linking context with reward: a functional circuit from hippocampal CA3 to ventral tegmental area. *Science*, *333*(6040), 353-357.

Lustberg, D., Iannitelli, A. F., Tillage, R. P., Pruitt, M., Liles, L. C., & Weinshenker, D. (2020). Central norepinephrine transmission is required for stress-induced repetitive behavior in two rodent models of obsessive-compulsive disorder. *Psychopharmacology*, *237*(7), 1973-1987.

Mäki-Marttunen, V., & Espeseth, T. (2021). Uncovering the locus coeruleus: Comparison of localization methods for functional analysis. *Neuroimage*, *224*, 117409.

Mather, M., Clewett, D., Sakaki, M., & Harley, C. W. (2016). Norepinephrine ignites local hotspots of neuronal excitation: How arousal amplifies selectivity in perception and memory. *Behavioral and Brain Sciences*, 39.

McCutcheon, R. A., Abi-Dargham, A., & Howes, O. D. (2019). Schizophrenia, dopamine and the striatum: from biology to symptoms. *Trends in Neurosciences*, *42*(3), 205-220.

McNamara, C. G., & Dupret, D. (2017). Two sources of dopamine for the hippocampus. *Trends in neurosciences*, *40*(7), 383-384.

Minzenberg, M. J., Watrous, A. J., Yoon, J. H., Ursu, S., & Carter, C. S. (2008). Modafinil shifts human locus coeruleus to low-tonic, high-phasic activity during functional MRI. *Science*, *322*(5908), 1700-1702.

Morales, M., & Margolis, E. B. (2017). Ventral tegmental area: cellular heterogeneity, connectivity and behaviour. *Nature Reviews Neuroscience*, *18*(2), 73-85.

Neunuebel, J. P., Yoganarasimha, D., Rao, G., & Knierim, J. J. (2013). Conflicts between local

and global spatial frameworks dissociate neural representations of the lateral and medial entorhinal cortex. *Journal of Neuroscience*, *33*(22), 9246-9258.

Niv, Y., Daw, N. D., Joel, D., & Dayan, P. (2007). Tonic dopamine: opportunity costs and the control of response vigor. *Psychopharmacology*, *191*(3), 507-520.

Palaniyappan, L., & Liddle, P. F. (2012). Does the salience network play a cardinal role in psychosis? An emerging hypothesis of insular dysfunction. *Journal of Psychiatry and Neuroscience*, *37*(1), 17-27.

Pauli, W. M., Nili, A. N., & Tyszka, J. M. (2018). A high-resolution probabilistic in vivo atlas of human subcortical brain nuclei. *Scientific Data*, *5*(1), 1-13.

Pickel, V. M., Segal, M., & Bloom, F. E. (1974). A radioautographic study of the efferent pathways of the nucleus locus coeruleus. *Journal of Comparative Neurology*, *155*(1), 15-41.

Pioli, E. Y., Meissner, W., Sohr, R., Gross, C. E., Bezard, E., & Bioulac, B. H. (2008). Differential behavioral effects of partial bilateral lesions of ventral tegmental area or substantia nigra pars compacta in rats. *Neuroscience*, *153*(4), 1213-1224.

Power, J. D., Barnes, K. A., Snyder, A. Z., Schlaggar, B. L., & Petersen, S. E. (2012). Spurious but systematic correlations in functional connectivity MRI networks arise from subject motion. *Neuroimage*, *59*(3), 2142-2154.

Pruim, R. H., Mennes, M., Buitelaar, J. K., & Beckmann, C. F. (2015). Evaluation of ICA-AROMA and alternative strategies for motion artifact removal in resting state fMRI. *Neuroimage*, *112*, 278-287.

Pruim, R. H., Mennes, M., van Rooij, D., Llera, A., Buitelaar, J. K., & Beckmann, C. F. (2015). ICA-AROMA: A robust ICA-based strategy for removing motion artifacts from fMRI data. *Neuroimage*, *112*, 267-277.

Rajkowski, J., Majczynski, H., Clayton, E., & Aston-Jones, G. (2004). Activation of monkey locus coeruleus neurons varies with difficulty and performance in a target detection task. *Journal of neurophysiology*, *92*(1), 361-371.

Reineberg, A. E., Gustavson, D. E., Benca, C., Banich, M. T., & Friedman, N. P. (2018). The relationship between resting state network connectivity and individual differences in executive functions. *Frontiers in Psychology*, 1600.

Rice, M. W., Roberts, R. C., Melendez-Ferro, M., & Perez-Costas, E. (2016). Mapping dopaminergic deficiencies in the substantia nigra/ventral tegmental area in schizophrenia. *Brain Structure and Function*, *221*(1), 185-201.

Sämann, P. G., Iglesias, J. E., Gutman, B., Grotegerd, D., Leenings, R., Flint, C., ... & Schmaal, L. (2022). FreeSurfer‐based segmentation of hippocampal subfields: A review of methods and applications, with a novel quality control procedure for ENIGMA studies and other collaborative efforts. *Human Brain Mapping*, *43*(1), 207-233.

Sara, S. J., & Bouret, S. (2012). Orienting and reorienting: the locus coeruleus mediates cognition through arousal. *Neuron*, *76*(1), 130-141.

Schaefer, A., Kong, R., Gordon, E. M., Laumann, T. O., Zuo, X. N., Holmes, A. J., ... & Yeo, B. T. (2018). Local-global parcellation of the human cerebral cortex from intrinsic functional connectivity MRI. *Cerebral Cortex*, *28*(9), 3095-3114.

Schölvinck, M. L., Maier, A., Frank, Q. Y., Duyn, J. H., & Leopold, D. A. (2010). Neural basis of global resting-state fMRI activity. *Proceedings of the National Academy of Sciences*, *107*(22), 10238-10243.

Schultz, W., Dayan, P., & Montague, P. R. (1997). A neural substrate of prediction and reward. *Science*, *275*(5306), 1593-1599.

Schwarz, L. A., & Luo, L. (2015). Organization of the locus coeruleus-norepinephrine system. *Current Biology*, *25*(21), R1051-R1056.

Seeley, W. W. (2019). The salience network: a neural system for perceiving and responding to homeostatic demands. *Journal of Neuroscience*, *39*(50), 9878-9882.

Seeley, W. W., Menon, V., Schatzberg, A. F., Keller, J., Glover, G. H., Kenna, H., ... & Greicius, M. D. (2007). Dissociable intrinsic connectivity networks for salience processing and executive control. *Journal of Neuroscience*, *27*(9), 2349-2356.

Servan-Schreiber, D., Printz, H., & Cohen, J. D. (1990). A network model of catecholamine effects: gain, signal-to-noise ratio, and behavior. *Science*, *249*(4971), 892-895.

Sesack, S. R., & Grace, A. A. (2010). Cortico-basal ganglia reward network: microcircuitry. *Neuropsychopharmacology*, *35*(1), 27-47.

Shine, J. M. (2019). Neuromodulatory influences on integration and segregation in the brain. *Trends in cognitive sciences*, *23*(7), 572-583.

Smith, S. M., Fox, P. T., Miller, K. L., Glahn, D. C., Fox, P. M., Mackay, C. E., ... & Beckmann, C. F. (2009). Correspondence of the brain's functional architecture during activation and rest. *Proceedings of the national academy of sciences*, *106*(31), 13040-13045.

Solié, C., Contestabile, A., Espinosa, P., Musardo, S., Bariselli, S., Huber, C., ... & Bellone, C. (2022). Superior Colliculus to VTA pathway controls orienting response and influences social interaction in mice. *Nature Communications*, *13*(1), 1-15.

Song, A. H., Kucyi, A., Napadow, V., Brown, E. N., Loggia, M. L., & Akeju, O. (2017). Pharmacological modulation of noradrenergic arousal circuitry disrupts functional connectivity of the locus ceruleus in humans. *Journal of Neuroscience*, *37*(29), 6938-6945.

Suhara, T., Yasuno, F., Sudo, Y., Yamamoto, M., Inoue, M., Okubo, Y., & Suzuki, K. (2001). Dopamine D2 receptors in the insular cortex and the personality trait of novelty seeking. *Neuroimage*, *13*(5), 891-895.

Sutton, R. S., & Barto, A. G. (2018). *Reinforcement learning: An introduction*. MIT press.

Swanson, L. W., & Hartman, B. K. (1975). The central adrenergic system. An immunofluorescence study of the location of cell bodies and their efferent connections in the rat utilizing dopamine‐B‐hydroxylase as a marker. *Journal of Comparative Neurology*, *163*(4), 467-505.

Takeuchi, T., Duszkiewicz, A. J., Sonneborn, A., Spooner, P. A., Yamasaki, M., Watanabe, M., ...

& Morris, R. G. (2016). Locus coeruleus and dopaminergic consolidation of everyday memory. *Nature*, *537*(7620), 357-362.

Tang, W., Kochubey, O., Kintscher, M., & Schneggenburger, R. (2020). A VTA to basal amygdala dopamine projection contributes to signal salient somatosensory events during fear learning. *Journal of Neuroscience*, *40*(20), 3969-3980.

Theofilas, P., Ehrenberg, A. J., Dunlop, S., Alho, A. T. D. L., Nguy, A., Leite, R. E. P., ... & Grinberg, L. T. (2017). Locus coeruleus volume and cell population changes during Alzheimer's disease progression: a stereological study in human postmortem brains with potential implication for early-stage biomarker discovery. *Alzheimer's & dementia*, *13*(3), 236-246.

Trutti, A. C., Mulder, M. J., Hommel, B., & Forstmann, B. U. (2019). Functional neuroanatomical review of the ventral tegmental area. *Neuroimage*, *191*, 258-268.

Turker, H. B., Riley, E., Luh, W. M., Colcombe, S. J., & Swallow, K. M. (2021). Estimates of locus coeruleus function with functional magnetic resonance imaging are influenced by localization approaches and the use of multi-echo data. *Neuroimage*, *236*, 118047.

Van Den Brink, R. L., Nieuwenhuis, S., & Donner, T. H. (2018). Amplification and suppression of distinct brainwide activity patterns by catecholamines. *Journal of Neuroscience*, *38*(34), 7476-7491.

Van Den Brink, R. L., Pfeffer, T., & Donner, T. H. (2019). Brainstem modulation of large-scale intrinsic cortical activity correlations. *Frontiers in human neuroscience*, *340*.

Van Den Brink, R. L., Pfeffer, T., Warren, C. M., Murphy, P. R., Tona, K. D., van der Wee, N. J., ... & Nieuwenhuis, S. (2016). Catecholaminergic neuromodulation shapes intrinsic MRI functional connectivity in the human brain. *Journal of Neuroscience*, *36*(30), 7865-7876.

Vankov, A., Hervé‐Minvielle, A., & Sara, S. J. (1995). Response to novelty and its rapid habituation in locus coeruleus neurons of the freely exploring rat. *European Journal of Neuroscience*, *7*(6), 1180-1187.

Varazzani, C., San-Galli, A., Gilardeau, S., & Bouret, S. (2015). Noradrenaline and dopamine neurons in the reward/effort trade-off: a direct electrophysiological comparison in behaving monkeys. *Journal of Neuroscience*, *35*(20), 7866-7877.

Wagatsuma, A., Okuyama, T., Sun, C., Smith, L. M., Abe, K., & Tonegawa, S. (2018). Locus coeruleus input to hippocampal CA3 drives single-trial learning of a novel context. *Proceedings of the National Academy of Sciences*, *115*(2), E310-E316.

Wang, Y., Toyoshima, O., Kunimatsu, J., Yamada, H., & Matsumoto, M. (2021). Tonic firing mode of midbrain dopamine neurons continuously tracks reward values changing moment-by-moment. *eLife*, *10*, e63166.

Westfall, J., Kenny, D. A., & Judd, C. M. (2014). Statistical power and optimal design in experiments in which samples of participants respond to samples of stimuli. *Journal of Experimental Psychology: General*, *143*(5), 2020.

Wig, G. S., Laumann, T. O., & Petersen, S. E. (2014). An approach for parcellating human cortical areas using resting-state correlations. *Neuroimage*, *93*, 276-291.

Wilson, R. C., Geana, A., White, J. M., Ludvig, E. A., & Cohen, J. D. (2014). Humans use directed and random exploration to solve the explore–exploit dilemma. *Journal of Experimental Psychology: General*, *143*(6), 2074.

Wowk, B., McIntyre, M. C., & Saunders, J. K. (1997). k‐Space detection and correction of physiological artifacts in fMRI. *Magnetic Resonance in Medicine*, *38*(6), 1029-1034.

Yamashita, A., Rothlein, D., Kucyi, A., Valera, E. M., & Esterman, M. (2021). Brain state-based detection of attentional fluctuations and their modulation. *Neuroimage*, *236*, 118072.

Yeo, B. T., Krienen, F. M., Chee, M. W., & Buckner, R. L. (2014). Estimates of segregation and overlap of functional connectivity networks in the human cerebral cortex. *Neuroimage*, 88, 212-227.

Zhang, S., Hu, S., Chao, H. H., & Li, C. S. R. (2016). Resting-state functional connectivity of the locus coeruleus in humans: in comparison with the ventral tegmental area/substantia nigra pars compacta and the effects of age. *Cerebral Cortex*, *26*(8), 3413-3427.

CHAPTER 6

CONCLUSION

We regularly encounter events that are relevant to our ongoing behavior. They require that we act on them in some fashion, if we are to stay in line with our personal goals. However, such situations tax our attention and memory systems, as those systems need to reorient our focus and update any mental models about the state of the world. Unfortunately, attention is limited and memory is fallible (James, 1890; Kinchla, 1992). Prominent theories on these constraints have, for instance, proposed that control mechanisms bias resources towards attending, processing, and responding to information that is currently behaviorally relevant (e.g., Buschman & Kastner, 2015; Desimone & Duncan, 1995). Research on visuospatial attention has corroborated such proposals, by demonstrating that neurons in visual cortices can be tuned to preferentially represent relevant over irrelevant stimuli. At the same time, using dual-task paradigms, work on dividing attentional resources across simultaneous streams of information has demonstrated that, although dividing attention is possible to some extent, it typically results in poorer performance on both ongoing tasks (e.g., Pashler, 1994). Therefore, one might predict that acting on behaviorally relevant events while simultaneously performing another ongoing task would have a negative effect on attention and memory. My dissertation demonstrates that the opposite is the case.

6.1 Conclusions and Discussion of Theoretical and Methodological Implications

In Chapter 2 (Turker & Swallow, 2019), I replicated and extended what was known about the ABE (Swallow & Jiang, 2010). I asked if the effect was exclusive to the image participants

are instructed to memorize and showed that the effect is much more than that. Indeed, acting on behaviorally relevant events resulted in participants also better encoding task-relevant and task-irrelevant features about the target cues, despite not being instructed to memorize those features. This included a boost to task-irrelevant shape, location, and even unique identity of the cue. However, this raised the question to what extent these effects may be due to response bias or dependent upon instructions to participants.

In Chapter 3 (Turker & Swallow, under review), I used diffusion decision modeling and two new experiments to answer those questions. Modeling the data suggested that, in the few cases where response bias could have played a role, evidence for it contributing to the findings was minimal. Instead, it is more likely that temporal selection of and acting on behaviorally relevant events resulted in richer representations for information presented during those moments. This is corroborated by the experiments where a response bias strategy could not be employed by participants (Exp. 3 in Chapter 2, Exp. 4a-b in Chapter 3), because they nevertheless had retained information about the identity of the detection task cue that allowed them to match a unique face to a given image. Furthermore, when participants were instructed to actively memorize the images as well as the faces, thus dividing their attention and taxing their memory even further, the ABE increased, not reduced, in magnitude.

How could this be the case, given that seminal research on dual-tasking states there should be interference in performance, that presenting multiple stimuli concurrently results in competition for resources among them, and that this competition is resolved by biasing activity towards information that is relevant to ongoing goals (and thus away from task-irrelevant information)? Part of the issue is that this work has primarily focused on characteristics of attention that are spatial or feature-based, less on the idea that attention can also select moments

in time. Indeed, longstanding and extensive research on event cognition has demonstrated that moments of change are treated differently from moments of stability (e.g., Radvansky & Zacks, 2014; Zacks & Tversky, 2001). Therefore, a broader theoretical implication of this dissertation is that it contributes to the push to characterize attention as a mechanism that can select not just across space but also over time and it also contributes to the growing appreciation of the event as a unit on which cognition can operate. Indeed, if we do not keep this ability of the mind in mind, we may overlook important cognitive, computational, and neural features of attention and memory mechanisms.

Regarding those mechanisms, this dissertation builds on the proposal that a critical component of it is the locus coeruleus neuromodulatory system. Swallow & Jiang (2013) proposed a dual-task interaction (as opposed to interference) model, which states that behaviorally relevant events transiently increase activity in the LC and broadly enhance attention in a way that is not spatially or modality specific. How might the LC be involved in this? Neuromodulatory systems are theorized to modulate brain-wide network dynamics to optimize processing of, learning about, and responding to stimuli that carry behavioral relevance (Briand, Gritton, Howe, Young, & Sarter, 2007). With their widespread afferent projections, they are, therefore, in a good position to impact various neural networks around the brain underpinning attention and memory (Shine et al., 2019). At the neurophysiological level, the impact that these systems have is that they change signal-to-noise ratio and thereby strengthen long-term potentiation (e.g., Lisman & Grace, 2005), potentially contributing to a boost in encoding of any information being processed at that moment. However, showing a direct causal link between the LC and the ABE is still an ongoing line of research.

Chapter 4 (Turker, Riley, Luh, Colcombe, & Swallow, 2021) was an important step toward establishing the plausibility of that link, in addition to its methodological contributions to the human neuroimaging field focused on LC. Starting with the latter point, a recent systematic review of that literature showed fMRI studies of the LC often use different (or even underspecified) methodologies, resulting in conflicting conclusions, and it expressed the need to optimize reliability and validity in future LC imaging studies (Liu, Marijatta, Hämmerer, Acosta-Cabronero, Düzel, & Howard, 2017). This need comes within a context where the broader fMRI community is looking to establish more reliability in imaging research, because variations in analysis pipelines across labs can result in different findings on the same data (Botvinik-Nezer et al., 2020). Therefore, my work meets some of the needs for LC imaging researchers and is highly timely given the broader discourse surrounding fMRI methodology, by showing that characterization of the functional connectivity of the LC is impacted by localization method and scanning protocol. Moreover, I argue that its characterization is, most likely, improved by using multi-echo fMRI and neuromelanin scanning. Next, regarding the prior point concerning the role of LC in producing the ABE, in Chapter 4, it is shown that functional connectivity of the LC during a task-free resting-state scan is correlated with frontal areas important for cognitive control, posterior areas important for perceptual processing, and critical memory areas like the HPC. Previous fMRI studies have confirmed that auditory targets can enhance activity throughout the visual cortex (Swallow, Makovski, & Jiang, 2012) and that target-detection and subsequent memory can be shown to be correlated with putative LC (Yebra et al., 2019). Combined, this work suggests that LC may indeed be enhancing the quality of representations that co-occur with behaviorally relevant events.

This is supported by another recent fMRI study of ours, not included in this dissertation. Using multi-echo fMRI and manual tracing of LC with participants performing an attentional boost task (Moyal, Turker, Luh, & Swallow, under review), we confirmed an increase in LC activity following the appearance of auditory targets, but not for images paired with auditory distractors or no tones. Replicating Swallow et al. (2012), the detection of auditory targets was again accompanied by widespread increases in activity, including in the ventral visual cortex. Expanding on that study, activity in the hippocampus lowered with each subsequent detection of a given image-cue pairing, lowering it faster if the cue was a target. Such repetition suppression is often an indicator of facilitated processing (e.g., Segaert, Weber, De Lange, Petersson, & Hagoort, 2013). Furthermore, the functional connectivity between hippocampus and visual cortex was enhanced following auditory target cues, resulting in better image classification in the ventral visual cortex, thereby supporting the notion that quality of representation is enhanced during target-detection. This fMRI study, in part, was made possible by the insights from Chapter 4 on localizing LC and the use of ME-fMRI scanning protocols (Turker et al., 2021).

One may then ask to what extent it is LC, as opposed to other neuromodulator systems, that is critical for the ABE. Chapter 5 (Turker, Colcombe, & Swallow, submitted) investigated this by comparing the functional connectivity profile of LC against that of another widely-studied neuromodulatory system: the VTA-dopamine system. Whereas previous research on these two systems analyzed the fMRI with conjunctive analyses, I took a different approach that would inform us about the contributions of these systems to unshared variance around the brain. By taking this approach that is less common, I showed that LC accounted for variance above and beyond what was accounted for by VTA in various cortical networks around the brain. In particular, unshared functional connectivity of LC was shown to be biased towards posterior

and parietal areas, involved in perceptual processing. In doing so, we showed, for the first time, that, although the VTA and LC system have many similarities in their function and physiology, they are differentiable in this important way, where LC appears to have a unique impact on networks that control attention and perception. In these ways, my dissertation and some of my other work have strengthened the proposal that it is the LC specifically that is a critical mechanism involved in producing the ABE.

Finally, regarding the aforementioned dual-task interaction model (Swallow & Jiang, 2013), one theoretical implication of my work is that this account of the ABE requires updating. The original account proposed a temporal selection mechanism working independently from one that selects on spatial locations or features. My dissertation argues in favor of a spatiotemporal boost – an enhancement that impacts all constituent items, features, and spatiotemporal relationships of a given moment in time. If broader spatiotemporal features of stimuli can be enhanced in the ABE and the LC is indeed a critical component in that mechanism, the original account of the ABE was underspecified. To account for my work and recent other work on the ABE, we are in the process of releasing an update to the dual-task interaction model (Swallow, Broitman, Riley, & Turker, under review).

6.2 Limitations and Warranted Studies

There remain several outstanding questions after the work presented here. For instance, there is the issue of the time course of the effect. Although current views on the memory advantage suggest that the effect begins to take shape early during the encoding process ("early phase encoding", Mulligan & Spataro, 2015; "temporal selection", Swallow & Jiang, 2013), it is unclear what that early process is like and whether there is a role for later-stage processes like

maintenance, rehearsal, and elaboration of an encoded item's meaning. Though there is research on the effects of target-detection on low-level perceptual processing (e.g., Pascucci & Turatto, 2012) as well as on the contribution of conceptual processing during encoding to the ABE (e.g., Spataro et al., 2017), there is no clear consensus on which processes are the key contributors and how. Techniques with higher temporal resolution than fMRI, such as electroencephalograms, may offer new and valuable insights into how the ABE manifests.

This issue of timing is related to the specificity of the effect. Different features of natural visual scenes are perceived at different points in time (e.g., Greene & Oliva, 2009). Therefore, the time point at which target-paired encoding starts to differentiate itself from distractor-paired encoding will result in temporal selection affecting some features but not others. Chapter 2 and 3 demonstrated that the boost can impact a range of features – color, location, and even facial identity – to a sufficient degree to differentiate the paired-item or feature from any foils on a recognition memory test. But this does not yet tell us, for example, whether temporal selection can boost encoding enough to differentiate different hues within the same color (i.e. color precision) or whether it boosts high and low spatial frequencies differently, let alone features and their precision in non-visual modalities (e.g., identity of voice reading out a word as the word itself was being encoded).

Next, the increasing likelihood of the LC playing a critical role in the ABE demands that we take into consideration what else is known about this neuromodulatory system. Indeed, much of the seminal work on neuromodulatory systems comes from machine learning and psychiatry. Both LC and VTA, for instance, show high frequency burst firing that is time-locked to the appearance of a behaviorally salient stimulus (e.g., a reward; Briand et al., 2007). With repeated exposure to that stimulus, this response moves forward in time to be time-locked to any

predictive cues that may precede the stimulus. Thus, an understanding of how prediction and expectation (e.g., Friston, 2018) contribute to the ABE will also allow for a better understanding of how underlying neural mechanisms, like neuromodulators, contribute to its manifestation, and vice versa.

Finally, because I argue that LC is likely (even if not exclusively) playing a role in modulating various brainwide dynamics during temporal selection, my findings raise questions regarding healthy aging and our understanding of clinical conditions. For instance, LC integrity is an important preclinical marker for Alzheimer's dementia and often the first site where tau pathology develops (Mather & Harley, 2016). Indeed, the ABE may be abolished in healthy older adults (Bechi Gabrielli, Spataro, Pezzuti, & Rossi-Arnaud, 2018; Prull, 2019), as well as in both young and older adults with bipolar disorder (Bechi Gabrielli et al., 2021), and patients with schizophrenia (Rossi-Arnaud et al., 2014). Patients with Parkinson's disease, however, show a similar ABE to healthy controls (Kéri, Nagy, Levy-Gigi, & Keleman, 2013). In another study of ours, we collected multi-echo fMRI in a group of younger and older adults as they performed the attentional boost task and localized their LC manually (following the protocol from Chapter 4) to ensure better signal specificity. We also collected pupillometry data while they were in the scanner, because LC is one of the systems that drives pupil size (Larsen & Waters, 2018). Intriguingly, in the absence of differences in task performance, we found that older adults use more of their dynamic pupillary range, potentially reflecting compensatory LC signaling (Riley, Turker, Swallow, De Rosa, Anderson, & Wang, under review). Ongoing analyses into individual neuromelanin intensity in the LC are corroborating that LC integrity is more critical to the performance of older adults than younger adults and that pupil responses are more strongly related to neural activity in older adults. Thus, our work here along with that of others may offer

a novel, non-invasive avenue to investigate preclinical brain changes for preemptive clinical intervention, through investigating physiological markers (like pupil size and LC integrity with fMRI) that are correlated with the presence or absence of an ABE.

6.3 Final Thoughts

Behaviorally relevant events happen around us all the time. Despite our limitations, we are able to manage quite well in a world rife with events that require us to act on them if we want to stay on track to meet our goals. A lot of the seminal work on attention and memory has focused on where things break down and fall apart, but there are many scenarios – ones that we might think should overwhelm us, given that seminal research – where performance is boosted instead.

It is my belief that, at least in part, the reason the findings in this dissertation appear at odds with some of the seminal theories, but were predictable from long-standing work on event cognition, is because work on event cognition has been more inclined to utilize naturalistic and ecologically valid stimuli and scenarios. In addition to being a push for taking a more complex stance on attention and memory interactions, I aim for this dissertation to be a call for more naturalistic research in behavioral and brain sciences. In Cognition and Reality (1976), Ulric Neisser states:

> "*Demands for ecological validity are only intelligible if they are specific. They must point to particular aspects of ordinary situations that are ignored by current experimental methods, and there must be a good reason to suppose that those aspects are important. I believe that important aspects of the normal environment are being ignored in*

> *contemporary research paradigms. These aspects are the spatial, temporal, and intermodal continuities of real objects and events.*"(p.34).

Since its publication, appreciation for the study of spatiotemporal features of naturalistic and multimodal events has increased, but perhaps not to the extent needed. Some of the work in this dissertation argues that attention and memory function in a more sophisticated manner than sometimes assumed, interacting with each other to encode a range of spatiotemporal features for moments in time that are behaviorally relevant for our goals and ongoing actions. It is my hope that the work that builds on this dissertation will carry forward an appreciation of naturalistic, ecological stimuli and expand on my findings with valid, intelligible, and specific scenarios rich in spatial, temporal, and intermodal continuities of real objects and events to better understand perception-action cycles.

References

Bechi Gabrielli, G., Rossi-Arnaud, C., Spataro, P., Doricchi, F., Costanzi, M., Santirocchi, A., … & Cestari, V. (2021). The attentional boost effect in young and adult euthymic bipolar patients and healthy controls. *Journal of Personalized Medicine*, *11*(3), 185.

Bechi Gabrielli, G., Spataro, P., Pezzuti, L., & Rossi-Arnaud, C. (2018). When divided attention fails to enhance memory encoding: The attentional boost effect is eliminated in young-old adults. *Psychology and Aging*, *33*(2), 259.

Botvinik-Nezer, R., Holzmeister, F., Camerer, C. F., Dreber, A., Huber, J., Johannesson, M., ... & Rieck, J. R. (2020). Variability in the analysis of a single neuroimaging dataset by many teams. *Nature*, *582*(7810), 84-88.

Briand, L. A., Gritton, H., Howe, W. M., Young, D. A., & Sarter, M. (2007). Modulators in concert for cognition: modulator interactions in the prefrontal cortex. *Progress in neurobiology*, *83*(2), 69-91.

Buschman, T. J., & Kastner, S. (2015). From behavior to neural dynamics: an integrated theory of attention. *Neuron*, *88*(1), 127-144.

Desimone, R., & Duncan, J. (1995). Neural mechanisms of selective visual attention. *Annual review of neuroscience*, *18*(1), 193-222.

Friston, K. (2018). Does predictive coding have a future? *Nature neuroscience*, *21*(8), 1019-1021.

Greene, M. R., & Oliva, A. (2009). The briefest of glances: The time course of natural scene understanding. *Psychological Science*, *20*(4), 464-472.

James, W. (1890). The Principles of Psychology. Dover Publications.

Kéri, S., Nagy, H., Levy‐Gigi, E., & Kelemen, O. (2013). How attentional boost interacts with reward: the effect of dopaminergic medications in Parkinson's disease. *European Journal of Neuroscience*, *38*(11), 3650-3658.

Kinchla, R. A. (1992). Attention. *Annual Review of Psychology*, *43*, 711-742.

Larsen, R. S., & Waters, J. (2018). Neuromodulatory correlates of pupil dilation. *Frontiers in neural circuits*, *12*, 21.

Lisman, J. E., & Grace, A. A. (2005). The hippocampal-VTA loop: controlling the entry of information into long-term memory. *Neuron*, *46*(5), 703-713.

Liu, K. Y., Marijatta, F., Hämmerer, D., Acosta-Cabronero, J., Düzel, E., & Howard, R. J. (2017). Magnetic resonance imaging of the human locus coeruleus: A systematic review. *Neuroscience & Biobehavioral Reviews*, *83*, 325-355.

Mather, M., & Harley, C. W. (2016). The locus coeruleus: essential for maintaining cognitive function and the aging brain. *Trends in cognitive sciences*, *20*(3), 214-226.

Mulligan, N. W., & Spataro, P. (2015). Divided attention can enhance early-phase memory encoding: The attentional boost effect and study trial duration. *Journal of Experimental Psychology: Learning, Memory, and Cognition*, *41*(4), 1223.

Neisser, U. (1976). Cognition and Reality. W. H. Freeman and Company.

Pascucci, D., Mastropasqua, T., & Turatto, M. (2012). Permeability of priming of pop out to expectations. *Journal of Vision*, *12*(10), 21-21.

Pashler, H. (1994). Dual-task interference in simple tasks: data and theory. *Psychological bulletin*, *116*(2), 220.

Prull, M. W. (2019). The attentional boost effect for words in young and older adults. *Psychology and Aging*, 34(3), 405.

Radvansky, G. A., & Zacks, J. M. (2014). Event cognition. Oxford University Press.

Rossi-Arnaud, C., Spataro, P., Saraulli, D., Mulligan, N. W., Sciarretta, A., Marques, V. R., & Cestari, V. (2014). The attentional boost effect in schizophrenia. *Journal of abnormal psychology*, *123*(3), 588.

Segaert, K., Weber, K., de Lange, F. P., Petersson, K. M., & Hagoort, P. (2013). The suppression of repetition enhancement: a review of fMRI studies. *Neuropsychologia*, *51*(1), 59-66.

Shine, J. M. (2019). Neuromodulatory influences on integration and segregation in the brain. *Trends in cognitive sciences*, *23*(7), 572-583.

Spataro, P., Mulligan, N. W., Bechi Gabrielli, G., & Rossi-Arnaud, C. (2017). Divided attention enhances explicit but not implicit conceptual memory: An item-specific account of the attentional boost effect. *Memory*, *25*(2), 170-175.

Swallow, K. M., & Jiang, Y. V. (2010). The attentional boost effect: Transient increases in attention to one task enhance performance in a second task. *Cognition*, *115*(1), 118-132.

Swallow, K. M., & Jiang, Y. V. (2013). Attentional load and attentional boost: A review of data and theory. *Frontiers in Psychology*, *4*, 274.

Swallow, K. M., Makovski, T., & Jiang, Y. V. (2012). Selection of events in time enhances activity throughout early visual cortex. *Journal of Neurophysiology*, *108*(12), 3239-3252

Turker, H. B., Riley, E., Luh, W. M., Colcombe, S. J., & Swallow, K. M. (2021). Estimates of locus coeruleus function with functional magnetic resonance imaging are influenced by localization approaches and the use of multi-echo data. *Neuroimage*, *236*, 118047.

Turker, H. B., & Swallow, K. M. (2019). Attending to behaviorally relevant moments enhances incidental relational memory. *Memory & Cognition*, *47*(1), 1-16.

Yebra, M., Galarza-Vallejo, A., Soto-Leon, V., Gonzalez-Rosa, J. J., de Berker, A. O., Bestmann, S., ... & Strange, B. A. (2019). Action boosts episodic memory encoding in humans via engagement of a noradrenergic system. *Nature Communications*, *10*(1), 1-12.

Zacks, J. M., & Tversky, B. (2001). Event structure in perception and conception. *Psychological Bulletin*, *127*(1), 3.